Structures and internal dynamics of methylated nitrogen containing aromatic rings probed by means of microwave spectroscopy, quantum chemical calculation and spectral modelling

Thuy Thi Nguyen

Université de Paris

lisa

Thèse de doctorat de l'Université de Paris

École doctorale 129 – Sciences de l'Environnement d'Île-de-France

Spécialité : Chimie de la pollution atmosphérique et physique de l'environnement

Structures and internal dynamics of methylated nitrogen containing aromatic rings probed by means of microwave spectroscopy, quantum chemical calculation and spectral modelling

présentée par

Thi Thuy NGUYEN

pour obtenir le grade de

Docteur de l'Université de Paris

Thèse dirigée par Mme Isabelle KLEINER

au Laboratoire Interuniversitaire des Systèmes Atmosphériques

Soutenue publiquement le 06 july 2021 devant le jury composé de :

Mme Halima MOUHIB	Maître de Conférences HDR Université Gustave Eiffel	Rapportrice
M. Vincent BOUDON	Directeur de Recherche Centre National de la Recherche Scientifique	Rapporteur
M. Majdi HOCHLAF	Professeur Université Gustave Eiffel	Examinateur
M. Arnaud CUISSET	Professeur Université du Littoral Côte d'Opale	Examinateur
Mme Souad AMMAR	Professeur Université de Paris	Examinatrice
M. Jens-Uwe GRABOW	Professeur Leibniz Universität Hannover	Examinateur
Mme Isabelle KLEINER	Directeur de Recherche Centre National de la Recherche Scientifique	Directrice de thèse

“Education is what remains after one has forgotten
what one has learned in school,,

-Albert Einstein-

RÉSUMÉ

Ce travail est dédié à l'étude des signatures de rotation de six cycles aromatiques contenant de l'azote et un ou deux groupes méthyles (2-méthylthiazole (2MTA), 2-méthypyrrole (2MP), 3-méthylpyrrole (3MP), 2,5-diméthylpyrrole (25DMP) 4,5-diméthylthiazole (45DMTA), 4-méthylpyrimidine (4MPY)) - des précurseurs d'hydrocarbures aromatiques polycycliques qui jouent un rôle crucial en astrochimie et ont le potentiel d'être détectés dans l'espace. Notre étude vise à affiner la compréhension des effets de mouvement(s) de grande amplitude du (des) groupe(s) méthyle(s), en produisant des constantes moléculaires précises en phase gazeuse et des listes de positions de raies utiles pour la recherche astronomique. Les spectres de rotation de ces molécules ont été étudiés en détails par une combinaison de méthodes de spectroscopie micro-onde, de calculs de chimie quantique et modélisation spectrale, permettant la détermination des paramètres géométriques, des barrières de rotation internes ainsi que des constantes de couplage quadripolaire nucléaire.

Pour les molécules de 2MTA, 2MP et 3MP, qui contiennent un groupe ^{14}N et un groupe méthyle, nos travaux confirment que les calculs de chimie quantique avec un ensemble de bases suffisamment larges donnent des résultats fiables pour les paramètres géométriques (p.ex., les constantes de rotation, les constantes de distorsion centrifuge) mais échouent souvent à prédire la valeur de la barrière à la rotation interne du groupe méthyle, en particulier lorsque le groupe méthyle possède une barrière assez basse. Nos résultats montrent que les atomes du cycle aromatique ainsi que la symétrie de ce dernier jouent un rôle important dans la hauteur de la barrière résultante. En étudiant la liaison chimique au site du ^{14}N au sein des cycles aromatiques, nous avons pu relier les configurations électroniques aux signes des constantes de couplage quadripolaire χ_{cc}.

Pour les molécules de 25DMP et 45DMTA, de nouvelles fonctionnalités du code *BELGI* ont été implémentées pour modéliser les spectres rotationnels de molécules à deux rotors et un ^{14}N. Un nouveau code appelé *WS18* a été utilisé qui traite séparément chaque espèce de symétrie permet de vérifier les attributions spectrales. Des paramètres moléculaires très précis sont rapportés pour le 25DMP et le 45DMTA. Contrairement au 25DMP qui ne montre aucun couplage entre les deux toupies, de forts couplages entre les deux rotateurs internes sont observés pour le 45DMTA où les effets de distribution électronique s'avèrent plus significatifs que dans le cas du 25DMP.

Pour la molécule de 4MPY, nous avons développé un nouveau code appelé *TW21*, afin de modéliser le spectre micro-onde d'une molécule avec un rotateur interne et jusqu'à deux couplages quadripolaires faiblement nucléaires. Une fonctionnalité similaire a également été implémentée dans le code *BELGI-2N* ainsi que dans les codes *WS18*. Le nouveau code *TW21* a été appliqué avec succès pour sur les molécules de 2MTA, 2MP et 3MP, obtenant des résultats en excellent accord avec les résultats du code *BELGI*. La signature rotationnelle de la molécule de 4MPY a été analysée à l'aide des programmes *WS18*, *BELGI-2N* et *TW21*, conduisant à des paramètres moléculaires très précis.

Mots clés : Spectroscopie rotationnelle, mouvements de grande amplitude, 2-méthylthiazole, 2-méthylpyrrole, 3-méthylpyrrole, 2,5-diméthylpyrrole, 4,5-diméthylpyrrole, 4-méthylpyrimidine.

ABSTRACT

This work is dedicated to the study of rotational signatures of six methylated nitrogen containing aromatic rings (2-methylthiazole (2MTA), 2-methypyrrole (2MP), 3-methylpyrrole (3MP), 2,5-dimethylpyrrole (25DMP), 4,5-dimethylthiazole (45DMTA), 4-methylpyrimidine (4MPY) – some important precursors of polycyclic aromatic hydrocarbon which play crucial roles in astrochemistry and have potential to be detected in space. Our study focuses on sharpening the understanding on the large amplitude motion(s) effects of the methyl group(s), providing accurate molecular parameters in the gas phase and a list of precise line positions for astronomical search. Probed by means of microwave spectroscopy, quantum chemistry and spectral modelling, the rotational spectra of those molecules were studied in details, allowing the determination of accurate geometries, internal rotation potential barriers and nuclear quadrupole coupling constants.

For the 2MTA, 2MP and 3MP molecules which contain one ^{14}N and one internal rotation methyl group, our investigations confirm that quantum chemical calculations with sufficient large basis set often yielded reliable results for geometrical parameters (e.g., rotational constants, centrifugal distortion constants) but often failed in predicting the value of barrier to internal rotation of methyl group, especially when the methyl group possesses a rather low barrier. Our results show that the skeleton atom as well as the frame symmetry plays an important role in the resulting barrier height. By studying the chemical bond at the site of the ^{14}N within the rings, we were able to link the electronic configurations to the signs of quadrupole coupling constants χ_{cc}.

For the 25DMP and 45DMTA molecules, new features of the *BELGI* code were implemented to model the rotational spectra of molecules with two rotors and one ^{14}N. A new code called *WS18* was introduced and used to fit each species separately which helped confirming the assignments. With regard on the value of methyl torsional barrier, while steric hindrance was mainly found in case of the 25DMP, the electronic distribution is found to have more significant effect in case of 45DMTA.

For the 4MPY molecule we introduced a new code called *TW21*, written for modelling the microwave spectrum of molecule with one rotor and up to two weakly nuclear quadrupole coupling. Similar feature was also implemented into the *BELGI-2N* code as well as *WS18* codes. The new code *TW21* was successfully tested on the 2MTA, 2MP and 3MP molecules, obtaining results in excellent agreement with the findings from *BELGI* code. The rotational signature of 4MPY was investigated and analyzed using the *WS18*, *BELGI-2N* and *TW21* programs, leading to very accurate molecular parameters.

Key words: Rotational spectroscopy, large amplitude motions, 2-methylthiazole, 2-methylpyrrole, 3-methylpyrrole, 2,5-dimethylpyrrole, 4,5-dimethylpyrrole, 4-methylpyrimidine.

*This thesis is conducted at the **L**aboratoire **I**nteruniversitaire des **S**ystèmes **A**tmosphériques (LISA) from Octocber 2018 to July 2021. Part of this dessertation were already published in scientific journals, some results were presented on national/international workshop(s)/ conferences as talks or posters*

A. Articles

1. **Thuy Nguyen**, Vinh Van, Claudine Gutlé, Wolfgang Stahl, Martin Schwell, Isabelle Kleiner, and Ha Vinh Lam Nguyen, The microwave spectrum of 2-methylthiazole: ^{14}N nuclear quadrupole coupling and methyl internal rotation, *J. Chem. Phys.* **152**, 134306 (2020).

2. **Thuy Nguyen**, Christina Dindic, Wolfgang Stahl, Ha Vinh Lam Nguyen, and Isabelle Kleiner, ^{14}N Nuclear quadrupole coupling and methyl internal rotation in the microwave spectrum of 2-methylpyrrole, *Mol. Phys.* **18**, 1668572 (2020).

3. **Thuy Nguyen**, Wolfgang Stahl, Ha Vinh Lam Nguyen, and Isabelle Kleiner, ^{14}N Nuclear quadrupole coupling and methyl internal rotation in 3-methylpyrrole investigated by microwave spectroscopy, *J. Mol. Spectros*. **372**, 111351 (2020).

4. Vinh Van, **Thuy Nguyen**, Wolfgang Stahl, Ha Vinh Lam Nguyen and, Isabelle Kleiner, Coupled Large Amplitude Motions: The Effects of Two Methyl Internal Rotations and ^{14}N Quadrupole Coupling in 4,5-Dimethylthiazole Investigated by Microwave Spectroscopy, *J. Mol. Struct.* **1207**, 127787, 14 (2020).

5. **Thuy Nguyen**, Wolfgang Stahl, Ha Vinh Lam Nguyen, and Isabelle Kleiner, Local versus global approaches to treat two equivalent methyl internal rotations and ^{14}N nuclear quadrupole coupling of 2,5-dimethylpyrrole, *J. Chem. Phys*. (accepted).

B. Conferences / workshops

04. – 05 April 2019 Young researchers meet molecular spectroscopy, 04-05 April (2019), Pisa, Italia

Thuy Nguyen, Christina Dindic, Wolfgang Stahl, Ha Vinh Lam Nguyen, and Isabelle Kleiner

Talk: Microwave spectroscopic and quantum chemical investigations on 2-methylpyrrole.

21. – 23 May 2019 Journée de Spectroscopie Moléculaire (JSM), LISA, France

Thuy Nguyen, Christina Dindic, Wolfgang Stahl, Ha Vinh Lam Nguyen, and Isabelle Kleiner

Poster: *Microwave spectroscopy as a tool to study internal rotation and ^{14}N nuclear quadrupole hyperfine structure.*

26. – 30. Aug. 2019 The 26th Colloquium on High-Resolution Molecular Spectroscopy HRMS, Dijon, France, **Thuy Nguyen**, Christina Dindic, Wolfgang Stahl, Ha Vinh Lam Nguyen, and Isabelle Kleiner, *Poster: Methyl internal rotation and ^{14}N quadrupole coupling in 2-methylpyrrole and 2,5-dimethylpyrrole: A comparative study.*

22. – 26. June 2020 2020 International Symposium on Molecular Spectroscopy, Champaign-Urbana, USA

Vinh Van, **Thuy Nguyen**, Wolfgang Stahl, Ha Vinh Lam Nguyen, and Isabelle Kleiner

Talk: *Coupled large amplitude motions: The effects of two methyl internal rotations and ^{14}N quadrupole coupling in 4,5-dimethylthiazole*, postponed due to the COVID-19.

ACKNOWLEDGEMENT

I would like to thank the Universite de Paris for the fellowship that has allowed me to do my thesis. I would like to express my sincere appreciation and thanks to all those who provided me the possibility to complete this thesis and all the academic supporting that I have received during my time at the hosted lab LISA.

I want to thank my advisor, Dr. Isabelle Kleiner, for giving me the chance to begin with microwave spectroscopy. I still remember her talks at USTH, she strongly said to us "Woman never give up", to my mind at the time she was a real inspiration. She also likes it to take care of those surrounding. When I participated the only conference with her, competing for a student prize, I thought she was much more worried than myself. She pushed me to do the work as best as possible. When the juries were listening to my talk, she with her camera in front of her chest taking photos. It was that funny that all of the juries and myself looking at her. Later on, she said to me: "Well, if we do not have the prize, we still have those pictures". Time does fly, it has been more than three years since we first met and many things had happened in those three years. Obviously, we did not agree on so many things and have real different views on stuffs but I really appreciate her protective actions and always response in very timely manner.

I would also like to thank my co-authors, Christina Dindic, Dr. Vinh Van, Dr. Ha Vinh Lam Nguyen, Dr. Claudine Gutle and Prof. Martin Schwell for cooperations which yielded successful publications during my thesis.

I indebt to all my teachers. From a small student project during my bachelor to the bachelor thesis, Dr. Ngo Ngoc Hoa taught me that for the tiny little things that I do, do it in the most careful possible way so that others can rely on my results. I would have never been able to speak English and have no chance for higher education without the encouragements from Dr. Ngo Duc Thanh. He taught me to trust in myself and to pursue what I like regardless any circumstances. Dr. Guillaume Patanchon with his enthusiasm for research and his open-mind, inspires me to do research and was the one who was always willing to share his precious time to write me countless recommendation letters. Finally, in this non-full list, I would like to mention Yannick for his significant contributions to the study and research of Vietnamese students. I wish that he will get recover soon, we still have a party that we wanted to gather together with all USTH students in France.

My dear friend Rebecca told all of us in the Ph.D.'s room, that no one can ever succeed a Ph.D. alone and I found that statement cannot be more correct. I am deeply grateful to members in SPECAT teams: Anusanth, Rebecca, Henda, Yoursa, Yohann, Farouk. Thank you, Anusanth for always be there even when I was not really reasonable, listening to all my complaints, and yes enjoying to tell me that I adapted to the Parisian style in complaining. When things do not go right, I know who to go to and can trust blindly. Thank you, Rebecca for sharing with me this journey. There were blue days, the days I had no motivations even to get up, but you patiently sent me pictures with quotes telling me how much you care about me. Whatever happens, I know there is someone always on my side. Thank you, Henda

for look after me even when you have a little beautiful baby Rana and a teaching job at the same time. Thank you for always take me back to the track if I was not in the right path. I miss so much the tea party with Yohann, perhaps the best tea I have tested is his Kusmi tea that he gave me as a present. He was very generous and it was great pleasure sharing the office with him. It was really fun talking with Yoursa with my broken French. And finally, the silent friend Farouk, he does not talk much but if I need helps and if he can, he will.

I thank all of my friends during the time I stay in Paris who made the stress time perusing a Ph.D. far more manageable. If I have any issue on renting a room or buying specific things, etc., Dung was always willing to give his hands. Remi mocked me that only after my time in France, I would obtain the carte de sejour and carte vital, but thanks to his helps with French translation, things were done much faster than expected.

My gratitude goes to my families. They were there regardless things were in dark or pink, they always support me in all ways possible. They do not love me more or less whether I finish the Ph.D. or not and I know that whatever happens, there will be a place where I can go back.

Inexpressively, I am thankful to Professor Wolfgang Stahl, without whom this thesis would never be written. From the beginning of my master thesis, he welcomed and taught me in the best way possible. He would sit down, take a pencil together with some white papers and teach me about irreducible tensors, operators, Wigner theory, etc., and listen to my crazy ideas about Zeeman effects. He is perhaps the most patient person I have met in my entire life so far. Three years ago, I told him that I am not afraid of operators, Hamiltonian, etc., but I have difficulties in programming. He patiently gave me some small projects, waited for me to struggle solving them myself. When I came up with a version, regardless it ran or not, he corrected them all. I will forever remember his sentences: “Always solve the first statement that compiler spots”, “Compiler never lies”, etc. I remember one day he told me: “Please bring me a bug-spray, I want to put it on my computer.” It was when he was fighting with the bug in his program for almost two weeks. He was a really humble person. We often argued about scientific stuffs, and yes, he dominantly won (I did win a few times). He was afraid if I would get upset, he told me: “Remember that I have 20 years more to learn all things you have just started”. I cannot count how many things he taught me, how many hours he spent on teaching me and the saddest thing is that I can never pay him back. I was a believer, that whatever we want, we could make it. But now I understand that there are certain things that we cannot dream of regardless how hard we wish. The last conversations before you left us, I will always keep with me and I will make it. I hope that this thesis brings you some happiness, it is written for you with all knowledge that you successfully transferred to me. I truly miss you.

TABLE OF CONTENTS

RÉSUMÉ DE THESE

"Structures and internal dynamics of methylated nitrogen containing aromatic rings probed by means of microwave spectroscopy, quantum chemical calculations and spectral modelling"

I. INTRODUCTION

Les spectromètres micro-ondes à transformée de Fourier couplés à un jet moléculaire font partie des techniques les plus précises pour la détermination des structures des molécules en phase gazeuse. Cette technique offre une très grande précision de mesure (environ 2 kHz)[1-3] et constitue donc un excellent outil pour l'obtention de nouvelles connaissances sur les structures chimiques. Elle peut aussi apporter des informations nécessaires aux recherches astrophysiques ou servir de base à de futures détections atmosphériques. Pour permettre ces détections, des paramètres très précis tels que les positions et intensités des raies sont indispensables. Ces données spectroscopiques de laboratoire sont collectées pour les astronomes dans des bases de données comme par exemple la *Cologne Database for Molecular Spectroscopy* CDMS[4,5], et pour les spécialistes de l'atmosphère dans la base de données *HIgh-resolution TRANsmission molecular absorption database* (HITRAN)[6].

Une molécule peut absorber ou émettre un rayonnement en acquérant un mouvement de rotation autour de son centre de gravité ou son centre de masse. La spectroscopie rotationnelle (3 - 300 GHz) étudie l'absorption et l'émission d'une onde électromagnétique par les molécules. Les transitions énergétiques se produisent entre leurs niveaux d'énergie de rotation. Le spectre rotationnel d'une molécule n'existe que si la molécule possède un moment dipolaire permanent. L'existence de ce moment dipolaire permet au champ électrique d'exercer un couple sur la molécule, ce qui la fait tourner plus rapidement ou plus lentement. La spectroscopie rotationnelle a fait l'objet d'études approfondies avec deux principaux domaines d'application. Le premier concerne la détection des molécules dans l'espace et le second est lié à la détermination précise de la structure tridimensionnelle des molécules.

En effet, la spectroscopie rotationnelle a permis de détecter plus de 200 molécules à présent[7]. Un certain nombre d'études ont été effectuées au sein de l'équipe SPECAT du Laboratoire Interuniversitaire des Systèmes Atmosphériques (LISA), permettant pour la première fois la détection dans l'espace de l'acétamide[8] CH_3CONH_2, des isotopomères du formiate de méthyle[9] $HCOOCH_3$, et de l'acétate de

méthyle[10] CH_3COOCH_3. Des limites de détection ont été également déterminées pour le thioformate de S-méthyle[11] $CH_3SC(O)H$ dans le nuage interstellaire Orion et une liste de raies a été établie pour chercher le sulfure de diméthyle[12] CH_3SCH_3. Le succès de la spectroscopie rotationnelle est dû au fait que le signal micro-onde provenant des sources dans l'espace peut traverser l'atmosphère terrestre sans être absorbé. Avec le développement de la prochaine génération de radiotélescopes, la détection de nouvelles molécules dans l'espace est très prometteuse. Néanmoins, de telles détections reposent sur des études intensives préalablement effectuées au laboratoire et sur la compréhension précise des spectres de ces molécules.

Le cas le plus simple à traiter du point de vue de l'analyse des spectres rotationnels est celui du spectre d'une molécule rigide. Avec les molécules non rigides, le spectre est plus compliqué comme expliqué ci-après. La non-rigidité peut provenir des forces de distorsion centrifuge qui vont légèrement modifier les niveaux d'énergie et donc déplacer les raies dans le spectre observé. Le spectre devient également plus compliqué lorsque la molécule est constituée d'un ou plusieurs groupes d'atomes qui peuvent tourner par rapport au reste de la molécule (mouvements de rotations internes d'un (ou de plusieurs) groupe(s) méthyle $-CH_3$ ou mouvements d'inversion comme dans l'ammoniac par exemple). Enfin le spectre peut se compliquer lorsque la molécule contient des noyaux de spin nucléaire $I \geq 1$, entraînant un dédoublement des raies dans le spectre observé en raison du couplage hyperfin des noyaux, par exemple pour ^{14}N, ^{33}S, ^{35}Cl, ^{37}Cl, etc.

1. Rotation interne

Au cours de ma thèse, je me suis intéressée à des molécules aromatiques contenant un ou deux groupes de rotation interne $-CH_3$ (appelés aussi « toupie(s) ou tops ») par rapport au reste de la molécule formant le « squelette » ou « frame » en anglais. Si une molécule comporte un seul rotateur interne, chaque transition rotationnelle sera divisée en deux composantes appelées A ($\sigma = 0$) et E ($\sigma = \pm 1$) où σ est un indice de symétrie. Le spectre de rotation d'une molécule avec deux rotateurs internes est encore plus compliqué.

La Fig. 1 illustre le dédoublement des niveaux d'énergie en présence d'un ou deux rotateur(s) interne(s). A gauche de cette Fig. 1, en absence de rotation interne, on trouve un niveau d'énergie (et donc une

seule transition rotationnelle est observée dans les spectres). Lorsqu'il y a un rotateur interne, chaque niveau d'énergie et donc chaque transition rotationnelle est dédoublée en deux composantes étiquetées en utilisant l'indice de symétrie σ (0) et (1) et elles sont situées à $-2\Delta_1$ et $+\Delta_1$, respectivement (avec $\Delta_1 > 0$). Si on tient compte de la rotation interne d'une seconde toupie Top 2, chacune de ces composantes est à nouveau divisée en deux autres niveaux, qui sont décalés vers des positions à $-2\Delta_2$ et $+\Delta_2$, respectivement (avec $\Delta_2 > 0$). Au total, cela produira quatre niveaux d'énergie notés (00), (01), (10), (11). Enfin, s'il y a une interaction entre les deux toupies, le niveau d'énergie (11) se divisera en deux composantes appelées (11) et (12).

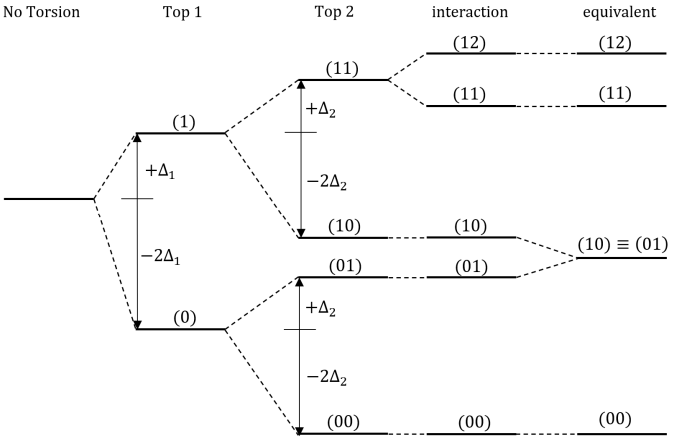

FIG. 1. Diagramme d'énergie pour le niveau $J = K = 0$ pour les molécules avec (de gauche à droite) absence de torsion, avec une toupie (dédoublement Δ_1), et deux toupies (dédoublement Δ_2) pour deux toupies inéquivalentes et deux toupies équivalentes. Le diagramme illustre la situation avec $\Delta_1 > \Delta_2 > 0$. Chaque niveau d'énergie est étiqueté en utilisant la notation semi-directe (σ_1,σ_2). Ce diagramme est similaire à celui de la Fig.2 présentée par *Ohashi et al.*[13]

Pour deux toupies inéquivalentes, on obtient cinq niveaux d'énergie présentés sous la colonne (interaction). Si les deux toupies sont équivalentes, cela signifie que les niveaux (10) et (01) coïncident en raison de la symétrie.

La rotation interne d'un groupe d'atomes (le groupe méthyle CH_3) par rapport au reste de la molécule est un phénomène de non-rigidité moléculaire, appelé également mouvement de grande amplitude, qui est difficile à modéliser en spectroscopie. En effet, l'effet tunnel résultant d'une barrière de potentiel

finie se traduit par des dédoublements des niveaux d'énergie et des raies des molécules, ce qui complique les spectres. Le(s) mouvement(s) de grande amplitude d'un ou deux rotateurs internes sont entravés par une barrière de potentiel, et ne peuvent pas être traités par les modèles théoriques "traditionnels" applicables aux mouvements de faible amplitude autour de la position d'équilibre des noyaux. L'étude de ce type de molécules nécessite donc l'utilisation de modèles théoriques spécifiques et de programmes informatiques appropriés[14]. L'amplitude des dédoublements de la rotation interne est proportionnelle à la hauteur de barrière "réduite", $s = 4V_3/9F$, où V_3 est la hauteur de la barrière de potentiel d'ordre trois et F est la constante cinétique de rotation interne. Cette constante F est l'inverse du moment d'inertie du groupe méthyle, mais elle dépend également de la direction du groupe méthyle dans la molécule, et est donc liée à la géométrie de la molécule. Plus la barrière réduite est élevée (basse), plus les dédoublements des niveaux d'énergie sont petits (grands).

2. Couplage quadripolaire nucléaire

L'effet du couplage quadripolaire nucléaire provient de l'interaction entre une distribution non sphérique de la charge du noyau (ce qui entraîne un moment quadripolaire électrique nucléaire) et une distribution non sphérique de la charge électronique autour du noyau (ce qui entraîne un gradient de champ électrique au niveau du noyau). Tout noyau avec un spin I > 1/2 génère une distribution non sphérique de sa charge nucléaire, et possède un moment quadripolaire nucléaire non nul. L'effet quadripolaire nucléaire entraîne également des dédoublements des niveaux d'énergie et des transitions dans le spectre.

La Fig. 2 montre l'effet d'une distribution non sphérique de la charge électronique autour du noyau ^{14}N avec des projections différentes du moment angulaire **I** suivant l'axe fixe ($M_I = -I, -I+1, \ldots, I$) sur deux niveaux d'énergie d'une toupie asymétrique pour le nombre quantique de rotation $J = 0$ et 1. Chaque niveau d'énergie de rotation est divisé en différentes composantes hyperfines. En raison de cet effet, plusieurs composantes hyperfines seront observées au lieu d'une seule transition rotationnelle avec les règles de sélection[13] $\Delta F = 0, \pm 1$.

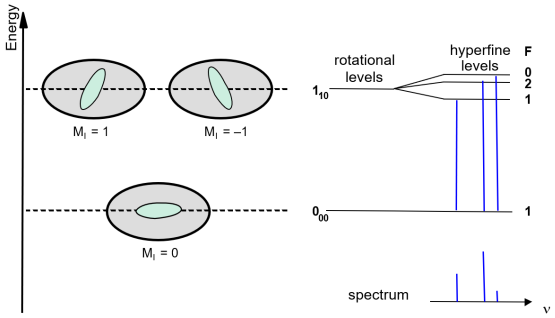

FIG.2. Côté gauche : Description schématique de la distribution non sphérique de la charge électronique autour du noyau ^{14}N correspondant à différentes projections de **I** (M_I). Côté droit : Différentes composantes hyperfines correspondant à différentes valeurs du nombre quantique total F pour deux niveaux de rotation $J_{KaKc} = 0_{00}$ et 1_{10}. Chaque niveau de rotation peut être divisé en plusieurs niveaux hyperfins, donnant lieu à plusieurs raies dans le spectre obtenu. Notons que la figure est présentée comme une illustration uniquement qualitative du phénomène.

3. Travaux antérieurs

La complexité des molécules étudiées par spectroscopie micro-onde à transformée de Fourier à jet moléculaire (MJ-FTMW) n'a cessé d'augmenter aux cours des dernières décennies, fournissant un nombre important de spectres à haute résolution pour tester les modèles théoriques. Si la molécule peut être décrite par un rotateur semi-rigide, un ajustement (ou « fit ») de haute qualité entre les spectres calculés et observés peut être obtenu en utilisant l'Hamiltonien du rotateur rigide H_r complété par des termes de distorsion centrifuge H_{cd}, prenant en compte des transitions avec des valeurs des nombres quantiques de rotation J et K encore plus élevées.

Cependant lorsqu'une molécule contient un groupe méthyle qui subit une rotation interne, entravée par une barrière de potentiel d'ordre trois suffisamment faible, son spectre micro-onde comporte des dédoublements de toutes les raies rotationnelles en composantes de torsion notées A et E. Dans ce cas, le spectre rotationnel ne peut plus être traité en utilisant un modèle de rotateur semi-rigide. Plusieurs modèles et programmes théoriques ont été développés dans la littérature pour traiter l'effet de la rotation interne. Parmi les codes existants on trouve le code écrit par Woods[15] basé sur la méthode appelée initialement Méthode de l'Axe Interne (*IAM*) et que nous appelons aujourd'hui la Méthode de l'Axe Rho (*RAM*), ainsi que les codes *XIAM*[16], *BELGI* dans ses versions C_s et C_1[17,18], *Erham*[19], et *RAM36*[20]

(voir aussi le site web géré par le Prof. Kisiel[1]) où des termes supplémentaires pour tenir compte de la rotation interne et du couplage avec la rotation globale de la molécule H_{ir} sont ajoutés dans l'Hamiltonien. Certaines molécules associées à une hauteur de barrière faible ou intermédiaire peuvent également être traitées par le programme *JB95* fourni par Plusquellic[21] ainsi que par le programme *IAMCALC* qui est intégré dans la suite des programmes de Pickett appelés les codes *SPFIT* et *SPCAT*[22].

Un noyau de spin nucléaire $I \geq 1$ implique un moment quadripolaire nucléaire électrique. Des structures hyperfines apparaissent dans le spectre micro-onde, c'est-à-dire que les niveaux de rotation avec $J > 0$ du rotateur rigide se divisent en plusieurs composantes hyperfines. La taille des dédoublements dépend de la transition respective. Dans le cas du noyau ^{14}N, le moment quadripolaire est relativement faible et peut souvent être traité en utilisant une approximation perturbative de premier ordre.

La combinaison d'un seul noyau de couplage quadripolaire ^{14}N et d'un groupe méthyle de rotation interne peut être traitée avec le programme *RAM36*, qui implique que la symétrie moléculaire du « squelette » ou « frame » soit C_s[23]. Avec le programme *XIAM*, la symétrie n'est pas limitée à C_s. Cependant, *XIAM* rencontre souvent des difficultés dans le traitement des rotations internes avec de faibles hauteurs de barrière, car (i) seul un nombre limité de paramètres d'ordre élevé peut être ajusté et (ii) les interactions de torsion entre les différents états v_t ne sont pas prises en compte de façon explicite. Le programme *BELGI*, dans ses versions hyperfines étendues au cas du « squelette » possédant un plan de symétrie (*BELGI-C_s-hyperfine*) et au cas où le « squelette » moléculaire n'en possède pas (*BELGI-C_1-hyperfine*) peut traiter les molécules avec un rotateur interne et un noyau de faible couplage comme ^{14}N.

La barrière de rotation interne des dérivés mono-méthylés pour des hétérocycles aromatiques à cinq chaînons contenant un azote couvre une large gamme allant des barrières faibles comme celle du 2-méthylthiazole (34.9 cm^{-1})[24] et du 4-méthylisothiazole (105.8 cm^{-1})[25] aux barrières intermédiaires comme celles du 4- et du 5-méthylthiazole (357.6 et 332.0 cm^{-1}, respectivement)[26,27], ainsi que dans les 2-, 4-, et 5-méthyloxazole (252.0, 428.0, et 477.9 cm^{-1}, respectivement)[28]. Bien qu'un certain nombre

[1] PROSPE - Programs for ROtational SPEctroscopy, http://info.ifpan.edu.pl/~kisiel/prospe.htm

d'études soient disponibles, aucune règle efficace et phénoménologique pour la prédiction de la barrière de torsion du groupe méthyle n'a pu être déduite. En d'autres termes, la manière dont les effets stériques et l'environnement électronique affectent la barrière de rotation interne du groupe méthyle dans les hétérocycles à cinq chaînons reste une question quantitative déroutante.

En présence de deux rotateurs internes méthyle, la structure fine est constituée de quartets (pour deux toupies équivalentes) ou de quintuplets (pour deux toupies non équivalentes). La modélisation du spectre avec une précision suffisante nécessite souvent d'inclure des Hamiltoniens effectifs dans le modèle. En raison des difficultés liées à l'attribution et l'ajustement des spectres, seul un nombre très restreint de molécules à deux rotateurs ont été étudiées, comme l'ont examiné Nguyen et Kleiner[29]. Pour les cas de deux groupes méthyles équivalents, le nombre d'études publiées dans la littérature est encore plus faible. Les exemples typiques sont l'acétone[30] et l'éther diméthylique[31], suivis de la diéthylcétone[32], du sulfure de diméthyle[12], du 2,5-diméthylthiophène[33], du 2,5-diméthylfurane[34], et du 2,6-diméthylfluorobenzène[35]. À notre connaissance, seuls deux hétérocycles aromatiques à cinq chaînons substitués par deux groupements méthyles, 2,5-diméthylthiophène[33] et 2,5-diméthylfurane[34], ont été étudiés par spectroscopie micro-onde jusqu'à présent.

Nous avons donc décidé d'étudier les spectres micro-ondes des cycles aromatiques azotés à cinq chaînons afin de comprendre ce qui influence la barrière à la rotation interne, apportant ainsi une partie d'information importante à la littérature.

Les progrès expérimentaux et théoriques de la spectroscopie micro-onde au cours des deux dernières décennies ont permis une résolution et une précision suffisantes pour permettre des études de spectroscopie ayant un impact important sur diverses applications chimiques ou biochimiques telles que la caractérisation rotationnelle des sucres, les tautomères de haute énergie[36-38], l'étude de molécules comportant jusqu'à quatre mouvements de grande amplitude[39], ainsi que l'analyse de la structure hyperfine avec maintenant jusqu'à quatre noyaux quadripolaires ^{14}N[37,38]. Avant ma thèse, à ma connaissance aucun programme ne pouvait traiter de manière globale les composés contenant un groupe méthyle et deux noyaux ^{14}N. Cependant, cette classe de molécules a gagné un intérêt considérable comme le montre un certain nombre d'études spectroscopiques expérimentales sur la 2-

méthylpyrimidine[40], la 5-méthylpyrimidine[41], et très récemment les quatre isomères du méthylimidazole[42]. Durant ma thèse, j'ai écrit un nouveau code (*TW21*) et participé à l'adaptation d'une version du code *BELGI* afin d'analyser les spectres micro-ondes de ces molécules avec les premières applications sur la 4-méthylpyrimidine. Les détails des objectifs de recherche et les résultats obtenus au cours de ma thèse sont résumés ci-après.

II. OBJECTIFS DE RECHERCHE

1. Molécules ciblées

Au cours de ma thèse, les objectifs de mes travaux ont consisté à étudier les structures moléculaires et la dynamique interne de quelques cycles aromatiques à cinq et six chaînons, substitués par des groupes méthyles. Je me suis intéressée à des molécules dérivées du thiazole, du pyrrole, et de la pyrimidine, avec un accent sur les effets de la rotation interne et du couplage quadripolaire. Au total, j'ai étudié cinq molécules appartenant au groupe de symétrie C_s ainsi qu'une molécule de symétrie C_{2v}, qui sont représentées dans la Fig. 3.

Ces six molécules peuvent être réparties en trois classes (Fig. 3), selon l'augmentation progressive du degré de complexité :

Class I : Cycles aromatiques contenant un groupe méthyle CH_3 + un atome d'azote ^{14}N (**1**-**3**).

Class II : Cycles aromatiques contenant des rotations internes de deux groupes méthyles CH_3 + un atome d'azote ^{14}N (**4**, **5**).

Class III : Cycles aromatiques contenant une rotation interne d'un groupe méthyle CH_3 + deux atomes d'azote ^{14}N (**6**).

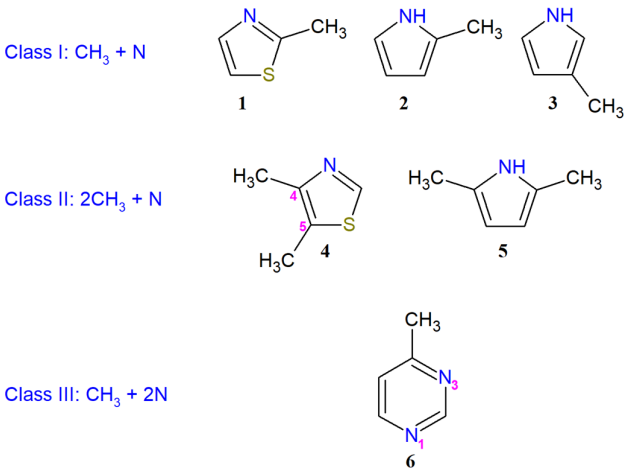

FIG. 3. Molécules étudiées dans cette thèse : (**1**) 2-méthylthiazole, (**2**) 2-méthylpyrrole, (**3**) 3-méthylpyrrole, (**4**) 4,5-diméthylthiazole, (**5**) 2,5-diméthylthiazole, (**6**) 4-méthylpyrimidine.

2. Importance de l'étude

Mes travaux ont pour but de :

- Fournir des paramètres géométriques (à savoir les constantes rotationnelles, les constantes de distorsion centrifuge, les constantes hyperfines nucléaires) et dynamiques (barrière de rotation interne V_3) précis pour l'état fondamental, qui peuvent servir de références pour des calculs *ab initio* ou de chimie quantique, ou qui peuvent être utilisés comme constantes de l'état de base dans d'autres études de spectroscopie, par exemple des études dans d'autres domaines spectraux.

- Fournir une première liste de positions de raies dans l'état fondamental de torsion et pour de faibles valeurs du nombre quantique de rotation J, qui pourra servir de base pour des recherches astronomiques sur ces molécules.

- Apporter une compréhension fondamentale importante sur les mouvements de grande amplitude de la (des) rotation(s) interne(s) et sur le couplage quadripolaire nucléaire dans les cycles aromatiques, en particulier dans la famille des cycles à cinq chaînons.

- Fournir des codes adéquats pour de futures études sur le même type de molécules.

III. MATÉRIELS ET MÉTHODOLOGIES

L'ensemble des méthodes expérimentales et théoriques utilisées pendant ma thèse est décrit en détail dans la Partie I de ma thèse.

1. Dispositifs expérimentaux

La spectroscopie micro-onde à transformée de Fourier à jet moléculaire (*Molecular Jet - Fourier Transform MicroWave*, MJ-FTMW) a été utilisée pour mesurer les spectres micro-ondes de toutes les molécules étudiées dans ma thèse. Tous les détails de ces dispositifs peuvent être trouvés dans les Refs.[1-3]. Dans toutes les études, un mélange de gaz contenant 1% de substance dans de l'hélium à une pression totale d'environ 100 hPa a été utilisé. Afin d'observer des transitions avec des valeurs de *J* plus élevées, l'hélium a été choisi comme gaz vecteur car le refroidissement n'est pas aussi efficace avec l'argon ou le néon. Tous les spectres ont été enregistrés dans la gamme de fréquences 2-40 GHz en utilisant deux spectromètres MJ-FTMW, montrés dans la Fig. 4.

L'un de ces spectromètres fonctionnant dans la gamme spectrale de 2 à 26.5 GHz se trouve dans le groupe du Prof. W. Stahl à l'Université RWTH de Aachen (Allemagne) tandis que l'autre, fonctionnant entre 26.6 et 40 GHz se trouve au Laboratoire LISA à Créteil.

FIG. 4. Spectromètres MJ-FTMW utilisés dans ce travail, situés à Aachen (2-26.5 GHz) et à Créteil (26.5-40.0 GHz)[1-3].

2. Codes pour l'analyse des spectres micro-ondes

Pour l'analyse des spectres micro-ondes, j'ai utilisé durant ma thèse plusieurs codes, basés sur des développements théoriques appropriés traitant la rotation interne et les effets hyperfins quadripolaires électriques. En particulier, j'ai utilisé les codes *XIAM*[16], *BELGI* dans ses versions C_s (pour les molécules contenant un plan de symétrie)[17] et C_1 (pour les molécules sans plan de symétrie)[18] et le code *WS18*. Ce code *WS18*, écrit par le Prof. W. Stahl de l'Université de Aachen, permet d'ajuster séparément les transitions rotationnelles pour chaque état de symétrie A et E et nous a permis ainsi de commencer le processus d'attribution pour certaines des molécules étudiées.

Dans le code *XIAM*, les énergies de torsion de chaque toupie sont évaluées dans leur système d'axe rho (RAM) individuel, puis sont transformées dans le système d'axe principal (PAM). Dans le système RAM, les valeurs propres sont calculées de façon appropriée dans la base du produit des fonctions des toupies symétriques pour la rotation globale et des fonctions du rotateur interne pour la torsion. Le programme *XIAM* permet de « fitter » ou d'ajuster les énergies de transitions moléculaires calculées et observées pour les spectres de rotation des molécules comportant jusqu'à trois rotateurs internes et d'inclure un noyau quadripolaire hyperfin. Il s'agit d'un code très facile à utiliser et très efficace pour l'attribution globale des molécules de différentes symétries. Cependant, la version originale de *XIAM* ne nous permettait de prendre en compte que l'état fondamental de torsion et n'incluait pas les termes d'ordre supérieur de l'Hamiltonien. Ceci explique pourquoi dans certains cas, pour des barrières de torsion plus basses, *XIAM* ne nous a pas permis d'atteindre la précision expérimentale.

Les codes *BELGI-C_s-hyperfine* et *BELGI-2Tops-C_{2v}* surmontent ces inconvénients en incluant de nombreux termes d'ordre supérieur. Ces codes prennent également en compte les termes d'interaction rotation-torsion entre les neuf premiers états de torsion d'un état vibrationnel donné, ce qui nous a donc permis de calculer correctement les énergies des états de torsion les plus bas. C'est pourquoi la méthode utilisée dans le code *BELGI* est souvent appelée "méthode globale" tandis que celle utilisés dans le code *XIAM* est appelé "méthode locale". Au cours de ma thèse, le code *BELGI-2Tops-C_{2v}* a été étendu pour prendre en compte l'effet du couplage quadripolaire en présence de deux rotateurs internes équivalents (le code *BELGI-2Tops-C_{2v}-hyperfine*). La version *BELGI-2N* a également été développée durant ma thèse pour traiter de manière globale les cas de molécules avec deux atomes d'azote ^{14}N et un rotateur interne. Finalement, au cours de ma thèse, j'ai participé au développement d'un nouveau code : le code

TW21, qui permet de traiter également la combinaison d'un rotateur CH_3 et de deux faibles couplages quadripolaires nucléaires de ^{14}N, comme décrit dans les résultats.

3. Méthodologie de recherche

La stratégie générale adoptée pour mes recherches en spectroscopie micro-onde est donnée dans la Fig. 5.

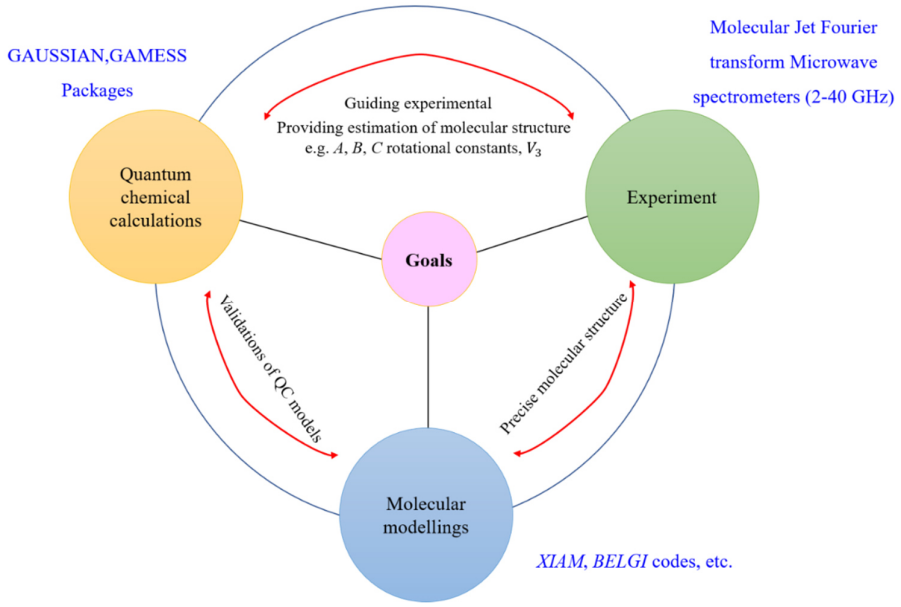

FIG. 5. Méthodologie de recherche.

Dans un premier temps, les estimations des structures des molécules sont effectuées par des calculs de chimie quantique à l'aide des progiciels GAUSSIAN[43-45] ou GAMESS[46]. Les résultats calculés, par exemple les constantes de rotation, les angles entre l'axe *a* et l'axe interne *i*, la barrière à la rotation interne V_3, ainsi que les constantes hyperfines quadripolaires, sont utilisés pour prédire un premier spectre des molécules et pour donner une indication de l'endroit où les chercheurs devraient regarder dans les spectres micro-ondes.

La deuxième étape consiste à enregistrer et mesurer les données expérimentales à l'aide des spectromètres décrits ci-dessus. La technique utilisée est la spectroscopie micro-onde à transformée de Fourier à jet moléculaire (MJ-FTMW) qui fonctionne à très basse température (≈ 2 K) et permet d'atteindre une très haute résolution de 2-5 kHz.

La troisième étape consiste à analyser les données expérimentales à l'aide du modèle Hamiltonien approprié qui vise à reproduire le spectre dans les limites de la résolution expérimentale. Cela nous permet de déterminer précisément la structure de la molécule, la (les) barrière(s) de torsion, et les constantes de couplage quadripolaire nucléaire. La comparaison entre les paramètres moléculaires dérivés expérimentalement et ceux issus des modèles de chimie quantique nous permet finalement de valider la théorie.

IV. RÉSULTATS

1. Class I : Cycles aromatiques azotés avec un rotateur et un noyau ^{14}N

Dans la partie II de cette thèse, je présente les recherches effectuées sur le 2-méthylthiazole (Chapitre II.1), le 2-méthylpyrrole (Chapitre II.2) et le 3-méthylpyrrole (Chapitre II.3) en combinant la spectroscopie micro-onde, les calculs de chimie quantique et l'analyse spectrale. Dans tous les cas, les données expérimentales ont été enregistrées à l'aide des spectromètres micro-ondes à transformée de Fourier à jet moléculaire dans la gamme de fréquences 2 – 26.5 GHz et/ou 26.5 – 40 GHz. La structure fine de la torsion du méthyle et les dédoublements provenant des effets de couplage hyperfin nucléaire ont pu être entièrement résolus. J'ai réussi à analyser et à ajuster toutes les transitions observées à l'aide des programmes *XIAM* et *BELGI-C_s-hyperfine* dans les limites de la précision de mesure. Le travail de spectroscopie a été complété par des calculs de chimie quantique. Le plus souvent, les valeurs sont calculées à différents niveaux de théorie tels que MP2, B3LYP en combinaison avec des ensembles de bases différents, par exemple cc-pVDZ, aug-cc-pVDZ, cc-pVTZ, etc. Les valeurs des constantes rotationnelles expérimentales diffèrent d'environ 1% par rapport aux constantes calculées, ce qui constitue un excellent accord pour ce type de molécules. La méthode de calcul des Constantes de Couplage Quadripolaire Nucléaire (Nuclear Quadrupole Coupling Constant or NQCC) introduite par Bailey[47] a donné des résultats satisfaisants, les déviations maximales observées étant de l'ordre de 8%. Les résultats obtenus au cours de ma thèse sur les molécules de 2-méthylthiazole, (2MTA) 2-méthylpyrrole (2MP) et 3-méthylpyrrole (3MP) ont été comparés à ceux d'autres cycles aromatiques à cinq chaînons étudiés dans les travaux antérieurs afin d'acquérir de nouvelles connaissances sur (i) les

effets qui peuvent affecter l'amplitude de la barrière de torsion du méthyle, et (ii) la manière dont le couplage quadripolaire nucléaire peut refléter la situation de la liaison sur le site de l'atome ^{14}N dans les molécules. Dans la Fig. 6, nous présentons toutes les molécules pour lesquelles la comparaison est effectuée.

Concernant la barrière de torsion du méthyle, la valeur du potentiel V_3 varie significativement suivant la position du groupe méthyle sur le cycle, ou si l'hétéroatome change. Pour les thiazoles, imidazoles et oxazoles mono-méthylés, la valeur la plus faible de V_3 est toujours obtenue pour les isomères où le groupé méthyle est en position 2-, tandis que les barrières les plus élevées correspondent aux isomères en position 5-. Le rôle crucial de la symétrie est également prouvé par la barrière intermédiaire de 123 cm^{-1} observée pour le 2-méthylimidazole (**10**). Si l'atome d'hydrogène n'était plus substitué à l'atome N(1) dans le 2-méthylimidazole, la symétrie locale du groupe CH_3 serait un C_{2v} parfait et un terme principal de potentiel d'ordre six V_6 serait obtenu. La déviation causée par le petit atome d'hydrogène rattaché à l'atome d'azote N(1) brise la parfaite symétrie C_{2v} et la distribution des électrons, ce qui entraîne un changement significatif de la hauteur de la barrière.

Enfin, la barrière de torsion du méthyle de 252 cm^{-1} obtenue pour le 2-méthyloxazole (**14**) est plus élevée que celle du 2-méthylimidazole (**10**). La tendance selon laquelle la barrière à la rotation interne augmente des méthylthiazoles aux méthylimidazoles en passant par les méthyloxazoles est généralement observée non seulement pour les isomères 2-, mais également pour les isomères 4- et 5-. De toute évidence, la distribution électronique d'un atome d'azote est plus proche de celle d'un atome de soufre que celle d'un groupe NH, et l'écart avec celle d'un atome d'oxygène est encore plus grand. Pour les isomères 2-, le 2MP (**7**) peut également être considéré dans la comparaison, qui possède la barrière la plus élevée, indiquant la plus grande différence dans les distributions électroniques entre un atome d'azote et un atome de carbone.

En conclusion, la barrière à la rotation interne d'un groupe méthyle dépend fortement de la présence d'hétéroatomes dans le cycle, puisque les effets électroniques se propagent facilement dans les cycles aromatiques par la conjugaison des électrons π. En ce sens, la barrière d'un groupe méthyle peut être

considérée comme une mesure directe de la distribution électronique au sein du cycle attaché. Cependant, ces interprétations ne sont qu'intuitives et nécessitent des preuves à partir de plus de données de mesure ainsi que des calculs théoriques.

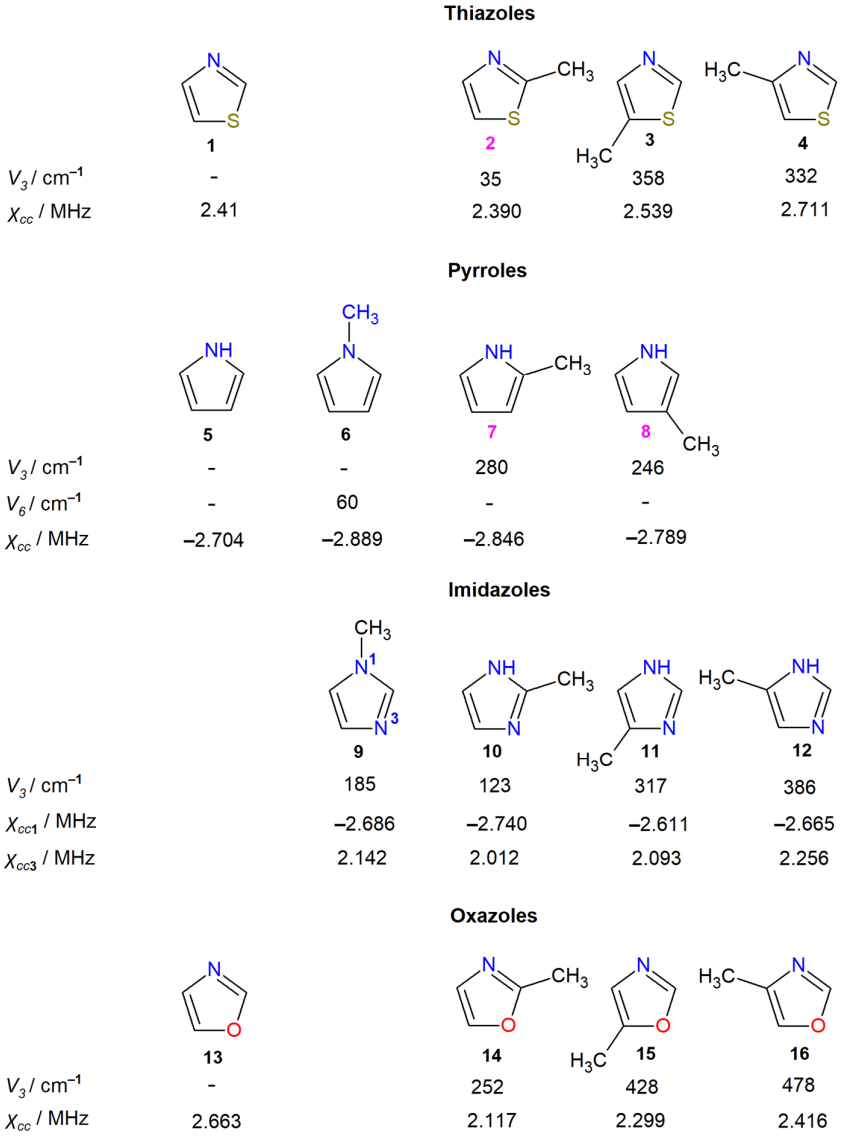

FIG. 6. Le potentiel de torsion du méthyle V_3 et les NQCC (Nuclear Quadrupole Couplig Constant) χ_{cc} du 2MTA, 2MP, et 3MP étudiés dans ma thèse en comparaison avec le thiazole, le pyrrole, l'imidazole, l'oxazole ainsi que leurs dérivés mono-méthylés. (**1**) thiazole[48], (**2**) 2-méthylthiazole, (**3**) 5-méthylthiazole[27], (**4**) 4-méthylthiazole[26], (**5**) pyrrole[49], (**6**) N-méthylpyrrole[50], (**7**) 2-méthylpyrrole, (**8**) 3-méthylpyrrole, (**9**) N-méthylimidazole[42], (**10**) 2-méthylimidazole[42], (**11**) 4-méthylimidazole[42], (**12**) 5-méthylimidazole[42], (**13**) oxazole, (**14**) 2-méthyloxazole[28],

(**15**) 5-méthyloxazole[28], (**16**) 4-méthyloxazole[28]. Les numéros sont indiqués en rose les molécules examinées dans cette thèse, tandis que les autres (dans la littérature) sont indiqués en noir.

En raison de la structure plane de toutes les molécules représentées sur la Fig. 6, l'axe principal d'inertie *c* est colinéaire avec un axe principal du tenseur de couplage de l'azote, permettant ainsi une comparaison directe des valeurs de la constante de couplage quadripolaire, χ_{cc} entre ces molécules. Les valeurs de χ_{cc} peuvent être classées en deux groupes, l'un avec des valeurs positives et l'autre avec des valeurs négatives.

Dans le thiazole, l'oxazole et leurs dérivés méthylés ((**1-4**) et (**13-16**)) ainsi que les χ_{cc} de N(1), les signes de χ_{cc} sont positifs alors que dans le pyrrole, y compris son dérivé mono-méthylé et les χ_{cc} de N(3), les signes de χ_{cc} sont négatifs. La raison sous-jacente est une situation de liaison très différente au niveau de l'atome d'azote qui entraîne un gradient de champ électrique différent au niveau du noyau d'azote. La configuration électronique de l'azote est $[He]2s^22p^3$. Dans tous les composés de la Fig. 6, trois orbitales hybrides sp^2 sont formées, dont deux sont utilisées pour former les liaisons σ avec les atomes voisins. Une orbitale p est restante et fait partie du système d'électrons π. Comme le montre la Fig. 7, dans le cas du pyrrole, trois des cinq électrons de l'azote sont nécessaires dans les trois orbitales sp^2 pour former les deux liaisons N-C et une liaison N-H (non illustrée). Les deux électrons restants sont contenus dans l'orbitale p (illustrée) et contribuent au système d'électrons π. En tout, il y a 6 électrons π, ce qui, selon la règle 4n + 2, fait du pyrrole un composé aromatique.

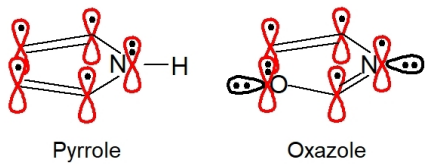

FIG. 7. Le système d'électrons π dans le pyrrole et l'oxazole.

Dans les autres hétérocycles, la situation est tout à fait différente. Pour l'oxazole, deux orbitales sp^2 de l'atome d'azote avec un électron chacune forment les liaisons avec les atomes voisins (non illustré). La troisième orbitale sp^2 contient une paire d'électrons (illustré). Il ne reste qu'un seul électron pour l'orbitale p contribuant au système d'électrons π. Il convient de noter que dans ce groupe de molécules, il faut donc qu'un atome de soufre ou d'oxygène fournisse deux électrons pour leur orbitale p afin de

remplir la condition d'un composé aromatique (6 électrons dans le système π). Des considérations similaires sont possibles pour le thiazole et l'isothiazole.

Malgré l'effet +I bien connu des groupes méthyles, seule une petite modification du tenseur de gradient de champ est observée. Dans le cas du pyrrole, des Pyrroles (**5**-**8**) et des Imidazoles (**9**-**12**), l'effet de la méthylation sur χ_{cc} est faible, par exemple les valeurs de χ_{cc} du pyrrole (**5**), du N-méthylpyrrole (**6**), du 2MP (**7**), et du 3MP (**8**) sont respectivement de –2.704, –2.889, –2.846, –2.789 MHz. Les plus grandes déviations sur χ_{cc} sont obtenues pour les Thiazoles (1-4) et (13-16).

2. Class II : Cycles aromatiques azotés avec deux rotateurs et un noyau ^{14}N

Dans le Partie III, deux molécules ont été étudiées, à savoir le 2,5-diméthylpyrrole (25DMP) (Chapitre III.1) et le 4,5-diméthylpyrrole (45DMTA) (Chapitre III.2). Les deux molécules possèdent un plan de symétrie, le 25DMP contient deux groupes méthyles équivalents alors que le 45DMTA possède deux groupes méthyles non équivalents. Les spectres de rotation des deux molécules ont été enregistrés à l'aide du spectromètre fonctionnant dans la gamme de fréquences 2-26.5 GHz. Les dédoublements fins provenant du couplage des deux rotateurs internes ainsi que la structure hyperfine ont été entièrement résolus et attribués.

Nous avons modifié les codes *BELGI*[12,52] pour modéliser les spectres de ces deux molécules, en prenant correctement en compte les effets des rotations internes des deux groupes méthyles en combinaison d'un faible couplage hyperfin de ^{14}N. Les attributions de chacune des molécules ont été effectuées en utilisant l'approche locale du code *WS18* et les ajustements globaux ont été réalisés en utilisant les codes *XIAM* et *BELGI-2Tops-C_s-hyperfine* ou *BELGI-2Tops-C_{2v}-hyperfine*.

Pour le 25DMP, les deux groupes méthyles équivalents provoquent le dédoublement de chaque transition rotationnelle en quatre composantes de torsion, qui est combinée avec les dédoublements hyperfins quadrupolaires provenant du noyau ^{14}N qui se produisent avec le même ordre de grandeur. Il en résulte une signature spectrale très compliquée. J'ai d'abord effectué l'attribution spectrale séparément pour chacune des composantes de symétrie. Deux ajustements automatiques des paramètres (« fits ») globaux ont ensuite été effectués en utilisant le code *XIAM* et le code *BELGI-C_{2v}-2Tops-hyperfine*, une version modifiée du code *BELGI-C_{2v}-2Tops*, sur 274 transitions donnant des écarts

quadratiques moyens satisfaisants (proches de la précision de mesure, soit 4.8 kHz et 3.4 kHz pour les codes *XIAM* et *BELGI-C_{2v}-2Tops-hyperfine* respectivement). Les barrières de potentiel de rotation interne des deux groupes méthyles ont été déterminées comme étant V_3 = 317.208(16) cm^{-1}. Les paramètres moléculaires ont été obtenus avec une grande précision, fournissant toutes les informations nécessaires sur l'état fondamental pour de futures recherches dans des gammes de fréquences plus élevées ou pouvant servir de base pour étudier les états excités de vibration-torsion. Un seul conformère stable a été observé dans le spectre micro-onde, comme confirmé par les calculs de chimie quantique, effectués pour guider les attributions initiales et compléter l'analyse expérimentale. En analysant les constantes de couplage quadripolaire nucléaire du 2-méthylpyrrole (Chapitre II.2) et du 25DMP (Chapitre III.1), nous avons pu conclure que le second groupe méthyle, adjacent à l'atome d'azote dans le 25DMP, augmente les valeurs des NQCC, en particulier χ_{zz}, de l'atome d'azote.

Pour le 45DMTA, la rotation interne des deux groupes méthyles non équivalents donne lieu à cinq composantes de torsion, révélant des barrières relativement faibles entravant la rotation interne. Les structures hyperfines de l'azote étaient bien résolues. Au total, nous avons analysé 1009 composantes hyperfines de 315 transitions rotationnelles. L'ensemble des données a été analysé avec le programme *XIAM* et notre code adapté *BELGI-C_s-hyperfine*. Le code *XIAM* a rencontré des difficultés pour la modélisation des spectres rotationnels du 45DMTA, donnant un *écart quadratique moyen* de 399.8 kHz, alors que le code *BELGI-C_s-hyperfine* a pu réduire l'*écart quadratique moyen* à 4.2 kHz, ce qui est proche de notre précision de mesure.

Contrairement au 25DMP qui ne montre aucun couplage entre les deux toupies, de forts couplages toupie-toupie faisant intéragir des termes d'énergie potentielle et cinétique de l'Hamiltonien ont été observés dans le cas du 45DMTA. Les barrières des rotations internes du 25DMP et du 45DMTA, ainsi que celles d'autres cycles à cinq chaînons, sont listées dans la Fig. 8 à des fins de comparaison.

Il existe deux principaux types d'effets qui influencent la barrière des rotations internes : l'effet stérique et l'effet électronique. Dans la partie gauche de la Fig. 8, nous avons constaté que la barrière est toujours plus grande dans les hétérocycles diméthylés dérivés du thiphène, du pyrrole et du furane que dans ceux monométhylés. Plus la barrière est faible, plus cet effet est prononcé. Ceci indique l'effet stérique

dominant sur les valeurs de V_3. Le contraire est obtenu pour le groupe des dérivés du thiazole, du côté droit de la Fig. 8. Alors que les cycles monométhylés (**7**, **8**) ont donné une grande valeur de V_3, les cycles diméthylés montrent des V_3 plus petits (**9**). Cela ne peut s'expliquer que par la distribution électronique équivalente des deux côtés du plan local auquel le groupe méthyle est attaché.

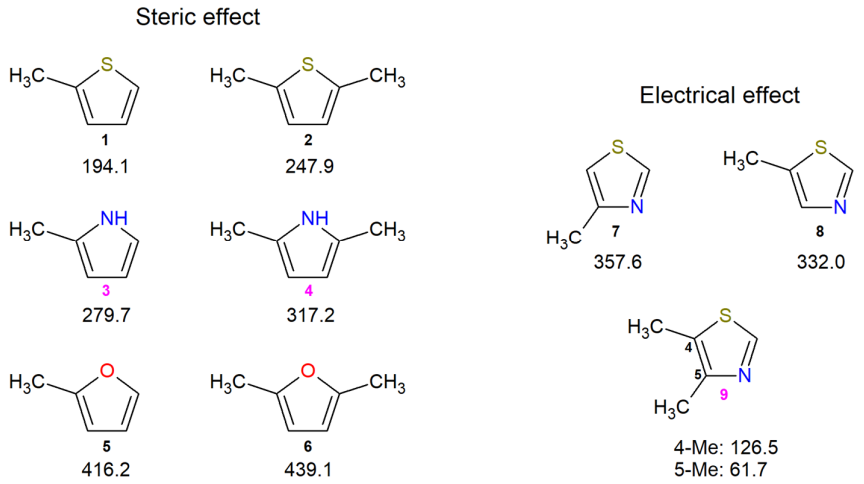

FIG. 8. Comparaison des barrières de rotation interne (en cm^{-1}) du (**1**) 2-méthylthiophène[53], (**2**) 2,5-diméthylthiophène[33], (**3**) 2-méthylpyrrole (Chapitre II.2, présente thèse), (**4**) 2,5-diméthylpyrrole (Chapitre III.1, présente thèse), (**5**) 2-méthylfurane[54], (**6**) 2,5-diméthylfurane[34], (**7**) 4-méthylthiazole[26], (**8**) 5-méthylthiazole[27] et (**9**) 4,5-diméthylthiazole (Chapitre III.2, présente thèse). Les numéros sont indiqués en rose les molécules examinées dans cette thèse, tandis que les autres (dans la littérature) sont indiqués en noir.

Dans la Partie III, des calculs ont été aussi effectués à différents niveaux de théorie en utilisant la chimie quantique. Les constantes de rotation déduites expérimentalement sont en accord de près de 2% avec celles qui ont été calculées, tandis que les barrières prédites ne sont pas aussi bien en accord avec les barrières expérimentales, ce qui montre les difficultés qui subsistent dans le calcul théorique de la valeur de V_3. Les mêmes constatations ont été effectuées lorsque les calculs de chimie quantique ont été menés avec des ensembles de base suffisamment grands.

3. Class III : Cycles aromatiques azotés avec un rotateur et deux noyaux ^{14}N

Dans la Partie IV sont décrits de nouvelles fonctionnalités qui ont été implémentées dans les programmes *WS18* et *BELGI-2N* et un nouveau code appelé *TW21* qui a été écrit pour permettre l'analyse des spectres complexes de la 4-méthylpyrimidine provenant de la combinaison d'un rotateur

CH_3 et de faibles couplages quadripolaires nucléaires issus de deux atomes de ^{14}N. Le spectre rotationnel de la 4-méthylpyrimidine dans des conditions de jet moléculaire a été enregistré et attribué avec succès en utilisant initialement des calculs complémentaires de chimie quantique. Dans le cadre de ce travail, des approches locales et globales ont été employées pour étudier les spectres. Les paramètres moléculaires obtenus avec une grande précision en utilisant les codes *WS18*, *TW21* ainsi que le code *BELGI-2N* fournissent des informations utiles pour une étude plus approfondie de la 4-méthylpyrimidine.

Les résultats sur les constantes de rotation *A*, *B*, *C* obtenus à partir des deux fits de *TW21* ainsi que *BELGI-2N* sont en très bon accord. Le calcul le plus long effectué au niveau de théorie MP2/6-311++G(d,p) donne les résultats les plus satisfaisants. Tous les autres calculs ont sous-estimé la valeur des constantes *A*, *B*, *C* et dans le cas du 4MPY, nous pouvons observer une tendance selon laquelle plus l'ensemble des bases est grand, plus les constantes rotationnelles prédites sont proches des valeurs expérimentales. En ce qui concerne les constantes de couplage quadripolaire nucléaire, toutes les valeurs calculées à différents niveaux de théorie ont donné des résultats en bon accord avec les valeurs expérimentales. Les résultats avec MP2/6-311++G(d,p) sont légèrement plus proches des valeurs expérimentales que les autres.

La valeur expérimentale déduite du potentiel V_3 à la rotation interne du méthyle est déterminée avec précision comme étant 94.390920(19) et 94.391728(99) cm^{-1} avec les codes *TW21* et *BELGI*, respectivement. Ces valeurs sont en excellent accord car les deux codes ont utilisé le même système de coordonnées, le même ensemble de données, et ont calculé le même ensemble de paramètres. Les valeurs de la barrière de potentiel calculées par les méthodes *ab initio* vont de 5 à 50 cm^{-1}, soit un facteur de 2 à 20 fois différent. Avec une barrière aussi faible, l'attribution spectrale était très difficile. Dans le cas du 4MPY, le résultat calculé au niveau de théorie MP2/cc-pVDZ est toujours le plus proche de la valeur expérimentale déduite.

Le nouveau code *TW21* nous a permis d'analyser en détail le spectre micro-onde de la 4-méthylpyrimidine. Nous avons conclu que pour l'ajustement des transitions rotationnelles correspondant à de faibles valeurs de *J* pour l'état fondamental de torsion $v_t = 0$, les interactions entre les différents

états de torsion supérieurs v_t jouent un rôle faible par rapport à celui de l'ajout des paramètres de rotation-torsion. Par conséquent, nous encourageons les utilisateurs à utiliser $v_{t_{max}} = 0$ pour les attributions dans les conditions de jet, car cette méthode est rapide et offre une précision suffisante dans les étapes des premières attributions. Ensuite, nous recommandons d'augmenter lentement $v_{t_{max}}$ à la fin du processus d'ajustement pour obtenir les meilleurs *écarts quadratiques moyens*.

V. CONCLUSIONS ET PERSPECTIVES

En combinant la spectroscopie micro-onde à transformée de Fourier à jet moléculaire, les calculs de chimie quantique et la modélisation moléculaire, au total six cycles aromatiques azotés ont été étudiés dans le cadre de ma thèse. Les molécules ciblées présentent une ou plusieurs rotations internes en présence d'un ou de deux couplages hyperfins faiblement quadripolaires de ^{14}N. Les paramètres de géométrie, par exemple les constantes rotationnelles, les constantes de distorsion centrifuge, les constantes de couplage quadripolaire, etc., ainsi que les paramètres de dynamique tels que la barrière à la (aux) rotation(s) interne(s) ont été déterminés avec une grande précision. Ces paramètres peuvent être utilisés comme données de référence pour les calculs de chimie quantique. Ils peuvent également servir de point de départ pour des recherches plus approfondies en phase gazeuse dans d'autres domaines spectraux (IR, THz), et sont d'une bonne utilité pour les recherches astrophysiques.

Des calculs de chimie quantique ont été effectués à différents niveaux de théorie. Les résultats montrent qu'avec un ensemble de base suffisamment large, les paramètres géométriques (les constantes rotationnelles *A*, *B*, *C*) peuvent être prédits avec une erreur inférieure à 2% et constituent un bon outil pour guider les attributions spectrales. Par ailleurs, nos travaux montrent également que la prédiction de la barrière à la rotation interne de V_3 reste un défi. Les barrières empêchant la(es) rotation(s) interne(s) calculées *ab initio* présentent des déviations par rapport aux valeurs expérimentales d'environ 10% sont généralement obtenues. Les surfaces d'énergie potentielle 2D sont un bon outil pour l'étude d'un possible couplage dans le cas où plusieurs rotations internes existent dans la (les) molécule(s). La méthode de Bailey a encore prouvé son pouvoir prédictif dans le calcul du couplage quadripolaire

nucléaire. Généralement, les constantes de couplage quadripolaire nucléaire prédites sont en excellent accord avec celles déduites expérimentalement. Cela facilite les processus d'attributions spectrales.

Les transitions rotationnelles ont été analysées localement en utilisant le code *WS18*. Dans les cas complexes tels que la barrière élevée en combinaison avec le couplage hyperfin, c'est un excellent outil pour l'attribution des spectres. Nous pensons qu'il peut être utile dans beaucoup de cas parce qu'il permet à l'utilisateur d'être sûr que l'attribution est correcte avant la poursuite du processus d'ajustement. Les spectres micro-ondes de toutes les molécules étudiées pendant ma thèse ont été reproduits en utilisant le code *XIAM* et les codes de la famille *BELGI*, et les résultats ont été comparés. Souvent, les codes de la famille *BELGI* montrent de grands avantages par rapport au code *XIAM* en réduisant les *écarts quadratiques moyens*. Dans les cas où les barrières de rotation interne sont faibles comme pour le 2MTA (Chapitre II.1) ou le 45DMTA (Chapitre III.2), un facteur d'environ 200 est observé pour ces écarts quadratiques moyens. Néanmoins, l'approche *XIAM* est extrêmement rapide car elle néglige les interactions entre les états v_t de torsion, alors que les codes *BELGI* prennent en compte les neuf premiers états de torsion ce qui les rend la vitesse de calcul plus lente. Cependant, il n'était pas clair au début de ma thèse que les interactions entre les états v_t jouent un rôle majeur dans la réduction des *écarts quadratiques moyens* dans le cas de transitions se produisant dans l'état fondamental de torsion $v_t = 0$.

Au cours de cette thèse, un nouveau code *TW21* a été écrit et été appliqué à quatre molécules. Comme le code *BELGI*, *TW21* diagonalise l'hamiltonien du système en deux étapes. Dans la première étape l'Hamiltonien de torsion est diagonalisé. Dans la deuxième étape l'Hamiltonien de rotation et les termes d'interaction rotation-torsion sont diagonalisés. Le résultat obtenu avec ce code pour la 4-méthylpyrimidine prouve que les interactions entre les états v_t ont un effet mineur sur l'ajustement des transitions rotationnelles (qui concernent des transitions avec de faibles *J*) alors que l'effet d'ajout des termes supplémentaires d'ordre supérieur de rotation-torsion joue un rôle majeur. Cela explique pourquoi le code *BELGI* a réussi à modéliser les spectres micro-ondes des molécules (dans des conditions de jet) avec de faibles barrières alors que le code *XIAM* rencontre souvent des difficultés. Le code *TW21* permet de déterminer quelle valeur de $v_{t_{max}}$ est la mieux adaptée pour une molécule donnée,

ce qui permet d'obtenir un ajustement suffisamment précis en un minimum de temps. La flexibilité du choix de $v_{t_{max}}$ (utilisée dans le code pour tronquer la matrice de l'Hamiltonien lors de la diagonalisation de la deuxième étape) et également k_{max} (utilisée dans le code pour tronquer la matrice de l'Hamiltonien lors de la diagonalisation de la première étape) devrait également être appliquée systématiquement pour les programmes à l'avenir, en particulier pour les programmes traitant de multiples rotations internes dans une molécule.

Pour la première fois, la combinaison d'une rotation interne et de deux faibles couplages quadripolaires nucléaires des noyaux ^{14}N est modélisée avec succès à l'aide de méthodes locales (*WS18*) et globales (*BELGI-2N*, *TW21*). Les développements de ces codes permettront de futures études sur ces composés et fourniront les outils appropriés pour les processus d'ajustement. Et par conséquent, ils permettront de mieux comprendre les liaisons chimiques sur les sites des noyaux ^{14}N dans ces molécules.

Enfin, les résultats de nos études ont été comparés avec ceux d'autres composés existant dans la littérature et ont permis d'observer la tendance d'augmentation de la barrière de rotation interne pour les composés ayant le même cycle mais substitués par des atomes S, N et O. Les effets stériques ainsi que la distribution électronique à l'intérieur du cycle jouent également des rôles importants dans la hauteur de barrière résultante. En étudiant les configurations électroniques à l'intérieur des cycles étudiés, les constantes de couplage quadripolaire nucléaire suivant la direction *c* de l'axe principal d'inertie peuvent être réparties en deux classes, l'une avec des signes positifs et l'autre avec des signes négatifs. Ces résultats permettent de mieux comprendre les cycles aromatiques azotés, en particulier les cycles à cinq chaînons.

RÉFÉRENCES

[1]U. Andresen, H. Dreiler, U. Kretschemer, W. Stahl, C. Thomsen, *Fresen J Anal Chem* **349**, 272 (1994).

[2]J. Grabow, W. Stahl, H. Dreiler, *Rev. Sci. Instrum.* **67**, 4072 (1996).

[3]I. Merke, W. Stahl, H. Dreiler, *Z. Naturforsch.* **49a**, 490 (1994).

[4]H.S.P. Müller, S. Thorwirth, D.A. Roth, G. Winnewisser, *Astron. Astrophys.* **370**, L49 (2001).

[5]H.S.P. Müller, F. Schlöder, J. Stutzki, G. Winnewisser, *J. Mol. Struct.* **742**, 215 (2005).

[6]I.E. Gordon, L.S. Rothman, C.Hill, R.V. Kochanov, Y. Tan, P.F. Bernath, M. Birk, V. Boudon, A. Campague, K.V. Chance, B.J. Drouin, J.-M. Flaud, R.R. Gamache, J.T. Hodges, D. Jacquemart, V.I. Perevalov, A. Perrin, K.P. Shine, M.-A.H. Smith, J. Tennyson, G.C. Toon, H. Tran, V.G. Tyuterev, A. Barbe, A.G. Császár, V.M. Devi, T. Furtenbacher, J.J. Harrison, J.-M. Hartmann, A. Jolly, T.J. Johnson, T. Karman, I. Kleiner, A.A. Kyuberis, J. Loos, O.M. Lyullin, S.T. Massie, S.N. Mikhailenko, N. Moazzen-Ahmadi, H.S.P. Müller, O.V. Naumenko, A.V. Nikitin, O.L. Polyansky, M. Rey, M. Rotger, S.W. Sharpe, K. Sung, E. Starikova, S.A. Tashkun, J. Vander Auwera, G. Wagner, J. Wilzewski, P. Wcisło, S. Yu, E.J. Zak, *J. Quant. Spectrosc. Radiat. Transf.* **203**, 3 (2017). See also HITRAN website at http://hitran.org for more detailed information.

[7]B.A. McGuire, *Astrophys. J., Suppl. Ser.* **239**, 48pp (2018).

[8]J.M. Hollis, F.J. Lovas, A.J. Remijan, P.R. Jewell, V.V. Ilyushin, I. Kleiner, *Astrophys. J.* **643**, 25 (2006).

[9]M. Carvajal, L. Margulès, B. Tercero, K. Demyk, I. Kleiner, J. C. Guillemin,V. Lattanzi, A. Walters, J. Demaison, G. Wlodarczak, T. R. Huet, H. Møllendal, V.V. Ilyushin, J. Cernicharo, *Astron. Astrophys.* **3**, 1109 (2009).

[10]B. Tercero, I. Kleiner, J. Cernicharo, H.V.L. Nguyen, A. López, and G. M. Muñoz Caro, *ApJL* **770**, 6 (2013).

[11]A. Jabri, B. Tercero, L. Margulès, R.A. Motiyenko, E.A. Alekseev, I. Kleiner, J. Cernicharo, J.-C. Guillemin, *Astron. Astrophys.* **A120**, 9 (2020).

[12]A. Jabri, V. Van, H.V.L. Nguyen, H. Mouhib, F. Kwabia-Tchana, L. Manceron, W. Stahl, I. Kleiner, *Astron. Astrophys.* **A127**, 589 (2016).

[13]N. Ohashi, J.T. Hougen, R.D. Suenram, F.J. Lovas, Y. Kawashima, M. Fujitake, J. Pykad, *J. Mol. Spectrosc.* **227**, 28 (2004).

[14]C.C. Lin, J. D. Swalen, *Rev. Mod. Phys.* **31**, 841 (1959).

[15]R.C. Woods, *J. Mol. Spectrosc.* **22**, 49 (1967).

[16]H. Hartwig, H. Dreizler, *Z. Naturforsch.* **51a**, 923 (1996).

[17]J.T. Hougen, I. Kleiner, M. Godefroid, *J. Mol. Spectrosc.* **163**, 559 (1994).

[18]I. Kleiner, J.T. Hougen, *J. Chem. Phys.* **119**, 5505 (2003).

[19]P. Groner, *J. Chem. Phys.* **107**, 4483 (1997).

[20]V.V. Ilyushin, Z. Kisiel, L. Pszczółkowski, H. Mäder, J.T. Hougen, *J. Mol. Spectrosc.* **259**, 26 (2010).

[21]D.F. Plusquellic, R.D. Suenram, B. Mate, J.O. Jensen, A.C. Samuels, *J. Chem. Phys.* **115**, 3057 (2001).

[22]See http://spec.jpl.nasa.gov/ for downloading and instruction of the program.

[23]A. Belloche, A.A. Meshcheryakov, R.T. Garrod, V.V. Ilyushin, E.A. Alekseev, R.A. Motiyenko, L. Margulès, H.S.P. Müller, K.M. Menten, *Astron. Astrophys.* **601**, A49 (2017).

[24]J.-U. Grabow, H. Hartwig, N. Heineking, W. Jäger, H. Mäder, H.W. Nicolaisen, W. Stahl, *J. Mol. Struct.* **612**, 349 (2002).

[25]H.-W. Nicolaisen, J.-U. Grabow, N. Heineking, W. Stahl, *Z. Naturforsch.* **46a**, 635 (1991).

[26]W. Jäger, H. Mäder, *Z. Naturforsch.* **42a**, 1405 (1987).

[27]W. Jäger, H. Mäder, *J. Mol. Struct.* **190**, 295 (1988).

[28]E.R.L. Fliege, *Z. Naturforsch.* **45a**, 911 (1990).

[29]H.V.L. Nguyen, I. Kleiner, *Phys. Sci. Rev.* (2020), DOI: 10.1515/psr-2020-0037, in press

[30]P. Groner, S. Albert, E. Herbst, F.C. De Lucia, F.J. Lovas, B.J. Drouin, J.C. Pearson, *Astrophys. J.* **142**, 145 (2002).

[31]W. Neustock, A. Guarnieri, J. Demaison, G. Wlodarczak, *Z. Naturforsch.* **45a**, 702 (1990).

[32]H.V.L. Nguyen, W. Stahl, *ChemPhysChem* **12**, 1900 (2011).

[33]V. Van, W. Stahl, H.V.L. Nguyen, *Phys. Chem. Chem. Phys.* **17**, 32111 (2015).

[34]V. Van, J. Bruckhuisen, W. Stahl, V.V. Ilyushin, H.V.L. Nguyen, *J. Mol. Spectrosc.* **343**, 121 (2018).

[35]S. Khemissi, H.V.L. Nguyen, *ChemPhysChem* **21**, 1682 (2020).

[36]J.L. Alonso, I. Pena, J. C. Lopez, V. Vaquero, *Angew. Chem. Int. Ed.* **48,** 6141 (2009).

[37]J.L. Alonso, V. Vaquero, I. Peña, J.C. López, S. Mata, W. Caminati, *Angew. Chem. Int. Ed.* **52**, 2331 (2013).

[38]L.B. Favero, I. Uriarte, L. Spada, P. Ecija, C. Calabrese, W. Caminati, E.J. Cocinero, *J. Phys. Chem. Lett.* **7**, 1187 (2016).

[39]V. Van, W. Stahl, A. R. Philipps, H.V.L. Nguyen, The internal rotation of four methyl groups in Tetramethylthiophene, *HRMS*, *24th Colloquium*, Dijon, France, 24-28 Aug (2015).

[40]W. Caminati, G. Cazzoli, D. Troiano, *Chem. Phys. Letters.* **43**, 65 (1976).

[41]W. Caminati, G. Cazzoli, A.M. Mirri, *Chem. Phys. Letters.* **31**, 104 (1975).

[42]E. Gougoula, C. Medcraft, M. Heitkämper, N.R. Walker, *J. Chem. Phys.* **151**, 144301 (2019).

[43]M. J. Frisch, G. W. Trucks, H. B. Schlegel, G. E. Scuseria, M. A. Robb, J. R. Cheeseman, J. A. Montgomery Jr, T. Vreven, K. N. Kudin, J. C. Burant, J. M. Millam, S. S. Iyengar, J. Tomasi, V. Barone, B. Mennucci, M. Cossi, G. Scalmani, N. Rega,G. A. Petersson, H. Nakatsuji, M. Hada, M. Ehara, K. Toyota, R. Fukuda, J. Hasegawa, M. Ishida, T. Nakajima, Y. Honda, O. Kitao, H. Nakai, M. Klene, X. Li, J. E. Knox, H. P. Hratchian, J. B. Cross, V. Bakken, C. Adamo, J. Jaramillo, R. Gomperts, R. E. Stratmann, O. Yazyev, A. J. Austin, R. Cammi, C. Pomelli, J. W. Ochterski, P. Y. Ayala, K. Morokuma, G. A. Voth, P. Salvador, J. J. Dannenberg, V. G. Zakrzewski, S. Dapprich, A. D. Daniels, M. C. Strain, O. Farkas, D. K. Malick, A. D. Rabuck, K. Raghavachari, J. B. Foresman, J. V. Ortiz, Q. Cui, A. G. Baboul, S. Clifford, J. Cioslowski, B. B. Stefanov, G. Liu, A. Liashenko, P. Piskorz, I. Komaromi, R. L. Martin, D. J. Fox, T. Keith, M. A. Al-Laham, C. Y. Peng, A. Nanayakkara, M. Challacombe, P. M. W. Gill, B. Johnson, W. Chen, M. W. Wong, C. Gonzalez, and J. A. Pople, Gaussian03, Revision D.01, Gaussian, Inc., Wallingford, CT, 2004.

[44]Gaussian 09 (Revision A.02), M.J. Frisch, G.W. Trucks, H.B. Schlegel, G.E. Scuseria, M.A. Robb, J.R. Cheeseman, G. Scalmani, V. Barone, B. Mennucci, G.A. Petersson, H. Nakatsuji, M. Caricato, X. Li, H.P. Hratchian, A.F. Izmaylov, J. Bloino, G. Zheng, J.L. Sonnenberg, M. Hada, M. Ehara, K. Toyota, R. Fukuda, J. Hasegawa, M. Ishida, T. Nakajima, Y.Honda, O. Kitao, H. Nakai, T. Vreven, J.A. Montgomery Jr., J.E. Peralta, F. Ogliaro, M. Bearpark, J.J. Heyd, E. Brothers, K.N. Kudin, V.N. Staroverov, R. Kobayashi, J. Normand, K. Raghavachari, A. Rendell, J.C. Burant, S.S. Iyengar, J. Tomasi, M. Cossi, N. Rega, J.M. Millam, M. Klene, J.E. Knox, J.B. Cross, V. Bakken, C. Adamo, J. Jaramillo, R. Gomperts, R.E. Stratmann, O. Yazyev, A.J. Austin, R. Cammi, C. Pomelli, J.W. Ochterski, R.L. Martin, K. Morokuma, V.G. Zakrzewski, G.A. Voth, P. Salvador, J.J. Dannenberg, S. Dapprich, A.D. Daniels, O. Farkas, J.B. Foresman, J.V. Ortiz, J. Cioslowski, D.J. Fox, Gaussian, Inc., Wallingford CT, 2009.

[45]M.J. Frisch, G.W. Trucks, H.B. Schlegel, G.E. Scuseria, M.A. Robb, J.R. Cheeseman, G. Scalmani, V. Barone, G.A. Petersson, H. Nakatsuji, X. Li, M. Caricato, A.V. Marenich, J. Bloino, B.G. Janesko, R. Gomperts, B. Mennucci, H.P. Hratchian, J.V. Ortiz, A.F. Izmaylov, J.L. Sonnenberg, D. Williams-Young, F. Ding, F. Lipparini, F. Egidi, J. Goings, B. Peng, A. Petrone, T. Henderson, D. Ranasinghe, V.G. Zakrzewski, J. Gao, N. Rega, G. Zheng, W. Liang, M. Hada, M. Ehara, K. Toyota, R. Fukuda, J. Hasegawa, M. Ishida, T. Nakajima, Y. Honda, O. Kitao, H. Nakai, T. Vreven, K. Throssell, J.A. Montgomery Jr, J.E. Peralta, F. Ogliaro, M.J. Bearpark, J.J. Heyd, E.N. Brothers, K.N. Kudin, V.N. Staroverov, T.A. Keith, R. Kobayashi, J. Normand, K. Raghavachari, A.P. Rendell, J.C. Burant, S.S. Iyengar, J. Tomasi, M. Cossi, J.M. Millam, M. Klene, C. Adamo, R. Cammi, J.W.

Ochterski, R.L. Martin, K. Morokuma, O. Farkas, J.B. Foresman, D.J. Fox, Gaussian 16, Revision B.01, Gaussian, Inc., Wallingford CT, 2016.

[46]M.W. Schmidt, K.K. Baldridge, J.A. Boatz, S.T. Elbert, M.S. Gordon, J.H. Jensen, S. Koseki, N. Matsunaga, K.A. Nguyen, S.J. Su, T.L. Windus, M. Dupuis, J.A. Montgomery, *J. Comput. Chem.* **14**, 1347 (1993).

[47]W.C. Bailey, http://nqcc.wcbailey.net/.

[48]L. Nygaard, E. Asmussen, J.H. Høg, R.C. Maheshwari, C.H. Nielsen, I.B. Petersen, J. Rastrup-Andersen, G.O. Sørensen, *J. Mol. Struct.* **8**, 225 (1971).

[49]L. Nygaard, J.T. Nielsen, J. Kirchheiner, G. Maltesen. J.R. Andersen, G.O. Sørensen, *J. Mol. Struct.* **3**, 491 (1969).

[50]J. Makarewicz, S. Huber, B. B.-Gatehouse, A. Bauder, *J. Mol. Struct*. **612**, 117 (2002).

[51]A. Kumar, J. Sheridan, O.L. Stiefvater, *Z. Naturforsch.* **33a**, 145 (1978).

[52]M. Tudorie, I. Kleiner, J.T. Hougen, S. Melandri, L.W. Sutikdja, W. Stahl, *J. Mol. Spectrosc.* **269**, 211 (2011).

[53]N. M. Pozdeev, L.N. Gunderova, A.A. Shapkin, *Opt. Spektrosk.* **28**, 254 (1970).

[54]I. A. Finneran, S.T. Shipman, S.L. Widicus Weaver, *J. Mol. Spectrosc.* **280**, 27 (2012).

INTRODUCTION

The rotational spectroscopy studies the absorption and emission of an electromagnetic wave (usually in the microwave region of the electromagnetic spectrum) by molecules. Spectroscopy studies the exchanges between the rotational energy of molecules and the electromagnetic energy of photons. A molecule can absorb or emit radiation by acquiring a rotational motion around its center of gravity or center of mass. Energy transitions occur between its rotational energy levels. The rotational spectrum of a molecule requires that the molecule has a dipole moment. The existence of this dipole moment allows the electric field to exert a torque on the molecule, which makes it spin more quickly or slowly. The field of rotational spectroscopy has been intensively studied with two main fields of applications. The first one is related to the detection of molecules in space and the second is related to the precise determination of the molecular structures.

About 70 years since the first interstellar molecule CH was discovered[1], the attention to the field of astrochemistry increasingly grew up. Much efforts have been made towards the detection of more complex molecular systems in space. Polycyclic aromatic hydrocarbons (PAHs) are believed to contribute as much as 25% of the interstellar carbon budget[2]. They are seen to be the most ubiquitous and abundant in all galactic and extragalactic sources which have sufficient UV fields to permit the detection of identifiable fluorescence emission signal. The studies of PAHs receive a considerable interest because they allow to understand: the astrophysical and astrochemical conditions in galaxies, the interactions between PAHs and nano-dust grains and how PAHs control their surface properties can be obtained and possibly the chemical evolution of life.

It is well-known that simple molecules condense to form complex molecules, then tiny nanoparticles (including PAHs) which can be ejected later into the interstellar medium. In the later stage of star envelopes (red giant, planetary nebula), the PAHs features are observed, i.e., C_{60}, C_{70} via infrared emission[3]. It is because at the late stage, the temperatures at the central stars are high enough, thus provide sufficient UV fields to trigger mid-IR emission of PAHs. In the contrary, at their early stage the temperatures are often low, lead to the lacking of UV emission. To have complete understanding on the

chemical evolution in star envelopes, relying on IR-emission is not sufficient and therefore other methods of observations are needed.

PAHs, which have permanent electric dipole moments, can emit microwave emission thus enable the observation of rotational transitions in the absence of UV fields and therefore can be seen as a unique way for us probe PAHs in ISM. The problem is that often PAHs have very tiny permanent dipole moments which also reduces our chance to detect them. This can be overcome by searching for possible aromatic molecules precursors to the PAH's and this method shows a surprisingly rapid succession in the last three years. In 2018, *McGuire et al.*[4] reported for the first time the detection of a CN-functionalized in a six membered ring called benzonitrile (C_6H_5N) in Taurus Molecular Cloud-1 (TCM-1). The detection of benzonitrile was supported by the microwave spectroscopic laboratory work investigated much earlier[5]. This work has shed light on the detections of new aromatic organic chemistry in space which had not been explored yet. Later on, *McGuire* and his co-workers reported a new finding of two bicyclic aromatic rings in a primordial gas cloud[6]. Even more recent, for the first time five-membered ring are detected which are 1-cyano-1,3-cyclopentadiene (also called 1-cyanocyclopentadiene)[7] and 2-cyano-1,3cyclopentadiene (or named as 2-cyanocyclopentadiene)[8].

Those studies opened up a new channel for the search and detection of yet undetected species precursors of PAHs, such as their substituted with -CN, -OH and -CH_3. The reason is that their substituted species offer much larger dipole moments and therefore stronger line intensities which significantly increase the chance for detection. Studying those species will provide direct information about the pathways to the formation of PAHs and will finally enable scientists to acquire a better understanding of the chemical evolution of how PAHs reacts and evolves in the process of stars and planets formations. The potential observations via microwave emission are in fact very promising because of the already existing radio telescopes operating in the microwave spectral range as GBT (Green Bank Telescope, USA) but also with upcoming advanced ones, i.e., Atacama Large Millimeter/submillimeter Array (ALMA) band 1 receiver covering the frequency range between 35 and 50 GHz, the Square Kilometer Array (SKA) and the next generation of the Very Large Array (ngVLA). In order to achieve the complete understanding of the chemical and physical pathways to the prebiotic molecules, much effords will still have to be made, but generally it is obvious that each of the aspects: (i) spectroscopic laboratory data, both

experimental and theoretical works, (ii) astronomical observations and (iii) astrochemical theoretical models must be carried out.

So far rotational spectroscopy has allowed the detection and the determination of the abundance of more than 200 molecules[9] in the interstellar medium, providing useful information about the chemical evolution of these media. A summary of detected molecules and a listing of tentative detections is reported by *McGuire*[9]. A number of spectroscopic studies were performed in the SPECAT group of the Laboratoire Interuniversitaire des Systèmes Atmosphériques (LISA), allowing the detection in space for the first time of acetamide[10] CH_3CONH_2, the isotopologues of methyl formate[11] HCOOCH3, and methyl acetate[12] CH_3COOCH_3. Upper limit detections were also calculated for S-methyl thioformate[13] $CH_3SC(O)H$ and line lists with line positions and intensities were established for dimethylsulfide[14] CH_3SCH_3.

The detectability of N-heterocycles molecules in astronomical environment was studied in details by *Z. Peeters et al.*[15] in which the authors suggested that these compounds could be found in dense clouds. During my thesis, we aimed at studying the molecular structures and dynamics of some five- and six-membered rings, methyl substituted derivatives of pyrrole, thiazole and pyrimidine, with focus on the effects of internal rotation and quadrupole coupling. In total, we studied six molecules, all molecules have a plane of the frame symmetry at equilibrium. The investigated molecular systems are summarized in Fig. 1.

These six molecules can be classified into three classes (Fig. 1), gradually increasing the degree of complexity:

Class I: Aromatic rings containing one methyl group CH_3 + one nitrogen atom ^{14}N (**1**-**3**).

Class II: Aromatic rings containing two internal rotations methyl groups CH_3 + one nitrogen atom ^{14}N (**4**, **5**).

Class III: Aromatic rings containing one internal rotation methyl group CH_3 + two nitrogen atoms ^{14}N (**6**).

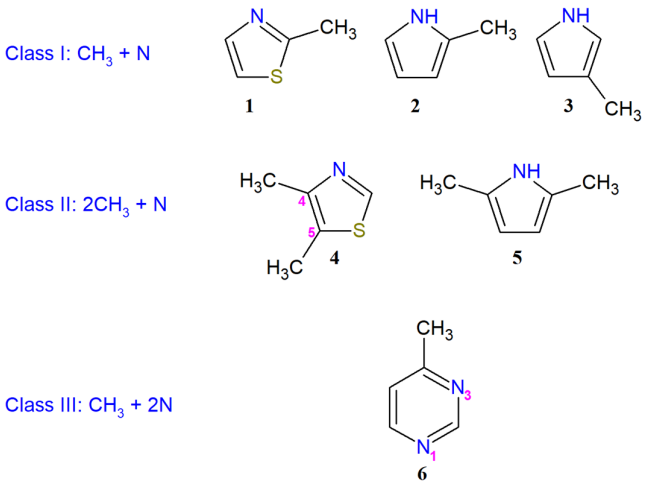

FIG. 1. Investigated molecular systems in this thesis: (**1**) 2-methylthiazole, (**2**) 2-methylpyrrole, (**3**) 3-methylpyrrole, (**4**) 4,5-dimethylthiazole, (**5**) 2,5-dimethylthiazole, (**6**) 4-methylpyrimidine.

The internal rotation of a group of atoms (in this case the methyl -CH_3 group) relative to the rest of the molecule is a phenomenon of molecular non-rigidity, also called large amplitude motion, which is difficult to model in spectroscopy. Indeed, the tunnelling effect originating from a finite potential barrier results in the splittings of the energy levels and of the molecular lines, which complicates the spectra. The large amplitude motion(s) of one or two internal rotors are hindered by a potential barrier and cannot be treated by "traditional" theoretical models applicable to small amplitude motions around the equilibrium position of the nuclei. The study of this type of molecules therefore requires the use of specific theoretical models and appropriate computer programs[16]. The magnitude of the internal rotation splittings is proportional to the “reduced” barrier height, $s = 4V_3/9F$, where V_3 is the height of the potential barrier and F is the kinetic internal rotation constant. F is the inverse of the moment of inertia of the methyl group, but it also depends on the direction of the methyl group in the molecule and is thus related to the geometry of the molecule. In general, the higher (lower) the reduced barrier is, the smaller (larger) the splittings of the energy levels are.

The nuclear quadrupole coupling effect arises from the interaction between a non-spherical distribution of the nuclear charge (which results in a nuclear electric quadrupole moment) and a non-spherical distribution of the electronic charge around the nucleus (which results in an electric field gradient from at the nucleus). Any nucleus with spin I > 1/2 causes a non-spherical distribution of its nuclear charge

and possesses a non-zero nuclear quadrupole moment. The nuclear quadrupole effect also results in splittings of the energy levels and transitions in the spectrum. All molecules targeted in my thesis contain ^{14}N nucleus with the quadrupole splittings are smaller or of the same magnitude as the internal rotation splittings. Therefore, both effects need to be taken into account properly to analyze the microwave spectra.

During my thesis we did not focus on the line intensities, even though they are essential for the astrophysical detection. However, our theoretical models can provide the permanent dipole moments, spin statistics and line strengths which are necessary to estimate the relative line intensities. The aims of our studies are to: (i) provide the accurate geometrical (rotational constants, centrifugal distortion constants) and dynamical (barrier to internal rotation V_3) for further studies, e.g., IR investigations of those investigated molecules, (ii) provide line positions in the microwave spectral range for astronomical search on those molecules, (iii) add knowledge to the understanding of the internal rotation(s) and nuclear quadrupole coupling in aromatic rings, especially those five-membered rings and finally (iv) provide proper codes to asset future studies on the same type of molecules.

The following of this thesis will be organized into four parts. In the Part I, we will briefly introduce the theoretical background necessary to understand the effects of internal rotation raising from methyl group as well as nuclear quadrupole coupling originating from ^{14}N and shortly describe of the experimental setups. Part II focuses the microwave spectroscopy investigations of nitrogen containing of five-membered rings which contains one ($-CH_3$) methyl group (2-methylthiazole, 2-methylpyrrole and 3-methylpyrrole in Chapter II.1, II.2 and II.3, respectively) while Part III reports our studies on di-methylated of nitrogen containing of five-membered rings (2,5-dimethylpyrrole and 4,5-dimethylthiazole in Chapter II.1 and III.2, respectively). In part IV, we will introduce the new codes called *TW21* and *BELGI-2N* with their first application on studying the rotational signatures of 4-methylpyrimidine. Finally, the thesis will end with a chapter dedicated to the conclusions and perspectives.

REFERENCES

[1]B.A. McKellar, *PASP.* **52**, 187 (1940).

[2]A.G.G.M. Tielens, *Annu. Rev. Astron. Astrophys.* **46**, 289 (2008).

[3]J. Cami, J. Bernard-Salas, E. Peeters, S.E. Malek, *Sci*. **329**, 1180 (2010).

[4]B.A. McGuire, A. Burkhardt, S. Kalenskii, C. Shingledecker, A. Remijan, E. Herbst, M. McCarthy. *Sci.* **359**, 202 (2018).

[5]U. Dahmen, W. Stahl, H. Dreizler, *Ber. Bunsenges. Phys. Chem.* **98**, 970 (1994).

[6]B.A. McGuire, R.A. Loomis, A.M. Burkhardt, K.L.K. Lee, C.N. Shingledecker, S.B. Charnley, I.R. Cooke, M.A. Cordiner, E. Herbst, S. Kalenskii, M.A. Siebert, E.R. Willis, C. Xue, A.J. Remijan, M.C. McCarthy, *Sci*. **371**, 1265 (2021).

[7]M.C. McCarthy, K.L.K. Lee, R.A. Loomis, A.M. Burkhardt, C.N. Shingledecker, S.B. Charnley, M.A. Cordiner, E. Herbst, S. Kalenskii, E.R. Willis, C. Xue, A.J. Remijan, B.A. McGuire, *Nat. Astron.* **5**, 176 (2021).

[8]K.L.K. Lee, P.B. Changala, R.A. Loomis, A.M. Burkhardt, C. Xue, M.A. Cordiner, S.B. Charnley, M.C. McCarthy, B.A. McGuire, *ApJL.* **910**, 1 (2021).

[9]B.A. McGuire, *Astrophys. J., Suppl. Ser.* **239**, 48pp (2018).

[10]J.M. Hollis, F.J. Lovas, A.J. Remijan, P.R. Jewell, V.V. Ilyushin, I. Kleiner, *Astrophys. J.* **643**, 25 (2006)

[11]M. Carvajal, L. Margulès, B. Tercero, K. Demyk, I. Kleiner, J. C. Guillemin,V. Lattanzi, A. Walters, J. Demaison, G. Wlodarczak, T. R. Huet, H. Møllendal, V.V. Ilyushin, J. Cernicharo, *Astron. Astrophys.* **3**, 1109 (2009).

[12]B. Tercero, I. Kleiner, J. Cernicharo, H.V.L. Nguyen, A. López, G. M. Muñoz Caro, *ApJL.* **770**, 6 (2013).

[13]A. Jabri, B. Tercero, L. Margulès, R. A. Motiyenko, E. A. Alekseev, I. Kleiner, J. Cernicharo, J.-C. Guillemin, *Astron. Astrophys.* **A120** 9 (2020).

[14]A. Jabri, V. Van, H.V.L. Nguyen, H. Mouhib, F. K.-Tchana, L. Manceron, W. Stahl, I. Kleiner, *Astron. Astrophys.* **A127**, 589 (2016).

[15]Z. Peeters, O. Botta, S. B. Charnley, Z. Kisiel, Y.-J. Kuan, P. Ehrenfreund, *Astron. Astrophys.* **433**, 583 (2005).

[16]C. C. Lin and J.D. Swalen, *Rev. Mod. Phys.* **31**, 841 (1959).

PART I: EXPERIMENTAL AND THEORETICAL METHODS

I. EXPERIMENTAL TECHNIQUES

The Molecular Jet-Fourier Transform Microwave (MJ-FTMW) technique was used to measure the microwave spectra of all investigated molecular systems in my thesis. Here, only a short description of how the spectrometer works will be given. All the details of those machines can be found in the Refs.[1-3]. Fig. 1 shows the block diagram for the instrument. The synthesizer generates a microwave frequency ν (GHz). Via a power divider, the microwave signal is led into a polarization and a detection branch. In the polarization branch the microwave signal is mixed in a single side band (SSB) mixer with a pulsed radio frequency of 160 MHz, so that an upper sideband of ν + 160 MHz is obtained. The frequency of 160 MHz is produced as the 16th harmonic of 10 MHz.

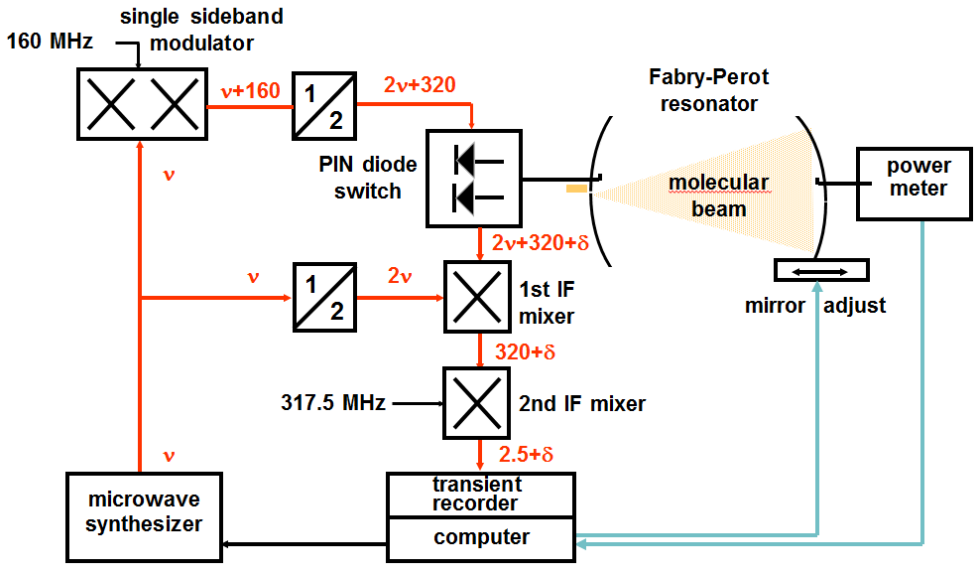

FIG. 1. Block diagram of Molecular Jet-Fourier Transform Microwave (MJ-FTMW) spectrometer operating in the 2-26.5 GHz spectral range.

The microwave pulses are amplified and their frequency is doubled, that finally pulses of a frequency of 2ν+320 MHz are available. They are amplified again and led via 2 PIN diode switches to the antenna inside the Fabry-Perot cavity where they are used to polarize the molecules. The transient emission signal is received with the same antenna and led via another microwave switch into the detection branch,

where it is amplified and downconverted with the doubled frequency of the synthesizer 2ν to a first intermediate frequency of 320 MHz. The downconverted signal is amplified, filtered and downconverted again with a frequency of 317.5 MHz to a second intermediate frequency of 2.5 MHz. The signal is digitized in a transient recorder and averaged. After a Fourier transform the spectrum is obtained. All Transitor-Transitor Logic (TTL) signals needed to control the microwave switches, the beam nozzle, and the transient recorder are generated by multi-channel pulse generator.

A gas mixture containing 1% substance in helium at a total pressure of about 100 hPa was used throughout. In order to observe molecular transitions with higher *J* values helium has been chosen as a carrier gas because the cooling is not as effective as with argon or neon. All spectra were recorded in frequency range of 2-40 GHz of frequency using two MJ-FTMW spectrometers. One of those spectrometers is located at the Institut für Physikalische Chemie, Rheinisch-Westfälische Technische Hochschule (RWTH), in Aachen (Germany), with the frequency range from 2 to 26.5 GHz and was available thanks our collaboration with the group of Prof. W. Stahl. The other spectrometer is located at the LISA laboratory in Créteil (France) and operates in the 26.5 to 40 GHz spectral range. I participated to the recordings and measurements using both spectrometers.

FIG. 2. MJ-FTMW spectrometers used in this work, located in Aachen (2-26.5 GHz) and in Paris (26.5-40.0 GHz).

II. QUANTUM CHEMISTRY

In order to facilitate the spectral assignment, initial values of the rotational constants, the torsional potential, and the ^{14}N quadrupole coupling constants were calculated by quantum chemical methods. The quantum chemical calculations were performed using the GAUSSIAN package[4-6] for the 2-methylthiazole, 4,5-dimethylthiazole, and 2-methyllpyrrole as well as with GAMESS[7] program for 3-methylpyrrole, 2,5-dimethylpyrrole, and 4-methylpyrimidine. Graphical representations were produced with MacMolPlt, version 7.7[8] for the calculations performed with GAMESS[7] package.

The molecular geometries of the molecules we studied were optimized at different levels of theory with various combinations of the Møller Plesset perturbation theory of second order, (MP2)[9], the functional density B3LYP (Becke, 3-parameter, Lee–Yang–Parr)[10], M06-2X, and the Coupled Cluster Singles and Doubles (CCSD) methods with different basis sets in order to check for the convergence and to find out the level of theory yielding rotational constants showing the best agreement with the experimental values.

Quantum chemistry calculations also allowed us to determine the torsional potential barrier hindering the internal rotation. For the potential curve, scan calculations are created by varying step-wise a given dihedral angle. At each stage the potential energy of a new structure (corresponding with a new energy E) is optimized. Finally, potential energy curves are plotted as function of the scanned dihedral angle. Furthermore, for the cases of two internal methyl tops, two-dimensional potential energy surfaces (PESs) can also be calculated and depicted as color contour plots. These surfaces provide the information for the internal rotation coupling terms.

All the molecular systems that we studied contain ^{14}N nitrogen atom(s). Thus, the nuclear quadrupole coupling constants had to be computed which enabled us to assign the hyperfine structure. As recommended for π-conjugated systems, the calculations were done using Bailey method[11]. After the geometries of the molecules were optimized at different levels of theory, we performed single point electric field gradient calculations at the B3PW91/6-311+G(d,p) level of theory with the calibration factor of –4.599(12)[12] MHz $a.u^{-1}$.

III. THEORETICAL CONSIDERATIONS

Microwave spectroscopy of static gases or molecular jet belongs to the most accurate experimental methods to get geometrical and dynamical information of isolated molecules, as the main geometry parameters, the rotational constants, which are proportional to the inverse of the principal moments of inertia, are obtained. The values of those experimental rotational constants can be compared with the results of quantum chemical calculations for a given conformer and can be used as a reference for quantum chemical benchmark calculations. Dynamic parameters obtained from microwave investigations are most often used to describe the internal rotation of methyl groups. Among these parameters are the hindering potential(s), the inertial moment of the methyl group(s) and the orientation of the internal rotor within the molecule.

When the molecules are not rigid due to additional effects, e.g., due to the centrifugal distortion force, the internal rotation, the energy levels cannot be calculated with sufficient accuracy based on only the three principal moments of inertia. Indeed, the energy levels are shifted or split due to those effects and we need to take them into account in the theoretical models. The internal rotation can usually be treated by two different theoretical approaches. One family of methods is based on the rigid top-rigid frame (RTRF) Hamiltonian model, the other one uses effective Hamiltonians including non-rigidity. Since distortion effects (due to centrifugal distortion, or due to non-C_{3v} methyl groups) are not included in the RTRF model, effective parameters are added in the Hamiltonian to accurately describe the spectra. From a more technical point of view, the internal rotation theoretical methods can be also classified according to the coordinates systems they use. Best known are probably the principal axis method (PAM) and the rho axis method (RAM)[13,14].

In this chapter, we will focus on describing the fundamental foundation to understand the necessary background, then describing some Hamiltonian methods for one or two rotors and the computer programs used in this thesis (the newly developed program, *TW21*, will be presented along with the results in Chapter IV). Note that most of the details for the Hamiltonian can be found in Refs.[13, 14].

1. Rigid rotor model

In the rigid rotor model, particles rotate with a fixed distance from each other. The kinetic energy T of a system can be written as:

$$\mathrm{T} = \frac{1}{2}\vec{\omega}^{+}\mathrm{I}\vec{\omega} = \frac{1}{2}\vec{\mathrm{P}}^{+}\mathrm{I}^{-1}\vec{\mathrm{P}} \tag{1}$$

here, $\vec{\omega}$ represents the angular velocity and I is the moment of inertia tensor which can be described as:

$$\mathrm{I} = \begin{pmatrix} I_{xx} & I_{xy} & I_{xz} \\ I_{yx} & I_{yy} & I_{yz} \\ I_{zx} & I_{zy} & I_{zz} \end{pmatrix} \tag{2}$$

Each element of the matrix is defined in the following equations:

$$I_{xx} = \sum_{\mathrm{i}=1}^{\mathrm{N}} \mathrm{m_i}(\mathrm{y_i^2} + \mathrm{z_i^2}) \tag{3}$$

$$I_{yy} = \sum_{\mathrm{i}=1}^{\mathrm{N}} \mathrm{m_i}(\mathrm{z_i^2} + \mathrm{x_i^2}) \tag{4}$$

$$I_{zz} = \sum_{\mathrm{i}=1}^{\mathrm{N}} \mathrm{m_i}(\mathrm{x_i^2} + \mathrm{y_i^2}) \tag{5}$$

$$I_{xx} = I_{yx} = -\sum_{\mathrm{i}=1}^{\mathrm{N}} \mathrm{m_i x_i y_i} \tag{6}$$

$$I_{zx} = I_{xz} = -\sum_{\mathrm{i}=1}^{\mathrm{N}} \mathrm{m_i x_i z_i} \tag{7}$$

$$I_{xy} = I_{yx} = -\sum_{\mathrm{i}=1}^{\mathrm{N}} \mathrm{m_i x_i y_i} \tag{8}$$

$$I_{yz} = I_{zy} = -\sum_{\mathrm{i}=1}^{\mathrm{N}} \mathrm{m_i y_i z_i} \tag{9}$$

where m_i represents the mass of the i[th] particle, x_i, y_i, z_i are the coordinates of the particle in a coordinate system fixed to the centre of gravity of the molecule and the number of all particles of the molecule is presented by N.

The coordinate axes can be always chosen in a way that all the off-diagonal elements of the inertia tensor I are zero so that it can be written as:

$$I = \begin{pmatrix} I_a & 0 & 0 \\ 0 & I_b & 0 \\ 0 & 0 & I_c \end{pmatrix} \tag{10}$$

This coordinate system (a, b, c) is called the principal inertial system or in short the principal axis system.

In the principal axis system, the components of the angular momentum are given accordingly:

$$\mathbf{P_a} = I_a \boldsymbol{\omega}_\mathbf{a} \tag{11}$$

$$\mathbf{P_b} = I_b \boldsymbol{\omega}_\mathbf{b} \tag{12}$$

$$\mathbf{P_c} = I_c \boldsymbol{\omega}_\mathbf{c} \tag{13}$$

From the Eqn. (11) to (13) and Eqn. (1), the kinetic energy is derived:

$$\mathbf{T} = \frac{1}{2}\left(\frac{\mathbf{P_a^2}}{I_a}\right) + \frac{1}{2}\left(\frac{\mathbf{P_b^2}}{I_b}\right) + \frac{1}{2}\left(\frac{\mathbf{P_c^2}}{I_c}\right) \tag{14}$$

If there is no torque, the classical Hamiltonian only consists of the kinetic energy, thus:

$$\mathbf{H_r} = \frac{1}{2}\left(\frac{\mathbf{P_a^2}}{I_a} + \frac{\mathbf{P_b^2}}{I_b} + \frac{\mathbf{P_c^2}}{I_c}\right) \tag{15}$$

Depending on the values of I_a, I_b, I_c, a rigid molecule can be classified into one of different classes which is given in the following:

Asymetric top	Symmetric top (prolate top)	Symmetric top (oblate top)
$I_a \neq I_b \neq I_c$	$I_a < I_b = I_c$	$I_a = I_b < I_c$

The rotational constants A, B, C are defined as:

$$A = \frac{\mathrm{h}^2}{8\pi^2 I_a} \tag{16}$$

$$B = \frac{\mathrm{h}^2}{8\pi^2 I_b} \tag{17}$$

$$C = \frac{\mathrm{h}^2}{8\pi^2 I_c} \tag{18}$$

a. Symmetric Tops

In the case of a prolate top, we have

$$\mathbf{P^2} = \mathbf{P_a^2} + \mathbf{P_b^2} + \mathbf{P_c^2} \tag{19}$$

the following Hamiltonian is obtained:

$$\mathbf{H_r} = \frac{\mathbf{P^2}}{2I_b} + \frac{1}{2}\left(\frac{1}{I_a} - \frac{1}{I_b}\right)\mathbf{P_a^2} \tag{20}$$

Since $\mathbf{H}_\mathrm{r}$, $\mathbf{P}^2$ and $\mathbf{P}_\mathrm{a}^2$ are commutable operators, they share a set of common symmetric-top eigenfunctions $\Psi_{J,K_a} = |JKM\rangle$ with M is the projection of the angular momentum on a fixed direction of the laboratory coordinate system. Therefore, we have:

$$\mathbf{P^2}\Psi_{J,K_a} = \hbar^2 J(J+1)\Psi_{J,K_a} \tag{21}$$

$$\mathbf{P_a}\Psi_{J,K_a} = \hbar^2 K_a \Psi_{J,K_a} \quad (22)$$

$$\mathbf{H_r}\Psi_{J,K_a} = E_{J,K_a}\Psi_{J,K_a} \quad (23)$$

where J is the quantum number associated with the rotational angular momentum, K_a is the quantum number associated with the projection of the angular momentum on the a-axis of the molecular coordinate system with $K_a = -J, -J+1, \ldots, J-1, J$ and ħ is defined as the reduced Planck constant ħ = h/2π.

By solving the Schrodinger equation, given in Eqn. (23), the energy eigenvalues of a prolate top are given as:

$$E_{J,K_a} = \mathrm{h}[BJ(J+1) + (A-B)K_a^2] \quad (24)$$

Analogously, the energy of an oblate top is written:

$$E_{J,K_c} = \mathrm{h}[BJ(J+1) + (C-B)K_a^2] \quad (25)$$

here K_c is a quantum number associated with the projection of the angular momentum on the c-axis of the molecular coordinate system.

b. Asymmetric Tops

To indicate the asymmetry of a molecule, we use the Ray's asymmetry parameter κ[15]:

$$\kappa = \frac{2B - A - C}{A - C} \quad (26)$$

The value of κ is in the range of [−1,1] with two limitations of κ = −1,1 for prolate tops and oblate tops, respectively. All other values of κ associate with asymmetric molecules.

The selection rules for an asymmetric top are are $\vec{\mu} \neq 0$, and $\Delta J = 0, \pm 1$. Based on the value of ΔJ, the rotational transition can be classified into several branches, e.g.,

P-branch	Q-branch	R-branch
$\Delta J = -1$	$\Delta J = 0$	$\Delta J = +1$

Depending on the value(s) of projected dipole moment $\vec{\mu}$ into the *a*-, *b*-, *c*- inertial principal axes, *a*, *b*, *c* type transitions can be observable. The classifications of different types rotational transitions are based on

a-type ($\vec{\mu}_a \neq 0$)	*b*-type ($\vec{\mu}_b \neq 0$)	*c*-type ($\vec{\mu}_c \neq 0$)
ΔK_a = even ΔK_c = odd	ΔK_a = odd ΔK_c = odd	ΔK_a = odd ΔK_c = even

For an asymmetric top, each rotational energy associated with a quantum number J has $2J + 1$ sub-levels energies (Fig. 3). The $2J + 1$ energy sub-levels of an asymmetric top are labeled as JK_aK_c with K_a of a prolate top and K_c of an oblate top quantum numbers as indicating in Fig. 3.

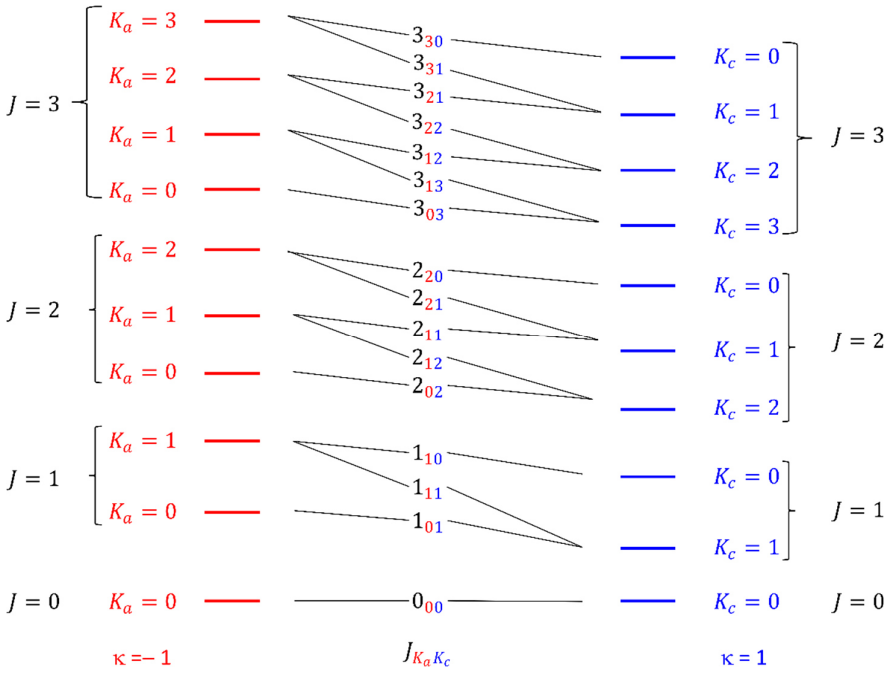

FIG. 3. Labelling scheme of the rotational energy levels for oblate (κ = 1), prolate (κ = −1), and asymmetric tops using angular momentum quantum numbers *J*, and the quantum numbers K_a and K_c from the prolate and oblate side, respectively.

2. Semi-rigid rotor due to quartic centrifugal distortion

To take into account the centrifugal distortion effect, the Hamiltonian is extended by a term $\mathbf{H_{cd}}$

$$\mathbf{H} = \mathbf{H_r} + \mathbf{H_{cd}} \tag{27}$$

where $\mathbf{H_r}$ is the Hamiltonian of the rigid rotor described in section **1** and $\mathbf{H_{cd}}$ is the Hamiltonian related to the centrifugal distortional energy.

In **1977**, Watson introduced the Watson's A and Watson's S reductions which are two main methods to deal with semi-rigid rotor effects due to quartic centrifugal distortion[16].

In order to treat an asymmetric top, Watson's A reduction is used and the Hamiltonian can be written as the following equation:

$$\begin{aligned}\mathbf{H_{cd}} = -\Delta_J \mathbf{P^4} - \Delta_{JK}\mathbf{P^2 P_a^2} - \Delta_K \mathbf{P_a^4} - 2\delta_J \mathbf{P^2}\left(\mathbf{P_b^2} - \mathbf{P_c^2}\right) \\ - \delta_K\left[\mathbf{P_a^2}\left(\mathbf{P_b^2} - \mathbf{P_c^2}\right) + \left(\mathbf{P_b^2} - \mathbf{P_c^2}\right)\mathbf{P_a^2}\right]\end{aligned} \tag{28}$$

where Δ_J, Δ_{JK}, Δ_K, δ_J, δ_K are the five quartic centrifugal distortion constants.

Watson's S reduction is used for near symmetric top and $\mathbf{H_{cd}}$ is written as:

$$\mathbf{H_{cd}} = -D_J \mathbf{P^4} - D_{JK}\mathbf{P^2 P_a^2} - D_K \mathbf{P_a^4} + d_1 \mathbf{P^2}(\mathbf{P_+^2} - \mathbf{P_-^2}) + d_2(\mathbf{P_+^4} - \mathbf{P_-^4}) \tag{29}$$

where $\mathbf{P_+} = \mathbf{P_a} + i\mathbf{P_b}$ and $\mathbf{P_-} = \mathbf{P_a} - i\mathbf{P_b}$ are the step-up and step-down operators.

3. Nuclear Quadrupole Coupling

a. One ^{14}N nucleus

For molecules which contain ^{14}N with nuclear spin $I = 1$, their spectra are complicated due to the nuclear quadrupole hyperfine effects. The nuclear quadrupole coupling effect arises due to the interaction between a non-spherical distribution of the nuclear charge (which results in a nuclear electric quadrupole moment) and a non-spherical distribution of the electronic charge around the nucleus. A nuclear with nuclear spin $I > ½$ causes non-spherical distribution of its nuclear charge, thus inducing a non-zero nuclear quadrupole moment.

The rotational angular momentum (**J**) vector couples with the nuclear spin angular momentum (**I**) to give the total angular momentum vector (**F**):

$$\mathbf{F} = \mathbf{J} + \mathbf{I} \tag{30}$$

here F can take the values of $F = |J - \mathrm{I}|, \ldots, J + \mathrm{I}$.

With the targeted molecular systems in my thesis, we will only consider the nuclear hyperfine interaction originating from the nitrogen atom ^{14}N with $I = 1$. As derived by Casimir[17], the Hamiltonian describing the quadrupole coupling interaction of ^{14}N is expressed as:

$$\mathbf{H_Q} = \frac{eQq_J}{2J(2J-1)I(2I-1)}\left[3(\mathbf{I}.\mathbf{J})^2 + \frac{3}{2}\mathbf{I}.\mathbf{J} - \mathbf{I^2J^2}\right] \tag{31}$$

with e is the charge of an electron, Q is the nuclear quadrupole moment and q_J is associated with electric field gradient at the site of the nucleus, **I**, **J** are nuclear spin and rotational angular momentum, both are given in the units of h/2π.

The energy eigenvalues of $\mathbf{H_Q}$ are given by:

$$E_Q = \frac{eQq_J}{2J(2J-1)I(2I-1)}\left[\frac{3}{4}C(C+1) - J(J+1)I(I+1)\right] \tag{32}$$

with

$$C = F(F+1) - J(J+1) - I(I+1) \tag{33}$$

The term eQq_J is known as the quadrupole coupling tensor χ, defined as:

$$\chi = eQq_J \tag{34}$$

Fig. 4 shows the effect of a non-spherical distribution of the electronic charge around the ^{14}N nucleus with the different projections of the angular momentum **I** along a fixed axis ($M_I = -I, -I+1, \ldots, I$) on two energy levels of an asymmetric top for the rotational quantum number $J = 0$ and 1. Each rotational energy level is split into different hyperfine components. Because of this effect, several hyperfine transitions will be observed (instead of only one rotational transition, with the selection rules[13] $\Delta F = 0, \pm 1$.

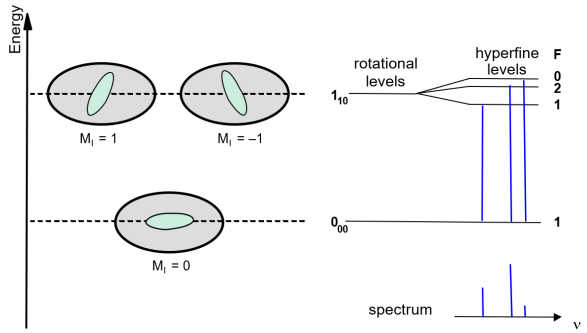

FIG. 4. Schematic description of the non-spherical distribution of the electronic charge around the ^{14}N nucleus corresponding with different projection of **I** (M_I) in the left-hand side. In the right-hand side, different hyperfine levels of given rotational levels for different values of the total quantum number F. Each rotational level can be split into several hyperfine levels resulting in several lines in obtained spectrum. Note that the figure is intended for qualitative illustration only.

b. Two ^{14}N nuclei

To treat the quadrupole coupling arising from two ^{14}N atoms, there are two coupling schemes: either ($I_1I_2I_{12}JFM_F$) as chosen in the *SPFIT*[18] and *PGOPHER*[19] codes, or the coupling ($JI_1F_1I_2FM_F$) which was implemented in the *WS18*, *TW21* and *BELGI-2N* programs. This later couping scheme means:

$$\begin{aligned} F_1 &= J + I_1, \\ F &= F_1 + I_2. \end{aligned} \tag{35}$$

For a given value of J, I_1, and I_2, the F can take the value in range of $F_{min} = \left||J - I_1| - I_2\right|$ and $F_{max} = J + I_1 + I_2$.

In case of two coupling nuclei, the Hamiltonian is

$$\mathbf{H_{hpf}} = \sum_{i=1}^{2} \mathbf{V(i)}^{(2)} \cdot \mathbf{Q(i)}^{(2)} \tag{36}$$

where $\mathbf{V(i)}^{(2)}$ and $\mathbf{Q(i)}^{(2)}$ are the electric field gradient and nuclear quadrupole second order tensor of the ith nuclear, respectively. Extensive explanations are given in Ref.[13]. In short, the matrix elements for the 1st and the 2nd nuclear atoms are given as (assuming $J = J'$)

$$\left\langle \tau J I_1 F_1 \middle| \mathbf{V(1)}^{(2)} \cdot \mathbf{Q(1)}^{(2)} \middle| \tau J I_1 F_1 \right\rangle = (-1)^{t_1} \left(eQq_{JJ}\right)_1 f(J) f(I_1) \begin{Bmatrix} F_1 & I_1 & J' \\ 2 & J & I_1 \end{Bmatrix} \tag{37}$$

$$\langle \tau J I_1 F_1' I_2 F | \mathbf{V}(\mathbf{2})^{(2)} \cdot \mathbf{Q}(\mathbf{2})^{(2)} | \tau J I_1 F_1 I_2 F \rangle$$
$$= (-1)^{t_2} \left(eQq_{JJ}\right)_2 f(J) f(I_2) [(2F_1+1)(2F_1'+1)]^{1/2} \times \begin{Bmatrix} J & F_1' & I_1 \\ F_1 & J & 2 \end{Bmatrix} \begin{Bmatrix} F & I_2 & F_1' \\ 2 & F_1 & I_2 \end{Bmatrix} \quad (38)$$

with

$$t_1 = J + I_1 + F_1, \qquad t_2 = J + I_1 + I_2 + 2F_1 + F, \quad (39)$$

$f(J)$, $f(I_1)$, $f(I_2)$ are calculated using Wigner *3j*-symbols, and $\begin{Bmatrix} F_1 & I_1 & J' \\ 2 & J & I_1 \end{Bmatrix}, \begin{Bmatrix} J & F_1' & I_1 \\ F_1 & J & 2 \end{Bmatrix}, \begin{Bmatrix} F & I_2 & F_1' \\ 2 & F_1 & I_2 \end{Bmatrix}$ are quantified using Wigner 6j-symbols, $\left(eQq_{JJ}\right)_i$ is quadrupole tensor χ of i^{th} N atom. τ represents additional quantum numbers.

4. Non-rigid rotor with internal rotation

For molecules which consist of two groups connected by a single bond, the groups can rotate with respect to each other about this bond. This large amplitude motion is called internal rotation. The effect of internal rotation on the rotational spectrum is that each rotational transition will exhibit a torsional find structure caused by the interaction of internal and overall rotation. This fine structure depends on the height of the potential barrier hindering the internal rotation. If the barrier is very high, the internal rotation of methyl group corresponds to simple harmonic torsional oscillation whereas if the barrier is very low, the internal motion corresponds to an almost free rotation. Internal rotation has been the subject of considerable number of investigations[14]. To describe the effects of internal rotation, additional terms must be added in the expression of the Hamiltonian with only pure rotation and centrifugal distortion:

$$\mathbf{H} = \mathbf{H_r} + \mathbf{H_{cd}} + \mathbf{H_{ir}} \quad (40)$$

The Hamiltonian $\mathbf{H_r} + \mathbf{H_{ir}}$ in Eqn. (40) can be expressed as:

$$\mathbf{H_r} + \mathbf{H_{ir}} = \mathbf{T} + \mathbf{V}(\boldsymbol{\alpha}) \quad (41)$$

where $\mathbf{T}$ is the kinetic energy and $\mathbf{V}(\boldsymbol{\alpha})$ represents the potential energy.

a. Kinetic energy T

In classical mechanics, the kinetic energy can be given as:

$$\mathrm{T} = \frac{1}{2}\vec{\omega}^{+}\mathrm{I}\vec{\omega} = \frac{1}{2}\vec{\mathrm{P}}^{+}\mathrm{I}^{-1}\vec{\mathrm{P}} \tag{42}$$

The form of Eqn. (42) is similar to what given in Eqn. (1). However, when internal rotations are observable, the dimensions of the angular velocity vector $\vec{\omega}$ and the moment of inertia tensor I increases by one per internal rotor.

For the molecules containing two internal tops (numbered 1 and 2), the angular velocity and the moment of inertia tensor will have the form[20]

$$\vec{\omega} = \begin{pmatrix} \omega_a \\ \omega_b \\ \omega_c \\ \omega_1 \\ \omega_2 \end{pmatrix} \tag{43}$$

and

$$\mathrm{I} = \begin{pmatrix} I_a & 0 & 0 & \lambda_{\alpha,1}I_{\alpha,1} & \lambda_{\alpha,2}I_{\alpha,2} \\ 0 & I_b & 0 & \lambda_{b,1}I_{\alpha,1} & \lambda_{b,2}I_{\alpha,2} \\ 0 & 0 & I_c & \lambda_{c,1}I_{\alpha,1} & \lambda_{c,2}I_{\alpha,2} \\ \lambda_{\alpha,1}I_{\alpha,1} & \lambda_{b,1}I_{\alpha,1} & \lambda_{c,1}I_{\alpha,1} & I_{\alpha,1} & 0 \\ \lambda_{\alpha,2}I_{\alpha,2} & \lambda_{b,2}I_{\alpha,2} & \lambda_{c,2}I_{\alpha,2} & 0 & I_{\alpha,2} \end{pmatrix} \tag{44}$$

with $\lambda_{i,n} = \cos(g_n, i)$, $i = a, b, c$ is the direction cosine of the internal rotation axis g_n (with n = 1 or 2) with respect to the principal axes, I_a, I_b, I_c are the moments of inertia of the whole molecule in the principal axis system and $I_{\alpha,n}$ is the moment of inertia of the internal rotor with n=1 or 2.

Due to the off-diagonal elements in the moment of inertia tensor I, the inverse moment of inertia tensors can be written as:

$$\frac{1}{2}\mathrm{I}^{-1} = \begin{pmatrix} \frac{1}{2I_a} + Z_{aa} & Z_{ba} & Z_{ac} & -Q_{\alpha,1} & -Q_{\alpha,2} \\ Z_{ba} & \frac{1}{2I_b} + Z_{bb} & Z_{bc} & -Q_{b,1} & -Q_{b,2} \\ Z_{ca} & Z_{cb} & \frac{1}{2I_c} + Z_{cc} & -Q_{c,1} & -Q_{c,2} \\ -Q_{\alpha,1} & -Q_{b,1} & -Q_{c,1} & F_1 & F_{12} \\ -Q_{\alpha,2} & -Q_{b,2} & -Q_{c,2} & F_{12} & F_2 \end{pmatrix} \tag{45}$$

with the elements of the tensor are:

$$Z_{ij} = Z_{ji} = \frac{\lambda_{i,1}\lambda_{j,1}I_{\alpha,1}^2}{I_i I_j} \cdot F_1 + \left(\frac{\lambda_{j,1}I_{\alpha,1}\lambda_{i,2}I_{\alpha,2}}{I_i I_j} + \frac{\lambda_{i,1}I_{\alpha,1}\lambda_{j,2}I_{\alpha,2}}{I_i I_j}\right) \cdot F_{12} + \frac{\lambda_{i,2}\lambda_{j,2}I_{\alpha,2}^2}{I_i I_j} \cdot F_2 \tag{46}$$

$$Q_{i,1} = \frac{\lambda_{i,1}I_{\alpha,1}}{I_i} \cdot F_1 + \frac{\lambda_{i,2}I_{\alpha,2}}{I_i} \cdot F_{12} \tag{47}$$

$$Q_{i,2} = \frac{\lambda_{i,1}I_{\alpha,1}}{I_i} \cdot F_{12} + \frac{\lambda_{i,2}I_{\alpha,2}}{I_i} \cdot F_2. \tag{48}$$

The remaining tensor elements can be calculated using the expression:

$$\begin{pmatrix} F_1 & F_{12} \\ F_{12} & F_2 \end{pmatrix} = \frac{1}{2} \cdot \begin{pmatrix} I_{\alpha,1}\left(1 - \sum_i \frac{\lambda_{i,1}^2 I_{\alpha,1}}{I_i}\right) & \sum_i \frac{\lambda_{i,1}\lambda_{i,2}I_{\alpha,1}I_{\alpha,2}}{I_i} \\ \sum_i \frac{\lambda_{i,1}\lambda_{i,2}I_{\alpha,1}I_{\alpha,2}}{I_i} & I_{\alpha,2}\left(1 - \sum_i \frac{\lambda_{i,2}^2 I_{\alpha,2}}{I_i}\right) \end{pmatrix}^{-1} \tag{49}$$

and the results are:

$$F_1 = \frac{1}{2} \cdot I_{\alpha,2}\left(1 - \sum_{\mathrm{i}} \frac{\lambda_{i,2}^2 I_{\alpha,2}}{I_i}\right) \cdot \mathrm{W} \tag{50}$$

$$F_2 = \frac{1}{2} \cdot I_{\alpha,1}\left(1 - \sum_{\mathrm{i}} \frac{\lambda_{i,1}^2 I_{\alpha,1}}{I_i}\right) \cdot \mathrm{W} \tag{51}$$

$$F_{12} = -\frac{1}{2} \cdot \mathrm{W} \cdot \sum_i \frac{\lambda_{i,1}\lambda_{i,2}I_{\alpha,1}I_{\alpha,2}}{I_i} \tag{52}$$

with

$$\mathrm{W} = \left[I_{\alpha,1}\left(1 - \sum_i \frac{\lambda_{i,1}^2 I_{\alpha,1}}{I_i}\right) I_{\alpha,2}\left(1 - \sum_i \frac{\lambda_{i,2}^2 I_{\alpha,2}}{I_i}\right) - \left(\sum_i \frac{\lambda_{i,1}\lambda_{i,2}I_{\alpha,1}I_{\alpha,2}}{I_i}\right)^2\right]^{-1} \tag{53}$$

From the Eqn. (46) to (49) above, F_1 and F_2 represent the reduced internal rotation constants which consider not only the motion of the top but also the countermotion of the frame. $F_{0,1}$ and $F_{0,2}$ are the rotational constants of the internal rotor(s), inversely proportional to the moment of inertia of the top ($I_{\alpha,n}$). Their values are usually found in range from 158 to 160 GHz for methyl groups. The relation between F_1 and $F_{0,1}$ is similar to the *mass* in the one-particle harmonic oscillator model and the *reduced mass* of a diatomic molecule. This is why during the fitting process, keeping the $F_{0,n}$ at a value compatible with the range mentioned above is encouraged. Finally, F_{12} is a parameter representing the kinetic coupling term between top 1 and top 2.

From Eqn. (44), it is clear that the rotational constants of molecules which contain internal rotation change to $A' = \frac{1}{2I_a} + Z_{aa}$, $B' = \frac{1}{2I_b} + Z_{bb}$, and $C' = \frac{1}{2I_c} + Z_{cc}$. The Eqn. (44) can then be rewritten as:

$$\frac{1}{2}\mathrm{I}^{-1} = \begin{pmatrix} A' & Z_{ba} & Z_{ac} & -Q_{\alpha,1} & -Q_{\alpha,2} \\ Z_{ba} & B' & Z_{bc} & -Q_{b,1} & -Q_{b,2} \\ Z_{ca} & Z_{cb} & C' & -Q_{c,1} & -Q_{c,2} \\ -Q_{\alpha,1} & -Q_{b,1} & -Q_{c,1} & F_1 & F_{12} \\ -Q_{\alpha,2} & -Q_{b,2} & -Q_{c,2} & F_{12} & F_2 \end{pmatrix} \tag{54}$$

Replacing the expression of I^{-1} into Eqn. (42), the kinetic energy **T** can be written as:

$$\mathbf{T} = \left(\frac{\mathbf{P_a^2}}{2I_a}\right) + \left(\frac{\mathbf{P_b^2}}{2I_b}\right) + \left(\frac{\mathbf{P_a^2}}{2I_a}\right) + F_1(\mathbf{p_1} - \boldsymbol{\pi_1})^2 + F_2(\mathbf{p_2} - \boldsymbol{\pi_2})^2 + F_{12}[(\mathbf{p_1} - \boldsymbol{\pi_1})(\mathbf{p_2} - \boldsymbol{\pi_2}) + (\mathbf{p_2} - \boldsymbol{\pi_2})(\mathbf{p_1} - \boldsymbol{\pi_1})] \tag{55}$$

with

$$\boldsymbol{\pi_n} = \sum_i \frac{\lambda_{i,n} I_{\alpha,n}}{I_i} \mathbf{P_i}\,, (i = a, b, c) \tag{56}$$

b. Potential energy $V(\alpha)$

The potential energy $V(\alpha)$ is described by a periodic function of the torsional angle α (defined in Ref.[13], page 572). The periodicity of the function depends on the number of equivalent configurations of the internal rotations (N). For a methyl group, usually N is 3 or 6 depending on the geometry of the attached frame.

Generally, for a molecule containing n methyl group(s), the potential energy can be written as a Fourier series:

$$V(\alpha) = \sum_{i=1}^{\mathrm{n}} \left[\frac{V_{3,i}}{2}(1 - \cos 3\alpha_i) \;+\; \frac{V_{6,i}}{2}(1 - \cos 6\alpha_i) \;+ \cdots\right] \tag{57}$$

For the seek of simplification, we will consider here the case of a molecule consisting of one internal rotor (n=1). Because there is only one rotor, the index *i* will also be omitted. In this case, the function can be given in the following form:

$$V(\alpha) = \frac{V_3}{2}(1 - \cos 3\alpha) \;+\; \frac{V_6}{2}(1 - \cos 6\alpha) \;+ \cdots \tag{58}$$

here, V_3 represents the "effective" height of the potential barrier of the internal rotation.

The Schrödinger equation which describes the one-dimensional internal rotation of a methyl group in the molecular potential $V(\alpha)$ can be written as:

$$\mathbf{H}\varphi(\alpha) = \left[-F\frac{\partial^2}{\partial\alpha^2} + V(\alpha)\right] = E\varphi(\alpha) \tag{59}$$

with F is the reduced internal rotational constant, as defined in Eqn. (50) or (51).

For the two limiting cases $V_3 \to 0$ and $V_3 \to \infty$, the solution for the equation above can be easily obtained.

- In case $V_3 \to 0$, the rotation of the methyl group is considered as an almost free rotor. The eigenfunction $\varphi^{(0)}(\alpha)$ and the energy eigenvalues $E^{(0)}$ are given[13]:

$$\varphi^{(0)}(\alpha) = Ae^{im\alpha} \tag{60}$$

$$E^{(0)} = Fm^2 \tag{61}$$

By applying the boundary condition $\varphi^{(0)}(\alpha) = \varphi^{(0)}(\alpha + 2\pi)$, the values for the quantum m can be easily obtained (m = 0, ±1, ±2, ±3, etc.). Each level is two-fold degenerate (except for m = 0), which corresponds to the different directions of the rotation in a classical picture.

- In case $V_3 \to \infty$ as presenting in Fig. 5

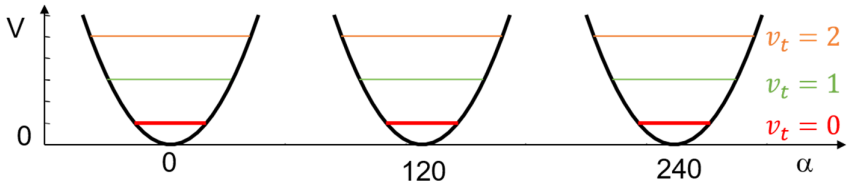

FIG. 5. The potential energy $V_3 \to \infty$ is described by a periodic function of the torsional angle α.

In this case, the term $\cos 3\alpha$ can be expressed using the Taylor series and the energy level can be described as:

$$E^{(\infty)} = \sqrt{3V_3F}\left(v_t + \frac{1}{2}\right), \tag{62}$$

with the quantum number v_t can take integer values. Each of torsional state is triply degenerate, which corresponds to a vibration in every well of the potential which are showed in Fig. 5.

- For the general problem when internal rotation is hindered by a finite barrier height, the periodic potential is illustrated in Fig. 6.

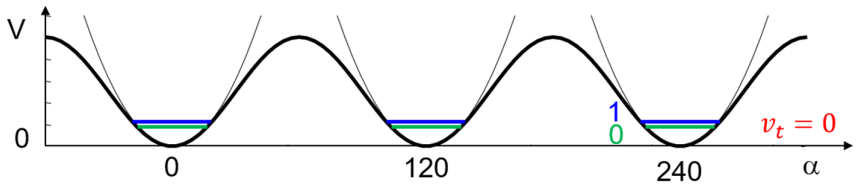

FIG. 6. The potential energy curve with finite height V_3 plotted as function of the torsional angle α.

Here, the Schrödinger equation can be rewritten as Mathieu equation[21], and the solutions are given by:

$$\varphi_{v_t\alpha} = |v_t\alpha\rangle = \sum_{k=-\infty}^{\infty} A_k^{(v_t)} e^{i(3k+\sigma)\alpha} \tag{63}$$

with k is an integer number. In Chap. 12 of Ref.[13], the calculation of the eigenvalues and the $A_k^{(v_t)}$ are given. When the barrier height is finite, tunneling can occur and the triply degenerate vibrational sub-levels mentioned above split into two degenerate levels designated with the quantum number $\sigma = \pm 1$ (associated with the symmetry label E) and one degenerate level with the quantum number $\sigma = 0$ (associated with the symmetry label A). The new quantum number σ defines the symmetry of the corresponding torsional wavefunction. It should also be noted that the transitions between $\sigma = 0$ or (0) and $\sigma = \pm 1$ or (1) are forbidden and that the only allowed transitions occur between two (0) or two (1) energy levels. Due to the Coriolis-like interaction which affects differently the (0) and the (1) levels, the energies of the rotational levels in (0) and (1) states are slightly different. This results in a (0)-(1) doublet in the rotational spectrum as depicted in Fig. 7.

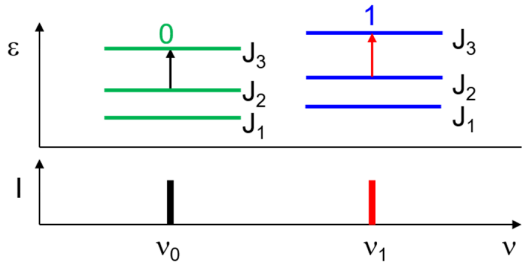

FIG. 7. Upper trace describes the rotational levels in (0) and (1) states whereas the lower trace illustrates the (0)-(1) doublet in the rotational spectrum.

In order to model the spectra of molecules which originating internal rotation, it is essential to derive an appropriate Hamiltonian which must take into account the over-all, the internal rotation and the coupling

of these two motions. In the following sections, several methods that we used during my thesis, e.g., the Principal Axis Method (PAM) and the Rho-Axis Method (RAM) for one- and two-top problems will be discussed.

5. Qualitative energy level diagram, from one-top to two-top

As mentioned above, when molecules contain one internal rotor, each rotational transition is split into two components call A ($\sigma = 0$) and E ($\sigma = \pm 1$). The rotational spectrum of a molecule with two internal rotors is even more complicated. For simplification, we will use here the semi-direct product notation reported by Ezra[22], using the quantum number σ level to characterize the energy diagram. This will intuitively guide us to understand how the rotational spectra look like when the effects from either one or two rotors are present. Fig. 8 shows a qualitative energy level diagram of $J = K = 0$ transitions, going from molecules with no torsion to one top, two inequivalent tops as well as two equivalent tops. In this figure, we use the notation (σ_1, σ_2) with $\sigma_i = 0, \mp 1$. For a better readability, we will designate the $\sigma_i = -1$ always by number 2.

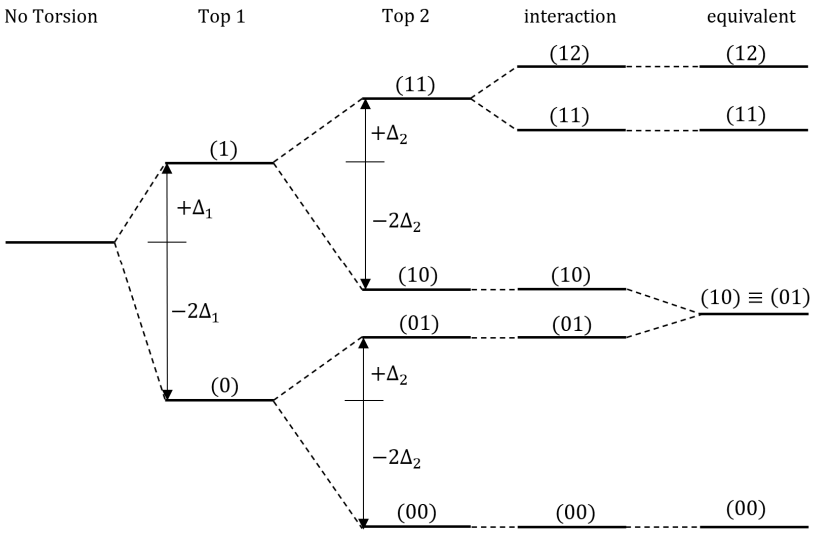

FIG. 8. Energy diagram of $J = K = 0$ transition for molecules with no torsion, with one top, and two tops in case inequivalent as well as equivalent. The diagram illustrated for $\Delta_1 > \Delta_2 > 0$ using semi-direct notation (σ_1, σ_2). This diagram is similar to Fig.2 introduced by *Ohashi et al.*[23]

At the very left side of Fig. 8, without any internal rotation, only one rotational transition is observed in the spectra. When one internal rotor is present, each rotational transition will be split into two

components (0) and (1) and they will be located at $-2\Delta_1$ and $+\Delta_1$, respectively (with $\Delta_1 > 0$). When the internal rotation of Top 2 is taken into account, each of those components will split into (0) and (1) levels, they will be shifted to positions at $-2\Delta_2$ and $+\Delta_2$, respectively (with $\Delta_2 > 0$) and in total will form four energy levels denoted as (00), (01), (10), (11). When there are some interactions between the two tops, the energy level (11) will split into two components called (11) and (12).

For two inequivalent tops, the five-energy level presented under the column (interaction) of Fig. 8. is obtained. In case the two tops are equivalent, that means (10) and (01) coincide due to symmetry. Details of group theory, spin statistic and selections rules will be further discussed in each chapter to report specific molecular characteristics.

6. Effective non-rigid Hamiltonians

a. Hamiltonian in the PAM for one top

For simplification, we will consider first the Hamiltonian for one top molecules. In the PAM method, the axis of internal rotation does not necessarily coincide with one of the principal axes. Using the Eqn. (55) with $F_2 = F_{12} = 0$, $F_1 = F$, and $\mathbf{p_1} = \mathbf{p_\alpha}$, we obtained the kinetic term for one top molecules. The Hamiltonian can then be given as:

$$\mathbf{H_{PAM}} = A\mathbf{P_a^2} + B\mathbf{P_b^2} + C\mathbf{P_c^2} + F(\mathbf{p_\alpha} - \rho_a\mathbf{P_a} - \rho_b\mathbf{P_b} - \rho_c\mathbf{P_c})^2 + \mathbf{V(\alpha)} \tag{64}$$

with

$$\mathbf{p_\alpha} = -i\frac{\partial}{\partial\alpha}, \quad \rho_g = \frac{\lambda_g I_\alpha}{I_g}, \quad g = a, b, c \tag{65}$$

and

$$F = \frac{\hbar}{2\mathrm{r}I_\alpha}, \quad r = 1 - \sum_{g=a,b,c}\lambda_g^2\frac{I_\alpha}{I_g} \tag{66}$$

In the expression from Eqn. (64) and (65), $\mathbf{p_\alpha}$ and $\mathbf{I_\alpha}$ are the angular momentum operator and the moment of inertia of the internal rotor in the principal axis system, respectively. The cross terms (also called as Coriolis-like terms, e.g., $-2F\mathbf{p_\alpha}\rho_g\mathbf{P_g}$) act on both, the symmetric rotor basic $|JKM\rangle$ (see Eqn.

(21-23)) and the torsional wavefunction $|v_t\sigma\rangle$ (see Eqn. (63)), therefore it is not possible to separate the Hamiltonian into a pure rotational part and a pure torsional part.

If the barrier height is high enough, it will give rise to larger difference between each v_t torsional energy levels compared with the rotational levels. In such cases, the internal rotation can be considered parametrically into the Hamiltonian as perturbation terms. The PAM Hamiltonian can be rewritten for a given torsional state $|v_t\sigma\rangle$ using Van-Vleck transformation[14] as:

$$\mathbf{H_{int,\,v_t\sigma}} = A\mathbf{P_a^2} + B\mathbf{P_b^2} + C\mathbf{P_c^2} + F\sum_n W_{v_t\sigma}^{(n)}\,(\rho_a\mathbf{P_a} + \rho_b\mathbf{P_b} + \rho_c\mathbf{P_c})^{\mathrm{n}} \tag{67}$$

with the first three perturbation coefficients[14]:

$$W_{v_t\sigma}^{(0)} = E_{v_t\sigma} \tag{68}$$

$$W_{v_t\sigma}^{(1)} = -2\langle v_t\sigma|\mathbf{p_\alpha}|v_t\sigma\rangle \tag{69}$$

$$W_{v_t\sigma}^{(2)} = 1 + 4F\sum_{v_t'}\frac{|\langle v_t\sigma|\mathbf{p_\alpha}|v_t'\sigma\rangle|^2}{E_{v_t\sigma} - E_{v_t'\sigma}} \tag{70}$$

The perturbation coefficients $W_{v_t\sigma}^{(n)}$ depend on the reduced barrier height $s = 4V_3/9F$. These coefficients (except for n = 0) increase with the barrier height. The zeroth order term ($W_{v_t\sigma}^{(0)}$) is only a torsional energy contribution and does not affect the rotational spectrum. The first order term ($W_{v_t\sigma}^{(1)}$) is zero for the (0) species, but non-zero for the degenerate (1) species. The second order term ($W_{v_t\sigma}^{(2)}$) is different for the (0) and (1) species of a given v_t state[13, 14].

In general, the Hamiltonian for any molecules with n rotors can also be written as sum of the kinetic term given in Eqn. (55) and the potential term given in Eqn. (57).

b. Hamiltonian in the RAM for one top

A more general approach to overcome the problem of impeding a separation of the Hamiltonian is called RAM method. In the RAM, which was initially developed by Dennison, Hecht and others who called internal axis method, (see the review of Ref.[14] and references therein) and in its modern form by Herbst

et al.[24], the coupling terms between internal and global rotation are eliminated at the zeroth order. This was an important simplification for the calculation at that time.

This elimination of the zeroth order coupling terms is accomplished through a rotation of the axes by an angle judiciously chosen (θ_{RAM}). In the case of molecules which have a plane of symmetry, θ_{RAM} can be calculated using the following equation:

$$\theta_{\mathrm{RAM}} = \arctan\left(\frac{\rho_x}{\rho_z}\right) = \arctan\left(\frac{I_z\lambda_x}{I_x\lambda_z}\right) \tag{71}$$

This rotation with respect to the system of principal axes makes the new z-axis parallel to the ρ vector. This is why it was called the Rho method (Rho Axis Method)[25, 26].

The RAM torsion-rotation Hamiltonian[25] can be given as:

$$\begin{aligned}\mathbf{H_{RAM}} = F(\mathbf{p_\alpha} - \rho\mathbf{P_z})^2 + \mathbf{V}(\boldsymbol{\alpha}) + A(\cos\theta_{\mathrm{RAM}}\mathbf{P_z} - \sin\theta_{\mathrm{RAM}}\mathbf{P_x})^2 \\ +B(\sin\theta_{\mathrm{RAM}}\mathbf{P_z} + \cos\theta_{\mathrm{RAM}}\mathbf{P_x})^2 + C\mathbf{P_y^2}\end{aligned} \tag{72}$$

with the torsional Hamiltonian

$$\mathbf{H_T} = F(\mathbf{p_\alpha} - \rho\mathbf{P_z})^2 + \mathbf{V}(\boldsymbol{\alpha})\,, \tag{73}$$

the over-all rotation Hamiltonian

$$\mathbf{H_r} = A(\cos\theta_{\mathrm{RAM}}\mathbf{P_z} - \sin\theta_{\mathrm{RAM}}\mathbf{P_x})^2 + B(\sin\theta_{\mathrm{RAM}}\mathbf{P_z} + \cos\theta_{\mathrm{RAM}}\mathbf{P_x})^2 + C\mathbf{P_y^2}. \tag{74}$$

By transformation, the rotational Hamiltonian can be given in form:

$$\mathbf{H_r} = A_{RAM}\mathbf{P_z^2} + B_{RAM}\mathbf{P_x^2} + C_{RAM}\mathbf{P_y^2} + D_{ab}(\mathbf{P_z}\mathbf{P_x} + \mathbf{P_x}\mathbf{P_z}) \tag{75}$$

In the case of prolate top, using I^r representation ($z \to a, x \to b$ and $y \to c$) and the rotational Hamiltonian will be written as:

$$\mathbf{H_r} = A_{RAM}\mathbf{P_a^2} + B_{RAM}\mathbf{P_b^2} + C_{RAM}\mathbf{P_c^2} + D_{ab}(\mathbf{P_a}\mathbf{P_b} + \mathbf{P_b}\mathbf{P_a}) \tag{76}$$

here

$$A_{RAM} = A\cos^2\theta_{\mathrm{RAM}} + B\sin^2\theta_{\mathrm{RAM}}, \tag{77}$$

$$B_{RAM} = A\sin^2\theta_{\mathrm{RAM}} + B\cos^2\theta_{\mathrm{RAM}}, \tag{78}$$

$$C_{RAM} = C \tag{79}$$

$$D_{ab} = (B - A)\cos\theta_{\mathrm{RAM}}\sin\theta_{\mathrm{RAM}} \tag{80}$$

where A, B, C are the rotational constants in PAM and

$$\tan(2\theta_{RAM}) = \frac{-2D_{ab}}{A_{RAM} - B_{RAM}}. \quad (81)$$

It should be mentioned that the RAM approach is only applicable for molecules with only one internal rotation and although the use of the RAM approach allows us to eliminate the torsion-rotation coupling terms at zeroth order, higher order terms of the Hamiltonian still contain torsion-rotation interaction terms. The higher order terms are product of one (or several) torsion operator(s) and one or several over-all rotation operator(s) at different powers. All terms are used for investigated molecular systems are given in Table 1. We note that the *BELGI* codes and the *TW21* code as well as the *RAM36* code written by *Ilyushin et al.* rely on this RAM method.

Table 1: Non-exhaustive list of high order terms for a C_s asymmetric top molecule containing an C_{3v} internal rotor in the RAM axis system implemented in program *BELGI*.

Rotation \ Torsion	1	$\mathbf{1-\cos(3\alpha)}$	$\mathbf{p_\alpha^2}$	$\mathbf{P_a p_\alpha}$
$\mathbf{1}$		$\frac{V_3}{2}$	F	ρ
$\mathbf{P^2}$	$\frac{B+C}{2}$	F_v	G_v	L_v
$\mathbf{P_a^2}$	$A-\frac{B+C}{2}$	k_5	k_2	k_1
$\mathbf{P_b^2 - P_c^2}$	$\frac{B-C}{2}$	c_2	c_1	c_4
$\{\mathbf{P_a}, \mathbf{P_b}\}$	D_{ab}	d_{ab}	Δ_{ab}	δ_{ab}
$\mathbf{-P^4}$	D_J	f_v	g_v	l_v
$\mathbf{-P^2 P_a^2}$	D_{JK}	k_{5J}	$-k_{2J}$	$-k_{1J}$
$\mathbf{-P_a^4}$	D_K	k_{5K}	k_{2K}	k_{1K}
$\mathbf{-2P^2(P_b^2 - P_c^2)}$	δ_J	c_{2J}	c_{1J}	c_{4J}
$-\{\mathbf{P_a^2}, (\mathbf{P_b^2 - P_c^2})\}$	δ_K	c_{2K}	c_{1K}	c_{4K}

$\mathbf{P_a}$, $\mathbf{P_b}$ and $\mathbf{P_c}$ are the rotational angular momentum components. $\mathbf{p_\alpha}$ is the internal angular momentum associated with the methyl group rotation by an angle α. {u,v} is the anti-commutator uv + vu. I^r representation and the A reduction of the Watson Hamiltonian for the centrifugal distortions are used.

c. Hamiltonian in the quasi-PAM for two-top

To analyze the spectrum of a two-top molecule, we used the Hamiltonian in the axis system called "quasi-PAM". This method takes its name from the fact that the coefficient of the three quadratic terms of the operators $\left(\mathbf{P_x P_y + P_y P_x}\right)$, $(\mathbf{P_x P_z + P_z P_x})$ and $\left(\mathbf{P_y P_z + P_z P_y}\right)$ from Eqn. (55) are set to zero. Following this procedure described by *Ohashi et al.*[23] for the N-methylacetamide, the rotation-torsion Hamiltonian $\mathbf{H_{RT}}$ is given as:

$$\begin{aligned}
\mathbf{H_{RT}} = {} & A'\mathbf{P_z^2} + B'\mathbf{P_x^2} + C'\mathbf{P_y^2} - \Delta_J\mathbf{P^4} - \Delta_{JK}\mathbf{P^2P_z^2} - \Delta_K\mathbf{P_z^4} - \delta_J 2\mathbf{P^2}\left(\mathbf{P_x^2} - \mathbf{P_y^2}\right) \\
& - \delta_K\{\mathbf{P_z^2}, \left(\mathbf{P_x^2} - \mathbf{P_y^2}\right)\} + f_1\mathbf{p_{\alpha 1}^2} + f_2\mathbf{p_{\alpha 2}^2} + f_{12}\mathbf{p_{\alpha 1}p_{\alpha 2}} \\
& + \frac{1}{2}V_{31}(\mathbf{1 - \cos 3\alpha_1}) + \frac{1}{2}V_{32}(\mathbf{1 - \cos 3\alpha_2}) \\
& + V_{12C}\,(\mathbf{1 - \cos 3\alpha_1})(\mathbf{1 - \cos 3\alpha_2}) + V_{12S}\,\mathbf{\sin 3\alpha_1 \sin 3\alpha_2} \\
& + \left(q_1 + q_{1J}\,\mathbf{P^2} + q_{1K}\mathbf{P_z^2}\right)\mathbf{P_z p_{\alpha 1}} + \left(q_2 + q_{2J}\,\mathbf{P^2} + q_{2K}\mathbf{P_z^2}\right)\mathbf{P_z p_{\alpha 2}} \\
& + \left(r_1 + r_{1J}\mathbf{P^2}\right)\mathbf{P_x p_{\alpha 1}} + \frac{1}{2}r_{1K}\,\{\mathbf{P_z^2}, \mathbf{P_x}\}\mathbf{p_{\alpha 1}} + \left(r_2 + r_{2J}\mathbf{P^2}\right)\mathbf{P_x p_{\alpha 2}} \\
& + \frac{1}{2}r_{2K}\,\{\mathbf{P_z^2}, \mathbf{P_x}\}\mathbf{p_{\alpha 2}} + \left(A_1\mathbf{p_{\alpha 1}^2} + A_2\mathbf{p_{\alpha 2}^2}\right)\mathbf{P_z^2} \\
& + \left(B_1\mathbf{p_{\alpha 1}^2} + B_2\mathbf{p_{\alpha 2}^2} + B_{12}\mathbf{p_{\alpha 1}p_{\alpha 2}}\right)\mathbf{P_x^2} \\
& + \left(C_1\mathbf{p_{\alpha 1}^2} + C_2\mathbf{p_{\alpha 2}^2} + C_{12}\mathbf{p_{\alpha 1}p_{\alpha 2}}\right)\mathbf{P_y^2} - \left(\Delta_{1J}\mathbf{p_{\alpha 1}^2} + \Delta_{2J}\mathbf{p_{\alpha 2}^2}\right)\mathbf{P^4} \\
& - \left(\Delta_{1JK}\mathbf{p_{\alpha 1}^2} + \Delta_{2JK}\mathbf{p_{\alpha 2}^2}\right)\mathbf{P^2P_z^2} - \left(\Delta_{1K}\mathbf{p_{\alpha 1}^2} + \Delta_{12K}\mathbf{p_{\alpha 1}p_{\alpha 2}}\right)\mathbf{P_z^4} \\
& + q_{12p}\mathbf{p_{\alpha 1}p_{\alpha 2}}(\mathbf{p_{\alpha 1}} + \mathbf{p_{\alpha 2}})\mathbf{P_z} + q_{12m}\mathbf{p_{\alpha 1}p_{\alpha 2}}(\mathbf{p_{\alpha 1}} - \mathbf{p_{\alpha 2}})\mathbf{P_z} \\
& + r_{12p}\mathbf{p_{\alpha 1}p_{\alpha 2}}(\mathbf{p_{\alpha 1}} + \mathbf{p_{\alpha 2}})\mathbf{P_x} + r_{12m}\mathbf{p_{\alpha 1}p_{\alpha 2}}(\mathbf{p_{\alpha 1}} - \mathbf{p_{\alpha 2}})\mathbf{P_x}
\end{aligned} \tag{82}$$

7. Computer programs

Several programs have been developed in the literature in order to deal with internal rotation, i.e., *XIAM*[27], *BELGI* in its C_s (for molecules containing a plane of symmetry)[28] and C_1 (for molecules with no plane of symmetry)[29] versions, *ERHAM*[30], *RAM36*[31] and more recently an extended version of *XIAM*, *XIAMmod*[32]. These programs and their guideline are available at the website managed by Prof. Z. Kisiel, http://www.ifpan.edu.pl/~kisiel/prospe.htm. A number of investigated molecules containing internal rotation were also studied using the *JB95* program provided by Plusquellic[33] which used a perturbative

method in the principal axis system as well as by the program *IAMCALC* which is integrated in Pickett's suite containing *SPFIT* and *SPCAT* codes (see also http://spec.jpl.nasa.gov/). Recently two new codes, *ntop*[34] and *aixPAM*[35], were also written by Prof. Wolfgang Stahl. Both programs employed the principal axis system. While *aixPAM* is restricted to the fitting one internal rotation, *ntop* code can treat an arbitrary number of tops. However, no hyperfine interactions are implemented yet in those two last codes.

In the following of this chapter, only a short review about the three programs which were used in my thesis, the progams *XIAM*, *BELGI* and *WS18* will be given.

a. The *XIAM* code

One of the most-used programs to fit internal rotation is the *XIAM*[27] program which employs the so-called Combined Axis Method (CAM) for which a first version was initially developed by Woods[36]. In the *XIAM* code, the torsional energies of each single top are evaluated in their individual rho-axis system (RAM) and then they are transformed to the principal axis system (PAM). In the RAM, the eigenvalues are conveniently calculated in the product basis of symmetric top functions for the overall rotation and internal rotor functions for the torsion (due to the elimination of coupling terms as mentioned earlier).

With the *XIAM* program[27], the rotational spectra of molecules with up to three internal rotors can be fitted. We can float the following molecular parameters: the rotational constants (*A*, *B*, *C*), centrifugal distortion constants, both Watson's A and Watson's S reductions are allowed (see Eqn. (28) and (29)), the potential value V_3, the angles which determine the internal axis within the principal system, the reduced rotational constants *F* and some higher order terms such as D_{pi2J}, D_{pi2K}, and D_{pi2-} which are associated with the operators $2(\mathbf{p_\alpha} - \rho\mathbf{P_r})^2\mathbf{P^2}$, $\{(\mathbf{p_\alpha} - \rho\mathbf{P_r})^2, \mathbf{P_a^2}\}$, and $\{(\mathbf{p_\alpha} - \rho\mathbf{P_r})^2, (\mathbf{P_b^2} - \mathbf{P_c^2})\}$[27] with $\mathbf{P_r}$ is the angular momentum vector along the rho axis. More details given by the authors as well as guidelines on the available parameters and how to use program are given in the website http://www.ifpan.edu.pl/~kisiel/prospe.htm.

b. The *BELGI* codes

The *BELGI* programs are also well-known for treating internal rotation(s). The codes exist in various versions dealing with one internal rotor (written exclusively using the RAM approach) and with two internal rotors (using the quasi-PAM approach). There are also versions which take into account either one or two weakly nuclear quadrupole coupling arising from ^{14}N.

- ***BELGI-C_s* code**

Note that in the Hamiltonian in the rho-axis system as given in Eqn. (72), all operators contain the torsional angle α or its zeroth order conjugate momentum p_α are diagonal in the quantum number *K*. All non-diagonal matrix elements in *K* come from the rotational part of this Hamiltonian. It enables the separation of the wavefunctions and therefore allows to perform the matrix elements in two-step procedure. In the first step, the matrix of torsional Hamiltonian is setup and diagonalized for each *K* value and each symmetry species (A and E). In the second step, the matrix elements of the rotational, centrifugal distortion and higher order terms of the rotation-torsion interactions are calculated and diagonalized. A number of allowed terms are listed in Table. 1 above.

This two-step diagonalization procedure enabled Herbst and his collaborators to offer for the first time a modern version of RAM method[24]. The authors applied this method to a series of molecules, including for example the acetaldehyde[37] CH_3CHO and the methanol[24,38] CH_3OH molecules. The *BELGI* program is based on the same procedure as presented by Herbst *et al*[24].

In the first step, the matrix elements of torsion Hamiltonian $\mathbf{H_T}$:

$$\mathbf{H_T} = F(\mathbf{p_\alpha} - \rho\mathbf{P_z})^2 + \mathbf{V(\alpha)} \tag{83}$$

is diagonalized for each value of *K* and for each symmetry species σ (A and E) using the following basis set wavefunctions

$$|Kk\sigma\rangle = \frac{1}{\sqrt{2\pi}} |K\rangle e^{i(3k+\sigma)\alpha} \tag{84}$$

where *k* is an integer between -10 and $+10$, $|K\rangle$ is the eigenfunction for a symmetric top and σ is a symmetry index, $\sigma = 0$ for the A species and $\sigma = \pm 1$ for the E species as mentioned above.

The torsional eigenvectors obtained from the first step are:

$$\varphi = \sum_{k=-10}^{10} A_{3k+\sigma}^{K,v_t} \exp[i(3k+\sigma)\alpha]\,|K\rangle \tag{85}$$

In the second step, the rest of the Hamiltonian is setup and then diagonalized with the basis set is product of the eigenvectors in Eqn. (84) and the symmetric top eigenfunctions $|JKM\rangle$.

While *XIAM* code treats each J block considering only the torsional ground state $v_t = 0$, in the *BELGI-C_s* code, the truncation of the second matrix is fixed at $v_t = 8$ and thus it involves the first nine torsional states. Therefore, this enables us to correctly calculate the energy of the lowest torsional states. That is why *BELGI* code is often called a "global" method whereas *XIAM* is called a "local" method.

- ***BELGI-hyperfine* codes**

The program *BELGI* has been extended in its hyperfine versions named *BELGI-C_s-hyperfine* for molecules which contain one rotor and have all heavy atoms lying in a plane of symmetry (C_s symmetry), allowing us to take into account the effects arising from one weakly coupling nucleus as ^{14}N. Prior to my work, this code has successfully applied for several molecules such as *N-tert*-butylacetamide[39] and 3-nitrotoluence[40].

In the *BELGI-C_s-hyperfine* code, the quadrupole energies for each rotational transition in a given torsional state caused by the ^{14}N nucleus are calculated using the perturbation approach. The hyperfine energy expression is:

$$\begin{aligned} E_{hf}\,(I,J,F) = 2\frac{f(I,J,F)}{J(J+1)}[\chi_{aa}\langle \mathbf{P_z^2}\rangle + \chi_{bb}\langle \mathbf{P_x^2}\rangle - (\chi_{aa}+\chi_{bb})\,\langle \mathbf{P_z^2}\rangle \\ + \chi_{ab}\langle \mathbf{P_z P_x} + \mathbf{P_x P_z}\rangle] \end{aligned} \tag{86}$$

with the Casimir function $f(I,J,F)$[17].

In *BELGI-C_s-hyperfine*, the numerical expectation values of the quadratic angular momentum components $\langle \mathbf{P_x^2}\rangle$, $\langle \mathbf{P_y^2}\rangle$, $\langle \mathbf{P_z^2}\rangle$ and $\langle \mathbf{P_z P_x} + \mathbf{P_x P_z}\rangle$ are first quantified. They are then included into the Eqn. (86). This method allows us to determine the structure of all hyperfine patterns and subsequently take the nuclear quadrupole coupling constants into account in a global fit which already treats the internal rotation of the methyl group.

During my thesis, to analyze the spectra of 45DMTA and 25DMP, I participated to implement the extension of the *BELGI-C_s-2Tops-hyperfine* and *BELGI-C_{2v}-2Tops-hyperfine*. The calculation of the hyperfine splittings is essentially the same as what had been done for one top code. To consider the effects of one internal rotor and two ^{14}N quadrupole nuclei, a new feature was implemented into the *BELGI* code. The new version is called *BELGI-2N*, the implementations were done based on Eqn. (35-39).

c. The *WS18* code

The *WS18* code was written by Prof. W. Stahl in 2018 at the RWTH Aachen University. It was tested on a number of molecules and it was also used during my thesis. The *WS18* code shows some similarities to the *JB95* code[33], as both programs allow to separately fit each symmetry and therefore, we refer to their Hamiltonian as effective Hamiltonian using the local approach. The Hamiltonian in *WS18* is highly flexible, it can be conveniently used for molecules with one but also two or even an arbitrary number of internal rotors. The Hamiltonian is developed in an expansion of the even and odd order terms of angular momentum operators of the overall rotation. The fitted parameters usually show less correlations than those obtained with the RTRF model. However, it is more difficult to give a physical interpretation of the effective Hamiltonian.

The effective Hamiltonian as it is used in our study is:

$$\mathbf{H} = \mathbf{H_r} + \mathbf{H_{cd}} + \mathbf{H_o} + \mathbf{H_{nq}} \tag{87}$$

The pure rotational part:

$$\mathbf{H_r} = A\mathbf{P_z^2} + B\frac{1}{4}(\mathbf{P_+^2} + \mathbf{P_-^2} + \mathbf{P_+P_-} + \mathbf{P_-P_+}) - C\frac{1}{4}(\mathbf{P_+^2} + \mathbf{P_-^2} - \mathbf{P_+P_-} - \mathbf{P_-P_+}) \tag{88}$$

the quartic centrifugal distortion terms:

$$\begin{aligned}\mathbf{H_{cd}} = -\Delta_J\mathbf{P^4} - \Delta_{JK}\mathbf{P^2P_z^2} - \Delta_K\mathbf{P_z^4} - \delta_J(\mathbf{P^2P_+^2} + \mathbf{P^2P_-^2}) \\ - \delta_K\tfrac{1}{2}\{\mathbf{P_z^2P_+^2} + \mathbf{P_z^2P_-^2} + \mathbf{P_+^2P_z^2} + \mathbf{P_-^2P_z^2}\}\end{aligned} \tag{89}$$

the odd order terms:

$$\mathbf{H_o} = q\mathbf{P_z} + r\frac{1}{2}(\mathbf{P_+} + \mathbf{P_-}) + q_J\mathbf{P^2P_z} + q_K\mathbf{P_z^3} + r_J\frac{1}{2}(\mathbf{P^2P_+} + \mathbf{P^2P_-}) + \cdots \quad (90)$$

and the nuclear quadrupole coupling Hamiltonian:

$$\mathbf{H_{nq}} = \mathbf{V^{(2)}} \cdot \mathbf{Q^{(2)}},\ \chi_{aa} = 2eQV_0^{(2)},\ \chi_{bb} - \chi_{cc} = \sqrt{6}eQ(V_2^{(2)} + V_{-2}^{(2)}) \quad (91)$$

where the operators are written in terms of the $\mathbf{P_z}$ and the step-up, step-down operators:

$$\mathbf{P_+} = \mathbf{P_x} + i\mathbf{P_y},\ \mathbf{P_-} = \mathbf{P_x} - i\mathbf{P_y}. \quad (92)$$

The Hamiltonian matrix is set up in the symmetric top basis, only matrix elements diagonal in the rotational quantum number J were considered, leading to a matrix size of $(2J + 1)$ x $(2J + 1)$ which makes it comparably fast and well-suited for the assignment processes. Both real and complex matrices elements are allowed, therefore the code can be used for all point groups of the frame symmetry. An important feature of the *WS18* code is the possibility to add effective Hamiltonian terms from the input file. These terms are given as sum of products of the

fundamental operator $\mathbf{P^2}$, $\mathbf{P_z}$, $\mathbf{P_+} = \mathbf{P_x} + i\mathbf{P_y}$, $\mathbf{P_-} = \mathbf{P_x} - i\mathbf{P_y}$ which are coded as P^2, P_z, P+, and P-, respectively. As an example, the operator $r_J\frac{1}{2}\left(\mathbf{P^2P_+} + \mathbf{P^2P_-}\right)$ is coded as

rJ 0.5 P2 P + (93)

rJ 0.5 P2 P − (94)

REFERENCES

[1]U. Andresen, H. Dreiler, U. Kretschemer, W. Stahl, C. Thomsen, *Fresen J Anal Chem.* **349**, 272 (1994).

[2]J. Grabow, W. Stahl, H. Dreiler, *Rev. Sci. Instrum.* **67**, 4072 (1996).

[3]I. Merke, W. Stahl, H. Dreiler, *Z. Naturforsch.* **49a**, 490 (1994).

[4]M. J. Frisch, G. W. Trucks, H. B. Schlegel, G. E. Scuseria, M. A. Robb, J. R. Cheeseman, J. A. Montgomery, Jr., T. Vreven, K. N. Kudin, J. C. Burant, J. M. Millam, S. S. Iyengar, J. Tomasi, V. Barone, B. Mennucci, M. Cossi, G. Scalmani, N. Rega,G. A. Petersson, H. Nakatsuji, M. Hada, M. Ehara, K. Toyota, R. Fukuda, J. Hasegawa, M. Ishida, T. Nakajima, Y. Honda, O. Kitao, H. Nakai, M. Klene, X. Li, J. E. Knox, H. P. Hratchian, J. B. Cross, V.

Bakken, C. Adamo, J. Jaramillo, R. Gomperts, R. E. Stratmann, O. Yazyev, A. J. Austin, R. Cammi, C. Pomelli, J. W. Ochterski, P. Y. Ayala, K. Morokuma, G. A. Voth, P. Salvador, J. J. Dannenberg, V. G. Zakrzewski, S. Dapprich, A. D. Daniels, M. C. Strain, O. Farkas, D. K. Malick, A. D. Rabuck, K. Raghavachari, J. B. Foresman, J. V. Ortiz, Q. Cui, A. G. Baboul, S. Clifford, J. Cioslowski, B. B. Stefanov, G. Liu, A. Liashenko, P. Piskorz, I. Komaromi, R. L. Martin, D. J. Fox, T. Keith, M. A. Al-Laham, C. Y. Peng, A. Nanayakkara, M. Challacombe, P. M. W. Gill, B. Johnson, W. Chen, M. W. Wong, C. Gonzalez, and J. A. Pople, Gaussian03, Revision D.01, Gaussian, Inc., Wallingford, CT, 2004.

5 Gaussian 09 (Revision A.02), M.J. Frisch, G.W. Trucks, H.B. Schlegel, G.E. Scuseria, M.A. Robb, J.R. Cheeseman, G. Scalmani, V. Barone, B. Mennucci, G.A. Petersson, H. Nakatsuji, M. Caricato, X. Li, H.P. Hratchian, A.F. Izmaylov, J. Bloino, G. Zheng, J.L. Sonnenberg, M. Hada, M. Ehara, K. Toyota, R. Fukuda, J. Hasegawa, M. Ishida, T. Nakajima, Y.Honda, O. Kitao, H. Nakai, T. Vreven, J.A. Montgomery Jr., J.E. Peralta, F. Ogliaro, M. Bearpark, J.J. Heyd, E. Brothers, K.N. Kudin, V.N. Staroverov, R. Kobayashi, J. Normand, K. Raghavachari, A. Rendell, J.C. Burant, S.S. Iyengar, J. Tomasi, M. Cossi, N. Rega, J.M. Millam, M. Klene, J.E. Knox, J.B. Cross, V. Bakken, C. Adamo, J. Jaramillo, R. Gomperts, R.E. Stratmann, O. Yazyev, A.J. Austin, R. Cammi, C. Pomelli, J.W. Ochterski, R.L. Martin, K. Morokuma, V.G. Zakrzewski, G.A. Voth, P. Salvador, J.J. Dannenberg, S. Dapprich, A.D. Daniels, O. Farkas, J.B. Foresman, J.V. Ortiz, J. Cioslowski, D.J. Fox, Gaussian, Inc., Wallingford CT, 2009.

[6]M.J. Frisch, G.W. Trucks, H.B. Schlegel, G.E. Scuseria, M.A. Robb, J.R. Cheeseman, G. Scalmani, V. Barone, G.A. Petersson, H. Nakatsuji, X. Li, M. Caricato, A.V. Marenich, J. Bloino, B.G. Janesko, R. Gomperts, B. Mennucci, H.P. Hratchian, J.V. Ortiz, A.F. Izmaylov, J.L. Sonnenberg, D. Williams-Young, F. Ding, F. Lipparini, F. Egidi, J. Goings, B. Peng, A. Petrone, T. Henderson, D. Ranasinghe, V.G. Zakrzewski, J. Gao, N. Rega, G. Zheng, W. Liang, M. Hada, M. Ehara, K. Toyota, R. Fukuda, J. Hasegawa, M. Ishida, T. Nakajima, Y. Honda, O. Kitao, H. Nakai, T. Vreven, K. Throssell, J.A. Montgomery, Jr., J.E. Peralta, F. Ogliaro, M.J. Bearpark, J.J. Heyd, E.N. Brothers, K.N. Kudin, V.N. Staroverov, T.A. Keith, R. Kobayashi, J. Normand, K. Raghavachari, A.P. Rendell, J.C. Burant, S.S. Iyengar, J. Tomasi, M. Cossi, J.M. Millam, M. Klene, C. Adamo, R. Cammi, J.W. Ochterski, R.L. Martin, K. Morokuma, O. Farkas, J.B. Foresman, D.J. Fox, Gaussian 16, Revision B.01, Gaussian, Inc., Wallingford CT, 2016.

[7]M.W. Schmidt, K.K. Baldridge, J.A. Boatz, S.T. Elbert, M.S. Gordon, J.H. Jensen, S. Koseki, N. Matsunaga, K.A. Nguyen, S.J. Su, T.L. Windus, M. Dupuis, J.A. Montgomery, *J. Comput. Chem.* **14**, 1347 (1993).

[8]B.M. Bode, M.S. Gordon, *J. Mol. Graphics and Modeling* **16**, 133 (1998).

[9]C. Møller, M.S. Plesset. *Phys. Rev.* **46**, 618 (1934).

[10]C. Lee, W. Yang, R.G. Parr, *Phys. Rev. B* **37**, 785 (1988).

[11]W.C. Bailey, *Chem Phys.* **252**, 57 (2000).

[12]R. Kannengießer, W. Stahl, H.V.L. Nguyen, W.C. Bailey, *J. Mol. Spectrosc.* **317**, 50 (2015).

[13]W. Gordy, R.L. Cook. *Microwave molecular spectra*. Wiley (1984).

[14]C.C. Lin, J.D. Swalen, *Rev. Mod. Phys.* **31**, 841 (1959).

[15]D.S. Ray, *Z. Physik* **78**, 74 (1932).

[16]J.K.G. Watson, *J. Mol. Spectrosc.* **65**, 123 (1977).

[17] H.B.G. Casimir, *Teyler's Tweede Genootschap*, E.F. Bohn, Harlem (1936).

[18]See http://spec.jpl.nasa.gov/ for downloading and instruction of the program.

[19]C.M. Western, PGOPHER, a program for simulating rotational structure, http://pgopher.chm.bris.ac.uk

[20]H. Dreizler, *Fortschr. Chem.Forsch.* **10**, 59 (1968).

[21]D.R. Herbschbach, *J. Chem. Phys.* **31**, 91 (1959).

[22]G.S. Ezra, Symmetry Properties of Molecules, Lecture Notes in Chemistry 28, Springer-Verlag, Berlin, Heidelberg, New York (1982).

[23]N. Ohashi, J.T. Hougen, R.D. Suenram, F.J. Lovas, Y. Kawashima, M. Fujitake, J. Pykad, *J. Mol. Spectrosc.* **227**, 28 (2004).

[24]E. Herbst, J. K. Messer, F. C. De Lucia, P. Helminger, *J.Mol. Spectrosc.* **108**, 42 (1984).

[25]J. T. Hougen, I. Kleiner, M. Godefroid, *J. Mol. Spectrosc.* **163**, 559 (1994).

[26]I. Kleiner, *J. Mol. Spectrosc.* **260**, 1 (2010).

[27]H. Hartwig, H. Dreizler, *Z. Naturforsch.* **51a**, 923 (1996).

[28]J.T. Hougen, I. Kleiner, M. Godefroid, *J. Mol. Spectrosc.* **163**, 559 (1994).

[29]I. Kleiner, J.T. Hougen, *J. Chem. Phys.* **119**, 5505 (2003).

[30]P.Groner, *J. Chem. Phys.* **107**, 4483 (1997).

[31]V.V. Ilyushin, Z. Kisiel, L. Pszczólkowski, H. Mäder, J.T. Hougen, *J. Mol. Spectrosc.* **259**, 26 (2010).

[32]S. Herbers, H.V.L. Nguyen, *J. Mol. Spectrosc.* **370**, 111289 (2020).

[33]See JB95 Spectral fitting program | NIST for downloading and instruction of the program.

[34]L. Ferres, W. Stahl, H.V.L. Nguyen, *J. Chem. Phys.* **151**, 104310 (2019).

[35]L. Ferres, W. Stahl, H.V.L. Nguyen, *J. Chem. Phys.* **148**, 124304 (2018).

[36]R.C. Woods, *J. Mol. Spectrosc.* **22**, 49 (1967).

[37]W.Liang, J.G. Baker, E. Herbst, R.A. Booker, F.C. De Lucia, *J. Mol. Spectrosc.***120**, 298 (1896).

[38]F.C. De Lucia, E. Herbst, T. Anderson, P. Helminger, *J. Mol. Spectrosc.* **134**, 395 (1989).

[39]R. Kannengießer, W. Stahl, H.V.L. Nguyen, and I. Kleiner, *J. Phys. Chem. A* **120**, 3992 (2016).

[40]A. Roucou, I. Kleiner, M. Goubet, S. Bteich, G. Mouret, R. Bocquet, F. Hindle, W.L. Meerts, A. Cuisset, *ChemPhysChem* **19**, 1056 (2018).

PART II: NITROGEN AROMATIC RINGS WITH ONE ROTOR AND ONE ^{14}N NUCLEUS

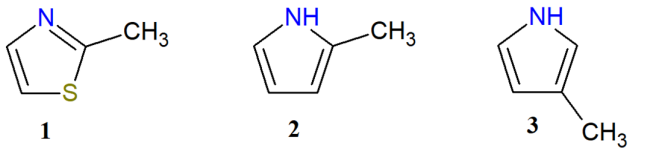

1 2-methylthiazole **2** 2-methylpyrrole **3** 3-methylpyrrole

The microwave spectra of 2-methylthiazole, 2-methylpyrrole and 3-methylpyrrole were recorded using the two molecular jet Fourier transform spectrometers operating in the frequency range of 2-40 GHz. All spectra were successfully assigned, the effects arising from internal rotation as well as quadrupole coupling were resolved with the complementary of quantum chemical calculations. Experimental data were analyzed using programs *XIAM* and *BELGI-C_s-hyperfine*, obtaining fits permitted the determinations of molecular parameters with high accuracy.

Our results allowed to conclude that the frame symmetry plays a crucial role in the resulting barrier height values. The question of how the position of the methyl group and the presence of the heteroatoms in the ring influence the barrier height was addressed. In addition, the results also enabled us to link the signs of the nuclear quadrupole coupling constants χ_{cc} with the chemical bonds at the sites of the nitrogen atoms in the rings.

In the following sub-sections, we will report the results on microwave investigations on 2-methylthiazole (Chapter II.1), 2-methylpyrrole (Chapter II.2) and 3-methylpyrrole (II.3).

Chapter II.1: The microwave spectrum of 2-methylthiazole: ^{14}N nuclear quadrupole coupling and methyl internal rotation

This is an Accepted Manuscript of an article published by AIP publisher in Journal of Chemical Physiscs: "Thuy Nguyen, Vinh Van, Claudine Gutlé, Wolfgang Stahl, Martin Schwell, Isabelle Kleiner, and Ha Vinh Lam Nguyen, The microwave spectrum of 2-methylthiazole: ^{14}N nuclear quadrupole coupling and methyl internal rotation, J. Chem. Phys. 152. 134306 (2020) available online: https://doi.org/10.1063/1.5142857*"*

ABSTRACT

The rotational spectrum of 2-methylthiazole was recorded using two pulsed molecular jet Fourier transform microwave spectrometers operating in the frequency range of 2 – 40 GHz. Due to internal rotation of the methyl group, all rotational transitions were split into A and E symmetry species lines, which were analyzed using the programs *XIAM* and *BELGI-C_s-hyperfine*, yielding the methyl torsional barrier of 34.79675(18) cm^{-1}. This value was compared with that found in other monomethyl substituted aromatic five-membered rings. The ^{14}N quadrupole coupling constants were accurately determined to be χ_{aa} = 0.5166(20) MHz, $\chi_{bb} - \chi_{cc}$ = –5.2968(50) MHz, and χ_{ab} = –2.297(10) MHz by fitting 531 hyperfine components. The experimental results were supplemented by quantum chemical calculations.

I. INTRODUCTION

The complexity of molecules studied by molecular jet Fourier transform microwave (MJ-FTMW) spectroscopy is steadily increasing, providing an enormous number of high-resolution spectra for testing theoretical models. If the molecule can be described by a semi-rigid rotor, a fit of high quality can be achieved using a rigid rotor Hamiltonian H_r supplemented by centrifugal distortion terms H_{cd}, taking into account even higher J and K transitions.

When a molecule contains a methyl group undergoing internal rotation hindered by a sufficiently low threefold potential barrier, its microwave spectrum exhibits splittings of all rotational lines into A and E torsional components, and can no longer be treated using a semi-rigid rotor model. Several programs have been developed to treat the effect of internal rotation, i.e. a code written by Woods named after what was called the Internal Axis Method (IAM) at that time and we refer to as the Rho Axis Method (RAM) today,[1] *XIAM*,[2] *BELGI* in its C_s and C_1 version,[3,4] *Erham*,[5] and *RAM36*[6] (see http://www.ifpan.edu.pl/~kisiel/prospe.htm) where additional terms to account for the internal rotation H_{ir} are added in the Hamiltonian. Some molecules associated with low or intermediate barrier height can also be treated by the program *JB95* provided by Plusquellic,[7] as well as by the program *IAMCALC* which is integrated in Pickett's CALPGM suite of programs containing the *SPFIT* and *SPCAT* codes.[8] An overview of internal rotation programs can be found in Ref. [9].

A nucleus with a nuclear spin $I \geq 1$ implies a spectroscopic electric nuclear quadrupole moment. Hyperfine structures occur in the microwave spectrum, i.e., the rotational levels with $J > 0$ of the rigid rotor split into several hyperfine components. The size and pattern of the splittings depend on the respective transition. In the case of a ^{14}N nucleus, the quadrupole moment is relatively small and can often be treated using a first order perturbation approximation.

The combination of a single ^{14}N quadrupole coupling nucleus and methyl internal rotation can be handled with the program *RAM36*, which implies the molecular symmetry to be C_s.[10] With the program *XIAM*, the symmetry is not restricted to C_s. However, *XIAM* often experiences difficulties in treating internal rotations with low barrier heights, because (i) only a limited number of high order parameters can be fitted and (ii) the torsional interactions between different v_t states are not taken into account explicitly. The program *BELGI* has been extended in its hyperfine versions *BELGI-C_s-hyperfine* and

BELGI-C_1-hyperfine, which can treat molecules with one internal rotor and one weakly coupling nucleus like ^{14}N. Its predictive power has been proven for several molecules containing one methyl rotor and a nitrogen nucleus such as *N-tert*-butylacetamide (C_s),[11] *N*-ethylacetamide (C_1),[11] 3-nitrotoluene (C_s),[12] and 2-methylpyrrole (C_s).[13]

Monomethyl derivatives of aromatic heterocyclic five-membered rings containing a nitrogen nucleus are ideally suited to test the Hamiltonian model because the V_3 potential value of the methyl group covers a wide range from low barriers like that in 2-methylthiazole (34.9 cm^{-1})[14] and 4-methylisothiazole (105.8 cm^{-1})[15] to intermediate barriers such as in 4- and 5-methylthiazole (357.6 and 332.0 cm^{-1}, respectively),[16,17] as well as in 2-, 4, and 5-methyloxazole (252.0, 428.0, and 477.9 cm^{-1}, respectively).[18] The first molecule mentioned above, 2-methylthiazole (2MTA), has been studied by *Grabow et al.* in the frequency range from 7 to 13 GHz.[14] The V_3 potential of 34.938(20) cm^{-1} is the lowest of all examples. Two independent fits were performed in this previous investigation using the program *XIAM*.[2] In the first fit, 16 torsional transitions were fitted with a standard deviation of 443 kHz, which is more than 200 times the measurement accuracy. The centrifugal distortion constants could not be determined. In order to deduce the ^{14}N nuclear quadrupole coupling constants (NQCCs), only the splittings of 44 hyperfine components were fitted in a second fit with a standard deviation of 2.7 kHz. We believe that the Hamiltonian which describes the microwave spectrum of 2MTA requires some higher order terms which are beyond the model used in *XIAM*. Therefore, we decided to (i) extend the data set to cover a much larger frequency range from 2 to 40 GHz to measure higher J and K values, and (ii) refit the data set using the program *BELGI-C_s-hyperfine*[11] by including higher order terms in the Hamiltonian. The goal is to achieve a global fit with a standard deviation close to the measurement accuracy and a set of molecular parameters with high predictive power.

II. EXPERIMENTAL AND QUANTUMCHEMICAL METHODS

A. Quantum Chemical Calculations

1. Structure optimizations

In order to predict the structure of 2MTA, the *Gaussian 03* program package[19] was used with three quantum chemistry methods: the Hartree-Fock self-consistent field method, the B3LYP density functional method, and the second-order Møller-Plesset perturbation theory with all electrons explicitly included (MP2ae). The Pople 6-311++G(d,p) basis set was chosen in all cases. These three levels of theory were chosen a priori, expected to provide reasonable predictions at an affordable cost for a medium-sized molecule like 2MTA. The equilibrium geometry of 2MTA optimized at the B3LYP/6-311++G(d,p) level is shown in Figure 1. The rotational constants are collected in Table I.

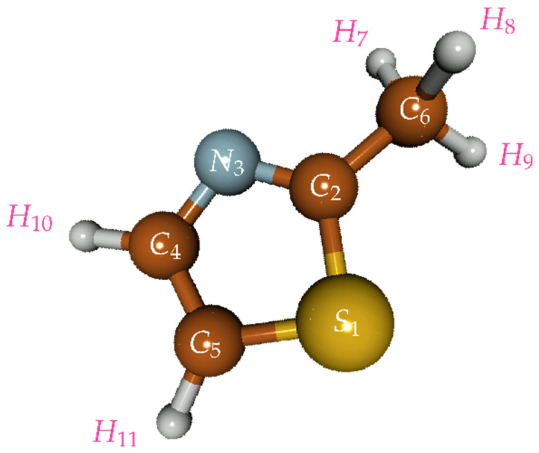

FIG. 1. Geometry of 2MTA optimized at the B3LYP/6-311++G(d,p) level of theory.

Table I. The rotational constants (in MHz) of the most stable geometry of 2-methylthiazole calculated at the B3LYP/6-311++G(d,p), HF/6-311++G(d,p), and MP2(ae)/6-311++G(d,p) levels of theory. The dihedral angle α is defined as ∠(S_1,C_2,C_6,H_9). For comparison, the data for the conformation with α = 60° calculated at the MP2(ae)/6-311++G(d,p) level of theory is also given.

B3LYP/6-311++G(d,p) α = 60°			
	(e)[a]	(00)[b]	(0)[c]
A	5287.361	5256.606	5256.607
B	3238.812	3219.713	3219.711
C	2033.933	2021.676	2021.677
HF/6-311++G(d,p) α = 60°			
A	5414.526	5388.873	5388.873
B	3273.155	3254.854	3254.854
C	2065.917	2054.512	2054.512
MP2(ae)/6-311++G(d,p) α = 32.9°			

A	5319.383	5287.236	5287.236
B	3273.476	3250.856	3250.856
C	2052.720	2038.443	2038.443
MP2(ae)/6-311++G(d,p) α = 60°			
A	5317.821	5284.436	5284.436
B	3271.103	3249.920	3249.920
C	2051.308	2037.267	2037.267

[a] Equilibrium constants. [b] Constants including the vibrational correction. [c] Constants including the vibrational correction and the centrifugal distortion.

Four conformations are of interest for studying the rotation of the methyl group relative to the thiazole ring, which can be characterized by the value of the dihedral angle $\alpha = \angle(S_1,C_2,C_6,H_9)$. In the first conformation at $\alpha = 0°$, the proton H_9 is eclipsed with the sulfur atom if we look along the $C_2{-}C_6$ bond. The second one with $\alpha = 60°$ has the H_8 atom eclipsed with the nitrogen atom. In the third conformation at $\alpha \approx 30°$, the $C_6{-}H_7$ bond is roughly perpendicular to the ring plane. Finally, the fourth conformation at $\alpha \approx 90°$ with the $C_6{-}H_9$ bond being roughly perpendicular to the ring plane is equivalent to the $\alpha \approx 30°$ position, assuming that the ring is planar as expected for an aromatic system. Due to symmetry, each of those four conformations appears three times during a full rotation of the methyl group about the $C_2{-}C_6$ bond. As summarized in Table II, they all give rise to a stationary point of the electrostatic energy at the MP2(ae)/6-311++G(d,p) level with those at $\alpha = 32.9°$ and $\alpha = 87.1°$ as the most stable rotamers and two saddle points at $\alpha = 0°$ and 60°, while only the first two conformations are found to be stationary in calculations at the B3LYP/6-311++G(d,p) and HF/6-311++G(d,p) levels with the most stable rotamer at $\alpha = 60°$.

Table II. Dihedral angle α, the difference Δα between the conformers, the energy at the stationary points *E*, the energy difference Δ*E* between the conformers, the energy with vibrational corrections *E*+*ZPE*, and the energy difference Δ(*E*+*ZPE*) between the conformers of 2-methylthiazole obtained while rotating the methyl group.

Method	α / °	Δα / °	Type	*E* / Hartree	Δ*E* / cm^{-1}	*E*+*ZPE* / Hartree	Δ(*E*+*ZPE*) / cm^{-1}
B3LYP	0.0		max	–608.4535876		–608.3713686	
	60.0	60.0 → 0.0	min	–608.4538273	52.61	–608.3715613	42.29
HF	0.0		max	–606.4056155		–606.3173985	
	60.0	60.0 → 0.0	min	–606.4061723	122.20	–606.3178393	96.74
MP2	0.0	0.0 → 32.9	max	–607.4967712	–29.37	–607.4138412	6.41
	32.9	60.0 → 32.9	min	–607.4969050	–25.52	–607.4138120	22.98
	60.0	60.0 → 0.0	max	–607.4967887	3.84	–607.4139167	16.57

For all above-mentioned conformers, the zero-point energy (ZPE) correction to the electrostatic energy were calculated as given in Table II. For all maxima, geometry optimizations to a first-order transition state were performed in addition by using the Berny algorithm,[20] which yielded the same results as those given in Table II. With the MP2 method, the ZPE corrected difference is greater than the non-corrected difference, indicating that the lowest vibrational level lies above the local maximum at $\alpha = 60°$. However, this difference is still smaller than the maximum value of the V_3 potential, suggesting that the V_6 contribution of the potential cannot be determined from transitions of the vibrational ground state, and only the effective V_3 term should be well-determined. The Cartesian coordinates of the atoms are reported in Table S-I of the Appendix AII.1.

2. Methyl Internal Rotations

Potential energy scans were generated by rotating the methyl group about the C_2–C_6 bond. The dihedral angle α was varied in a grid of 10° (2° around the stationary points). All other geometry parameters were optimized. The potential energy curves showing the rotation of the methyl group are presented in Figure 2, where the minima of all curves have been translated to the energy origin. The corresponding data points are available in Table S-II of the Appendix AII.1. While the potential curves calculated with the B3LYP and the HF methods show normal three-fold potentials without V_6 contribution, the MP2 method predicts V_6 as the dominating term with a value of 26.92 cm^{-1} and a V_3 contribution of 6.92 cm^{-1}. These values were obtained by parameterizing the data points given in Table S-II with a one-dimensional Fourier expansion as

$$V(\alpha) = -607.496842\ Hartree + \frac{6.92cm^{-1}}{2}cos(3\alpha) + \frac{26.92cm^{-1}}{2}cos(6\alpha) - \frac{2.82cm^{-1}}{2}cos(9\alpha).$$

Therefore, they slightly deviate from those given in Table II.

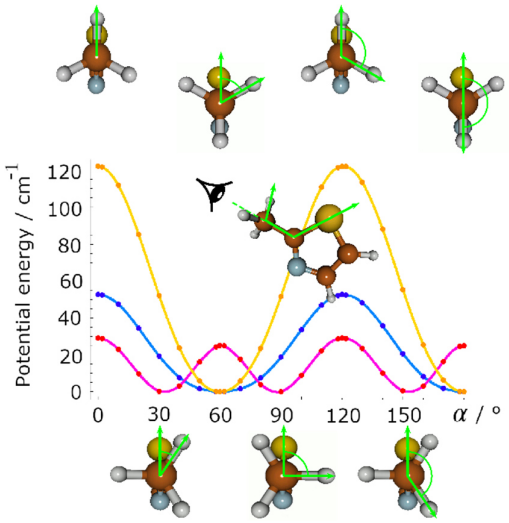

FIG. 2. Potential energy curves of 2-methylthiazole (in cm^{-1}) obtained by rotating the methyl group about the C_2–C_6 bond. The dihedral angle $\alpha = \angle(S_1,C_2,C_6,H_9)$ was varied in a grid of 10° (2° around stationary points), while all other molecular parameters were optimized at the B3LYP/6-311++G(d,p) (in blue), HF/6-311++G(d,p) (in orange), and MP2(ae)/6-311++G(d,p) (in magenta) levels of theory. The energies are relative to the energetically lowest conformations.

Our best estimate for the V_3 potential includes the *ZPE* correction, as shown in Table II under $\Delta(E + ZPE)$, whose value depends on the method in use. The Hartree-Fock method is not expected to be quantitative, whereas the V_3 potential of 42.29 cm^{-1} from calculations using the density functional is presumed to be more quantitatively realistic. Finally, as the MP2 results are not in agreement with those of the Hartree-Fock (96.74 cm^{-1}) and the B3LYP methods, experimental results are important to validate results from calculations. We emphasize that the small value of the methyl torsional barrier of 2MTA is a significant challenge for quantum chemistry.

B. Measurements

2MTA, purchased from TCI Europe, Zwijndrecht, Belgium, has a stated purity of 98% and was used without further purification. The colorless liquid with a typical aromatic smell was placed on a pipe cleaner in a stainless-steel tube upstream the nozzle. Under a helium stream at a backing pressure of 2 bar, the helium-2MTA mixture was expanded into the vacuum chamber. The spectra were recorded using two supersonic jet Fourier transform microwave spectrometers operating in the frequency range

from 2 to 26.5 GHz (the Aachen big cavity)[21] and 26.5 to 40 GHz (the Paris small cavity).[22] All lines appear as doublets because of the Doppler effect. A typical spectrum is shown in Figure 3. Some intense lines can be measured with a linewidth at FWHH smaller than 20 kHz, corresponding to a measurement accuracy of 2 kHz, but in most cases the line widths are larger. In some transitions, small splittings up to 10 kHz were observed, probably due to proton spin-spin and spin-rotation coupling. The measurement accuracy is thus about 3 kHz. In all fits carried out in the present work, all lines were equally weighted.

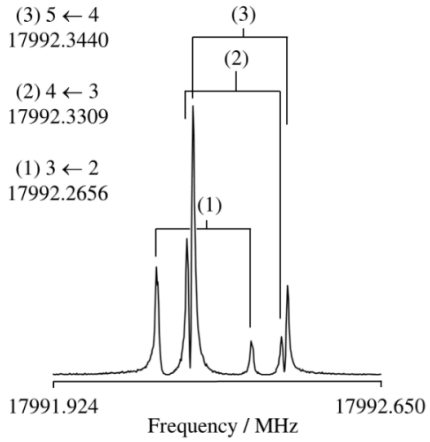

FIG. 3. The $4_{04} \leftarrow 3_{13}$ transition of the A species of 2MTA with its quadrupole hyperfine components given as F′ ← F. The splittings indicated by brackets are due to the Doppler effect. For this spectrum, 41 free-induction decays were co-added.

III. MICROWAVE SPECTRUM

A. ^{14}N nuclear quadrupole coupling

In the first step, we neglected the methyl internal rotation effect and treated 2MTA as an effective rigid rotor with ^{14}N nuclear quadrupole coupling. The 34 A species transitions (including their hyperfine splittings) reported in Ref. [14] were refitted with the program *XIAM* in its rigid rotor mode with a root-mean-square (rms) deviation of about 3 kHz. This fit allowed us to predict the whole rigid rotor spectrum with sufficient accuracy to measure new A species lines in the frequency range from 2 to 40 GHz. All lines appear as multiplets with a different number of components, which could be straightforwardly attributed to the ^{14}N hyperfine structure. Three rotational constants *A*, *B*, *C*, five quartic centrifugal distortion constants, and two NQCCs were fitted for a total of 278 A species hyperfine components to measurement accuracy. The molecular parameters are summarized as Fit *XIAM* A in Table III.

TABLE III. Molecular parameters in the principal axis system obtained using the *XIAM* code (*XIAM* A and *XIAM* A/E) and the *BELGI*-C_s-hyperfine code (*BELGI*). For the *BELGI* fits, the molecular parameters in the rho axis system were transformed into the principal axis system. Details on the conversion are given in Ref. [23].

Par. [a]	Unit	*XIAM* A	*XIAM* A/E	*BELGI*	MP2(ae)[b]
A	MHz	5490.32686(14)	5343.110(23)	5323.498(49)	5284.436
B	MHz	3266.223383(76)	3266.0697(98)	3264.1955(93)	3249.920
C	MHz	2052.328264(68)	2052.3963(88)	2051.5080(15)	2037.267
Δ_J	kHz	0.24007(63)	0.458(72)	0.23763(54)	0.223817
Δ_{JK}	kHz	1.2817(26)	1.01(29)		0.257817
Δ_K	kHz	15.3697(56)			0.883085
δ_J	kHz	0.07888(27)	0.180(30)		0.073732
δ_K	kHz	0.7404(20)	1.00(22)		0.369655
F_0	GHz		159[c]		159
F	GHz		164.5155[d]	164.5155[e]	
ρ			0.033540793[d]	0.03310670(95)	
V_3	cm^{-1}		34.79675(18)	34.2535(12)	6.92[f]
D_{pi2J}	kHz		–88.7(24)		
D_{pi2K}	MHz		0.3310(79)		
$\angle(i,a)$	°		4.4589(15)	4.6413(31)	5.5817
$\angle(i,b)$	°		94.4589(15)	94.6413(31)	95.5811
$\angle(i,c)$	°		90.0[g]	90.0[g]	89.9204
χ_{aa}	MHz	0.5407(16)	0.44(17)	0.5166(20)	0.462[h]
$\chi_{bb}-\chi_{cc}$	MHz	–5.3159(24)	–5.21(27)	–5.2968(50)	–5.044[h]
χ_{ab}[i]				–2.297(10)	–2.464[h]
N_A/N_E[j]		278/0	278/253	278/253	
rms[k]	kHz	3.0	455.9	3.2	

[a] Standard error in parentheses in the unit of the last digits. Watson's A reduction and I^r representation were used.

[b] Values calculated at the MP2(ae)/6-311++G(d,p) level including the vibrational and centrifugal distortion corrections with α = 60°, except the values for the NQCCs.

[c] Fixed to *ab initio* value.

[d] Derived parameter.

[e] Not fitted. Fixed to the *XIAM* A/E value.

[f] The potential energy contains a leading V_6 contribution of 26.92 cm^{-1}.

[g] Fixed due to symmetry.

[h] Calculated at the B3PW91/6-311+G(d,p)//MP2(ae)/6-311++G(d,p) level of theory. Values from Ref. [14] are χ_{aa} = 0.5239(30) MHz, $\chi_{bb} - \chi_{cc}$ = –5.239(15) MHz, and χ_{ab} = –2.279(14) MHz.

[i] Cannot be fitted in Fit *XIAM* A and not determinable in Fit *XIAM* A/E.

[j] Number of fitted A and E species lines.

[k] Root-mean-square deviation of the fit.

B. Methyl internal rotation

In the second step, we took into account the methyl internal rotation by including the 26 E species transitions from Ref. [14] in the fit, and achieved a standard deviation of over 400 kHz. With the parameters from this fit, a prediction of the E species frequencies was performed between 2 and 40 GHz. However, the predicted frequencies did not match the experimental ones. Consequently, the assignments of the hyperfine structure were carried out by analyzing the hyperfine splittings instead of the absolute frequencies. Finally, 278 A species and 253 E species lines were measured and fitted using the program *XIAM* with a rms deviation of 455.9 kHz, similar to the result of Ref. [14]. The molecular parameters from the so-called Fit *XIAM* A/E are presented in Table III. A list of all fitted transitions is given in Table S-III of the Appendix AII.1. All attempts to reduce the large rms deviation using *XIAM* failed.

TABLE IV. Molecular parameters of 2MTA in the rho axis system obtained using the *BELGI-C_s-hyperfine* code.

Par.[a]	Unit	Value	Operator
A	MHz	5318.408(48)	$\mathbf{P_a^2}$
B	MHz	3269.2857(64)	$\mathbf{P_b^2}$
C	MHz	2051.5081(15)	$\mathbf{P_c^2}$
D_{ab}	MHz	102.256(68)	$\mathbf{\{P_a,P_b\}}$
Δ_J	kHz	0.23763(54)	$\mathbf{-P^4}$
Δ_{JK}	kHz	0.9768(28)	$\mathbf{-P^2P_a^2}$
Δ_K	kHz	–2.978(14)	$\mathbf{-P_a^4}$
δ_J	kHz	0.07742(24)	$\mathbf{-2P^2(P_b^2-P_c^2)}$
δ_K	kHz	0.7517(27)	$\mathbf{-\{P_a^2,(P_b^2-P_c^2)\}}$
$2\chi_{aa}$	MHz	1.4725(34)	
$2\chi_{bb}$	MHz	–6.2528(31)	
$2\chi_{ab}$	MHz	–4.232(21)	
V_3	cm^{-1}	34.2535(12)	$\mathbf{(1/2)(1-\cos 3\alpha)}$
ρ	unitless	0.03310670(95)	$\mathbf{P_aP_\alpha}$
F	cm^{-1}	5.48765[b]	$\mathbf{P_\alpha^2}$
Δ_{ab}	MHz	–1.110(23)	$\mathbf{P_\alpha\{P_a,P_b\}}$
F_v	MHz	1.6234(67)	$\mathbf{(1-\cos 3\alpha)P^2}$
k_5	MHz	31.971(78)	$\mathbf{(1-\cos 3\alpha)P_a^2}$
c_2	MHz	0.4666(53)	$\mathbf{(1-\cos 3\alpha)(P_b^2-P_c^2)}$
d_{ab}	MHz	–3.192(61)	$\mathbf{(1-\cos 3\alpha)\{P_a,P_b\}}$
k_1	MHz	–0.10274(62)	$\mathbf{P_a^3P_\alpha}$
c_4	kHz	4.82(21)	$\mathbf{P_aP_\alpha(P_b^2-P_c^2)}$
N_A / N_E / N_q[c]		93/83/531	
rms[d]	kHz	3.2	

[a] All parameters refer to the rho axis system and cannot be directly compared to those referred to the principal axis system. $\mathbf{P_a}$, $\mathbf{P_b}$, and $\mathbf{P_c}$ are the components of the overall rotation angular momentum, $\mathbf{P_\alpha}$ is the angular momentum of the internal rotor rotating about the internal rotor axis by an angle α. {u,v} is the anti-commutator uv + vu. The product of the parameter and operator from a given row yields the term actually used in the vibration-rotation-torsion Hamiltonian, except for F, ρ, and A, which occur in the Hamiltonian in the form $F(\mathbf{P_\alpha}-\rho\mathbf{P_a})^2 + A\mathbf{P_a}^2$, where $F = h^2/8\pi^2 crI_\alpha$ (cm^{-1}). Statistical uncertainties are shown as one standard uncertainty in the last digit. [b] Fixed to the value from the *XIAM* A/E fit. [c] Number of A and E species transitions as well as hyperfine components. [d] Root-mean-square deviation of the fit.

In order to achieve a global fit with measurement accuracy, the program *BELGI-C_s-hyperfine*[11] was applied. By floating 21 parameters (plus the reduced rotational constant F of the methyl group fixed at the value from the *XIAM* A/E fit) which are the NQCCs χ_{aa}, χ_{bb}, and χ_{ab}, together with the three rotational constants A, B, C, five centrifugal distortion constants Δ_J, Δ_{JK}, Δ_K, δ_J, and δ_K, the D_{ab} parameter multiplying the off-diagonal $\{\mathbf{P_a},\mathbf{P_b}\}$ term, the torsional potential barrier height V_3, the unitless parameter ρ which, together with F, is associated with P_aP_α, and seven additional terms beyond the rigid top-rigid frame model, the rms deviation of the fit decreases to 3.2 kHz. All out-of-plane terms were set to zero due to the C_s symmetry of 2MTA. The *BELGI-C_s-hyperfine* parameters in the rho axis system are given in Table IV, and parameters that could be transferred to the principal axis system are presented in Table III.

IV. DISCUSSION

The *BELGI-C_s-hyperfine* code improves the rms deviation of 2MTA to measurement accuracy by adding 7 effective parameters which are not available in the *XIAM* code. The operators containing the (1–cos3α) term led to the most significant changes of the fit. The rotational constants A, B, C obtained from both fits, the *XIAM* A/E and the *BELGI* fits, are well-determined and they agree within 0.4 %. A better agreement is not expected because (i) different approaches are used in the two codes, (ii) different sets of parameters are used, and (iii) that the conversion of RAM parameters to PAM parameters is not unique. The accuracy of the rotational constants is higher by two orders of magnitude in the *XIAM* A fit. The rms deviation of 3.0 kHz of the *XIAM* A fit, which is essentially the measurement accuracy, also

indicates that for the A species of 2MTA, a semi-rigid rotor model with centrifugal distortion corrections is satisfactory. The inertial defect $\Delta_c = I_c - I_a - I_b = -3.083$ uÅ^2 confirms that the heavy atom skeleton is planar with a pair of methyl hydrogen atoms out of plane. This value is very close to that found for the isomers 4-methylthiazole (–3.092 uÅ^2)[16] and 5-methylthiazole (–3.077 uÅ^2).[17]

The rotational constants obtained from the *XIAM* A fit agree with the constants calculated at the MP2(ae)/6-311++G(d,p) level of theory including the vibrational correction and the centrifugal distortion. The deviation is 1.10% for *A*, 0.50% for *B*, and 0.74% for *C* with respect to the *XIAM* values. They are even smaller if the values obtained for the equilibrium structure are taken (0.48% for *A*, –0.16% for *B* and 0.06% for *C*), suggesting that geometry parameters of the equilibrium structure calculated at the MP2(ae)/6-311++G(d,p) level of theory could be used directly to support the vibrational ground state assignment in methyl substituted thiazoles. Results from calculations using the more cost-efficient B3LYP method are less accurate, but also reasonable.

The calculated centrifugal distortion constants are quite different from those deduced in Fit *XIAM* A, but in the same order of magnitude as the values in Fit *XIAM* A/E. The large rms deviation in the latter fit leads to low accuracy of the experimental values. The well-determined constants from the *BELGI-C_s-hyperfine* fit refer to the rho axis system and cannot be directly compared with the calculated values, which refer to the principal axis system.

The NQCCs cannot be determined well in the *XIAM* A/E fit because of the large rms deviation, but in the *XIAM* A and the *BELGI* fits they are accurately deduced and agree nicely in both fits as well as with the values from Ref. [14]. Due to the rather low barrier to internal rotation of the methyl group, the expectation value of the operator $\{P_a,P_b\}$ is not negligible and therefore χ_{ab} could be determined experimentally. Calculations of the ^{14}N NQCCs were performed by Bailey at the B3PW91/6-31G(2d,2pd) level based on optimized molecular structures as given in Ref. [24]. Using the density functional B3PW91, Bailey also reported two possible orientations of the methyl group where the in-plane C_6–H_9 bond is in *cis* or *trans* position with respect to the nitrogen atom. This agrees well with our results obtained with the B3LYP and HF methods, and the *cis* and *trans* conformers in Ref. [24] correspond to our conformers at $\alpha = 0°$ and $\alpha = 60°$, respectively. These calculated NQCCs for the *cis* conformer are $\chi_{aa} = 0.449$ MHz, $\chi_{bb}-\chi_{cc} = -5.269$ MHz, and $|\chi_{ab}| = 2.338$ MHz. The respective values for the

trans rotamer are 0.517, –5.186, and 2.307 MHz, showing that the experimentally deduced χ_{aa} value is much closer to the predicted value of the *trans* conformation with $\alpha = 60°$.

The program *XIAM* yielded a methyl torsional barrier of 34.79675(18) cm^{-1}, which is very close to the value of 34.2535(12) cm^{-1} determined by *BELGI-C_s-hyperfine*. The calculated barrier heights ΔE given in Table II are 52.61 cm^{-1}, 122.20 cm^{-1}, and 29.37 cm^{-1} using the B3LYP, HF, and MP2 methods, respectively. While the value predicted with the HF method are far from being accurate, the B3LYP method overestimates and the MP2 method underestimates the torsional barrier height. Considering the *ZPE* corrections has shifted the predicted barriers on the right direction for the B3LYP and HF methods with the respective values of 42.29 cm^{-1} and 96.74 cm^{-1}, but the results still do not satisfy the experimental requirements. For the MP2 method, it is difficult to evaluate because the ZPE corrected difference is greater than the non-corrected difference. Many of our previous studies have pointed out the challenge of predicting the torsional barrier heights.[25] The calculated values vary strongly depending on the level of theory in use.[26-28] No method currently exists to solve this problem in general. If the V_3 and V_6 terms are fitted using the program *XIAM*, both of them could be determined with respective values of 31.88(21) and 17.2(12) cm^{-1}, but the correlation between them is 1.000, because only rotational transitions from the vibrational ground state are available in the data set. If the V_6 term is fixed to different values from 0 (Fit XIAM A/E or Fit BELGI) to 20 cm^{-1}, the fits converge and the rms deviation remains almost unchanged. The V_3 value changes according to the fixed value of V_6 due to correlation. Therefore, the quantity of V_6 contribution cannot be determined and further investigation including higher torsional state is needed to lift its correlation with V_3. Therefore, the leading V_6 contribution found in calculations at the MP2/6-311++G(d,p) level cannot be validated by the experiment.

The V_3 potential of 2MTA (**1**) decreases approximately by one order of magnitude compared to the barrier heights of 357.55(14) cm^{-1} and 332.02(81) cm^{-1} observed for 4- (**2**)[16] and 5-methylthiazole (**3**),[17] respectively (for molecule numbering see Figure 4). If we consider that the electronic environment around the sulfur atom and the nitrogen atom were similar, there would be a methyl group with C_{3v} symmetry attached to a C_{2v} frame. In such cases, the V_3 contribution of the potential would be zero and only a V_6 term would exist in the potential function expression. However, in 2MTA (**1**) the frame symmetry is not C_{2v}. Therefore, the electronic distribution is out of balance, which causes a low, but

significant V_3 potential term. If the nitrogen atom disappears from the ring, as in the case of 2-methylthiophene (**4**), the barrier height increases to 194.1 cm^{-1},[29] indicating that not only the position of the methyl group but also the presence of the nitrogen atom is crucial for the value of this parameter.

The methyl torsional barrier of 34.1 cm^{-1} in 2MTA is much lower than that found in the oxygen analogue 2-methyloxazole (252.0 cm^{-1}).[30] This is in agreement with the trend observed for the monomethyl derivatives of furan and thiophene, e.g. 2-methylfuran (416.2 cm^{-1})[31] versus 2-methylthiophene (194.1 cm^{-1})[29] and 3-methylfuran (380.5 cm^{-1})[32] versus 3-methylthiophene (258.8 cm^{-1}).[33] The same is also found for the dimethyl substituted versions with the only example 2,5-dimethylfuran (439.2 cm^{-1})[34] versus 2,5-dimethylthiophene (248.0 cm^{-1}).[35]

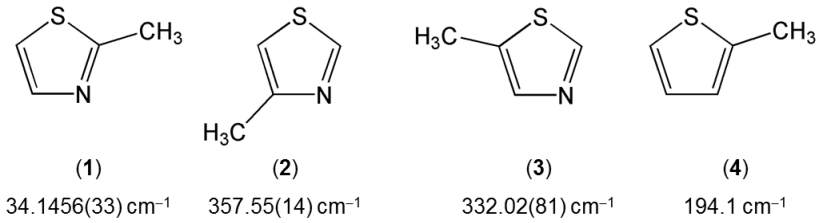

FIG. 4. Comparison of the methyl torsional barriers of 2MTA (**1**) (this work) and its two isomers 4- (**2**)[16] and 5-methylthiazole (**3**),[17] as well as 2-methylthiophene (**4**).[29]

V. CONCLUSION

The microwave spectrum of 2MTA containing a methyl group attached on the second position of the thiazole ring was assigned under molecular jet conditions with supports from quantum chemistry. Highly accurate molecular parameters were determined using the programs *XIAM* and *BELGI-C_s-hyperfine*. The internal rotation of the methyl group causes torsional splittings of all rotational transitions into the A and E species, which are additionally complicated by the quadrupole coupling arising from the ^{14}N nucleus. Using the *XIAM* code, the whole data set was reproduced with an rms deviation of 455.9 kHz while the *BELGI-C_s-hyperfine* code reduced this value to 3.2 kHz. The barrier to internal rotation of about 34 cm^{-1} is the lowest observed in three isomers of methylthiazole. Comparison to other methyl substituted sulfur-containing five-membered rings leads to the conclusion that not only the position of the methyl group, but also the presence of the nitrogen atom strongly influences the barrier height. The

results found for 2MTA also confirm the trend that the ring methyl torsion has a lower barrier in the sulfur analogue than in the oxygen analogue.

APPENDIX

See the Appendix section AII.1 for the Cartesian coordinates (Table S-I), data points of the potential energy curves (Table S-II), and frequency list (Table S-III). The *XIAM* and *BELGI-C_s-hyperfine* inputs and outputs are available as separate files. The *BELGI-C_s-hyperfine* code is currently available by one of the authors (I.K.).

ACKNOWLEDGMENTS

T.N. thanks the Department of Space and Aeronautics, University of Science and Technology of Hanoi, Vietnam, for a scholarship permitting to be enrolled in the USTH Space Master study, the Faculty of Sciences and Technology of University Paris-Est Créteil for a fellowship during her Master thesis, and University of Paris for a Ph.D. grant. V.V. is grateful to the Fonds der Chemischen Industrie for a Ph.D. fellowship. W.S. thanks the Université Paris Est for an invited researcher grant which enabled him to work at LISA. Alina Wildenberg and Ba Thanh Dang are acknowledged for performing some of the measurements during their student research projects. We thank Dr. Yannick Giraud-Héraud and Prof. Ngo Duc Thanh for their help and support in the master thesis of T.N. at LISA. This work was supported by the Agence Nationale de la Recherche ANR (project ID ANR-18-CE29-0011) and the Programme National "Physique et Chimie du Milieu Interstellaire" (PCMI) of CNRS/INSU with INC/INP co-funded by CEA and CNES.

REFERENCES

[1]R.C. Woods, *J. Mol. Spectrosc.* **22**, 49 (1967).

[2]H. Hartwig, H. Dreizler, *Z. Naturforsch.* **51a**, 923 (1996).

[3]J.T. Hougen, I. Kleiner, M. Godefroid, *J. Mol. Spectrosc.* **163**, 559 (1994).

[4]I. Kleiner, J.T. Hougen, *J. Chem. Phys.* **119**, 5505 (2003).

[5]P. Groner, *J. Chem. Phys.* **107**, 4483 (1997).

[6]V.V. Ilyushin, Z. Kisiel, L. Pszczółkowski, H. Mäder, J.T. Hougen, *J. Mol. Spectrosc.* **259**, 26 (2010).

[7]D.F. Plusquellic, R.D. Suenram, B. Mate, J.O. Jensen, A.C. Samuels, *J. Chem. Phys.* **115**, 3057 (2001).

[8]See http://spec.jpl.nasa.gov/ for downloading and instruction of the program.

[9] I. Kleiner, *ACS Earth Space Chem.* **3**, 1812 (2019).

[10]A. Belloche, A.A. Meshcheryakov, R.T. Garrod, V.V. Ilyushin, E.A. Alekseev, R.A. Motiyenko, L. Margulès, H.S.P. Müller, K.M. Menten, *Astron. Astrophys.* **601**, A49 (2017).

[11] R. Kannengießer, W. Stahl, H.V.L. Nguyen, I. Kleiner, *J. Phys. Chem. A* **120**, 3992 (2016).

[12] A. Roucou, I. Kleiner, M. Goubet, S. Bteich, G. Mouret, R. Bocquet, F. Hindle, W.L. Meerts, A. Cuisset, *ChemPhysChem* **19**, 1056 (2018).

[13]T. Nguyen, C. Dindic, W. Stahl, H.V.L. Nguyen, I. Kleiner, *Mol. Phys.* **118**, 1668572 (2020).

[14] J.-U. Grabow, H. Hartwig, N. Heineking, W. Jäger, H. Mäder, H.W. Nicolaisen, W. Stahl, *J. Mol. Struct.* **612**, 349 (2002).

[15] H.-W. Nicolaisen, J.-U. Grabow, N. Heineking, W. Stahl, *Z. Naturforsch.* **46a**, 635 (1991).

[16] W. Jäger, H. Mäder, *Z. Naturforsch.* **42a**, 1405 (1987).

[17] W. Jäger, H. Mäder, *J. Mol. Struct.* **190**, 295 (1988).

[18] E.R.L. Fliege, *Z. Naturforsch.* **45a**, 911 (1990).

[19] M.J. Frisch, G.W. Trucks, H.B. Schlegel, G.E. Scuseria, M.A. Robb, J.R. Cheeseman, J.A. Montgomery Jr, T. Vreven, K. N. Kudin, J.C. Burant, J.M. Millam, S.S. Iyengar, J. Tomasi, V. Barone, B. Mennucci, M. Cossi, G. Scalmani, N. Rega, G.A. Petersson, H. Nakatsuji, M. Hada, M. Ehara, K. Toyota, R. Fukuda, J. Hasegawa, M. Ishida, T. Nakajima, Y. Honda, O. Kitao, H. Nakai, M. Klene, X. Li, J.E. Knox, H.P. Hratchian, J.B. Cross, V. Bakken, C. Adamo, J. Jaramillo, R. Gomperts, R.E. Stratmann, O. Yazyev, A.J. Austin, R. Cammi, C. Pomelli, J.W. Ochterski, P.Y. Ayala, K. Morokuma, G.A. Voth, P. Salvador, J.J. Dannenberg, V.G. Zakrzewski, S. Dapprich, A.D. Daniels, M.C. Strain, O. Farkas, D.K. Malick, A.D. Rabuck, K. Raghavachari, J.B. Foresman, J.V. Ortiz, Q. Cui, A.G. Baboul, S. Clifford, J. Cioslowski, B.B. Stefanov, G. Liu, A. Liashenko, P. Piskorz, I. Komaromi, R. L. Martin, D. J. Fox, T. Keith, M.A. Al-Laham, C. Y. Peng, A. Nanayakkara, M. Challacombe, P. M. W. Gill, B. Johnson, W. Chen, M. W. Wong, C. Gonzalez, and J. A. Pople, Gaussian03, Revision D.01, Gaussian, Inc., Wallingford, CT, 2004.

[20] H.B. Schlegel, *J. Comput. Chem.* **3**, 214 (1982).

[21] J.-U. Grabow, W. Stahl, H. Dreizler, *Rev. Sci. Instrum.* **67**, 4072 (1996).

[22] I. Merke, W. Stahl, H. Dreizler, *Z. Naturforsch.* **49a**, 490 (1994).

[23] D. Jelisavac, D.C. Cortés-Gómez, H.V.L. Nguyen, L.W. Sutikdja, W. Stahl, I. Kleiner, *J. Mol. Spectrosc.* **257**, 111 (2009).

[24] W.C. Bailey, Calculation of Nuclear Quadrupole Coupling Constants in Gaseous State Molecules. <http://nqcc.wcbailey.net/index.html>.

[25] R. Kannengießer, S. Klahm, H.V.L. Nguyen, A. Lüchow, W. Stahl, *J. Chem. Phys.* **141**, 204308 (2014).

[26] V. Van, J. Bruckhuisen, W. Stahl, V.V. Ilyushin, H.V.L. Nguyen, *J. Mol. Spectrosc.* **343**, 121 (2018).

[27] A. Jabri, V. Van, H.V.L. Nguyen, W. Stahl, I. Kleiner, *ChemPhysChem* **17**, 2660 (2016).

[28] V. Van, W. Stahl, H.V.L. Nguyen, *ChemPhysChem* **17**, 3223 (2016).

[29] N.M. Pozdeev, L.N. Gunderova, A.A. Shapkin, *Opt. Spektrosk.* **28**, 254 (1970).

[30] E.R.L. Fliege, *Z. Naturforsch.* **45a**, 911 (1990).

[31] I.A. Finneran, S.T. Shipman, S.L.W. Weaver, *J. Mol. Spectrosc.* **280**, 27 (2012).

[32] T. Ogata, K. Kozima, *Bull. Chem. Soc. Jpn.* **44**, 2344 (1971).

[33] T. Ogata, K. Kozima, *J. Mol. Spectrosc.* **42**, 38 (1972).

[34] V. Van, J. Bruckhuisen, W. Stahl, V.V. Ilyushin, H.V.L. Nguyen, *J. Mol. Spectrosc.* **343**, 121 (2018).

[35] V. Van, W. Stahl, H.V.L. Nguyen, *Phys. Chem. Chem. Phys.* **17**, 32111 (2015).

Chapter II.2: ^{14}N nuclear quadrupole coupling and methyl internal rotation in the microwave spectrum of 2-methylpyrrole

This is an Accepted Manuscript of an article published by Taylor & Francis in Journal of Molecular Physics: "Thuy Nguyen, Christina Dindic, Wolfgang Stahl, Ha Vinh Lam Nguyen, and Isabelle Kleiner, ^{14}N Nuclear quadrupole coupling and methyl internal rotation in the microwave spectrum of 2-methylpyrrole, Molecular Physics, **18**, 1668572 (2020) *available online:* http://wwww.tandfonline.com/10.1080/00268976.2019.1668572*"*

ABSTRACT

Using two molecular jet Fourier transform microwave spectrometers, the rotational spectrum of 2-methylpyrrole was recorded in the frequency range from 2 to 40 GHz. From the torsional splittings due to the internal rotation of the methyl group a barrier height of 279.7183(26) cm^{-1} was deduced. Because of the ^{14}N nucleus, all lines show a quadrupole hyperfine structure. The microwave spectra were analyzed using the *XIAM* and *BELGI-C_s-hyperfine* codes. The *XIAM* code enabled us to reproduce the whole data set with a root-mean-square deviation of 5.6 kHz while the *BELGI-C_s-hyperfine* code could provide a better root-mean-square almost by a factor of 2 compared to that of *XIAM*. The experimental results were complemented by quantum chemical calculations. The values of the methyl torsional barrier and the ^{14}N nuclear quadrupole coupling constants are discussed and compared with other methyl substituted pyrroles as well as other aromatic five-membered rings.

Keywords: 2-methylpyrrole, microwave spectrum, internal rotation, nuclear hyperfine.

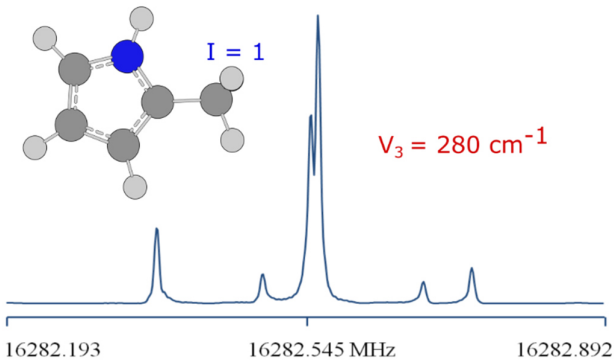

I. INTRODUCTION

For many years, the phenomenon of internal rotation has been a subject of considerable interest to both chemists and physicists. Studies of potential functions, barrier heights, stability of rotational isomers, and ring conformations provide basic information for testing and improving methods to understand the effects of internal rotation. Quantum chemical calculations together with molecular jet Fourier transform microwave (MJ-FTMW) spectroscopy allow us to obtain the torsional potential with high accuracy.

Due to steric and electronic interactions, the torsional potential of methyl groups attached to an aromatic compound are often hard to predict intuitively, while results from quantum chemical calculations are still rather not sufficiently accurate. Many investigations have been carried out on such aromatic systems, especially heterocyclic five-membered rings, to determine the methyl barrier heights, i.e., 2-methylthiazole[1] (34.9 cm^{-1}), 4-methylisothiazole[2] (105.8 cm^{-1}), 2,5-dimethylthiophene[3] (248.0 cm^{-1}), 2-acetyl-5-methylfuran[4] (369.8 cm^{-1} for the *trans* conformer and 356.5 cm^{-1} for the *cis* conformer), and 2,5-dimethylfuran[5] (439.2 cm^{-1}). From those studies it is obvious that the torsional potentials of methyl groups attached to planar aromatic rings vary in a wide range in both, shape and height.

Pyrroles are nitrogen containing five-membered ring systems which possess unique organoleptic properties[6]. Some pyrroles are used as flavor additives. In the 1960s, pyrroles became known to represent a minor class of potentially significant flavor-associated compounds that occur naturally in foods. Pyrrole and the methyl substituted compound, 2-methylpyrrole (2MP), are found in volatile compounds from fried chicken[7]. Pyrrole also provides the key structural subunit for many of the most important biological molecules, such as heme and chlorophyll. Pyrrole and its derivatives exhibit wide range of biological and pharmaceutical activities, i.e., antibacterial, anti-fungal, anti-viral, anti-inflammatory, anti-cancer and antioxidant activity[8].

From a spectroscopic point of view, 2MP contains a methyl group which undergoes internal rotation and a ^{14}N nucleus which causes a nuclear quadrupole hyperfine structure. Within the scope of this work, a combination of quantum chemical calculations and MJ-FTMW spectroscopy was used to determine the shape of the potential function and the barrier to internal rotation. The quadrupole

hyperfine structure yielded information on the electric field gradient at the site of the ^{14}N nucleus and consequently on the nature of its chemical bonds.

II. QUANTUM CHEMICAL CALCULATIONS

To facilitate the spectral assignment, initial values of the rotational constants, the torsional potential, and the ^{14}N nuclear quadrupole coupling constants (NQCCs) were calculated by quantum chemical methods using the *GAUSSIAN16* program package[9].

A. Geometry optimizations

The molecular geometry of 2MP was optimized at different levels of theory with various combinations of the MP2, B3LYP, M06-2X, and CCSD methods with different basis sets to check for the convergence and to find out the level of theory which yields rotational constants in best agreement with the experimental values. A selection of the calculations is presented in Table 1. The predicted rotational constants are given along with the dipole moment components and the angle between the inertial principal *a* axis and the methyl rotor axis. For comparison, the experimental rotational constants are also shown. A full list with all calculations is given in Table S-II in the Appendix AII.2. The molecular geometry as optimized at the MP2/cc-pVDZ level of theory is shown in Figure 1.

Table 1. The rotational constants (in MHz), the angle between the inertial principal *a* axis and the internal rotor axis *i* (in degree), and the dipole moment components (in Debye) obtained by optimizations of the molecular geometry of 2MP at various levels of theory.

	A	*B*	*C*	∠(*i*,*a*)	$\|\mu_a\|$	$\|\mu_b\|$	$\|\mu_c\|$
MP2/6-311+G(d,p)	8536.0	3417.4	2478.4	2.82	1.16	1.72	0.00
MP2/6-311++G(d,p)	8533.9	3419.1	2479.1	2.80	1.16	1.71	0.00
B3LYP-D3/6-311+G(d,p)	8594.5	3427.0	2488.1	2.87	1.09	1.67	0.00
B3LYP-D3/6-311++G(d,p)	8595.3	3427.0	2488.1	2.86	1.09	1.66	0.00
MP2/cc-pVDZ	8462.7	3398.5	2462.7	2.75	1.07	1.79	0.00
MP2/cc-pVTZ	8607.6	3446.9	2499.5	2.77	1.08	1.73	0.00
B3LYP-D3/ cc-pVDZ	8535.3	3415.7	2477.7	2.80	1.03	1.79	0.00
B3LYP-D3/ cc-pVTZ	8639.7	3444.5	2500.9	2.84	1.02	1.69	0.00
CCSD/6-311++G(d,p)	8549.4	3413.6	2477.6				
Experimental	8559.0	3432.5	2488.9	2.00			

It should be noted that the internal rotor axis is almost parallel to the principal *a* axis (see also the value of the angle $\angle(i,a)$ in Table 1). At equilibrium, the dihedral angle $\alpha = \angle(C_3,C_2,C_6,H_{11})$ is 0°, i.e. the methyl group is staggered with respect to the nitrogen atom.

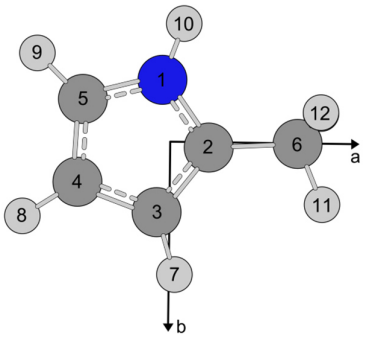

FIG. 1. The molecular geometry of 2MP optimized at the MP2/cc-pVDZ level of theory. The atom numbering and the *a* and *b* principal axes of inertia are given. The hydrogen atom H_{13} is located behind H_{12}.

B. Torsional potential of the methyl group

To obtain the barrier height to internal rotation and the shape of the potential function, geometry optimizations at the MP2/cc-pVDZ level of theory were carried out while the dihedral angle α was varied in steps of 10°. The resulting potential curve is given in Figure S1 in the Appendix AII.2. The potential was parameterized by a symmetry-adapted Fourier series with the Fourier coefficients given in Table S-III in the Appendix AII.2.

The torsional potential of 2MP displays the typical threefold shape caused by the symmetry of the methyl group. The potential consists of a V_3 value of 255.24 cm^{-1} with a V_6 contribution of 36.16 cm^{-1}.

C. ^{14}N nuclear quadrupole coupling constants (NQCCs)

In many previous studies on nitrogen containing molecules[10,11], the method of calculating ^{14}N NQCCs given by Bailey[12] turned out to be very reliable and was also applied in this work. At first, the molecular structure of 2MP was optimized at the MP2/cc-pVDZ level of theory. For this optimized structure, the electric field gradient tensor of the ^{14}N nucleus in 2MP was computed at the B3PW91/6-311+G(d,p) level of theory, as recommended for π-conjugated system [13]. Using the calibration factor eQ/h = –4.599 MHz/a.u.[13], the quadrupole coupling tensor with the diagonal elements χ_{aa} = 1.331 MHz, χ_{bb} =

1.665 MHz, and χ_{cc} = –2.996 MHz, as well as the off-diagonal element χ_{ab} = 0.091 MHz was obtained. Due to the symmetry of the molecule χ_{ac} and χ_{bc} are zero.

III. EXPERIMENT

A. Measurements

2MP was purchased from abcr GmbH, Karlsruhe, Germany, with a stated purity of 95% and was used without further purification. A piece of pipe cleaner was soaked with the substance and inserted into a stainless-steel tube placed upstream the nozzle. Helium, which was used as carrier gas, flowed over the substance at a pressure of 200-250 kPa.

All spectra were recorded using two MJ-FTMW spectrometers operating in the frequency ranges from 2.0 to 26.5 GHz[14] and from 26.5 to 40.0 GHz[15]. At first, a broadband scan was recorded from 12.0 to 14.9 GHz. The lines observed in the scan were remeasured at higher resolution. All lines show a hyperfine structure due to the nuclear quadrupole coupling of the ^{14}N nucleus. A typical spectrum is given in Figure 2.

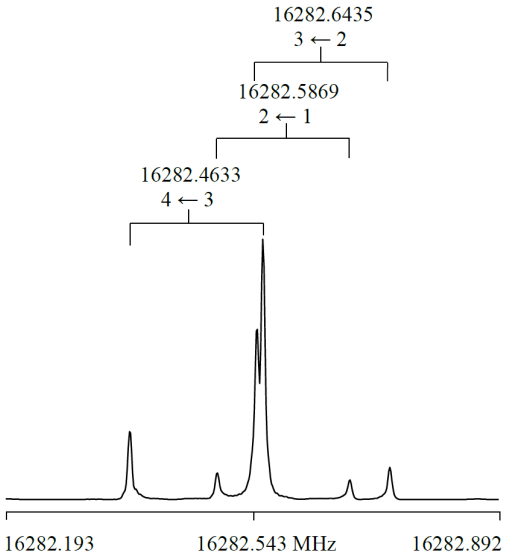

FIG. 2. A high-resolution spectrum of the $3_{13} \leftarrow 2_{12}$ E species transition of 2MP. The Doppler doublets are marked by brackets. The quantum numbers F' ← F are given at the respective hyperfine component. For this spectrum, 23 free induction decays were co-added prior to Fourier transformation.

B. Spectral assignment

At the beginning of the assignment, we predicted the spectrum with the *XIAM* code[16] using the rotational constants, the V_3 potential, and the angle between the internal rotor axis and the inertial *a* axis obtained by *ab initio* calculations at the MP2/cc-pVDZ level of theory, and neglected the quadrupole hyperfine splittings due to the ^{14}N nucleus. The predicted dipole moment components are $|\mu_a|$ = 1.07 D, $|\mu_b|$ = 1.79 D and $|\mu_c|$= 0.00 D (see Table 1). Therefore, A species *c*-type transitions were not expected to be observed in the spectrum. By comparing the broadband scan and the predicted spectrum the A and E torsional components of the $2_{11} \leftarrow 1_{10}$, $3_{03} \leftarrow 2_{12}$, $3_{21} \leftarrow 3_{12}$, and $4_{21} \leftarrow 4_{13}$ transitions could be identified. The linear combinations of the rotational constants $B_K = A - 0.5(B + C)$, $B_J = 0.5(B + C)$, $B_- = 0.5(B - C)$ and the V_3 potential were fitted, which enabled us to predict all other transitions with sufficient accuracy. Only one line in the scan region remained unassigned, which later turned out to be the *c*-type transition $1_{10} \leftarrow 0_{00}$ of the E species, which is nominally forbidden in the semi-rigid rotor approximation.

Afterwards, all lines were remeasured at high resolution. In this step, the quadrupole coupling effect was taken into account. The values of the NQCCs obtained by quantum chemical calculations were used to predict the hyperfine patterns, which fairly matched those of the experimental spectra. Due to spin-rotation and spin-spin interactions, some transitions show additional splittings of the order of 10 kHz. In those cases, the average of the individual components was taken.

IV. RESULT AND DISCUSSION

A. Results of the fits

Two global fits of 2MP with 62 A species and 67 E species lines with a total number of 359 hyperfine components were performed using the *XIAM* and *BELGI-C_s-hyperfine*[17] codes. The measurement accuracy is about 3.0 kHz for all lines. The root-mean-square (rms) deviations are 5.6 kHz and 3.1 kHz, respectively. The fit results are given in Table 2, the frequency list is available in Table S-IV of the Appendix AII.2. The fit with *BELGI-C_s-hyperfine* was carried out in the rho axis system with the parameters defined in this coordinate system are given in Table 3. For comparison with the *XIAM* results, some parameters were converted to the principal axis system (also presented in Table 2).

With the *XIAM* code, the three linear combination of rotational constants, five quartic centrifugal distortion constant Δ_J, Δ_{JK}, Δ_K, δ_J, δ_K, the ^{14}N NQCCs χ_{aa}, $\chi_{bb}-\chi_{cc}$, as well as the barrier to internal rotation V_3, the angle $\angle(i,a)$ between the *a* axis and the internal rotor axis and two higher order terms D_{pi2J}, D_{pi2K} enabled us to reproduce the experimental spectra to a *rms* deviation of 5.6 kHz.

In order to treat molecules containing one methyl rotor and one nitrogen nucleus, the *BELGI* code has been extended to its hyperfine versions *BELGI-C_s-hyperfine* and *BELGI-C_1-hyperfine*. Up to now, three molecular systems have been successfully treated by these codes, which are *N-tert*-butylacetamide (C_s)[17], *N*-ethylacetamide (C_1)[10] and 3-nitrotoluene (C_s)[18]. In this work, the *BELGI-C_s-hyperfine* code was applied, showing its capability to handle nuclear quadrupole coupling in the presence of internal rotation.

Table 2. Molecular parameters of 2MP in the inertial principal axis system obtained from fits with *XIAM* and *BELGI-C_s-hyperfine*.

Par.[a]	Unit	Fit *XIAM*	Fit *BELGI* [b]	*ab initio*[c]
A	MHz	8558.954(44)	8569.751(34)	8462.7
B	MHz	3432.5127(87)	3432.832(38)	3398.5
C	MHz	2488.8717(87)	2489.1935(69)	2462.7
Δ_J	kHz	0.2354(19)	0.2391 (11)	0.2236
Δ_{JK}	kHz	1.397(10)		1.4044
Δ_K	kHz	0.790(30)		0.5694
δ_J	kHz	0.06467(77)		0.0618
δ_K	kHz	0.401(18)		0.4222
F_o	GHz	158[d]		158.061
F	GHz	167.0422[e]	167.0422[f]	
V_3	cm^{-1}	279.7183(26)	278.9946(13)	255.24
ρ		0.0541[e]	0.0536021(93))	
D_{pi2J}	kHz	13.12(92)		
D_{pi2K}	MHz	1.1163(44)		
χ_{aa}	MHz	1.3345(20)	1.3342(11)	1.331
$\chi_{bb}-\chi_{cc}$	MHz	4.3599(36)	4.3600(33)	4.661
$\angle(i,a)$	°	2.002(46)	2.050(24)	2.75
$\angle(i,b)$	°	87.998(46)	87.950(24)	87.25
$\angle(i,c)$	°	90.0[g]	90.0[g]	90
rms[h]	kHz	5.6	3.1	
$N_A/N_E/Nq$[i]		62/67/359	62/67/359	

[a] All parameters refer to the inertial principal axis system. Statistical uncertainties are given as one standard uncertainty in the last digit. Watson's A reduction and I^r representation were used. [b] Obtained by transformation from the rho axis system to the principal axis system. [c] Calculated at the MP2/cc-pVDZ level. [d] Fixed to the calculated value. [e] Derived parameter. [f] Fixed to the value of Fit *XIAM*. [g] Fixed due to symmetry. [h] Root-mean-square deviation of the fit. [i] Number of A and E species transitions as well as number of the hyperfine components.

Table 3. Spectroscopic constants of 2MP in the rho axis system obtained using the program *BELGI-C_s-hyperfine*.

Par.[a]	Unit	Value	Operator
A	MHz	8568.696(23)	P_a^2
B	MHz	3433.887(29)	P_b^2
C	MHz	2489.1935(69)	P_c^2
D_{ab}	MHz	73.64(87)	$\{P_a,P_b\}$
Δ_J	kHz	0.2391 (11)	$-P^4$
Δ_K	kHz	0.736(17)	$-P_a^4$
Δ_{JK}	kHz	1.3174 (56)	$-P^2P_a^2$
δ_J	kHz	0.06585(43)	$-2P^2(P_a^2-P_c^2)$
δ_K	kHz	1.000(10)	$-\{P_a^2,(P_a^2-P_c^2)\}$
χ_{aa}	MHz	2.6683(22)	
χ_{bb}	MHz	3.0258(22)	
V_3	cm^{-1}	278.9946(13)	$(1/2)(1-\cos 3\alpha)$
ρ	unitless	0.0536021(93)	P_aP_α
F	cm^{-1}	5.57193[b]	$(P_\alpha-\rho P_a)^2$
F_v	MHz	-0.920(61)	$(1-\cos 3\alpha)P^2$
rms[c]	kHz	3.1	
$N_A/N_E/N_q$[d]		62/67/359	

[a] All parameters refer to the rho axis system and cannot be directly compared to those referring to the principal axis system. $\mathbf{P_a}$, $\mathbf{P_b}$, $\mathbf{P_c}$ are the components of the overall rotation angular momentum, $\mathbf{P_\alpha}$ is the angular momentum conjugate to the internal rotation angle α. {u,v} is the anti-commutator uv + vu. The product of the parameter and operator from a given row yields the term actually used in the vibration-rotation-torsion Hamiltonian, except for F, ρ and A which occur in the Hamiltonian in the form $F(\mathbf{P_\alpha}-\rho\mathbf{P_a})^2+A\mathbf{P_a^2}$, where $F = \hbar^2/2rI_\alpha$. Statistical uncertainties are shown as one standard uncertainty in the last digits. [b] Fixed to the value obtained from *XIAM* fit. [c] Root-mean-square deviation of the fit. [d] Number of A and E species transitions as well as hyperfine components. The nuclear quadrupole coupling constants are defined in the way that they are by a factor of two greater compared to their definitions in the *XIAM* program.

B. Discussion

The rotational constants from the *XIAM* and the *BELGI-C_s-hyperfine* fits are in good agreement, however, they do not agree within their standard errors. This is due to the fact that different sets of parameters were used, and that the conversion of some RAM parameters to PAM parameters is not unique and introduces some errors. It turned out that the MP2 method as well as the DFT method with the B3LYP functional in combination with Grimme's dispersion correction and Becke-Johnson damping[19] yielded a good agreement with the experimental rotational constants for most sufficiently large basis sets. Rotational constants predicted with Truhlar's M06-2X method[20] are in general further

off from the experimental values. Comparison between the rotational constants obtained from *XIAM* with those from *ab initio* calculations at the MP2/cc-pVDZ level of theory shows deviations of 1.13% for *A*, 1.01% for *B*, and 1.06% for *C* (with respect to the experimental values). A better agreement is not expected at the level of theory in use, because the experimental constants observed in the vibrational ground state are not directly comparable with the equilibrium values obtained from the *ab initio* calculations. From the results given in Table S2, the values of the rotational constants predicted at our most time-consuming calculations CCSD/6-311++G(d,p) are very close to the experimental values. Similar results can be achieved using a combination of the 6-31+G(d,p) or 6-31++G(d,p) basis set with the B3LYP or MP2 method, probably due to error compensation. From our experience, the same kind of error compensation always occurs at the same level of theory. Therefore, these levels might be chosen to predict reliable rotational constants to start the spectral assignment of future investigations on related methyl substituted pyrroles.

The parameters associated with the internal rotation, the V_3 potential and the angle between the principal *a* axis and the internal rotor axis $\angle(i,a)$, obtained from the *XIAM* and *BELGI* programs agree satisfactory, while the predicted V_3 potential is 8.8% lower than the experimental value. This deviation is rather large; however, it is in the expected range for quantum chemical calculations at the MP2/cc-pVDZ level of theory. In contrast to the geometry parameters, the calculations of the V_3 potential strongly depend on the method and basis set and a convergence is hard to achieve. Furthermore, the effects of zero-point vibrations are known to influence the calculated value. Though the calculated potential also contains contributions of V_6 and higher order terms, they are assumed to be negligible in the potential function fitted with the current experimental data. With only transitions in the torsional ground state, it is impossible to test the validity of this assumption, as V_6 cannot be determined.

The ^{14}N NQCCs obtained from the *XIAM* and the *BELGI* fits agree within the standard errors. The quantum chemical results obtained at the B3PW91/6-311+G(d,p)//MP2/cc-pVDZ level agree within 0.3% for χ_{aa} and −6.9% for $\chi_{bb} - \chi_{cc}$ (with respect to the experimental values). In the principal axis system, an experimental value for χ_{ab} cannot be obtained because it is associated with the expectation value of $\{P_a,P_b\}$ which is zero in the case of the A species and which cannot be determined well from the E species at rather high barriers such as 280 cm^{-1} . If we calculate the same quantity in

RAM and back-transform it to PAM, we will not be able to acquire χ_{ab}. Particularly in case of 2MP, the off-diagonal elements of the nuclear quadrupole coupling tensor could not be fitted with *BELGI-C_s-hyperfine* program and therefore a back-transformation on χ_{ab} was not possible.

Some results obtained for 2MP are compared with those of other five-membered heterocycles in Figure 3.

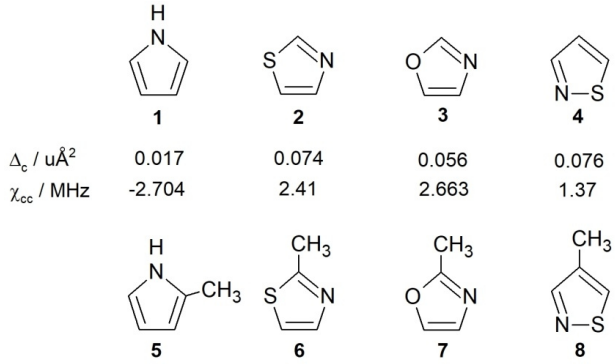

FIG. 3. Comparison of the V_3 potential, the inertial defect Δ_c, and the ^{14}N coupling constant χ_{cc} of 2MP with those of other five-membered heterocycles. (**1**) Pyrrole, (**2**) Thiazole, (**3**) Oxazole, (**4**) isothiazole, (**5**) 2-methylpyrrole, (**6**) 2-methylthiazole, (**7**) 2-methyloxazole, (8) 4-methylisothiazole.

The V_3 potential varies in a wide range from 34 cm^{-1} for 2-methylthiazole[1] (**6**), 106 cm^{-1} for 4-methylisothiazole[2] (**8**), 252 cm^{-1} for 2-methyloxazole[21] (**7**) to 280 cm^{-1} for 2MP (**5**). The V_3 potential is due to symmetry strictly 0 cm^{-1} for molecules with a C_{2v} symmetric frame and an internal rotor of C_{3v} symmetry. Only a small V_6 term is found in the cases of toluene[22], nitromethane[23, 24], and *N*-methylpyrrole[25]. If the frame symmetry is lowered from C_{2v} to C_s, then a V_3 contribution is observed, depending on the local asymmetry due to steric or electronic effects. In 2-methylthiazole (**6**) the nitrogen and sulfur atoms have similar effects on the methyl rotor and only a very low V_3 potential arises. In 4-methylisothiazole (**8**) a similar situation also leads to a rather low barrier of 106 cm^{-1}. In the title compound 2MP (**5**) the environment of the methyl group with a NH group on one side and a carbon atom on the other side is rather asymmetric which results in a much higher barrier. We note that such intuitive interpretations should be taken with caution because in aromatic systems electronic effects are easily propagated through the π system of the ring and affect the barrier height.

The aromaticity is associated with a planar structure of the π electron system. A direct measure for planarity is the inertial defect $\Delta_c = I_c - I_a - I_b$ with the principal moments of inertia I_a, I_b, I_c is calculated for all compounds in Figure 3. In the case of the non-methylated systems inertial defects of 0.017, 0.074, 0.056, and 0.076 uÅ^2 are found for pyrrole[26] (**1**), thiazole[27] (**2**), oxazole[28] (**3**), and isothiazole[29] (**4**), respectively. The deviation from zero can be explained by the zero point vibrations of the rings. If one methyl group is attached to the ring, the out-of-plane hydrogen atoms of the methyl group cause an inertial defect close to 3.2 uÅ^2. This is in agreement with the values of –3.223, –3.108, –3.127, and –3.012 uÅ^2 of 2MP (**5**), 2-methylthiazole (**6**), 2-methyloxazole (**7**), and 4-methylisothiazole (**8**), respectively.

In all systems given in Figure 3 the principal *c* axis perpendicular to the ring plane is collinear with one principal axis of the coupling tensor. Therefore, the χ_{cc} element of the ^{14}N quadrupole coupling tensor can be directly compared. In pyrrole (**1)** and 2MP (**5**), the values of χ_{cc} are very similar but have a different sign than in all other heterocycles (**2-4)** and **(6-8**). The reason is, that the two groups exhibit a very different bond situation at the nitrogen atom which causes different electric field gradients at the site of the nitrogen nucleus. The electron configuration of nitrogen is [He]2s^{2}2p^3. In all compounds of Figure 3, three sp^2 hybrid orbitals are formed, two of which are used to form the σ bonds to the neighboring atoms. One p orbital remains and becomes part of the π electron system. As shown in Figure 4, in the case of pyrrole three of five nitrogen electrons are needed in three sp^2 orbitals to form the two N-C bonds and one N-H bond (not illustrated). The other two electrons occupy the p orbital (illustrated in red) and contribute to the π electron system. Altogether, there are 6 π electrons which, according to the 4n + 2 rule, makes pyrrole an aromatic compound.

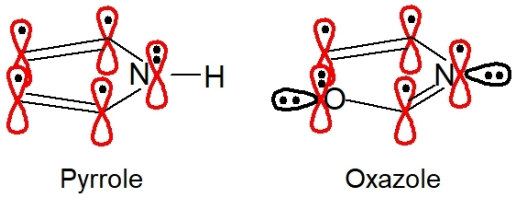

FIG. 4. The π electron system in pyrrole and oxazole.

In the other heterocycles, the situation is quite different. For oxazole, two sp^2 orbitals of the nitrogen atom with one electron each form the bonds to the neighboring atoms (not illustrated). The

third sp^2 orbital is occupied by an electron lone pair (illustrated in black). Only one electron remains in the p orbital (illustrated in red) contributing to the π electron system. It should be noted that in this group of molecules a sulfur or an oxygen atom is needed to donate two electrons for their p orbital to fulfill the condition for an aromatic compound (6 electrons in the π system). Similar considerations apply also to thiazole and isothiazole.

In the case of pyrrole, the effect of methylation on χ_{cc} is small. Despite the well-known +I effect[30] of methyl groups, only a small change in the field gradient tensor is observed. The values of χ_{cc} of pyrrole (**1**) and 2MP (**5**) are –2.704 and –2.846 MHz, respectively. Similar small effects are observed upon methylation of thiazole (**4**), oxazole (**6**), and isothiazole (**8**).

V. CONCLUSION

The methyl torsional fine structure and the quadrupole hyperfine structure in the rotational spectrum of 2MP could be fully resolved using two molecular jet Fourier transform microwave spectrometers operating in the frequency range from 2 to 40 GHz. All observed transitions were analyzed and fitted with the programs *XIAM* and *BELGI-C_s-hyperfine*, whereby the *BELGI-C_s-hyperfine* code enabled us to reproduce the whole data set close to measurement accuracy. The spectroscopic work was supplemented by quantum chemical calculations.

The methyl group undergoes internal rotation with a V_3 hindering potential of 279.7183(26) cm^{-1}. The quadrupole coupling constants of the ^{14}N nucleus were determined with very high accuracy. Calculations of the electric field gradient tensor with Bailey's method yielded nuclear coupling constants in good agreement with the experimental values.

APPENDIX

See the Appendix section AII.2 for Potential curve (Figure S-I), nuclear coordinates of 2MP (Table S-I), rotational constants at different levels of theory (Table S-II), Fourier coefficient of the fitted potential curve (Table S-III), and frequency list (Table S-IV).

FUNDING

T. N. thanks the Doctoral School of Environmental Science of Île-de-France (DS 129) for a Ph.D grant. Simulations were performed with computing resources granted by RWTH Aachen University under project rwth0369. W.S. thanks the Université Paris-Est for an invited researcher grant which enabled him to work at the Université Paris-Est Créteil. This work was supported by the Agence Nationale de la Recherche ANR (project ID ANR-18-CE29-0011).

ACKNOWLEDGEMENT

I.K., H.V.L.N., and T.N. thank the DIM Qi2 for supporting the organization of the Journées de Spectroscopie Moléculaire (JSM) in Créteil where T.N. presented a poster with the results. C.D. thanks the DIM Qi2 for supporting her trip to the JSM.

REREFRENCES

[1]J.-U. Grabow, H. Hartwig, N. Heineking, W. Jäger, H. Mäder, H.W. Nicolaisen, W. Stahl, *J. Mol. Struct.* **612**, 349 (2002).

[2]H.W. Nicolaisen, J.-U. Grabow, N. Heineking, W. Stahl, *Z. Naturforsch.* **46a**, 635 (1991).

[3]V. Van, W. Stahl, H.V.L. Nguyen, *Phys. Chem. Chem. Phys.* **17**, 32111 (2015).

[4]V. Van, W. Stahl, H.V.L. Nguyen, *ChemPhysChem*. **17**, 3223 (2016).

[5]V. Van, J. Bruckhuisen, W. Stahl, V.V. Ilyushin, H.V.L. Nguyen, *J. Mol. Spectrosc.* **343**, 121 (2017).

[6]J.A. Maga, J. Agric. *Food Chem.* **29**, 691 (1981).

[7]J. Tang, Q.Z. Jin, G.-H. Shen, C.T. Ho, S.S. Chang, *J. Agric. Food Chem.* **31**, 1287 (1983).

[8]R. Kaur, V. Rani, V. Abbot, Y. Kapoor, D. Konar, K. Kumar, *J. Pharm Chem Chem Sci.* **1**, 17 (2017).

[9]M. J. Frisch, G.W. Trucks, H.B. Schlegel, G.E. Scuseria, M.A. Robb, J.R. Cheeseman, G. Scalmani, V. Barone, B. Mennucci, G.A. Petersson, H. Nakatsuji, M. Caricato, X. Li, H.P. Hratchian, A.F. Izmaylov, J. Bloino, G. Zheng, J.L. Sonnenberg, M. Hada, M. Ehara, K. Toyota, R. Fukuda, J. Hasegawa, M. Ishida, T. Nakajima, Y. Honda, O. Kitao, H. Nakai, T. Vreven, J.A. Montgomery, Jr., J.E. Peralta, F. Ogliaro, M. Bearpark, J.J. Heyd, E. Brothers, K.N. Kudin, V. N. Staroverov, R. Kobayashi, J. Normand, K. Raghavachari, A. Rendell, J.C. Burant, S.S. Iyengar, J. Tomasi, M. Cossi, N. Rega, J. M. Millam, M. Klene, J.E. Knox, J.B. Cross, V. Bakken, C. Adamo, J. Jaramillo, R. Gomperts, R. E. Stratmann, O. Yazyev, A.J. Austin, R. Cammi, C. Pomelli, J.W. Ochterski, R.L. Martin, K. Morokuma, V.G. Zakrzewski, G.A. Voth, P. Salvador, J.J. Dannenberg, S. Dapprich, A.D. Daniels, Ö. Farkas, J. B. Foresman, J.V. Ortiz, J. Cioslowski, and D.J. Fox, Gaussian 09, Gaussian, Inc., Wallingford CT, 2009

[10]R. Kannengießer, M.J. Lach, W. Stahl, H.V.L. Nguyen, *ChemPhysChem* **16**, 1906 (2015).

[11]R. Kannengießer, S. Klahm, H.V.L. Nguyen, A. Lüchow, W. Stahl, *J. Chem. Phys.* **141**, 204308 (2014).

[12]W.C. Bailey, *Chem. Phys.* **252**, 57 (2000).

[13]R. Kannengießer, W. Stahl, H.V.L. Nguyen, W.C. Bailey, *J. Mol. Spectrosc.* **317**, 50 (2015).

[14]J.-U. Grabow, W. Stahl, H. Dreizler, *Rev. Sci. Instrum.* **67**, 4072 (1996).

[15]I. Merke, W. Stahl, H. Dreizler, *Z. Naturforsch.* **49a**, 490 (1994).

[16]H. Hartwig, H. Dreizler, *Z. Naturforsch*. **51a**, 923 (1996).

[17]R. Kannengießer, W. Stahl, H.V.L. Nguyen, I. Kleiner, *J. Phys. Chem. A* **120**, 3992 (2016).

[18]A. Roucou, I. Kleiner, M. Goubet, S. Bteich, G. Mouret, R. Bocquet, F. Hindle, W.L. Meerts, A. Cuisset, *ChemPhysChem* **19**, 1056 (2018).

[19]E. Caldeweyher, C. Bannwarth, S. Grimme, *J. Chem. Phys.* **147**, 034112 (2017).

[20]Y. Zhao, D.G. Truhlar, *Theor. Chem. Acc.* **120**, 215 (2008).

[21]E.R.L. Fliege, *Z. Naturforsch.* **45a**, 911 (1990).

[22]V.V. Ilyushin, E.A. Alekseev, Z. Kisiel, L. Pszczółkowski, *J. Mol. Spectrosc.* **339**, 31 (2017).

[23]F. Rohart, *J. Mol. Spectrosc.* **57**, 301 (1975).

[24]V. V. Ilyushin, *J. Mol. Spectrosc.* **345**, 64 (2018).

[25]J. Makarewicz, S. Huber, B. Brupbacher-Gatehouse, A. Bauder, *J. Mol. Struct*. **612**, 117 (2002).

[26]L. Nygaard, J.T. Nielsen, J. Kirchheiner, G. Maltesen, J.R. Andersen, G.O. Sørensen, *J. Mol. Struct.* **3**, 491 (1969).

[27]L. Nygaard, E. Asmussen, J.H. Høg, R.C. Maheshwari, C.H. Nielsen, I.B. Petersen, J. Rastrup-Andersen, G.O. Sørensen, *J. Mol. Struct.* **8**, 225 (1971).

[28]A. Kumar, J. Sheridan, O.L. Stiefvater, *Z. Naturforsch.* **33a**, 145 (1978).

[20]J.H. Griffiths, A. Wardley, V.E. Williams, N.L. Owen, J. Sheridan, *Nature* **216**, 1301 (1967).

[30]C.K. Ingold, *J. Chem. Soc.* **1120** (1933).

Chapter II.3: ^{14}N Nuclear Quadrupole Coupling and Methyl Internal Rotation in 3-Methylpyrrole Investigated by Microwave Spectroscopy

This is an Accepted Manuscript of an article published by Elsevier in Journal of Molecular Spectroscopy: "Thuy Nguyen, Wolfgang Stahl, Ha Vinh Lam Nguyen, and Isabelle Kleiner, ^{14}N Nuclear quadrupole coupling and methyl internal rotation in 3-methylpyrrole investigated by microwave spectroscopy, J. Mol. Spectros. ***372****, 111351 (2020) available online: https://doi.org/10.1016/j.jms.2020.111351"*

ABSTRACT

The molecular structure of 3-methylpyrrole in the gas phase has been determined using a combination of high-resolution spectroscopy and quantum chemical calculations. The rotational spectrum was recorded using a molecular jet Fourier transform microwave spectrometer covering the frequency range from 2.0 to 26.5 GHz. The experimental data were analyzed using the programs *XIAM* and *BELGI-C_s-hyperfine*. Because the internal rotor axis accidentally lies along the principal *a*-axis of inertia, the rho axis system and the principal axis system coincide, enabling a direct comparison of the fits. With the program *XIAM*, the rotational constants A = 8631.1629(12), B = 3342.19750(43), and C = 2445.73846(42) MHz were obtained. Torsional splittings due to internal rotation of the methyl group were observed, leading to the determination of the V_3 potential of 245.92445(31) cm^{-1}. Hyperfine splittings arising from the nuclear quadrupole coupling of the ^{14}N nucleus could be resolved, and the quadrupole coupling constants χ_{aa} = 1.4159(49) and $\chi_{bb} - \chi_{cc}$ = 4.1622(86) MHz were found.

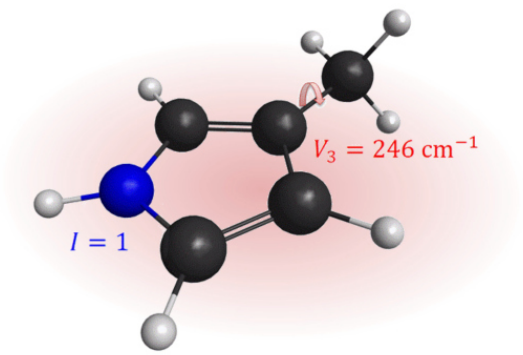

I. INTRODUCTION

Many studies on monomethyl-substituted five-membered heterocycles have been carried out in the microwave region in great detail, i.e., 2-methylfuran,[1] 3-methylthiophene,[2] the three isomers of methylthiazole,[3-5] the three isomers of methyl oxazole,[6] 3- and 5-methylisoxazole,[7] and the four isomers of methylimidazole.[8] Such molecules exhibit intramolecular dynamics, arising from the internal rotation of the methyl group, being important in physics, chemistry, and biology. Though a number of studies are available, still no effective, phenomenological rule for predicting the torsional barrier of the methyl group could be deduced. In other words, how the steric effects and the electronic environment affect the barrier to internal rotation of the methyl group in five-membered heterocycles is still a puzzling quantitative question, which might be answered by the complementary use of microwave spectroscopy and quantum chemical calculations.

Pyrrole is a nitrogen containing five-membered ring which appears as a structural component of several biologically important compounds, e.g., serotonin (5-hydroxytryptamine), a neurotransmitter and vasoconstrictor active in the central nervous system. It is also a subunit of some vitally important compounds called porphyrines, e.g., porphine, and substituted derivatives that form metal complexes like chlorophyll or hemoglobin. The derivatives of pyrrole are studied extensively by pharmacology.[9] Therefore, basic knowledge on the structure and dynamics of pyrrole derivatives underpins investigations and developments in biology.

Recently, the microwave spectrum of a mono-methyl substituted pyrrole derivative, 2-methylpyrrole (2MP), was studied, revealing torsional splittings from the three-fold hindered internal rotation of the methyl group and hyperfine structures from the quadrupole coupling of the ^{14}N nucleus.[10] The molecular structure as well as the effective V_3 potential and the ^{14}N nuclear quadrupole coupling constants (NQCCs) were determined with high accuracy. In order to answer how the steric effect and the electronic environment affect the methyl internal rotation, it is plausible to study substitution isomers. i.e., 3-methylpyrrole (3MP) and compare the methyl torsional barrier with that of 2MP. Moreover, the study on the ^{14}N NQCCs of 2MP states that the effect of methylation on χ_{cc} can be almost neglected. The NQCCs of 3MP will provide valuable data to confirm or deny the general validity of this statement.

The details of the present study will be divided into sections which describe the quantum chemical calculations, the experimental setup, the assignment of the spectra, the fits with molecular parameters deduced from the experimental data, followed by a discussion and our conclusion.

II. QUANTUM CHEMICAL CALCULATIONS

In order to get reasonable starting values for the spectral assignment, the *GAMESS*[11] program package was used to quantum-chemically optimize the structure of 3MP, to predict the barrier to internal rotation of the methyl group, and to compute the ^{14}N NQCCs.

A. Geometry optimizations

To obtain the molecular geometry of 3MP, optimizations were performed using the Kohn-Sham density functional theory[12] employing Becke's three parameters hybrid exchange functional,[13] the Lee-Yang-Parr correlation functional[14] (B3LYP) and the second order Møller-Plesset perturbation method (MP2)[15] in combination with the Dunning basis sets cc-pVDZ and cc-pVTZ.[16] In Table 1, the rotational constants and the angle $\angle(i,a)$ between the principal a axis and the internal rotor axis i are given along with the level of theory at which the calculation was performed.

Table 1. The rotational constants (in MHz) and the angle $\angle(i,a)$ (in degrees) of 3MP obtained at various levels of theory.

	A	*B*	*C*	$\angle(i,a)$
MP2/cc-pVDZ	8553.8	3305.9	2420.8	0.25
MP2/cc-pVTZ	8470.2	3445.8	2486.9	0.01
B3LYP/cc-pVDZ	8602.5	3321.6	2432.9	0.42
B3LYP/cc-pVTZ	8697.2	3352.1	2456.2	0.44
Experimental	8631.2	3342.2	2445.7	0.00

All calculations yielded only one stable conformer. The geometrical structure of 3MP optimized at the MP2/cc-pVDZ level of theory is illustrated in Figure 1, showing that the internal rotor axis is almost collinear with the principal inertial a axis. The Cartesian coordinates are given in Table S-I in the Appendix AII.3.

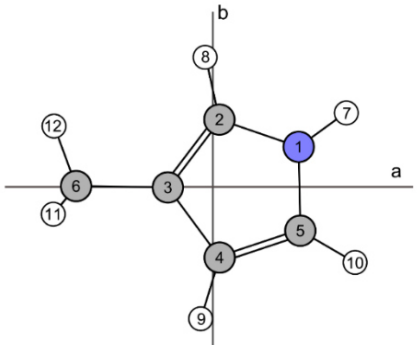

FIG. 1. The geometry of 3MP optimized at the MP2/cc-pVDZ level of theory. Atomic numbers and the inertial principal axes are given. The N atom is presented in blue; C atoms are given in grey and H atoms in white. The hydrogen atom H_{13} is located behind H_{12}. The internal rotor axis is almost collinear with the inertial principal *a* axis.

B. Methyl torsional barrier

The height and shape of the torsional potential of the methyl group were retrieved by optimizing the molecular geometry of 3MP in steps of 10° of the dihedral angle $\alpha = \angle(C_2,C_3,C_6,H_{12})$ at the MP2/cc-pVDZ level of theory. The V_3 term was determined to be 189.8 cm^{-1}. The potential curve is illustrated in Figure S-II, the fitted Fourier coefficients obtained by fitting the step-wise computed potential function are given in Table S-III in the Appendix AII.3.

C. ^{14}N nuclear quadrupole coupling constants

It is known from a number of previous studies that the method introduced by Bailey[17] to compute the ^{14}N NQCCs is rather reliable.[10,18-20] Therefore, we also apply this method for 3MP. With the molecular geometry optimized at the MP2/cc-pVDZ level of theory, the electric field gradient (EFG) tensor at the site of the ^{14}N nucleus was calculated at the B3PW91/6-311+G(d,p) level of theory, which is recommended for modeling of conjugated π-electron systems.[21] The quadrupole coupling tensor is directly proportional to the EFG tensor by the calibration factor eQ/h = –4.599 MHz/a.u.[21] The NQCCs were found to be χ_{aa} = 1.5054, χ_{bb} = 1.4234, χ_{cc} = –2.9288, and χ_{ab} = 0.1481 MHz. The off-diagonal χ_{ac} and χ_{bc} are zero due to symmetry.

III. EXPERIMENTAL SECTION

A. Measurements

The sample of 3MP was purchased from TCI Europe, Zwijndrecht, Belgium, with a stated purity of over 99% and used without further purification. A drop of 3MP was put on a pipe cleaner which is inserted into a stainless-steel tube placed upstream the nozzle. Helium, used as carrier gas, flowed over the substance at a backing pressure of 200-250 kPa. The spectra of 3MP were recorded using a molecular jet Fourier-transform microwave spectrometer covering the frequency region from 2.0 to 26.5 GHz.[22]

Guided by the theoretical spectrum using the rotational constants predicted at the MP2/cc-pVDZ level of theory, a broadband scan from 10 to 12 GHz in steps of 0.25 MHz was recorded for the spectral assignment. Subsequently, all lines were remeasured at higher resolution. The line widths are approximately 15-30 kHz for isolated lines, the measurement accuracy is about 2.5 kHz.

B. Spectral assignment

In the first approach, the effects arising from the nuclear quadrupole coupling were neglected and 3MP was treated as a one-top molecule. The values of the rotational constants, the barrier to internal rotation of the methyl group, and the angle $\angle(i,a)$ calculated at the MP2/cc-pVDZ level of theory were used as initial values in the program *XIAM*[23] to predict the spectrum of 3MP. The dipole moment components of 3MP were predicted to be $|\mu_a| = 1.49$, $|\mu_b| = 1.17$, and $|\mu_c| = 0.00$ D. Therefore, the spectrum should contain only *a*- and *b*-type transitions. By comparing the theoretical spectrum and the broadband frequency scan, we were able to identify the A and E torsional components of the $1_{11} \leftarrow 0_{00}$, $2_{12} \leftarrow 1_{01}$, $2_{12} \leftarrow 1_{11}$, and $4_{13} \leftarrow 4_{04}$ transitions. Fitting the frequencies of those transitions by adjusting the three linear combinations of the rotational constants $B_K = A - 0.5(B + C)$, $B_J = 0.5(B + C)$, $B_- = 0.5(B - C)$, and the V_3 potential minimized the root-mean-square (rms) deviation to about 0.5 MHz. This fit allowed us to record further lines at high resolution with sufficient accuracy. The quadrupole hyperfine structures due to the ^{14}N nucleus are well-resolved for all lines. The assignment of the hyperfine components was straightforward because the observed frequencies agreed fairly well with the predictions based on the predicted NQCC values. Finally, 89 rotational transitions including 36 A species and 53 E species lines with a total of 264 hyperfine components were measured and fitted with the program *XIAM*. The frequencies are given in Table S-IV of the Appendix AII.3.

Since the final rms deviation of 12.1 kHz obtained with *XIAM* is much higher than the measurement accuracy, the program *BELGI-C_s-hyperfine*[24] was applied on the same data set, aiming to reduce the rms deviation to measurement accuracy. The *BELGI-C_s-hyperfine* code is an extension of the *BELGI-C_s* code. While *BELGI-C_s* is suitable to treat the microwave spectra of molecules with one methyl internal rotation and C_s frame symmetry, the *BELGI-C_s-hyperfine* code takes into account in addition one weak nuclear quadrupole interaction, i.e., ^{14}N, using a perturbation approach to calculate the hyperfine splittings. The rotation-torsion eigenvalues and eigenvectors are first obtained from the usual two-step diagonalization of the rotation-torsion Hamiltonian in the rho axis system. Subsequently, the numerical values of the quadratic angular momentum components $\langle \mathbf{P_x^2} \rangle, \langle \mathbf{P_y^2} \rangle, \langle \mathbf{P_z^2} \rangle$, and $\langle \mathbf{P_z P_x} + \mathbf{P_x P_z} \rangle$ are quantified, and then put into the standard hyperfine energy expression as given in Eq. (1) of Ref. [24].

IV. FIT RESULTS

The experimental data were analyzed using two programs, *XIAM*[23] and *BELGI-C_s-hyperfine*.[24] The *XIAM* code uses a combined axis method where the internal rotation Hamiltonian of each single top is set up in the rho axis system and then transformed into the principal axis system, while in *BELGI-C_s-hyperfine* the Hamiltonian is written exclusively in the rho axis system. Therefore, molecular parameters obtained from *XIAM* and *BELGI-C_s-hyperfine* refer to different axis systems. For a comparison, parameters obtained from *BELGI-C_s-hyperfine* have to be transformed into the principal axis system, which is often not possible for all resultant parameters. In all previous investigations where the two approaches have been compared, this procedure could only be applied for the rotational constants[25,26] and the NQCCs.[24] Details of the conversions are given in Refs. [27,28].

Though *ab initio* calculations suggested that the angle $\angle(i,a)$ between the *a* principal axis and the internal rotor axis is approximately zero (see Table 1), we still tried to float this angle in the *XIAM* fit. However, it turned out to be badly determined and was highly correlated with the V_3 parameter with a correlation coefficient of 0.998. Therefore, we finally fixed the value of $\angle(i,a)$ at zero. In the *BELGI* code, the angle $\angle(i,a)$ is not available as a fit parameter, but another parameter called D_{ab} multiplying the $\mathbf{P_a P_b} + \mathbf{P_b P_a}$ off-diagonal Hamiltonian term. D_{ab} is related to the angle between the rho axis system

and the principal axis system. A detailed explanation can be found in Ref. [29]. Similar to the situation observed during the fitting with the program *XIAM*, attempts to float D_{ab} led to divergence. We then fixed D_{ab} at various values varying in the range from $1 \cdot 10^{-5}$ cm^{-1} (about 0.3 MHz) to $5 \cdot 10^{-3}$ cm^{-1} (about 150 MHz). In Figure 2, the rms deviation of the fits is plotted as a function of the fixed value of D_{ab}. The bottom of the curve is extremely flat until D_{ab} reaches the value of about 0.002 cm^{-1} where the rms deviation started to increase. Therefore, we decided to fix D_{ab} at zero. This means that in the case of 3MP, the principal axis system and the rho axis system coincide within the measurement accuracy and the results of the *XIAM* and *BELGI-C_s-hyperfine* fits are directly comparable for all resultant parameters.

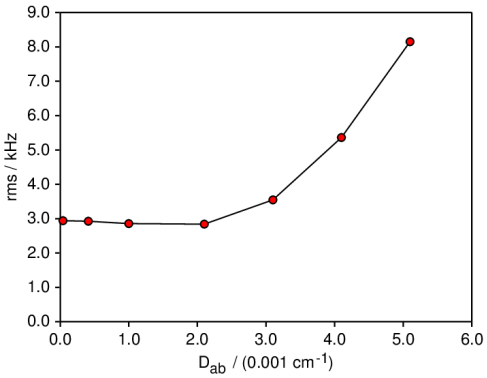

FIG. 2. Root-mean-square deviation of the *BELGI* fit as a function of D_{ab}.

In the *XIAM* fit, the main geometrical parameters (three rotational constants), the internal rotation parameters (barrier to internal rotation and the rotation distortion operators in the principal axis system terms D_{pi2J}, D_{pi2K}, and D_{pi2-}), the NQCCs (χ_{aa} and $\chi_{bb} - \chi_{cc}$) together with four centrifugal distortion constants using Watson's A reduction (Δ_J, Δ_{JK}, δ_J, δ_K) were fitted and determined with high accuracy. The rms deviation is 12.1 kHz which is approximately 5 times the estimated measurement accuracy.

The *BELGI-C_s-hyperfine* code succeeded to reproduce the experimental data of *N-tert*-butylacetamide,[24] 3-nitrotoluene,[30] and recently 2MP[10] with a satisfactory rms deviation. For 3MP, with 14 floated parameters (and fixing the two parameters F and D_{ab} at zero), the rms deviation of 2.9 kHz obtained with *BELGI-C_s-hyperfine* is almost the measurement accuracy. The molecular parameters of 3MP obtained from the two fits, and the results from *ab initio* calculations at the MP2/cc-pVDZ level of theory are presented in Table 2.

Table 2. Molecular parameters of 3MP in the principal axis system obtained from fits with the *XIAM* and the *BELGI-C_s-hyperfine* programs.

Operator	Par.[a]	Unit	Fit *XIAM*	Fit *BELGI*	*ab initio*[b]
$\mathbf{P_a^2}$	A	MHz	8631.1629(12)	8631.0585(40)	8553.8
$\mathbf{P_b^2}$	B	MHz	3342.19750(43)	3341.8407(43)	3305.9
$\mathbf{P_c^2}$	C	MHz	2445.73846(42)	2445.5916(45)	2420.8
$\mathbf{\{P_a,P_b\}}$	D_{ab}		-	0[c]	
$\mathbf{-P^4}$	Δ_J	kHz	0.2460(89)	0.2191(27)	0.2142
$\mathbf{-P^2P_a^2}$	Δ_{JK}	kHz	1.487(42)	1.586(10)	1.4488
$\mathbf{-P_a^4}$	Δ_K	kHz	-	0.525(14)	0.6462
$\mathbf{-2P^2(P_a^2 - P_c^2)}$	δ_J	kHz	0.0645(32)	0.0608(78)	0.0582
$\mathbf{-\{P_a^2,(P_a^2 - P_c^2)\}}$	δ_K	kHz	0.445(70)	1.129(17)	0.3413
	F_0	GHz	158[d]	-	158
$\mathbf{(P_\alpha - \rho P_a)^2}$	F	GHz	167.130[e]	167.130[f]	
$\mathbf{(1/2)(1 - \cos 3\alpha)}$	V_3	cm^{-1}	245.92445(31)	245.14101(89)	189.8
$\mathbf{F P_a P_\alpha}$	ρ		0.0546[e]	0.05400716(72)	
$\mathbf{2(P_\alpha - \rho P_r)^2P^2}$	D_{pi2J}	kHz	21.9(19)	-	
$\mathbf{\{(P_\alpha - \rho P_r)^2,P_a^2\}}$	D_{pi2K}	MHz	1.3505(60)	-	
$\mathbf{\{(P_\alpha - \rho P_r)^2,(P_b^2 - P_c^2)\}}$	D_{pi2-}	kHz	13.20(89)		
$\mathbf{P^2P_\alpha^2}$	G_v	MHz	-	0.05832(93)	
$\mathbf{2(P_b^2 - P_c^2)P_\alpha^2}$	c_1	MHz	-	0.01200(22)	
	χ_{aa}	MHz	1.4159(49)	1.41345(12)	1.5054
	χ_{bb}	MHz	1.3732(68)	1.37535(12)	1.4234
	χ_{cc}[e]	MHz	–2.7890(19)	–2.78880(24)	–2.9288
	$\angle(i,a)$	°	0[c]	-	0.25
	$\angle(i,c)$	°	90[g]	90[g]	90
	rms[h]	kHz	12.1	2.9	
	$N_A/N_E/N$[i]		36/53/264	36/53/264	

[a] All parameters refer to the inertial principal axis system. $\mathbf{P_a}$, $\mathbf{P_b}$, $\mathbf{P_c}$ are the components of the overall rotation angular momentum, $\mathbf{P_\alpha}$ is the angular momentum conjugate to the internal rotation angle α and $\mathbf{P_r}$ is the angular momentum vector along the rho axis. For 3MP, the rho axis is collinear to the principal *a* axis, meaning that $\mathbf{P_r}$ lies in the same direction as $\mathbf{P_a}$. Statistical uncertainties are given as one standard uncertainty in the last digit. Watson's A reduction and I^r representation were used. {u,v} is the anti-commutator uv + vu. The product of the parameter and operator from a given row yields the term actually used in the vibration-rotation-torsion Hamiltonian, except for F, ρ, and A, which occur in the Hamiltonian in the form $F(\mathbf{P_\alpha} - \rho\mathbf{P_a})^2 - A\mathbf{P_a^2}$. [b] Calculated at the MP2/cc-pVDZ level. [c] Fixed to zero (see text). [d] Fixed to the calculated value. [e] Derived parameter. [f] Fixed to the value of *XIAM*. [g] Fixed due to symmetry. [h] Root-mean-square deviation of the fit. [i] Number of A and E species rotational transitions as well as number of the hyperfine components.

V. DISCUSSION

A. Geometry parameters

The rotational constants obtained with the *XIAM* and *BELGI-C_s-hyperfine* codes agree fairly well. The small differences in the different approaches probably arise from altered constraints that come with the different sets of parameters used in the two fits. When comparing the values obtained from the *XIAM* fit with those from quantum chemical calculation at the MP2/cc-pVDZ level of theory, we found deviations of –0.90% for *A*, –1.09% for *B*, and –1.02% for *C* (with respect to the *XIAM* value). Such deviations are frequently observed while comparing the experimental rotational constants, which refer to the vibrational ground state, with equilibrium constants calculated at the MP2/cc-pVDZ level.

Using the same data set, the *BELGI-C_s-hyperfine* code enables us to retrieve all five quartic centrifugal distortion constants Δ_J, Δ_{JK}, Δ_K, δ_J, δ_K whereas Δ_K cannot be determined with *XIAM*. Generally, a direct comparison between the centrifugal distortion constants obtained with *BELGI-C_s-hyperfine* and *XIAM*, except for Δ_J, is not possible. However, in the case of 3MP where the rho axis and the principal axis systems accidentally coincide, the parameters can be directly compared. While the values of Δ_J, Δ_{JK}, and δ_J from the *XIAM* fit, the *BELGI-C_s-hyperfine* fit, and *ab initio* calculations at the MP2/cc-pVDZ level of theory match fairly well, the δ_K value obtained with *BELGI-C_s-hyperfine* is significantly higher. To test the effects of centrifugal distortion in *BELGI*, we switched to Watson's S reduction, since some studies in the literature, e.g. 1,1-difluoroacetone[31] and aziridine,[32] have indicated fitting problems arising from the dependence of δ_K on the ratio $(2A - B - C)/(B - C)$,[33] from which Δ_J, Δ_{JK}, Δ_K, δ_J and all of five quartic centrifugal distortion terms in the S reduction are free of. A comparison of the quartic centrifugal distortion constants obtained from *BELGI* and *XIAM* is given in Table 3.

Table 3. Comparison of quartic centrifugal distortion constants (in kHz) using Watson's S reduction in I^r representation obtained from fits with the *XIAM* and the *BELGI-C_s-hyperfine* programs.

Par.[a]	Fit *XIAM*	Fit *BELGI*	*ab initio*
D_J	0.2387(90)	0.1777(33)	0.2010
D_{JK}	1.592(35)	1.990(11)	1.5284
D_K	-	0.292(17)	0.5798
d_1	–0.0644(32)	–0.05888(95)	–0.0582
d_2	–0.0088(14)	–0.02429(42)	–0.0066

Since Δ_K (or D_K) is not well-determined with *XIAM*, we performed several tests where Δ_K (or D_K) is fixed to zero, fitted, and fixed to the values obtained from *BELGI-C_s-hyperfine*. The results from all these tests showed that all other four quartic centrifugal distortion parameters as well as the rms deviation did not change much upon variations in the value of Δ_K (or D_K), and the value of δ_K or d_2 deduced from *XIAM* always differs significantly to that from *BELGI*. This indicates that the reduction is not responsible for the different values of δ_K or d_2, but the contamination of this parameter by the internal rotation effects reflected in different sets of internal rotation parameters used in *BELGI-C_s-hyperfine* and *XIAM*.

B. ^{14}N nuclear quadrupole coupling constants

The NQCCs obtained from the two fits are in very good agreement. The values of χ_{aa}, χ_{bb}, and χ_{cc} predicted at the B3PW91/6-311+G(d,p)//MP2/cc-pVDZ level deviate by 6.32%, 3.65%, and 5.01%, respectively, compared to those deduced by the *XIAM* fit. The χ_{cc} value found for 3MP is –2.7890(19) MHz which is smaller than that found for 2MP (–2.846(36) MHz) and even closer to that of pyrrole (–2.66(2) MHz).[34] This observation confirmed the negligible methylation effect on χ_{cc} perpendicular to the aromatic rings plane of the methyl derivatives of pyrrole. As χ_{ab} is associated with the expectation value of $\{\mathbf{P_a},\mathbf{P_b}\}$, it can vanish if the coupling tensor aligns with the inertial principal *a*- or *b*-axis. This is only approximately true here. However, since the off-diagonal elements only contribute to the second order, an experimental value of χ_{ab} could not be determined for 3MP.

C. Barrier to methyl internal rotation

The V_3 potential values obtained with the *XIAM* and *BELGI-C_s-hyperfine* codes give satisfactory agreement. The value obtained from *BELGI* differs only by –0.32% from the *XIAM* value. The V_3 value predicted at the MP2/cc-pVTZ level of theory is –22.8% lower than the experimental value. At the same level, the difference of 8.8% observed for 2MP is much smaller.[10] Obviously, even within the same class of molecules, in this case methyl-substituted pyrroles, a level of theory which gives calculated results close to the experimental values for one isomer may not give such a satisfactory agreement for another isomer. It is hard to predict which level of theory is required for trustable value of V_3, thereby highlight

the need of microwave studies as the reliable source to quantify a molecule with large amplitude motion(s).

D. Comparison of nitrogen containing mono-methylated aromatic five-membered rings

A comparison between the results obtained for mono-methylated pyrroles, thiazoles, imidazoles, and oxazoles is given in Figure 3 with focus on the title molecule 3MP.

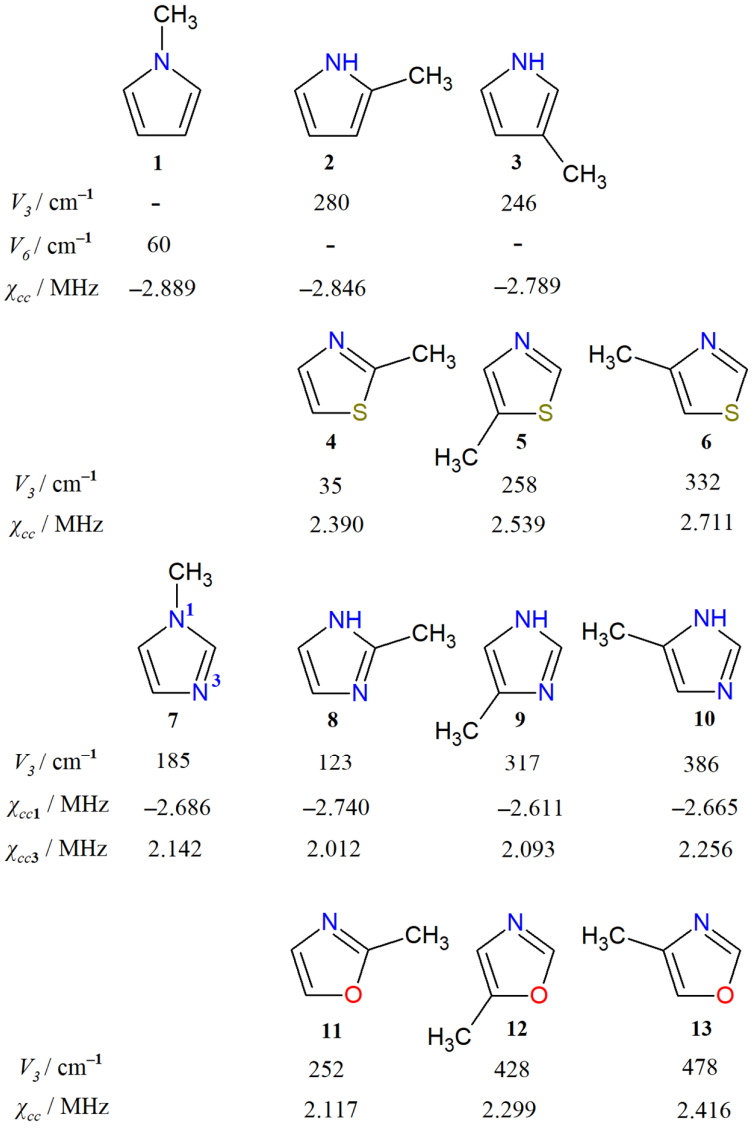

FIG. 3. The barrier to methyl internal rotation V_3, and the NQCC χ_{cc} of 3MP in comparison with mono-methylated thiazoles, imidazoles and oxazoles. (**1**) *N*-methylpyrrole,[28] (**2**) 2-methylpyrrole,[10] (**3**) 3-methylpyrrole (this work), (**4**) 2-methylthiazole,[3] (**5**) 4-methylthiazole,[4] (**6**) 5-methylthiazole,[5] (**7**) *N*-methylimidazole,[8] (**8**) 2-methylimidazole,[8] (**9**) 4-methylimidazole,[8] (**10**) 5-methylimidazole,[8] (**11**) 2-methyloxazole,[6] (**12**) 4-methyloxazole,[6] (**13**) 5-methyloxazole.[6]

The planar moment of 1.5639 uÅ^2 of 3MP (**3**) is very close to that of *N*-methylpyrrole (**1**) (1.652 uÅ^2)[35] and 2MP (**2**) (1.6115 uÅ^2),[10] confirming that there are two out-of-plane hydrogen atoms. Regarding the methyl torsion, the V_3 potential value changes significantly if the ring atom or the substitution at the heteroatom is varied. For mono-methylated thiazoles, imidazoles, and oxazoles, the lowest V_3 value is always found in the 2-isomer while the highest barriers correspond to the 5-isomer. The crucial role of the frame symmetry is also proven by the intermediate barrier of 123 cm^{-1} observed for 2-methylimidazole (**8**).[8] If the hydrogen atom would no longer attach to the N(1) atom in (**8**), the local frame symmetry of the CH_3 group would be C_{2v}, resulting in a leading V_6 potential term. The deviation caused by the small hydrogen atom attached to the nitrogen atom N(1) breaks the C_{2v} symmetry of the frame as well as the electron distribution, and leads to a significant change of the barrier height.

Finally, the methyl torsional barrier of 252 cm^{-1} found for 2-methyloxazole (**11**) is higher than that of 2-methylimidazole (**8**). The trend that the barrier to internal rotation increases from methylthiazoles[3-5] over methylimidazoles[8] to methyloxazoles[6] is generally observed not only for the 2-, but also for the 4- and 5-isomers. Obviously, the electronic distribution of a nitrogen atom is closer to that of a sulfur atom than that of a NH group, and the deviation to that of an oxygen atom is even greater. For the 2-isomers, 2MP (**2**) can also be considered in the comparison, which possesses the highest barrier,[10] indicating the largest difference in the electronic distributions between a nitrogen atom and a carbon atom. In conclusion, the barrier to internal rotation of a methyl group strongly depends on the presence of heteroatoms in the ring, since electronic effects are easily propagated in aromatic ring systems through the π electron conjugation. In this sense, the barrier of a methyl group can be considered as a direct measure for the electronic distribution within the attached ring. However, such interpretations are only intuitive and require proofs from more measurement data as well as theoretical calculations.

Due to the planar structure of all molecules shown in Figure 3, the principal *c*-axis of inertia is collinear with one principal axis of the nitrogen coupling tensor, therefore enabling a direct comparison of the values of χ_{cc} among these molecules. The values of χ_{cc} can be classified into two groups, one with positive values, and the other with negative values. They reflect different bond situations of the nitrogen nucleus. If the nitrogen atom is bond to a methyl group as in *N*-methylpyrrole (**1**) or a hydrogen atom

as in 2MP (**2**), 3MP (**3**), and the case of N(1) in methylimidazoles (**7**-**10**), it donates two electrons to create the aromatic system, and χ_{cc} is negative. In methylthiazoles (**4**-**6**) and methyloxazoles (**11**-**13**), χ_{cc} has a positive value, as the nitrogen atom provides only one electron to the ring systems. Detailed interpretations concerning the field gradient at the side of the nitrogen atom are explained in Ref. [10].

VI. CONCLUSION

The rotational spectra of 3MP were recorded using molecular jet Fourier transform microwave spectroscopy. Fine splittings arising from the internal rotation of the methyl group and hyperfine splittings from the ^{14}N quadrupole coupling were observed and analyzed using the programs *XIAM* and *BELGI-C_s-hyperfine*. While the program *XIAM* experienced some difficulties in reproducing the data set within the measurement accuracy, the *BELGI-C_s-hyperfine* yielded satisfactory result. Highly accurate molecular parameters were obtained. Because the internal rotor axis accidentally coincides with the principal *a*-axis of inertia, a direct comparison of the *XIAM* and *BELGI-C_s-hyperfine* parameters is possible. Comparison on the barrier height and the χ_{cc} quadrupole coupling constant among a selection of nitrogen containing aromatic five-membered rings has given insights into the dependence of these two parameters not only on the methyl position but also on the specific atom in the planar rings.

APPENDIX

See the Appendix section AII.3 for the nuclear coordinates of 3MP (Table S-I), torsional potential function of the methyl group (Figure S-II), Fourier coefficient of the potential energy curve (Table S-III) as well as the frequency list (Table S-IV).

ACKNOWLEDGEMENT

T.N. thanks the Université de Paris for a Ph.D grant. This work was supported by the Agence Nationale de la Recherche ANR (project ID ANR-18-CE29-0011).

REFERENCES

[1]I.A. Finneran, S.T. Shipman, S.L. Widicus Weaver, *J. Mol. Spectrosc.* **280**, 27 (2012).

[2]T. Ogata, K. Kozima, *J. Mol. Spectrosc.* **42**, 38 (1972).

[3]T. Nguyen, V. Van, C. Gutlé, W. Stahl, M. Schwell, I. Kleiner, H.V.L. Nguyen, *J. Chem. Phys.* **152**, 134306 (2020).

[4]W. Jäger, H. Mäder, *Z. Naturforsch.* **42a**, 1405 (1987).

[5]W. Jäger, H. Mäder, *J. Mol. Struct.* **190**, 295 (1988).

[6]E. Fliege, H. Dreizler, M. Meyer, K. Iqbal, J. Sheridan, *Z. Naturforsch.* **41a**, 623 (1986).

[7]E.R.L. Fliege, *Z. Naturforsch.* **45a**, 911 (1990).

[8]E. Gougoula, C. Medcraft, M. Heitkämper, N.R. Walker, *J. Chem. Phys.* **151**, 144301 (2019).

[9]R. Kaur, V. Rani, V. Abbot, Y. Kapoor, D. Konar, K. Kumar, *J. Pharm. Chem. Chem. Sci.* **1**, 17 (2017).

[10]T. Nguyen, C. Dindic, W. Stahl, H.V.L. Nguyen, I. Kleiner, *Mol. Phys.* **118**, 1668572 (2020).

[11]M.W. Schmidt, K.K. Baldridge, J.A. Boatz, S.T. Elbert, M.S. Gordon, J.H. Jensen, S. Koseki, N. Matsunaga, K.A. Nguyen, S.J. Su, T.L. Windus, M. Dupuis, J.A. Montgomery, *J. Comput. Chem.* **14**, 1347 (1993).

[12]W. Kohn, L.J. Sham, *Phys. Rev. A.* **140**, 1133 (1965).

[13]A.D. Becke, *J. Chem. Phys.* **98**, 5648 (1993).

[14]C.T. Lee, W.T. Yang, R.G. Paar, *Phys. Rev. B.* **37**, 785 (1988).

[15]C. Møller, M.S. Plesset, *Phys. Rev.* **46**, 618 (1934).

[16]T.H. Dunning, *J. Chem. Phys.* **90**, 1007 (1989).

[17]W.C. Bailey, *Chem. Phys.* **252**, 57 (2000).

[18]R. Kannengießer, M. J. Lach, W. Stahl, H.V.L. Nguyen, *ChemPhysChem* **16**, 1906 (2015).

[19]R. Kannengießer, S. Klahm, H.V.L. Nguyen, A. Lüchow, W. Stahl, *J. Chem. Phys.* **141**, 204308 (2014).

[20]R. Kannengießer, W. Stahl, H.V.L. Nguyen, *J. Phys. Chem. A* **120**, 5979 (2016).

[21]R. Kannengießer, W. Stahl, H.V.L. Nguyen, W.C. Bailey, *J. Mol. Spectrosc.* **317**, 50 (2015).

[22]J.-U. Grabow, W. Stahl, H. Dreizler, *Z. Naturforsch.* **45a**, 1043 (1990).

[23]H. Hartwig, H. Dreizler, *Z. Naturforsch.* **51a**, 923 (1996).

[24]R. Kannengießer, W. Stahl, H.V.L. Nguyen, I. Kleiner, *J. Phys. Chem. A.* **120**, 3992 (2016).

[25]K. Eibl, W. Stahl, I. Kleiner, H.V.L. Nguyen, *J. Chem. Phys.* **149**, 144306 (2018).

[26]M. Andresen, I. Kleiner, M. Schwell, W. Stahl, H.V.L. Nguyen, *J. Phys. Chem. A* **124**, 1353 (2020).

[27]D. Jelisavac, D.C. Cortés-Gómez, H.V.L. Nguyen, L.W. Sutikdja, W. Stahl, I. Kleiner, *J. Mol. Spectrosc.* **257**, 111 (2009).

[28]V. Van, T. Nguyen, W. Stahl, H.V.L. Nguyen, I. Kleiner, *J. Mol. Struct.* **1207**, 127787 (2020).

[29]I. Kleiner, *J. Mol. Spectrosc.* **260**, 1 (2010).

[30]A. Roucou, I. Kleiner, M. Goubet, S. Bteich, G. Mouret, R. Bocquet, F. Hindle, W.L. Meerts, A. Cuisset, *ChemPhysChem* **19**, 1056 (2018).

[31]G.S. Grubbs II, P. Groner, S.E. Novick, S.A. Cooke, *J. Mol. Spectrosc.* **280**, 21 (2012).

[32]R.A. Motiyenko, L. Margulès, E.A. Alekseev, J.-C. Guillemin, J. Demaison, *J. Mol. Spectrosc.* **264**, 94 (2010).

[33]W. Gordy, R.L. Cook, Microwave Molecular Spectra, Techniques of Chemistry Vol. XVIII, Table 8.14, Wiley, New York, (1984).

[34]L. Nygaard, J.T. Nielsen, J. Kirchheiner, G. Maltesen. J.R. Andersen, G.O. Sørensen, *J. Mol. Struct.* **3**, 491 (1969).

[35]J. Makarewicz, S. Huber, B. B.-Gatehouse, A. Bauder, *J. Mol. Struct.* **612**, 117 (2002).

PART III: NITROGEN AROMATIC RINGS WITH TWO ROTORS AND ONE ^{14}N NUCLEUS

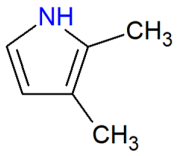

2,5-dimethylpyrrole

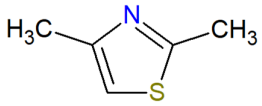

4,5-dimethylthiazole

The microwave spectra of 2,5-dimethylpyrrole (25DMP) and 4,5-dimethylthiazole (45DMTA) were recorded using the molecular jet Fourier transform spectrometers operating in the frequency range of 2-26.5 GHz. With the aids of quantum chemical calculations, all spectra were successfully analyzed. The fine structures originating from coupled internal rotation together with the nuclear quadrupole coupling were fully understood.

The *BELGI*-family code which treats two tops were extended to take into account the effect of weakly nuclear quadrupole coupling of ^{14}N, the so-called *BELGI-C_s-2Tops-hyperfine* and *BELGI-C_{2v}-2Tops-hyperfine*. In the case of 25DMP, results obtained with the *BELGI-C_{2v}-2Tops-hyperfine* and the *XIAM* codes are both very good and of a fairly good agreement. In the case of 45DMTA, the microwave spectra were analyzed using the *XIAM* and *BELGI-C_s-2Tops-hyperfine*. While the *XIAM* code failed to reproduce the experimental data to measurement accuracy, the *BELGI-C_s-2Tops-hyperfine* offered a much better *rms* deviation, showing its predictive power over *XIAM* code by adding additional rotation-torsion terms to the Hamiltonian which then reduced the *rms* by factor of 200 times compared to the *XIAM* code. The *WS18* code allowed to check the correctness of the assignment and is useful in both cases. The molecular parameters of those two molecules were obtained with very high accuracy. Our results showed that while the steric effect plays a major role in the obtained value of V_3 in case of 25DMP, it is not significant in case of 45DMTA. In contrast to 25DMP, the electric distribution within the ring has noticeable effect in case of 45DMTA compared to that of steric effect.

In the following sub-sections, we will report the results on microwave investigations on 2,5-dimethylpyrrole (Chapter III.1) and 4,5-dimethylthiazole (Chapter III.2).

Chapter III.1: Local versus global approaches to treat two equivalent methyl internal rotations and ^{14}N nuclear quadrupole coupling of 2,5-dimethylpyrrole

This is a manuscript of an accepted article in Journal of Chemical Physics: Thuy Nguyen, Wolfgang Stahl, Ha Vinh Lam Nguyen, and Isabelle Kleiner, Local versus global approaches to treat two equivalent methyl internal rotations and ^{14}N nuclear quadrupole coupling of 2,5-dimethylpyrrole.

ABSTRACT

The microwave spectrum of 2,5-dimethylpyrrole was recorded using a molecular jet Fourier transform microwave spectrometer operating in the frequency range from 2 to 26.5 GHz. Only one stable conformer was observed in the microwave spectrum as expected and confirmed by quantum chemical calculations which were carried out to complement the experimental analysis. The two equivalent methyl groups cause each rotational transition to split into four torsional species, which is combined with the quadrupole hyperfine splittings in the same order of magnitude arising from the ^{14}N nucleus. This results in a complicated spectrum feature. The spectral assignment was done separately for each torsional species. Two global fits were carried out using the *XIAM* code and the *BELGI-C_{2v}-2Tops-hyperfine* code, a modified version of the *BELGI-C_{2v}-2Tops* code, giving satisfactory root-mean-square deviations. The potential barriers to internal rotation of the two methyl groups were determined to be V_3 = 317.208(16) cm^{-1}. The molecular parameters were obtained with high accuracy, providing all necessary ground state information for further investigations in higher frequency ranges and on excited torsional-vibrational states.

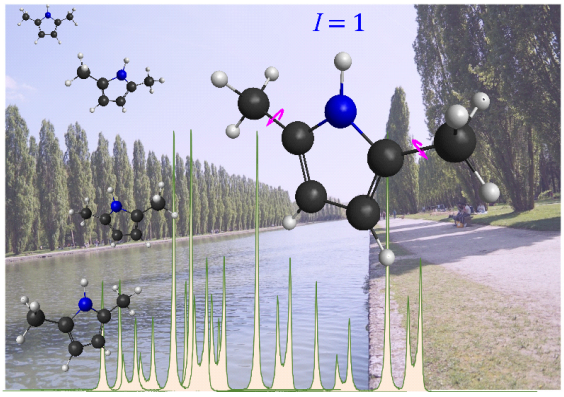

I. INTRODUCTION

Besides the classic topics in structural chemistry,[1] large amplitude motions (LAMs), e.g., internal rotation,[2] ring puckering,[3] and inversion motion,[4] form a very active area in microwave spectroscopy. The effect of a methyl internal rotation on the rotational spectrum is that each rotational transition exhibits a torsional fine structure caused by the interaction of the methyl internal and the overall rotation. This fine structure, consisting of A-E doublets, depends on the height of the potential barrier hindering the internal rotation. If the barrier is very high, the internal motion of the methyl group corresponds to simple harmonic oscillation, whereas if the barrier is very low, the internal motion corresponds to an essentially free rotation.

In the presence of two methyl internal rotors, the fine structure consists of quartets (two equivalent tops) and quintets (two inequivalent tops). Analyzing their microwave spectra is a rather complicated task. Fitting the spectrum with sufficient accuracy often requires effective Hamiltonians to be included in the model. Due to challenges in both spectral assignment and fit, only a limited number of two-top molecules have been investigated, as reviewed by Nguyen and Kleiner.[2] Unlike inequivalent two-top cases where the point group of the frame symmetry can be C_1 or C_s, in the cases of two equivalent methyl groups, due to the higher molecular symmetry requirement, e.g., C_2, C_{2h}, or C_{2v}, the number of studies reported in the literature are even smaller. Some examples of equivalent two-top molecules are dimethylgermane,[5] dimethylamine,[6] dimethylketene,[7] isobutylene,[8] propane,[9] 2,6-lutidine,[10,11] difluorodimethylsilane,[12] 2-bromopropane,[13] dimethyl sulfate,[14] acetone,[15,16] dimethyl ether,[17] diethyl ketone,[18] dimethyl sulfide,[19] 2,5-dimethylthiophene,[20] 2,5-dimethylfuran,[21] and 2,6-dimethylfluorobenzene.[22] The spectral analysis can be challenging enough that even until now our understanding about the microwave spectra of some compounds still remains incomplete, i.e., 2,6-lutidine,[10,11] 2-bromopropane[13]. In the present work, we studied the microwave spectrum of 2,5-dimethylpyrrole (25DMP), a nitrogen-containing five-membered ring which contains two equivalent methyl groups and a nitrogen atom with support from quantum chemical calculations. This investigation adds an important contribution to the limited number of studies on two equivalent methyl rotors.

While high barriers result in rather small torsional splittings in the order of a few tens of kHz to a few MHz as found for 4- and 5-methylthiazole,[23,24] or 2-chloro-4-fluorotoluene,[25] in the case of low barriers, the splittings can be up to several GHz,[26-28] making the spectral assignment difficult. If the molecule contains also a ^{14}N nucleus which causes a quadrupole hyperfine structure with splittings also from a few tens of kHz to 2 MHz in addition, the spectral analysis is even challenging for high barrier cases, since the hyperfine patterns overlap with the torsional splittings.[29] To confirm that the assignments are correct, it is often useful to fit each torsional species separately. For 25DMP, the *WS18* program was written, taking into account both, the internal rotation and the quadrupole coupling of one ^{14}N nucleus, enabling to confirm the correctness of the assignment.

The effects of internal rotation arising from two methyl groups in combination with one weakly coupling ^{14}N quadrupole nucleus can be treated in a global fit with the program *XIAM*.[30] However, *XIAM* has its weakness in reproducing the experimental data to measurement accuracy if the torsional barrier is low.[31-33] It is often discussed that a reason might be the neglection of interactions between different v_t states, but a study on *m*-methylanisole has proven this assumption to be false.[34] Recent studies on 4-methylacetophenone,[35] 3-fluorotoluene,[36] and *m*-methylanisole[37] strongly suggest the limited number of parameters available in *XIAM* to be the main reason.

The initial version of the *BELGI-C_s* program[38] has been extended to a hyperfine version for one-top, *BELGI-C_s-hyperfine*,[39] and recently also for molecules with two inequivalent methyl tops, *BELGI-C_s-2Tops-hyperfine*.[31] In many cases, the *BELGI* code shows great advantages over *XIAM* in reducing the root-mean-square (rms) deviations.[26,31,39-41] To treat the microwave spectrum of 25DMP, we modified the *BELGI-C_{2v}-2Tops* code which was used to fit the rotational spectrum of dimethyl sulfide, properly treating molecules containing two equivalent methyl tops with C_{2v} molecular symmetry,[19] to *BELGI-C_{2v}-2Tops-hyperfine* to consider the quadrupole coupling of one ^{14}N nucleus. The results of *BELGI-C_{2v}-2Tops-hyperfine* will be compared with those of *XIAM*.

II. THEORETICAL

A. Quantum chemical calculations

Quantum chemical calculations were performed at the MP2/cc-pVDZ level of theory using the *GAMESS* program.[42] The obtained rotational constants, the V_3 term of the methyl torsional potentials and the ^{14}N nuclear quadrupole coupling constants (NQCCs) were used as initial values for assigning the spectrum of 25DMP.

Optimizations of the molecular geometry of 25DMP at the MP2/cc-pVDZ level of theory yielded only one stable conformer with the geometry shown in Fig. 1. The dihedral angles $\alpha_1 = \angle(C_3,C_2,C_6,H_{13})$ and $\alpha_2 = \angle(C_4,C_5,C_7,H_{16})$ are 0° at equilibrium. The nuclear coordinates in the principal axis orientation are given in Table S-I in the Supplementary Material. In order to calculate the ^{14}N NQCCs, the method of Bailey[43] was applied as it is known to give very reliable results.[31,44-46] The electric field gradient at the site of the ^{14}N nucleus in 25DMP was calculated at the B3PW91/6-311+G(d,p) level using the molecular geometry given in Fig. 1. The calibration factor eQ/h = −4.599 MHz/a.u. recommended for conjugated π systems was used.[44] The resulting quadrupole coupling constants are χ_{aa} = 1.3243, χ_{bb} = 1.665, and χ_{cc} = −2.996 MHz. Due to the C_{2v} symmetry of the molecule, all off-diagonal elements are zero.

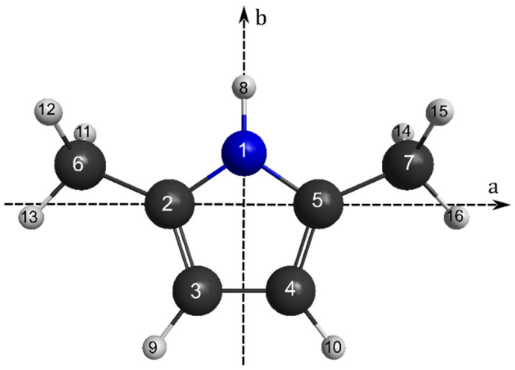

FIG. 1. The molecular geometry of 25DMP calculated at the MP2/cc-pVDZ level of theory. The atom numbering and the principal axis of inertia *a*- and *b*- are given.

A two-dimensional potential energy surface (2D-PES) was calculated at the MP2/cc-pVDZ level by varying the dihedral angles $\alpha_1 = (C_3,C_2,C_6,H_{13})$ and $\alpha_2 = (C_4,C_5,C_7,H_{16})$ to predict the barriers to internal rotation and to study the possible potential coupling effects between the two methyl rotors, as given in Fig. 2. The symmetry adapted Fourier coefficients describing the PES are collected in Table S-II in the Appendix AIII.1. From the PES, we obtain a V_3 value of 281.9 cm^{-1} for each top with a V_6

contribution of approximately 42.6 cm^{-1}. Moreover, the top-top potential coupling contributes with 10% to the value of the barrier to internal rotation, indicating a weak anti-gearing motion between the two tops, as will be discussed in detail in section IV.C.

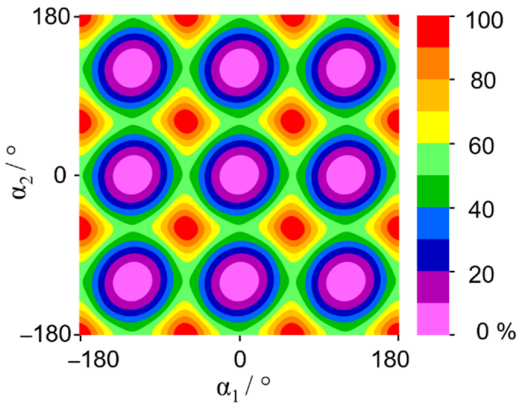

FIG. 2. The potential energy surface of 25DMP calculated at the MP2/cc-pVDZ level of theory obtained by varying the dihedral angles $\alpha_1 = (C_3,C_2,C_6,H_{13})$ and $\alpha_2 = (C_4,C_5,C_7,H_{16})$ in a 10° grid, corresponding to the rotations of the methyl groups. The energies (in percent) are color-coded. The global energy minimum is at $E = -287.897702$ Hartree (0 %).

B. Molecular symmetry

In 25DMP, two equivalent methyl groups are attached to a C_{2v} symmetric frame. Its molecular symmetry group is G_{36} with the well-known irreducible representations A_1, A_2, A_3, A_4, E_1, E_2, E_3, E_4, G and the character table[47] given in Table S-III in the Appendix AIII.1. In this work, we follow a labeling scheme (00), (01), (11), and (12) which naturally arises from the semi-direct product decomposition $G_{36} = (C_3^I \otimes C_3^I) \leftthreetimes C_{2v}$ as reported by Ezra[48] and discussed for 2,5-dimethylthiophene by Van *et al.*[49] but with detailed intuitive interpretation. The label (σ_1, σ_2)·X of the irreducible representations consists of two parts. The first part arises from the invariant subgroup of G_{36}, which is the direct product $C_3^I \otimes C_3^I$ of the two intrinsic (superscript I) C_3 permutation groups of the internal rotors. Their irreducible representations (σ_1, σ_2) with $\sigma_i = 0, -1, 1$ represent the transformation properties of the C_3-adapted planar rotor wave functions $e^{i(3k+\sigma)\alpha}$, $k \in Z$ and the torsional angle α, according to the three species A, E_a, E_b of the C_3 group, respectively. For a better readability, we use the number 2 in the symmetry labels for the $\sigma_i = -1$ irreducible representation. Under the C_{2v} frame symmetry, the direct product C_3^I

$\otimes C_3^I$ decomposes into four orbits {(00)}, {(12), (21)}, {(11), (22)}, and {(01), (10), (02), (20)}. One representative of each orbit is chosen for the symmetry label. The second part, the label X, is formed by the irreducible representations of the little co-group of a given (σ_1, σ_2) orbit. Here, we will give an intuitive description of this little co-group. The expectation values of the angular momentum of a methyl group are zero for the $\sigma_i = 0$ states. For σ_i = 1 and −1 states, the angular momenta are non-zero with opposite signs. This can be imagined as no rotation for $\sigma_i = 0$, and a clockwise or a counterclockwise rotation for $\sigma_i = \pm 1$. In the case of the (00) species, none of the tops rotates. There is no displacement of the methyl groups, and in this state the little co-group is C_{2v} with its irreducible representations A_1, B_1, A_2, B_2. Therefore, we have the G_{36} species (00)·A_1, (00)·B_1, (00)·A_2, (00)·B_2, corresponding to the traditional A_1, A_2, A_3, A_4 labels, respectively. For the (12) orbit, one top rotates clockwise, the other one counterclockwise. Looking at a snapshot at a given time, the point group of the frame symmetry is no longer C_{2v} but C_s symmetry. There is no longer an *ab* mirror plane but only a *bc* mirror plane. From the irreducible representations A′ and A″ of C_s, we obtain the G_{36} species (12)·A′ and (12)·A″ corresponding to E_1 and E_2, respectively. In the case of the (11) orbit, both tops rotate either clockwise or counterclockwise. Almost all the time, there is no longer any mirror plane in the molecule but the C_2 axis, coinciding with the *b* axis, remains. The little co-group of the (11) orbit is C_2 with the irreducible representations A and B. We obtain the G_{36} irreducible representations (11)·A and (11)·B, corresponding to E_3 and E_4. Finally, the (01) orbit describes the case where one top does not rotate and the other one rotates clockwise or counterclockwise. A snapshot of the molecule will not show any non-trivial symmetry elements. The little co-group is C_1 with the species A, and the G_{36} irreducible representation is therefore (01)·A corresponding to G. A comparison of both labeling schemes shows that direct information of the degeneracy of a species, i.e., the non-, double-, and four-fold degeneracy of A, E, G, respectively, is lost. Instead, we obtain intuitive information on the behavior of the internal rotors for a given G_{36} irreducible representation.

25DMP has 9 protons and one ^{14}N nucleus, from which $2^9 \cdot 3 = 1536$ spin functions arise. The selection rules along with the spin statistical weights is given in Table I. In comparison to 2,5-dimethylthiophene,[49] a factor of 6 was found because the NH group, replacing the sulfur atom in 2,5-dimethylthiophene, adds a proton with two spin states and a ^{14}N nucleus with three spin states while the

^{32}S nucleus has only one spin state. Without taking the spin statistical weights into account, the intensities of all torsional components are the same (see for example Fig. 4 in Ref. [35]). When the spin weight was taken into account, the calculated intensities of torsional components are in fairly good agreement with the observed intensities as depicted in Fig. 3. Only for the (12) species, which should be about half as intense as the (00) species, we found that the two lines feature almost the same intensity and have no reasonable explanation for this observation.

Table I. Spin statistical weights of torsional components of allowed transitions of 25DMP

ee ↔ oo		eo ↔ oe	
(00)·A_1 ↔ (00)·A_2	216	(00)·B_1 ↔ (00)·B_2	168
(12)·A′ ↔ (12)·A″	96	(12)·A′ ↔(12)·A″	96
(11)·A ↔ (11)·A	120	(11)·B ↔ (11)·B	72
(01)·A ↔ (01)·A	384	(01)·A ↔ (01)·A	384

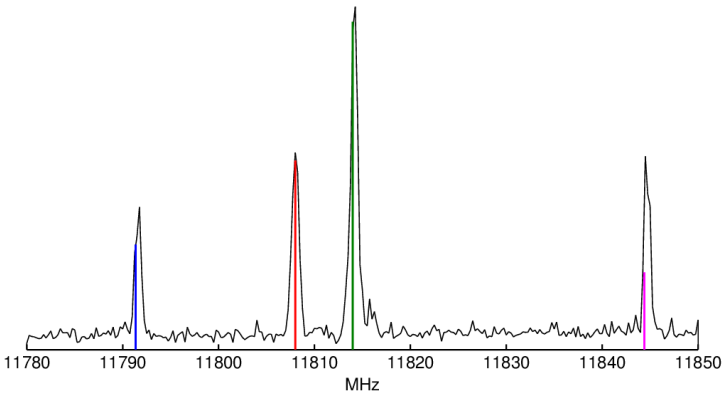

FIG. 3. The broadband scan and the simulated spectrum of the four torsional species (00) in red, (01) in green, (11) in blue, and (12) in purple of the rotational transition $4_{22} \leftarrow 4_{13}$ of 25DMP.

C. The *WS18* code

The complexity of the spectra of 25DMP caused by two equivalent methyl groups and the presence of a ^{14}N nucleus makes the spectral assignment a challenging task. The splittings of the torsional species for some rotational transitions are within 1 MHz and overlap with the hyperfine splittings of the ^{14}N nucleus. Using a global fit for assignments was very time-consuming and uncertain.

From experiences in the literature, separately fitting the torsional species is a good alternative to check the assignments, as successfully done in the investigations in Refs. [22,35,50]. To take into account the quadrupole coupling of the ^{14}N nucleus, the *WS18* code was written. The effective Hamiltonian used in our study is:

$$\mathbf{H} = \mathbf{H_r} + \mathbf{H_{cd}} + \mathbf{H_{op}} + \mathbf{H_{nq}}, \tag{95}$$

with the pure rotational part:

$$\mathbf{H_r} = A\mathbf{P_z^2} + B\frac{1}{4}(\boldsymbol{P_+^2} + \mathbf{P_-^2} + \mathbf{P_+P_-} + \mathbf{P_-P_+}) - C\frac{1}{4}(\mathbf{P_+^2} + \mathbf{P_-^2} - \mathbf{P_+P_-} - \mathbf{P_-P_+}), \tag{96}$$

the quartic centrifugal distortion terms:

$$\mathbf{H_{cd}} = -\Delta_J\mathbf{P^4} - \Delta_{JK}\mathbf{P^2P_z^2} - \Delta_K\mathbf{P_z^4} - \delta_J\mathbf{P^2}(\mathbf{P_+^2} + \mathbf{P_-^2}) - \delta_{K\frac{1}{2}}\{\mathbf{P_z^2}, (\mathbf{P_+^2} + \mathbf{P_-^2})\}, \tag{97}$$

the odd-order angular momentum terms:

$$\mathbf{H_{op}} = q\mathbf{P_z} + r\frac{1}{2}(\mathbf{P_+} + \mathbf{P_-}) + q_J\mathbf{P^2P_z} + q_K\mathbf{P_z^3} + \cdots, \tag{98}$$

and the nuclear quadrupole coupling Hamiltonian:

$$\mathbf{H_{nq}} = \mathbf{V^{(2)}} \cdot \mathbf{Q^{(2)}},\ \chi_{aa} = 2eQV_0^{(2)},\ \chi_{bb} - \chi_{cc} = \sqrt{6}eQ(V_2^{(2)} + V_{-2}^{(2)}). \tag{99}$$

The Hamiltonian matrix is set up in the symmetric top basis. Only matrix elements diagonal in J were considered, leading to a matrix size of $(2J + 1)(2J + 1)$. Both real and complex matrix elements are allowed. The code can be used for fitting microwave spectra of molecules with any point group of the frame symmetry. Effective Hamiltonian terms can be added from the input file in *WS18*, similar to the *aixPAM* code written for treating the rotational spectrum of one-top molecules.[34] These terms are given as a sum of products of the fundamental operator $\mathbf{P^2}$, $\mathbf{P_z}$, the step-up and step-down operators $\mathbf{P_+} = \mathbf{P_x} + i\mathbf{P_y}$, $\mathbf{P_-} = \mathbf{P_x} - i\mathbf{P_y}$ which are coded as P2, Pz, P+, and P–, respectively. As an example, the operator r_J, multiplying $\frac{1}{2}\left(\mathbf{P^2P_+} + \mathbf{P^2P_-}\right)$, is coded as:

```
rJ 0.5 P2 P+
rJ 0.5 P2 P–.
```
(100)

D. The *BELGI-C_{2v}-2Tops-hyperfine* code

In order to treat the LAMs originating from two methyl groups and a weak nuclear quadrupole coupling caused by a ^{14}N nucleus in the rotational spectrum of 25DMP, the *BELGI-C_{2v}-2Tops* code[19] was modified to *BELGI-C_{2v}-2Tops-hyperfine*. The method is similar to that applied for 4,5-dimethylthiazole.[31] The only difference is the molecular point group which is C_s in the case of 4,5-dimethylthiazole and C_{2v} in 25DMP.

The Hamiltonian used in *BELGI-C_{2v}-2Tops-hyperfine* is the same as in *BELGI-C_{2v}-2Tops*[19] which is based on the Hamiltonian initially introduced by *Ohashi et al.*[50] It is written in a slightly modified Principal Axis Method (quasi-PAM). In the Hamilton operator of Eqn. (6) from Ref. [50] which we also used, the axis system (x, y, z) is chosen in such a way that quadratic cross terms in the angular momentum components $\mathbf{P_x}$, $\mathbf{P_y}$, and $\mathbf{P_z}$ are kept fixed to zero at lowest order, which is different from the traditional PAM Hamiltonian with internal rotation (see Eqn. (7) of Ref. [50]). The relations between the parameters of our quasi-PAM and the traditional PAM system are defined in Eqn. (9) to (12) of Ref. [50]. Unlike in Ref. [50], we follow a two-steps diagonalization of the matrix associated to the Hamiltonian. More detailed descriptions are referred to Refs. [19] and [51].

The quadrupole energies for each rotational transition in a given torsional state caused by the ^{14}N nucleus are computed in the *BELGI-C_{2v}-2Tops-hyperfine* code using the perturbation approach where the hyperfine energy expression is

$$E_{hf}\ (I,J,F) = 2\frac{f(I,J,F)}{J(J\ +1)}\left[\chi_{aa}\langle\mathbf{P_z^2}\rangle\ +\ \chi_{bb}\langle\mathbf{P_x^2}\rangle - (\chi_{aa}+\chi_{bb})\,\langle\mathbf{P_y^2}\rangle\ +\chi_{ab}\langle\mathbf{P_zP_x}+\mathbf{P_xP_z}\rangle\right] \qquad (101)$$

with the Casimir function *f(I, J, F)*.[52]

To facilitate the calculations, the numerical expectation values of the quadratic angular momentum components $\langle\mathbf{P_x^2}\rangle, \langle\mathbf{P_y^2}\rangle, \langle\mathbf{P_z^2}\rangle$, and $\langle\mathbf{P_zP_x}+\mathbf{P_xP_z}\rangle$ are quantified and then transferred into Eqn. (7). This method allows us to determine the structure of all hyperfine patterns and take the nuclear quadrupole coupling constants into account in a global fit which already treats the internal rotation of two equivalent methyl groups in *BELGI-C_{2v}-2Tops*.[19]

III. EXPERIMENTAL

A. Measurements

The rotational spectra of 25DMP were measured with a molecular jet Fourier transform microwave spectrometer operating in the frequency range from 2.0 to 26.5 GHz.[53] 25DMP was purchased from TCI Europe, Zwijndrecht, Belgium, with a stated purity of over 97% and was used without any further purification. A small piece of a pipe cleaner containing the substance was put inside a steel tube close to the nozzle. Helium was used as carrier gas and flowed at a backing pressure of approximately 200 kPa over the substance. The mixture of helium and 25DMP was then expanded into the cavity. A broadband scan with a step width of 250 kHz was recorded in the frequency range from 10.6 to 12.5 GHz. All spectra were recorded at high resolution where Doppler splittings are observed due to the coaxial arrangement between the molecular beam and the resonators. The measurement accuracy is approximately 4 kHz for all lines.

B. Spectral analysis

Due to the C_{2v} symmetry of 25DMP, we only expected one dipole moment component along the *b* axis which is in agreement with results from quantum chemical calculations stating that $|\mu_a| = 0.00$, $|\mu_b| = 2.10$, and $|\mu_c| = 0.00$ D. Using the calculated rotational constants, V_3 potential of the methyl groups, and angles between the principal *a* axis and the internal rotor axes, a spectrum was predicted using the *XIAM* code.[30] We first neglected the nuclear quadrupole hyperfine structure and could identify the four torsional states (00), (01), (11), (12) of some intense transitions such as $2_{12} \leftarrow 1_{01}$, $4_{04} \leftarrow 3_{13}$, and $4_{22} \leftarrow 4_{13}$ by comparing the broadband scan and the predicted spectrum. Using those lines, a fit was carried out, and the fitted molecular parameters enabled us to predict and find further lines in the frequency range of the spectrometer.

The hyperfine structures arising from the nuclear quadrupole coupling of the ^{14}N nucleus were observed for all torsional transitions. The assignment of the hyperfine patterns was first done separately for each torsional species using the *WS18* code. Subsequently, all lines are fitted globally with the

programs *XIAM* and *BELGI-C_{2v}-2Tops-hyperfine*. The frequency list along with the residuals obtained with *XIAM*, *BELGI-C_{2v}-2Tops-hyperfine*, and *WS18* are given in Table S-IV in the Appendix AIII.1.

IV. RESULTS AND DISCUSSION

A. Separate fits

The four torsional species (00), (01), (11), and (12) were fitted separately with the parameters summarized in Table II. All separate fits yielded reasonable standard deviations which are close to the measurement accuracy, showing that all lines are assigned correctly. All geometry parameters in the separate fits are effective and do not present the real geometry of the molecule.

Table II. Molecular parameters of all torsional species of 25DMP obtained from fits with *WS18*.

Par.[a]	Unit	(00)	(01)	(11)	(12)
A	MHz	6294.59598(87)	6291.65826(19)	6288.7238(19)	6288.71917(62)
B	MHz	2016.97245(33)	2016.91615(10)	2016.86103(37)	2016.86032(23)
C	MHz	1557.13464(36)	1557.13473(10)	1557.13585(23)	1557.13595(14)
Δ_J	kHz	0.1258(82)	0.1004(11)	0.1034(41)	0.0991(22)
Δ_{JK}	kHz	–0.152(39)	–0.1723(52)	–0.235(23)	–0.259(13)
Δ_K	kHz	5.28(20)	3.913(23)	2.74(41)	2.30(12)
δ_J	kHz	0.0521(79)	0.0301(61)	0.0318(50)	0.0285(19)
q	MHz	-	44.94177(36)	-	89.8432(18)
r	MHz	-	6.086(37)	12.311(76)	-
q_J	kHz	-	–1.240(13)	-	–2.588(60)
q_K	kHz	-	–41.645(64)	-	–8.452(45)
χ_{aa}	MHz	1.3253(25)	1.3243(15)	1.3262(20)	1.3301(16)
χ_{bb}- χ_{cc}	MHz	4.6287(49)	4.6339(25)	4.6450(35)	4.6331(29)
N[b]		44	98	55	77
σ[c]	kHz	4.1	2.5	2.4	2.1

[a] All parameters refer to the principal axis system. Watson's A reduction and I^r representation were used. Single standard errors in the unit of the last digits are given in parentheses.

[b] Number of hyperfine components.

[c] Root-mean-square deviation of the fit.

B. Global fits

The microwave spectrum of 25DMP was fitted globally with the programs *XIAM* and *BELGI-C_{2v}-2Tops-hyperfine* with results given in Table III. Both fits give satisfactory rms deviations. In Table III, all parameters are referred to the principal axis system. As the *BELGI-C_{2v}-2Tops-hyperfine* program works

in the quasi-PAM system, the rotational and the quadrupole hyperfine constants need to be converted into the principal axis system for comparison. The complete set of fitted parameters using the *BELGI-C_{2v}-2Tops-hyperfine* code is presented in Table IV.

Table III. Molecular parameters of 25DMP in the principal axis system obtained with *XIAM* (Fit *XIAM*) and *BELGI-C_{2v}-2Tops-hyperfine* (Fit *BELGI*) as well as values calculated at the MP2/cc-pVDZ level of theory. Parameters from the quasi-PAM system are converted into the PAM system using the conversion code introduced in Section 2.3. of Ref. [31].

Operator	Par.[a]	Unit	Fit *XIAM*	Fit *BELGI* [b]	*ab initio*[c]
$\mathbf{P_a^2}$	A	MHz	6290.61862(82)	6290.69(32)	6192.8
$\mathbf{P_b^2}$	B	MHz	2016.95964(16)	2016.96(17)	1999.7
$\mathbf{P_c^2}$	C	MHz	1557.07334(14)	1557.06340(11)	1541.2
$-\mathbf{P^4}$	Δ_J	kHz	0.1010(16)		0.0964
$-\mathbf{P^2P_a^2}$	Δ_{JK}	kHz	–0.2058(96)		–0.2100
$-\mathbf{P_a^4}$	Δ_K	kHz	3.294(39)		3.3804
$-2\mathbf{P^2}(\mathbf{P_a^2}-\mathbf{P_c^2})$	δ_J	kHz	0.02840(99)		0.0289
$-\{\mathbf{P_a^2},(\mathbf{P_a^2}-\mathbf{P_c^2})\}$	δ_K	kHz	-		0.0580
	F_0	GHz	158[d]	160.238(72)[e]	158
$\left(\mathbf{p}_{\alpha_i}-\rho\mathbf{P_a}\right)^2$	F	GHz	164.0340[e]	164.9605[f]	
$\{(\mathbf{p}_{\alpha_1}-\vec{\rho}^{\dagger}\vec{\mathbf{P}}_{\mathbf{r}_1}),(\mathbf{p}_{\alpha_2}-\vec{\rho}^{\dagger}\vec{\mathbf{P}}_{\mathbf{r}_2})\}$	F_{12}	GHz	–5.4211[e]	–5.74(12)[e]	
(1/2)(1 – cos(3α))	V_3	cm^{-1}	317.208(16)	317.9205(41)	281.9
$F\mathbf{P_a}\mathbf{p}_{\alpha_i}$	ρ		0.0370[e]	0.036460(18)[e]	
$\{(\mathbf{p}_{\alpha_i}-\vec{\rho}^{\dagger}\vec{\mathbf{P}}_{\mathbf{r}_i}),\mathbf{P_a^2}\}$	D_{pi2K}	MHz	0.6996(89)		
	χ_{aa}	MHz	1.3272(21)	1.3267(14)	1.3243
	$\chi_{bb}-\chi_{cc}$	MHz	4.6390(36)	4.6388(31)	4.6610
	$\angle(i_1,a)$[g]	°	157.130(22)	156.955(24)[e]	156.41
	$\angle(i_1,b)$	°	67.123(22)	66.955(24)[e]	66.42
	$\angle(i_2,a)$[g]	°	22.888(22)	23.045(24)[e]	23.59
	$\angle(i_2,b)$	°	67.112(22)	113.045(24)[e]	66.42
	N_q[h]		274	274	
	rms[k]	kHz	4.8	3.4	

[a] All parameters refer to the principal axis system. Watson's A reduction and I^r representation were used.

[b] Rotational and quadrupole hyperfine constants obtained by transformation from the quasi-PAM to the PAM system.

[c] Calculated at the MP2/cc-pVDZ level. The centrifugal distortion constants were obtained by harmonic frequency calculations.

[d] Fixed to the calculated value.

[e] Derived parameter in *XIAM*. For *BELGI-C_{2v}-2Tops-hyperfine,* the fitted parameters are q_1 (= q_2) which multiplies the operator $\mathbf{P_z}\mathbf{p}_{\alpha_1}$ (see Table IV). The value of the ρ parameter can be obtained from $q_1 = q_2 = -2F_1\rho_{1z}$ and $r_1 = -r_2 = -2F_1\rho_{1x}$. f_{12} is a floated parameter, with the relation $f_{12} = -2F_{12}$ (see text).

[f] Fixed value. In *BELGI-C_{2v}-2Tops-hyperfine*, F_1 (or f_1 in the notation of Ref. [50]) = F_2 (or f_2), multiplying the operators $\mathbf{p}_{\alpha_1}^2 = \mathbf{p}_{\alpha_2}^2$.

[g] $\angle(i,c) = 90°$ for both rotors due to symmetry.

[h] Number of hyperfine components.

[k] Root-mean-square deviation of the fit.

Table IV. Spectroscopic constants of 25DMP in quasi-PAM obtained with the program *BELGI-C_{2v}-2Tops-hyperfine.*

Operator[a]	Par.[b]	Unit	Value
$\mathbf{P_z^2}$	A	MHz	6736.22(17)
$\mathbf{P_x^2}$	B	MHz	2024.689(11)
$\mathbf{P_y^2}$	C	MHz	1557.06340(11)
$-\mathbf{P^4}$	Δ_J	kHz	0.0392(17)
$-\mathbf{P_z^4}$	Δ_K	kHz	3.433(28)
$-\mathbf{P^2P_z^2}$	Δ_{JK}	kHz	–0.1561(69)
$\mathbf{p_1^2 = p_2^2}$	$F_1 = F_2$	GHz	164.9605[c]
$\mathbf{p_1p_2}$	f_{12}	GHz	11.47(12)
$(1/2)(1-\cos(3\alpha_1))$	$V_{3,1}$	cm^{-1}	317.9205(41)
$\mathbf{P_zp_1}$	q_1	GHz	–12.3329(45)
$\mathbf{P_xp_1}$	r_1	GHz	–1.5691(12)
$\mathbf{P_xp_1P^2}$	r_{1J}	MHz	–11.91(28)
	$2\chi_{aa}$	MHz	2.6533(29)
	$2\chi_{bb}$	MHz	3.3121(27)
	$2\chi_{cc}$	MHz	–5.9654(29)
	N_q[d]		274
	rms[e]	kHz	3.4

[a] All parameters refer to the quasi-PAM system. $\mathbf{P_x}$, $\mathbf{P_y}$, $\mathbf{P_z}$ are the components of the overall rotation angular momentum, $\mathbf{p_1}$ and $\mathbf{p_2}$ are the angular momentum of the first and the second top and α_i is the internal rotation angle.

[b] Notation used in the input and output. The relations between the parameters of top 1 and top 2 are: $V_{32} = V_{31}$, $V_{32J} = V_{31J}$, $q_1 = q_2$, $r_2 = -r_1$, $r_{2J} = -r_{1J}$.

[c] Fixed values.

[d] Number of hyperfine components.

[e] Root-mean-square deviation of the fit.

C. Discussion

The different approaches used in the *XIAM* and *BELGI-C_{2v}-2Tops-hyperfine* codes lead to different values of fitted parameters which are given in Table III and Table IV, respectively. The rotational constants obtained from the *BELGI-C_{2v}-2Tops-hyperfine* fit, after converting them to the principal axis system, agree well with those obtained from the *XIAM* program. The small deviations are probably not only due to different terms included in the two fits carried out in different coordinate systems but also

due to the conversion process. The values of the calculated rotational constants A, B, C deviate by −1.6%, −0.86%, −1.02%, respectively, to the experimental ones obtained with *XIAM*. Since the rotational constants obtained from *ab initio* calculations are evaluated at equilibrium geometry and the experimental constants refer to the vibrational ground state, an agreement better than 1% is hardly feasible. In the *XIAM* fit, four centrifugal distortion constants (except δ_K) are accurately determined while only three of them (Δ_J, Δ_K, Δ_{JK}) are needed to model the microwave spectra of 25DMP with *BELGI*. The calculated values of centrifugal distortion constants are in very good agreement with the experimental ones (see Table III).

To predict the V_3 potential and determine the contributions of higher order terms such as V_6, V_9, etc. in the Fourier expansion of the potential function, as well as to study the potential coupling between the methyl groups, three different sets of symmetry adapted terms were used to parameterize the potential functions. For comparison, the contour plots drawn with the Fourier coefficients obtained from those three different parameterizations are given in Fig. 4. Due to symmetry, only a portion of each PES with the dihedral angles α_1 and α_2 ranging from −60° to 60° is necessary.

The PES (**a**) in Fig. 4 is obtained after fitting the data points with a constant term and the Fourier term ($\cos(3\alpha_1) + \cos(3\alpha_2)$), with which all data points can be reproduced with a maximum deviation of 10% within the dynamic range. If we included in addition the Fourier terms ($\cos(6\alpha_1) + \cos(6\alpha_2)$) and ($\cos(9\alpha_1) + \cos(9\alpha_2)$), associating with V_6 and V_9, respectively, as illustrated in the PES (**b**), the maximum deviation decreased to 2.8 %, and the minimum in (**b**) is significantly broader than that in (**a**). The PES (**c**) represents one unit cell of the PES given in Fig. 2 where also potential coupling terms between the methyl groups are taken into account and the maximum deviation is 1.13%. The potential minimum is slightly distorted along the anti-diagonal which can be interpreted as an anti-gearing motion of the methyl groups close to the minimum. The V_6 and V_9 contributions are approximately 15% and 3%. Experimental information on these contributions cannot be obtained from our spectrum containing only vibrational ground state rotational transitions, which only yields an effective V_3 barrier for both rotors. The *ab initio* results show that the coupling between the two methyl groups is rather weak with contributions of 1.8% and 11% for V_{cc} and V_{ss}, respectively. This is in agreement with our experimental

finding that potential coupling terms were not needed in the fits. Details of symmetry adapted terms and their values are given in Table S-II in the Appendix AIII.1.

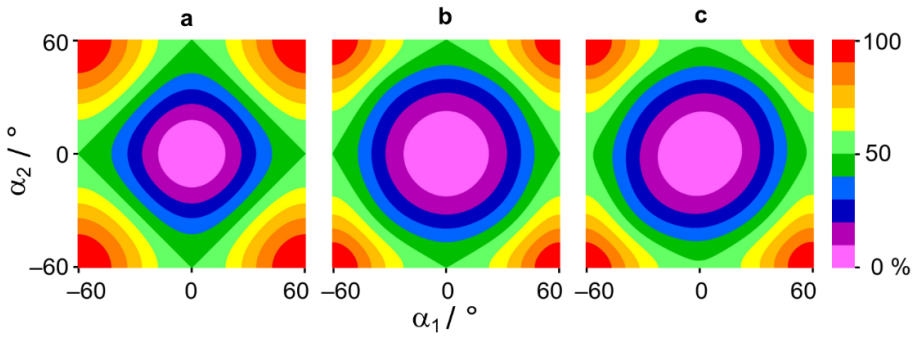

FIG. 4. The PES of 25DMP calculated at the MP2/cc-pVDZ level parameterized using three different sets of symmetry adapted terms.

The values of V_3 are determined to be 317.208(16) and 317.9205(41) cm^{-1} with *XIAM* and *BELGI*, respectively. They are in fairly well agreement but not within their error. Qualitatively speaking, the V_3 value should not depend on the axis system (PAM or quasi-PAM) in use. Nevertheless, it depends on different sets of parameters floated in the fit, causing the slight difference between *XIAM* and *BELGI*.

The V_3 potential calculated at the MP2/cc-pVDZ level of theory is 11.2% lower than the observed value, thus giving only the correct order of magnitude. While comparing the value of the V_3 potential obtained for 25DMP with that of 2-methylpyrrole[46] and those of other five-membered rings, as given in Fig. 5, we found that for 2- and 2,5-methylated heterocyclic rings, the barrier to internal rotation is lowest in mono-methylated and di-methylated thiophenes (**1**, **2**), higher in substituted pyrroles (**3**, **4**), and highest in substituted furans (**5**, **6**). The same holds true when comparing mono-methylated thiazoles, imidazoles, and oxazoles.[56] We also observe that the barrier is always larger in dimethylated heterocycles compared to the monomethylated ones. The lower the barrier, the more pronounced this effect.

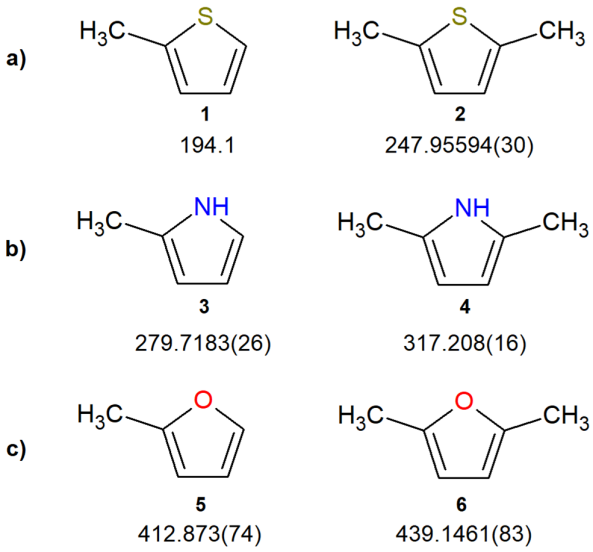

FIG. 5. Comparison of the barriers to internal rotation (in cm^{-1}) of **a)** 2-methylthiophene (**1**)[54] and 2,5-dimethylthiophene (**2**),[49] **b)** 2-methylpyrrole (**3**)[46] and 2,5-dimethylpyrrole (**4**, this study), and **c)** 2-methylfuran (**5**)[55] and 2,5-dimethylfuran (**6**).[21] For 2-methylthiophene, the uncertainty was not given in Ref. [54].

It should be noted that the correlation between the potential barrier V_3 and $\angle(i,a)$ is –1.000, showing that if the barrier of V_3 increases, the value of $\angle(i,a)$ will decrease simultaneously. In the *BELGI* approach, the angle $\angle(i,a)$ is not available as a floatable parameter directly but we observed a correlation between V_3 and $F_1 = F_2$. This problem has been solved in previous studies by fixing the values of F_1 and F_2 to those derived from the *XIAM* fit.[20] However, in the case of 25DMP, the fit did not converge and a slight change in F leads to a large different in V_3 even though the rms remains the same. We then tried several values of F starting from the value derived with *XIAM* in steps of 0.05. The value of $F_1 = F_2$ finally chosen yielded a nicely converged fit.

The *XIAM* code is based on the rigid top-rigid frame model in which parameters related with the molecular geometry such as $\angle(i,a)$, $\angle(i,b)$, and F_{12} are available as derived parameters. F_{12} can be floated but it is not recommended since it would lead to the distortion of the molecule. In contrast, the *BELGI* program employed a different approach in which the angles $\angle(i,a)$, $\angle(i,b)$ are not directly involved. Instead, several parameters related to those angles (q_1, r_1, f_{12}) can be floated, as for the two-inequivalent-top Hamiltonian introduced by Ohashi *et al*.[50] As given in the footnote of Table III, F_1 =

F_2 was kept fixed, and the constants q_1 and r_1 are floated. It is clear in Table IV from the operators they multiply that q_1 and r_1 are essentially $-2F_1\rho_{1a}$ and $-2F_1\rho_{1b}$,[51] respectively, with similar definitions for top 2. In the present study for two equivalent tops, the following parameters were set to be equal:

$$F_1 = F_2, \qquad V_{3,1} = V_{3,2}, \qquad q_1 = q_2. \tag{102}$$

To be consistent with the convention used in *Jabri et al.*,[19] r_2 was set to be equal but with opposite sign to r_1:

$$r_2 = -r_1. \tag{103}$$

The magnitude and the signs of those parameters can be derived from equations (11) of Ref. [50]. It should be noted that the angle θ about the y axis relating the a, b, c principal axes to the x, y, z rho-axes is zero in the case of two equivalent tops. Due to this choice of sign from $r_2 = -r_1$, we also have the relation $f_{12} = -2F_{12}$.

In our previous study on 2-methylpyrrole, the methylation effect arising from one methyl group attached to the pyrrole ring on NQCCs was found to be negligible.[46] In the present study, two methyl groups with similar functionalities are involved, raising an interesting question whether they possess more significant influence than that of one methyl group. Since the coupling constants obtained in the principal axes of inertia cannot be used directly for comparison, we attempt to compare their values in the principal axes of the field gradient at the nitrogen nucleus in each molecule. For molecules having a plane of symmetry, the principal axis of inertia and a principal axis of the field gradient are collinear with the axis perpendicular to the plane. Assuming that the c axis of the inertial moment coincides with the principal axis y of the field gradient, then the nuclear quadrupole coupling constants in the inertia χ_{aa}, χ_{bb} and those in the field gradient χ_{xx}, χ_{zz} are related by the expression:

$$\begin{pmatrix} \chi_{aa} \\ \chi_{bb} \end{pmatrix} = \begin{pmatrix} \sin^2\theta_{za} & \cos^2\theta_{za} \\ \cos^2\theta_{za} & \sin^2\theta_{za} \end{pmatrix} \cdot \begin{pmatrix} \chi_{xx} \\ \chi_{zz} \end{pmatrix} \tag{10}$$

where θ_{za} is the angle between the z-axis and the a-axis, as illustrated in Fig. 6.

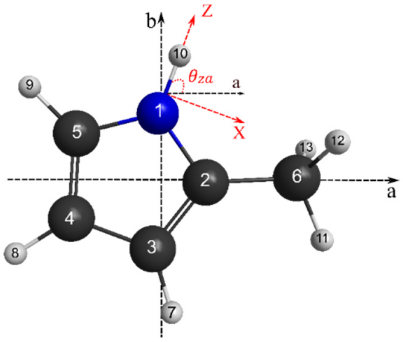

FIG. 6. The principal axes of inertia of the molecule and the principal axes of the field gradient at the nitrogen atom of 2-methylpyrrole.[46]

Because 25DMP has C_{2v} symmetry, the principal axes of the field gradient at the nitrogen nucleus are the same as the principal axes of inertia. Therefore, $\theta_{za} = 0°$, $\chi_{xx} = \chi_{aa} = 1.3272$ MHz and $\chi_{zz} = \chi_{bb} = 1.6559$ MHz. For 2-methylpyrrole,[46] using the experimentally deduced nuclear quadrupole constants $\chi_{aa} = 1.3345$ MHz and $\chi_{bb} = 1.5127$ MHz together with the calculated value of $\chi_{ab} = 0.0908$ MHz, the angle θ_{za} is determined to be 81.4°. Consequently, χ_{xx} and χ_{zz} are 1.2964 MHz and 1.5508 MHz, respectively. Since the two molecules both have a plane symmetry, the $\chi_{yy} = \chi_{cc}$ and χ_{yy} values are –2.9831 MHz and –2.8472 MHz for 25DMP and 2-methylpyrrole,[46] respectively. The results show that the second methyl group adjoining to the nitrogen atom in 25DMP increase the NQCC values, especially χ_{zz}, of the nitrogen atom. Nevertheless, the effect of methylations on the pyrrole ring is still negligible, confirming the results found in Ref. [46].

V. CONCLUSION

The microwave spectrum of 25DMP with four torsional species arising from two equivalent methyl internal rotations in combination with the presence of quadrupole hyperfine structures originating from a ^{14}N nucleus was recorded under molecular jet conditions and successfully assigned with support of quantum chemical calculations. The *WS18* code, a local approach where the different torsional species were fitted separately, enables us to verify the correctness of the assignment. The *BELGI-C_{2v}-2Tops-hyperfine* version of the *BELGI* code and the program *XIAM* offer a proper tool for a global fit of molecules featuring a C_{2v} symmetry and a weakly coupling quadrupole nucleus, yielding highly accurate

molecular parameters and NQCCs. Comparing 25DMP with the mono-methylated derivative 2-methylpyrrole, we conclude that the second methyl group adjoining to the nitrogen atom in 25DMP does not significantly change the field gradient around the nitrogen atom, but slightly increases the NQCC values.

APPENDIX

See Appendix AIII.1 for Cartesian coordinates, coefficients of the PESs, G_{36} character table with the adapted spin weight for 25DMP and frequency list.

ACKNOWLEDGMENTS

T.N. thanks the Université de Paris for a Ph.D. fellowship. This work is supported by the Agence Nationale de la Recherche ANR (project ID ANR-18-CE29-0011) and partly supported by the Programme National Physique et Chimie du Milieu Intestellaire (PCMI) of CNRS/INSU with INC/INP co-funded by CEA and CNES.

REFERENCES

[1]D. G. Lister, J. N. MacDonald, N. L. Owen, *Internal Rotation and Inversion: An Introduction to Large Amplitude Motions in Molecules*, Academic Press, New York (1978).

[2]H.V.L. Nguyen, I. Kleiner, *Phys. Sci. Rev.* (2021), DOI: 10.1515/psr-2020-0037 (in press).

[3]A. Legon, *Chem. Rev.* **80**, 231 (1980).

[4]H.V.L. Nguyen, I. Gulaczyk, M. Kręglewski, I. Kleiner, *Coord. Chem. Rev.* **436**, 213797 (2021).

[5]E.C. Thomas, V.W. Laurie, *J. Chem. Phys.* **50**, 8 (1969).

[6]J.E. Wollrab, V.W. Laurie, *J. Chem. Phys.* **54**, 532 (1971).

[7]K.P.R. Nair, H.D. Rudolph, H. Dreizler, *J. Mol. Spectrosc.* **48**, 571 (1973).

[8]H.S. Gutowsky, T.C. Germann, *J. Mol. Spectrosc.* **147**, 91 (1991).

[9]G. Bestmann, W. Lalowski, H. Dreizler, *Z. Naturforsch.* **40a**, 271 (1985).

[10]W. Caminati, S.D. Bernardo, *Chem. Phys. Lett.* **171**, 1 (1990).

[11]C. Thomsen, H. Dreizler, *Z. Naturforsch.* **48a**, 1093 (1993).

[12]M. Schnell, J.-U. Grabow, H. Hartwig, N. Heineking, M. Meyer, W. Stahl, W. Caminati, *J. Mol. Spectrosc.* **229**, 1 (2005).

[13]M. Meyer, W. Stahl, H. Dreizler, *J. Mol.Spectrosc.* **151**, 243 (1992).

[14]L.B. Favero, L. Evangelisti, G. Feng, L. Spada, W. Caminati, *Chem. Phys. Lett.* **517**, 139 (2011).

[15]P. Groner, S. Albert, E. Herbst, F.C. De Lucia, F. J. Lovas, B.J. Drouin, J. C. Pearson, *Astrophys. J.* **142**, 145 (2002).

[16]V.V. Ilyushin, J.T. Hougen, *J. Mol. Spectrosc.* **289**, 41 (2013).

[17]W. Neustock, A. Guarnieri, J. Demaison, G. Wlodarczak, *Z. Naturforsch.* **45a**, 702 (1990).

[18]H.V.L. Nguyen, W. Stahl, *ChemPhysChem* **12**, 1900 (2011).

[19]A. Jabri, V. Van, H.V.L. Nguyen, H. Mouhib, F.K.-Tchana, L. Manceron, W. Stahl, I. Kleiner, *Astron. Astrophys.* **A127**, 589 (2016).

[20]V. Van, W. Stahl, H.V.L. Nguyen, *Phys. Chem. Chem. Phys.* **17**, 32111 (2015).

[21]V. Van, J. Bruckhuisen, W. Stahl, V. Ilyushin, H.V.L. Nguyen, *J. Mol. Spectrosc.* **343**, 121 (2018).

[22]S. Khemissi, H.V.L. Nguyen, *ChemPhysChem* **21**, 1682 (2020).

[23]W. Jäger, H. Mäder, *Z. Naturforsch.* **42a**, 1405 (1987).

[24]W. Jäger, H. Mäder, *J. Mol. Struct.* **190**, 295 (1988).

[25]K.P.R. Nair, S. Herbers, W.C. Bailey, D.A. Obenchain, A. Lesarri, J.-U. Grabow, H.V.L. Nguyen, *Spectro. Chim. Acta A* **247**, 119120 (2021).

[26]T. Nguyen, V. Van, C. Gutlé, W. Stahl, M. Schwell, I. Kleiner, H.V.L. Nguyen, *J. Chem. Phys.* **152**, 134306 (2020).

[27]L. Ferres, W. Stahl, H.V.L. Nguyen, *J. Chem. Phys.* **151**, 104310 (2019).

[28]R. Kannengießer, M.J. Lach, W. Stahl, H.V.L. Nguyen, *ChemPhysChem* **16**, 1906 (2015).

[29]A. Roucou, M. Goubet, I. Kleiner, S. Bteich, A. Cuisset, *ChemPhysChem* **17**, 2523 (2020).

[30]H. Hartwig, H. Dreizler, *Z. Naturforsch.* **51a**, 923 (1996).

[31]V. Van, T. Nguyen, W. Stahl, H.V.L. Nguyen, I. Kleiner, *J. Mol. Struct.* **1207**, 127787 (2020).

[32]L. Ferres, W. Stahl, I. Kleiner, H.V.L. Nguyen, *J. Mol. Spectrosc.* **343**, 44 (2018).

[33]H.V.L. Nguyen, W. Stahl, *J. Mol. Spectrosc*. **264**, 120 (2010).

[34]L. Ferres, W. Stahl, H.V.L. Nguyen, *J. Chem. Phys.* **148**, 124304 (2018).

[35]S. Herbers, S.M. Fritz, P. Mishra, H.V.L. Nguyen, T.S. Zwier, *J. Chem. Phys.* **152**, 074301 (2020).

[36]K.P.R. Nair, S. Herbers, H.V.L. Nguyen, J.-U. Grabow, *Spectro. Chim. Acta A* **242**, 118709 (2020).

[37]S. Herbers, H.V.L. Nguyen, *J. Mol. Spectrosc.* **370**, 111289 (2020).

[38]J. T. Hougen, I. Kleiner, M. Godefroid, *J. Mol. Spectrosc.* **163**, 559 (1994).

[39]R. Kannengießer, W. Stahl, H.V.L. Nguyen, I. Kleiner, *J. Phys. Chem. A* **120**, 3992 (2016).

[40]K. Eibl, R. Kannengießer, W. Stahl, H.V.L. Nguyen, I. Kleiner, *Mol. Phys.* **114**, 3483 (2016).

[41]K. Eibl, W. Stahl, I. Kleiner, H.V.L. Nguyen, *J. Chem. Phys.* **149**, 144306 (2018).

[42]M.W. Schmidt, K.K. Baldridge, J.A. Boatz, S.T. Elbert, M.S. Gordon, J.H. Jensen, S. Koseki, N. Matsunaga, K.A. Nguyen, S.J. Su, T.L. Windus, M. Dupuis, J.A. Montgomery, *J. Comput. Chem.* **14**, 1347 (1993).

[43]W.C. Bailey, *Chem. Phys.* **252**, 57 (2000).

[44]R. Kannengießer, W. Stahl, H.V.L. Nguyen, W.C. Bailey, *J. Mol. Spectrosc.* **317**, 50 (2015).

[45]J.B. Graneek, W.C. Bailey, M. Schnell, *Phys. Chem. Chem. Phys.* **20**, 22210 (2018).

[46]T. Nguyen, C. Dindic, W. Stahl, H.V.L. Nguyen, I. Kleiner, *Mol. Phys.* **118**, 1668572 (2020).

[47]P. R. Bunker, P. Jensen, *Molecular Symmetry and Spectroscopy*, NRC Research Press, Ottawa, Ontario, Canada (2006).

[48]G.S. Ezra, *Symmetry Properties of Molecules*, *Lecture Notes in Chemistry 28*, Springer-Verlag, Berlin, Heidelberg, New York (1982).

[49]V. Van, W. Stahl, H.V.L. Nguyen, *Phys. Chem. Chem. Phys.* **17**, 32111 (2015).

[50]N. Ohashi, J.T. Hougen, R.D. Suenram, F.J. Lovas, Y. Kawashima, M. Fujitake, J. Pykad, *J. Mol. Spectrosc.* **227**, 28 (2004).

[51]M. Tudorie, I. Kleiner, J.T. Hougen, S. Melandri, L.W. Sutikdja, W. Stahl, *J. Mol. Spectrosc.* **269**, 211 (2011).

[52]H.B. G. Casimir, *Teyler's Tweede Genootschap*, E. F. Bohn, Harlem (1936).

[53]J.-U. Grabow, W. Stahl, H. Dreizler, *Rev. Sci. Instrum.* **67**, 4072 (1996).

[54]N.M. Pozdeev, L.N. Gunderova, A.A. Shapkin, *Opt. Spektrosk.* **28**, 254 (1970).

[55]I.A. Finneran, S.T. Shipman, S.L.W. Weaver, *J. Mol. Spectrosc.* **280**, 27 (2012).

[56]T. Nguyen, W. Stahl, H.V.L. Nguyen, I. Kleiner, *J. Mol. Spectrosc.* **372**, 111351 (2020).

Chapter III.2: Coupled large amplitude motions: The effects of two methyl internal rotations and ^{14}N quadrupole coupling in 4,5-dimethylthiazole investigated by microwave spectroscopy

This is an Accepted Manuscript of an article published by Elsevier publisher in Journal of Molecular Structure: "Vinh Van, Thuy Nguyen, Wolfgang Stahl, Ha Vinh Lam Nguyen and, Isabelle Kleiner, Coupled Large Amplitude Motions: The Effects of Two Methyl Internal Rotations and ^{14}N Quadrupole Coupling in 4,5-Dimethylthiazole Investigated by Microwave Spectroscopy, J. Mol. Struct. ***1207****, 127787, (2020), available online:* https://doi.org/10.1016/j.molstruc.2020.127787*"*

Abstract

The molecular jet Fourier-transform microwave spectrum of 4,5-dimethylthiazole has been recorded between 2.0 and 26.5 GHz, revealing torsional splittings arising from two inequivalent methyl internal rotations with relatively low hindering barriers and nitrogen quadrupole hyperfine structures. Two global fits with 1009 hyperfine components of 315 rotational transitions involving 5 torsional species were performed using the program *XIAM* and *BELGI-C_s-2Tops-hyperfine*, an extended version of the *BELGI-C_s-2Tops* code which includes the effect of the ^{14}N quadrupole coupling, giving a root-mean-square deviation of 399.8 kHz and 4.2 kHz, respectively. Compared to the monomethyl substituted thiazole derivatives, the barriers to internal rotation are drastically lower. This is also in contrast to chemical intuition which suggests high barriers due to steric hindrance. Because of the strong interaction between the methyl groups, strong top-top couplings in both the potential energy and kinetic parts of the Hamiltonian were observed.

Keywords: internal rotation, large amplitude motions, quadrupole hyperfine structure, rotational spectroscopy, dimethylthiazole

I. INTRODUCTION

Thiazole is a five-membered heterocyclic compound that contains a sulfur atom and a nitrogen atom in the ring. It exists as the basic structure element in a variety of organic compounds such as vitamin B_1 and clomethiazole[1]. It is also a precursor in the production of fungicides, drugs (e.g., alagebrium), and dyes[2]. Thiazole derivatives participate in several biosyntheses as required for the formation of thiamine[1], where the sulfur atom is obtained from cysteine. Whereas thiazoles are well-represented in biomolecules, their related compounds oxazoles, where the sulfur atom is replaced by an oxygen atom, are not.

Thiazole and its monomethyl derivatives have been studied thoroughly by microwave spectroscopy (see Figure 1)[3-6]. Whereas their structures are proved to be relatively rigid, the internal dynamics arising from the internal rotation of the substituted methyl group are hard to predict. It is particularly interesting to compare the hindering potentials of the methyl rotors, which strongly depend on the position of the methyl substituent. While changing the methyl group from the 4- (**3**)[5] to the 5-position (**4**)[6] does not significantly influence the hindering potential (357.6 cm^{-1} and 332.0 cm^{-1}, respectively), it decreases drastically to one tenth in 2-methylthiazole (**2**, 34.9 cm^{-1}, for molecule numbering see Figure 1)[4]. The same trend can be recognized in the related compounds, oxazoles, where the hindering potentials are 251.8 cm^{-1}, 428.0 cm^{-1}, and 477.9 cm^{-1} for 2- (**6**)[7], 4- (**7**)[8], and 5-methyloxazole (**8**)[7], respectively. It is also notable by comparing (**2**) and (**6**), (**3**) and (**7**), as well as (**4**) and (**8**) that substitution of an oxygen by a sulfur atom significantly reduces the hindering potential. An explanation for these observations is the aromatic character of azole rings. Thiazoles are characterized by larger π-electron delocalization than the corresponding oxazoles and have therefore greater aromaticity. This aromaticity is evidenced by the chemical shift of the ring protons in ^{1}H-NMR spectroscopy, which is between 7.27 and 8.77 ppm. It clearly indicates a strong diamagnetic ring current. The calculated π-electron density marks the 5-position as the primary site for electrophilic substitution and the 2-position as the site for nucleophilic substitution[9].

The question of how the hindering potentials are influenced if two positions in the thiazole ring are substituted by methyl groups prompted us to study 4,5-dimethylthiazole (**5**) (45DMTA). To the best

of our knowledge, only two dimethyl substituted aromatic five-membered heterocyclic compounds, 2,5-dimethylthiophene[10] and 2,5-dimethylfuran[11], have been studied by microwave spectroscopy so far.

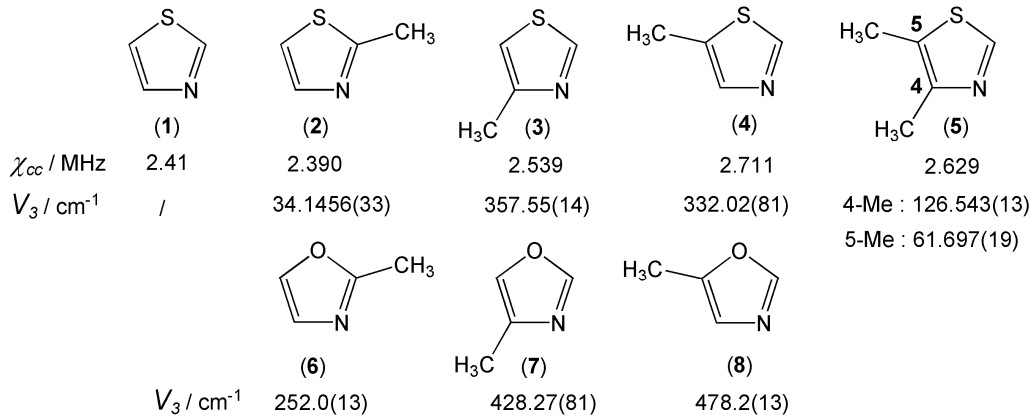

FIG. 1. The ^{14}N quadrupole coupling constant χ_{cc} (in MHz) of thiazole and its methyl-substituted derivatives as well as methyl torsional barriers in methyl substituted thiazoles and oxazoles (in cm^{-1}). (**1**) Thiazole, (**2**) 2-methylthiazole[4], (**3**) 4-methylthiazole[5], (**4**) 5-methylthiazole[6], (**5**) 4,5-dimethylthiazole (this work), (**6**) 2-methyloxazole[7], (**7**) 4-methyloxazole[8], (**8**) 5-methyloxazole[7].

Because 45DMTA has in addition to the two methyl tops a ^{14}N nucleus with a nuclear spin I = 1, hyperfine splittings occur in the microwave spectrum. Currently, the combination of two methyl internal rotations with one ^{14}N quadrupole coupling can be treated with only one program, the *XIAM* code, where nuclear quadrupole interactions are treated in a first order approximation[12]. However, spectra of molecules with low barriers to internal rotation often cannot be modeled correctly with *XIAM* due to the limited number of fit parameters[13-15]. Implementing higher order terms in the program is a difficult task.

The disadvantages of the *XIAM* code in dealing with low barriers to internal rotation can be overcome with the *BELGI-C_s-2Tops* program, which succeeded to fit the microwave spectra of molecules with C_s symmetry and two methyl tops to experimental accuracy, e.g., methyl acetate[16], ethyl methyl ketone[17], and dimethylbenzaldehyde[18], by adding higher order terms in the Hamiltonian[19]. However, *BELGI-C_s-2Tops* does not include the quadrupole coupling effect. Therefore, we decided to extend the program to a *BELGI-C_s-2Tops-hyperfine* version to treat the microwave spectrum of

45DMTA by taking into account the effect of weak nuclear quadrupole coupling using a first order perturbation approximation.

II. THEORETICAL PART

A. Quantum chemical calculations

1. Geometry optimizations

As other thiazole rings, 45DMTA is planar and aromatic because of the π electron delocalization of the two conjugated double bonds. This constraint confines the structural analysis to have only one starting geometry. Full geometry optimizations were performed on these initial forms using the B3LYP, M06-2X, MP2, and CCSD methods in combination with various Pople and Dunning basis sets[20,21] as implemented in the *GAUSSIAN09* package[22]. The geometry optimized at the MP2/6-311++G(d,p) level of theory is shown in Figure 2 in the principal axes of inertia. The nuclear Cartesian coordinates are given in Table S-I in the Appendix AIII.2. Harmonic frequency calculations were carried out to verify whether the stationary point is a saddle point or a true minimum geometry. An interesting feature of 45DMTA is that the dipole moment component in *a*-direction is accidentally almost zero. Therefore, the total dipole moment vector is almost exactly parallel to the *b* principal axis, and we expect a pure *b*-type spectrum.

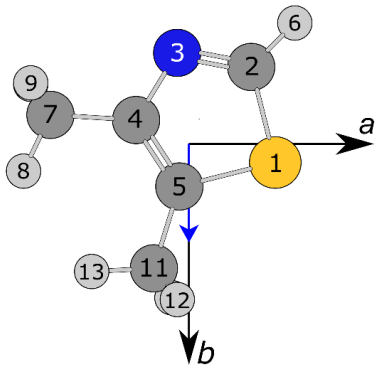

FIG. 2. The atom numbering and geometry of 4,5-dimethylthiazole calculated at the MP2/6-311++G(d,p) level of theory, as viewed along the *c* principal axis. The dipole moment is given as a blue arrow. The methyl groups attached to the 4- and 5-ring position are called the 4- and 5-methyl groups, respectively. The hydrogen atom H_{10} is located behind H_9, and H_{14} is behind H_{12}. This figure illustrates that: (i) all heavy atoms are located on the *ab*

plane and (ii) the dipole moment is almost exactly parallel to the *b* principal axis with the components of 0.01 D, 1.79 D, and 0.00 D in *a*-, *b*-, and *c*-direction, respectively.

2. ^{14}N nuclear quadrupole coupling constants

As mentioned in the introduction, 45DMTA contains one ^{14}N nucleus with a nuclear spin of $I = 1$. Therefore, nuclear quadrupole coupling will result in a hyperfine pattern for each rotational line. The splittings between the hyperfine components depend on the nuclear quadrupole coupling constants (NQCCs). From the optimized structure at the MP2/6-311++G(d,p) level, we carried out a single point electric field gradient calculation at the B3PW91/6-311+(d,p) level of theory using a calibration factor of eQ/h = 4.599[23] MHz a.u.$^{-1}$. This combination is a validated method for the prediction of NQCCs in π-conjugated amides in particular and might be also suitable for aromatic rings like 45DMTA. The calculation results in nuclear quadrupole coupling tensors with the diagonal elements $\chi_{aa} = 0.8070$, $\chi_{bb} = -3.2397$, $\chi_{cc} = 2.4327$ MHz, as well as the off-diagonal elements $\chi_{ab} = -2.1512$, $\chi_{ac} = 0.0117$, and $\chi_{bc} = 0.0028$ MHz. For comparison, we also performed calculations using the B3PW91/6-311+G(df,pd)//MP2/6-311++G(d,p) combination and the calibration factor of eQ/h = 4.5586(40)[24] MHz a.u.$^{-1}$. The respective values of the nuclear quadrupole coupling tensor elements are 0.7159, –3.2149, 2.4990, –2.1036, 0.0105, and 0.0030 MHz. Due to the C_s symmetry of the molecule, χ_{ac} and χ_{bc} should be zero. However, since no symmetry constraints were used during the geometry optimizations, a perfect C_s symmetry was not achieved, resulting in small, but non-zero values for these parameters.

3. Methyl internal rotations

Beside the ^{14}N nucleus which causes hyperfine splittings of all rotational transitions, 45DMTA features two methyl groups undergoing internal rotation. The resulting torsional fine splittings mainly depend on the orientations of the methyl groups in the molecule, the moment of inertia of the methyl group, and the barriers hindering the internal rotation. While the orientations of the methyl groups and their moments of inertia can be calculated well by geometry optimizations, predicting the barrier heights is a much more difficult task. The predicted values vary in a wide range and depend strongly on the level of

theory in use[10,25]. Even within the same molecule, a level that predicts reasonable value for one methyl group may fail for another methyl group[26]. High level quantum chemical methods such as coupled cluster and diffusion quantum Monte Carlo does not directly mean the best agreement with the experiments[27]. However, the magnitude (low, intermediate, or high) of the barrier heights is often correct, which serves as a good starting point for the spectral assignment.

For 45DMTA, we calculated the barrier heights of the methyl groups attached to the 4- and 5-ring position, henceforward called the 4- and 5-methyl groups, respectively, by varying the dihedral angles $\alpha_2 = \angle(N_3,C_4,C_7,H_8)$ and $\alpha_1 = \angle(S_1,C_5,C_{11},H_{12})$, respectively, in a grid of 2° (for atom numbering see Figure 2) with the MP2, B3LYP, M06-2X, and CCSD methods in combination with the 6-311++G(d,p) basis set. All other geometry parameters were optimized. A rotation of only 120° was sufficient due to the three-fold symmetry of the methyl groups. The potential energy curves corresponding to the 4-methyl group are depicted in the left panel of Figure 3, all of which have negligible V_6 contributions. The Fourier coefficients are available in Table S-2 in the Supplementary Material. It is interesting that the barrier height of 158.8 cm^{-1} calculated using the coupled cluster method is similar to that obtained with the much more cost-efficient B3LYP method (165.6 cm^{-1}), but significantly higher than that predicted by MP2 (63.0 cm^{-1}). The value of 98.2 cm^{-1} from calculations with Truhlar's M06-2X method[28] is in between.

In the case of the 5-methyl group, the potential energy curves predicted by the B3LYP, M06-2X, and CCSD methods, illustrated in the right panel of Figure 3, indicate normal three-fold potentials with no V_6 contributions. On the other hand, the MP2 method predicts a considerable V_6 contribution of about 55 % (see Table S-II in the Appendix AIII.2 for Fourier coefficients). For the 5-methyl group, like for the 4-methyl group, the calculated barrier heights are quite different and vary from about 25 cm^{-1} to 130 cm^{-1}. Again, the B3LYP method yields the highest value, the MP2 method the lowest, and the values from CCSD and M06-2X calculations are almost the mean value of them.

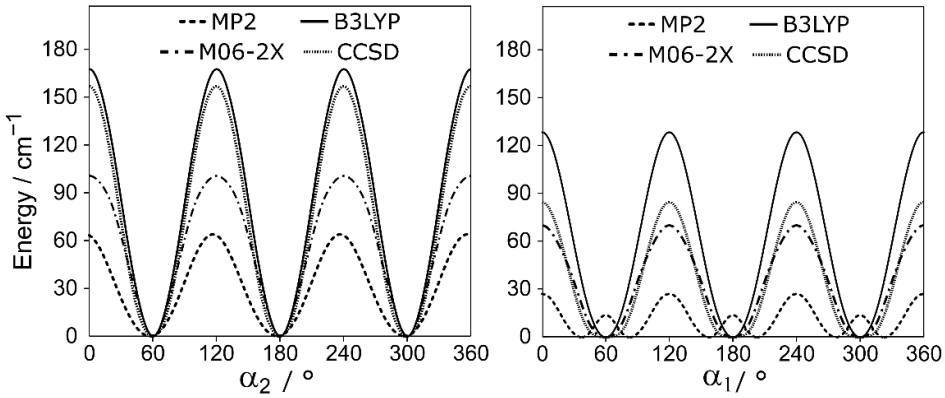

FIG. 3. *Left hand side:* The potential energy curves corresponding to a rotation of the 4-methyl group calculated using the MP2, B3LYP, M06-2X, and CCSD methods in combination with the 6-311++G(d,p) basis set. The dihedral angle $\alpha_2 = \angle(N_3,C_4,C_7,H_8)$ is varied over a grid of 2°. *Right hand side:* the respective potential energy curves corresponding to a rotation of the 5-methyl group by varying the dihedral angle $\alpha_1 = \angle(S_1,C_5,C_{11},H_{12})$. In both figures, energy values relative to the energetically lowest conformation with E_{min} = −646.4816118 (MP2), −647.7803704 (B3LYP), −647.6327793 (M06-2X), and −646.5253342 Hartree (CCSD) are used.

As an alternative, geometry optimizations to a first order transition state of the methyl groups were performed at various levels of theory using the Berny algorithm to calculate the barrier heights[29]. The rotational constants and angles between the internal rotor axes and the principal axes of inertia obtained from geometry optimizations as well as the V_3 potentials from the transition state calculations are collected in Table S-III, Appendix AIII.2.

The discrepancy in predicting the methyl barrier heights and especially the abnormally high V_6 contribution in MP2 calculations induced us to perform two-dimensional potential energy surfaces (2D-PES) depending on α_1 and α_2 to study the coupling between the two methyl rotors. The dihedral angles α_1 and α_2 were varied over a grid of 10°. The corresponding energies were parameterized with a 2D Fourier expansion based on terms representing the correct symmetry, which are listed in Table S-IV in the Appendix AIII.2. Using these Fourier terms, the PESs were drawn as a contour plot depicted in Figure 4. All PESs indicate significant coupling between the two rotors, shown by the deviation in forms of the minimum regions from circles (oval for calculations using the DFT and CCSD methods, rhomb

for the M06-2X method, and double minimum for the MP2 method). The top-top coupling will be revisited in the discussion.

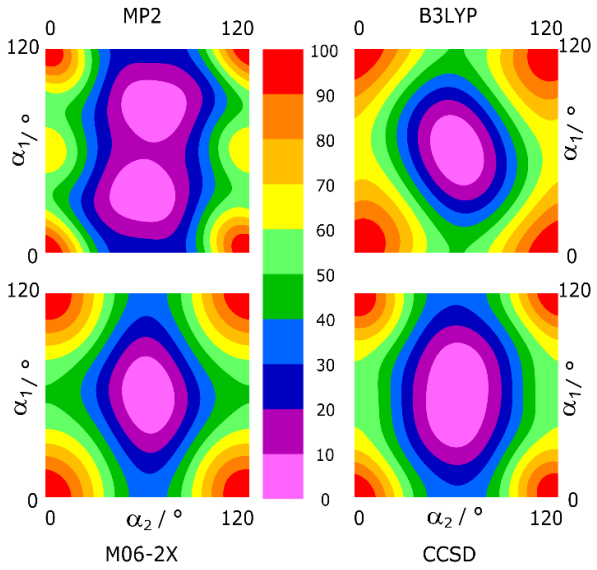

FIG. 4. The potential energy surfaces of 45DMTA depending on the rotation of the 4- and 5-methyl groups calculated with the MP2 (top left), B3LYP (top right), M06-2X (bottom left), and CCSD (bottom right) methods and the 6-311++G(d,p) basis set. The dihedral angles $\alpha_1 = \angle(S_1,C_5,C_{11},H_{12})$ and $\alpha_2 = \angle(N_3,C_4,C_7,H_8)$ were varied in 10° steps. The color codes indicate the energy (in percent) relative to the energy minima (0 %) and the energy maxima (100 %).

B. The *BELGI-C_s-2Tops-hyperfine* code

The *BELGI-C_s-2Tops* program has been slightly modified to treat hyperfine splittings in the rotational spectrum arising from weak nuclear quadrupole coupling of the nitrogen atom. A perturbation approach has been applied, which is similar to that used first for acetamide (see Eq. 1 of Ref.[30]), then for *N-tert*-butylacetamide (see Eq. 1 of Ref.[31]). The molecular symmetry is C_s in all cases, only the number of rotors increases to two in the present case.

In *BELGI-C_s-2Tops-hyperfine*, like in the *BELGI-C_s-2Tops* code[19], we follow the Hamiltonian initially described by *Ohashi et al.*[32]. The Hamiltonian is set up using a modified Principal Axis Method (PAM) in which the coefficients of the three quadratic rotational operators ($\mathbf{P_xP_y} + \mathbf{P_yP_x}$), ($\mathbf{P_yP_z} + \mathbf{P_zP_y}$), and ($\mathbf{P_zP_x} + \mathbf{P_xP_z}$) are kept fixed to zero in the fit (see Eq. (6) of Ref.[32]). We will refer to it hereafter as

the Ohashi-Hougen Hamiltonian. In this Hamiltonian, the nuclear quadrupole interaction terms were also included, taken from the usual form (e.g., Eq. (1) of Ref.[30]).

However, the *BELGI-C_s-2Tops-hyperfine* code differs from that in Ref.[32] because it solves the torsion-rotation Hamiltonian in a two-step diagonalization procedure[33], where the first step deals with the torsion-*K*-rotation part of the problem, and the second step deals with all the rest. This procedure is explained in details in Eq. (3) of Ref.[19] and in Eqs. (1) and (2) of Ref.[18].

In the *BELGI-C_s-2Tops-hyperfine* code, the expectation values of various combinations of angular momentum components $\langle \mathbf{P_a^2} \rangle$, $\langle \mathbf{P_b^2} \rangle$, $\langle \mathbf{P_c^2} \rangle$, and $\langle \mathbf{P_a P_b} + \mathbf{P_b P_a} \rangle$ are calculated. Subsequently, their numerical values are transferred into the standard hyperfine energy expression:

$$E_{hf}\ (I,J,F) = 2\frac{f(I,J,F)}{J(J\ +1)}\big[\chi_{aa}\langle \mathbf{P_a^2} \rangle\ +\ \chi_{bb}\langle \mathbf{P_b^2} \rangle - (\chi_{aa} + \chi_{bb}\ )\ \langle \mathbf{P_c^2} \rangle + \chi_{ab}\langle \mathbf{P_a P_b} + \mathbf{P_b P_a} \rangle\big] \quad (1)$$

where $f\,(I, J, F)$ is the Casimir function[34].

The shifts for each rotation-torsion energy level, and therefore those of the hyperfine components, can be calculated using Eq. (1). This enables us to take into account all hyperfine patterns as well as to fit the rotational and rotation-torsional molecular parameters together with the nuclear quadrupole coupling constants in a global fit. The *BELGI-C_s-2Tops-hyperfine* code is currently available by contacting one of the authors (I.K.).

In order to deduce physical meaning from the results of the fit, it is convenient to transform from the quasi-PAM parameters to PAM quantities. The details of the conversion program will be described in detail in section **2.3** below.

C. Conversion of the quasi-PAM parameters to PAM quantities

In section 6.1 of Ref.[32], the transformation of the rotation-torsion parameters obtained from the fit in quasi-PAM into PAM quantities is given. However, the transformation of the quadrupole coupling tensor into the principal axis system is not discussed. Here, we will briefly repeat the conversion from

quasi-PAM parameters into PAM quantities in the vector-matrix notation, give an algorithm facilitating the transformation, and extend it to the transformation of the quadrupole coupling tensor.

If we focus on the quadratic kinetic energy terms of the Ohashi-Hougen Hamiltonian (Eq. 6 of Ref.[32]), it can be conveniently written as

$$H_{kin}^{(2)} = \boldsymbol{P}^{\dagger}\boldsymbol{M}\boldsymbol{P} \tag{2}$$

with

$$\boldsymbol{P} = \begin{pmatrix} P_z \\ P_x \\ P_y \\ p_1 \\ p_2 \end{pmatrix}, \quad \boldsymbol{M} = \begin{pmatrix} A' & 0 & 0 & \frac{1}{2}q_1 & \frac{1}{2}q_2 \\ 0 & B' & 0 & \frac{1}{2}r_1 & \frac{1}{2}r_2 \\ 0 & 0 & C' & 0 & 0 \\ \frac{1}{2}q_1 & \frac{1}{2}r_1 & 0 & f_1 & \frac{1}{2}f_{12} \\ \frac{1}{2}q_2 & \frac{1}{2}r_2 & 0 & \frac{1}{2}f_{12} & f_2 \end{pmatrix}.$$

The quantities $A', B', C', f_1, f_2, f_{12}, q_1, q_2, r_1, r_2$ are the parameters obtained from a fit with the *BELGI-C_s-2Tops-hyperfine* code (e.g., see Table 5 of Ref.[19]).

In the same way, the quadratic kinetic energy terms in the classical PAM rigid frame-rigid top Hamiltonian for two internal rotors (Eq.7 of Ref.[32]) can be written as

$$\widetilde{H}_{kin}^{(2)} = \widetilde{\boldsymbol{P}}^{\dagger}\widetilde{\boldsymbol{M}}\widetilde{\boldsymbol{P}} \tag{3}$$

with

$$\widetilde{\boldsymbol{P}} = \begin{pmatrix} P_a \\ P_b \\ P_c \\ p_1 \\ p_2 \end{pmatrix}, \quad \widetilde{\boldsymbol{M}} = \begin{pmatrix} A'' & Z_{ab} & 0 & Q_1 & Q_2 \\ Z_{ab} & B'' & 0 & R_1 & R_2 \\ 0 & 0 & C'' & 0 & 0 \\ Q_1 & R_1 & 0 & F_1 & F_{12} \\ Q_2 & R_2 & 0 & F_{12} & F_2 \end{pmatrix}$$

and

$$A'' = A + F_1\rho_{1a}^2 + F_2\rho_{2a}^2 + 2F_{12}\rho_{1a}\rho_{2a} \tag{3a}$$

$$B'' = B + F_1\rho_{1b}^2 + F_2\rho_{2b}^2 + 2F_{12}\rho_{1b}\rho_{2b} \tag{3b}$$

$$C'' = C \tag{3c}$$

$$Z_{ab} = F_1\rho_{1a}\rho_{1b} + F_2\rho_{2a}\rho_{2b} + F_{12}(\rho_{1a}\rho_{2b} + \rho_{2a}\rho_{1b}) \tag{3d}$$

$$Q_1 = -F_1\rho_{1a} - F_{12}\rho_{2a} \tag{3e}$$

$$Q_2 = -F_2\rho_{2a} - F_{12}\rho_{1a} \tag{3f}$$

$$R_1 = -F_1\rho_{1b} - F_{12}\rho_{2b} \tag{3g}$$

$$R_2 = -F_2\rho_{2b} - F_{12}\rho_{1b}. \tag{3h}$$

We note that in Eq. (3), A'', B'', Z_{ab} are the same as A_{aa}, A_{bb}, and A_{ab} of Eq. (12) from Ref.[32].

The 5-dimensional angular momentum vector $\widetilde{\boldsymbol{P}}$ of the classical PAM Hamiltonian can be transformed to the $\boldsymbol{P}$ vector of the Ohashi-Hougen Hamiltonian by the application of the rotation matrix $\boldsymbol{T}$ (similar to the transformation matrix above Eq. (11) in Ref. [32]).

$$\boldsymbol{P} = \boldsymbol{T}\widetilde{\boldsymbol{P}} \tag{4}$$

with

$$\boldsymbol{T} = \begin{pmatrix} \cos\Theta & -\sin\Theta & 0 & 0 & 0 \\ \sin\Theta & \cos\Theta & 0 & 0 & 0 \\ 0 & 0 & 1 & 0 & 0 \\ 0 & 0 & 0 & 1 & 0 \\ 0 & 0 & 0 & 0 & 1 \end{pmatrix}.$$

Combining Eqs. (2), (3), and (4), we obtain

$$\widetilde{\boldsymbol{M}} = \boldsymbol{T}\boldsymbol{M}\boldsymbol{T}^{-1}. \tag{5}$$

From this transformation, it is obvious that

$$F_1 = f_1, F_2 = f_2, F_{12} = \tfrac{1}{2}f_{12}. \tag{6}$$

Eq. (5) is conveniently evaluated numerically by matrix multiplication for a given rotation angle Θ observing that $\boldsymbol{T}^{-1} = \boldsymbol{T}^{\dagger}$. However, there are only a few discrete angles which are consistent with the equations (3d-h). To find these angles, we vary Θ until consistency is achieved. Therefore, for a given Θ the quantities Q_1, Q_2, R_1, R_2 of $\widetilde{\boldsymbol{M}}$ as given in (3e-h) are used to obtain

$$\rho_{1a} = (Q_2 f_{12} - Q_1 F_2)/U, \quad \rho_{2a} = (Q_1 f_{12} - Q_2 F_1)/U \tag{6a}$$

$$\rho_{1b} = (R_2 f_{12} - R_1 F_2)/U, \quad \rho_{2b} = (R_1 f_{12} - R_2 F_1)/U \tag{6b}$$

with

$$U = F_1 F_2 - F_{12}^2.$$

Then Z_{ab}, also obtained for the given value of Θ, is used to calculate the expression

$$\Delta = Z_{ab} - F_1\rho_{1a}\rho_{1b} + F_2\rho_{2a}\rho_{2b} + F_{12}(\rho_{1a}\rho_{2b} + \rho_{2a}\rho_{1b}). \tag{7}$$

From Eq. (3d) it is clear that $\Delta = 0$ for a properly chosen value of the Θ angle. Therefore, to roughly determine all possible values of Θ, we calculated them in the range $[-\pi,\ \pi]$ in steps of 0.0001. If for two successive angles Θ_1, Θ_2 the condition $\Delta(\Theta_1) \cdot \Delta(\Theta_2) < 0$ is fulfilled, then there will be an angle Θ between Θ_1 and Θ_2 for which $\Delta = 0$. Four possible values of Θ were determined that way. Then we refined them to 10^{-9} using the bisection algorithm [35] and obtained $\Theta = 0.016699$ rad, $\Theta + \pi/2$, $\Theta - \pi/2$, and $\Theta - \pi$. Assuming that the coordinate system does not change much, i.e., the *a* axis (PAM) almost corresponds to the z axis (quasi-PAM), then only the angle $\Theta = 0.016699$ rad is a physically meaningful solution. The angle with the smallest absolute value was also chosen by *Ohashi et al.*[32]. The other angles corresponding to the change of the *x* and *z* axes and a rotation of 180°, which will change the directions of the *x* and *z* axes, are also allowed solutions.

Once the transformation of Eq. (5) is carried out with the correct value of Θ, the values for A'', B'', C'' in the matrix $\widetilde{\boldsymbol{M}}$ can be used to determine the structural rotational constants A, B, C from (3a-c).

The direction cosines λ between the internal rotor axes i_1 and i_2 and the inertial *a* and *b* axes are obtained using the equations (8c-d) of Ref. [32] together with $\lambda_{ga}^2 + \lambda_{gb}^2 = 1,\ g = 1{,}2$. We obtain

$$\lambda_{ga}^2 = \frac{w}{1+w}, \qquad \lambda_{gb}^2 = \frac{1}{1+w} \tag{8}$$

with

$$w = \left(\frac{I_a \rho_{ga}}{I_b \rho_{gb}}\right)^2 = \left(\frac{B \rho_{ga}}{A \rho_{gb}}\right)^2.$$

From equations (8c-d) of Ref.[32] it is clear that the signs of the direction cosines must be the same as the signs of the corresponding ρ values. The angles between the internal rotor axes and the principal axes of inertia are obtained then with $\angle(i_g, h) = \arccos \lambda_{gh}$, $h = a, b, c$.

Once the direction cosines are determined, equations (8c-d) of Ref.[32] also enable us to obtain the moments of inertia of the internal rotors I_g and the corresponding rotational constants F_{0g}.

$$I_g = \frac{I_a \rho_{ga}}{\lambda_{ga}}, \qquad F_{0g} = \frac{\lambda_{ga}}{\rho_{ga}} A. \tag{9}$$

We also use the rotation matrix $\boldsymbol{T}$ to transform the ^{14}N quadrupole coupling tensor $\boldsymbol{\chi}$ obtained from the *BELGI-C_s-2Tops-hyperfine* fit to the coupling tensor $\tilde{\boldsymbol{\chi}}$ which refers to the principal axes of inertia.

$$\tilde{\boldsymbol{\chi}} = \boldsymbol{T}\boldsymbol{\chi}\boldsymbol{T}^{-1} \tag{10}$$

with

$$\boldsymbol{\chi} = \begin{pmatrix} \chi_{zz} & \chi_{xz} & 0 & 0 & 0 \\ \chi_{xz} & \chi_{xx} & 0 & 0 & 0 \\ 0 & 0 & \chi_{yy} & 0 & 0 \\ 0 & 0 & 0 & 1 & 0 \\ 0 & 0 & 0 & 0 & 1 \end{pmatrix} \quad and \quad \tilde{\boldsymbol{\chi}} = \begin{pmatrix} \chi_{aa} & \chi_{ab} & 0 & 0 & 0 \\ \chi_{ab} & \chi_{bb} & 0 & 0 & 0 \\ 0 & 0 & \chi_{cc} & 0 & 0 \\ 0 & 0 & 0 & 1 & 0 \\ 0 & 0 & 0 & 0 & 1 \end{pmatrix}.$$

D. Symmetry considerations

G_{18} is the appropriate molecular symmetry group for 45DMTA which has a frame with C_s point-group symmetry and two inequivalent methyl groups[36,37]. There are different notations to describe the symmetry species of this group. In the Ohashi-Hougen code written to fit the microwave spectrum of *N*-methylacetamide[32], as well as in the *BELGI-C_s-2Tops-hyperfine* code, energy levels are labeled with A (=A_1+A_2), E_1, E_2, E_3, and E_4. Recently, another labeling scheme, for which the G_{18} group is written as the semi-direct product $(C_3^I \otimes C_3^I) \leftthreetimes C_s$, has been introduced for 3,4-dimethylanisole[38] and then applied for 2,4-dimethylanisole[39]. Using this scheme, the torsional species can be labeled by the first part (σ_1,σ_2) of the full symmetry label given in Table 1 of Ref.[38]. We will also use the abbreviated notations (00), (10), (01), (12), and (11) for 45DMTA, where σ_1 and σ_2 represent the 5- and the 4-methyl groups, respectively. The notations A, E_1, E_2, E_3, and E_4 correspond to (00), (10), (01), (12), and (11), respectively.

The seven protons and one nitrogen atom in 45DMTA result in 384 spin functions. The representation of the total nuclear spin function is Γ_{ns}= 96 (00)·A' + 48 (10)·A + 48 (01)·A + 24 (11)·A + 24 (12)·A. The selection rules for torsional components are (00)·A′ ↔ (00)·A″, (10)·A ↔ (10)·A, (01)·A ↔ (01)·A with the spin statistical weight of 96 and (11)·A ↔ (11)·A and (12)·A ↔ (12)·A with the spin weight of 48, showing that if only the spin statistical weight is considered, the intensity of the (11) and (12) torsional components are only half of that of the other species.

III. MICROWAVE SPECTRUM

A. Experimental setup

The sample of 45DMTA was purchased from TCI Deutschland GmbH, Eschborn, Germany, with a stated purity of over 97% and used without further purification. The rotational spectra were measured using a COBRA-type pulsed molecular jet Fourier transform microwave spectrometer covering the frequency range from 2.0 to 26.5 GHz[40]. The sample was placed on a piece of a pipe cleaner as carrier material, which was inserted in a stainless-steel tube close to the nozzle. Helium at a pressure of approximately 200 kPa flowed over the sample and the resulting 45DMTA-helium mixture was expanded into the Fabry-Pérot cavity.

To obtain the spectrum, the time domain signal was Fourier transformed. In our spectrometer, the supersonic jet and the resonator are coaxially aligned. Thus, each rotational transition is split into two components due to the Doppler effect. The rest frequency is calculated as the arithmetic mean of the frequencies of the Doppler components. The line widths are approximately 15-30 kHz for isolated lines. However, we observed additional splittings in the order of more than 10 kHz in many transitions, which are probably caused by spin-spin or spin-rotation coupling. Therefore, the estimated measurement accuracy is about 4 kHz.

B. Spectral analysis

The dipole moment components predicted at the MP2/6-311++G(d,p) level of theory are 0.01 D, 1.79 D, and 0.00 D in *a*-, *b*-, and *c*-direction, respectively. Because of the negligible components in *a*- in *c*-direction, we expect a pure *b*-type spectrum for 45DMTA.

Preliminary predictions of the spectrum using a rigid-rotor Hamiltonian were based on the rotational constants calculated at the MP2/6-311++G(d,p) level of theory given in Table S-3 of the Supplementary Material. A broadband scan in the frequency range 9.00 – 13.25 GHz was automatically recorded as overlapping spectra in steps of 0.25 MHz. It revealed a very dense spectrum, which made the assignment quite challenging. We searched first for the *b*-type $J+1_{0,J+1} \leftarrow J_{1,J}$, $J+1_{1,J+1} \leftarrow J_{0,J}$, and $J+1_{1,J} \leftarrow J_{2,J-1}$ lines with J ranging from 2 to 4. The (00) torsional state of these transitions could be identified by trial and error, which allowed us to predict other (00) lines well.

All rotational lines show hyperfine structures, as can be seen in Figure 5, due to the quadrupole coupling of the ^{14}N nucleus. As a next step, this effect was taken into account. Using the NQCCs calculated in section 2.1.2, the hyperfine structures of the (00) torsional state were readily assigned. A fit using a rigid-rotor model with centrifugal distortion correction and first order approximation for the quadrupole coupling yielded molecular parameters with sufficient accuracy.

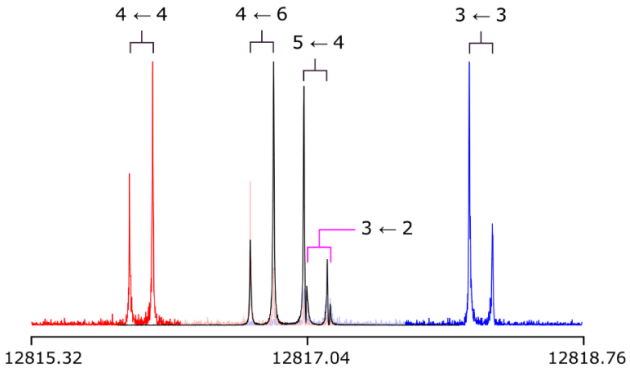

FIG. 5. Typical spectra of the (11) torsional species of the $4_{14} \leftarrow 3_{03}$ transition of 45DMTA recorded at high resolution. The frequencies are in MHz. The quadrupole components are given by F' ← F; the Doppler pairs are marked by brackets. Three spectra are illustrated and can be distinguished by different colors. For each spectrum, 50 decays were co-added.

After excluding all (00) lines, an amount of approximately four times of the assigned lines remains in the broadband scan. They belong to the other torsional species arising from the internal rotations of the two methyl groups. The program *XIAM*[12] was used to predict the torsional splittings. The initial values of the angles between the internal rotor axes and the principal axes of inertia as well as the hindering potentials were taken from *ab initio* calculation at the MP2/6-311++G(d,p) level of theory, those of the rotational constants, the centrifugal distortion constants, and the NQCCs from the rigid-rotor fit. The (01) and (10) species were assigned after a lot of trial and error, and we were able to get a satisfactory fit including the (00), (01), and (10) torsional species with their hyperfine components. However, we failed to assigned any (11) and (12) species with the prediction using molecular parameters from this fit.

In Figure 6, a portion of the broadband spectrum with the $4_{04} \leftarrow 3_{13}$ and $4_{14} \leftarrow 3_{03}$ rotational transitions is given as an example. It shows that the splitting between the (10), (11), and (12) torsional

species is rather small for some transitions, resulting in a triplet pattern. This gave us a hint to identify the (11) and (12) lines. Using the fit in which the (00), (01), and (10) lines are included with sufficient accuracy, all lines belong to those species were marked in the broadband scan. The remaining lines belong to the triplet were then identified as (11) and (12) lines of the same rotational transition as (10) in the same triplet.

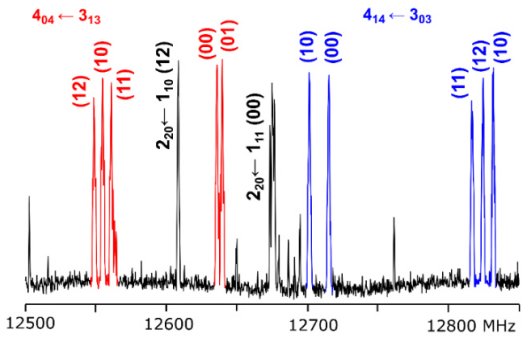

FIG. 6. A portion of the spectrum of 45DMTA showing the five torsional components (00), (10), (01), (11), and (12) of the $4_{04} \leftarrow 3_{13}$ (in red) and $4_{14} \leftarrow 3_{03}$ (in blue) rotational transitions. Two other intense lines (in black) are marked with their torsional species and rigid rotor quantum numbers *J, K_a, K_c*. The lines are broadened or split because of the quadrupole coupling arising from the ^{14}N nucleus.

Despite the fact that we were successful to find some (11) and (12) lines within the broadband scan range, the molecular parameters obtain from the *XIAM* fit, where all five torsional species were included, did not yield satisfactory results at this stage. Therefore, we were not able to assign any further (11) and (12) lines out of the range of the broadband scan. To overcome this problem, the (10) species, corresponding to the $\sigma = 1$ state of the 5-methyl group with lower barrier, had to be excluded, and we performed two separated fits, one with the (00), (01), (11) and the other with the (00), (01), and (12) species. With the predictions from these two fits, we were able to extend considerably the assignment of the (11) and (12) torsional species. The hyperfine structure analysis of the (10), (01), (11), and (12) species was straightforward. The frequency list is available in Table S-IV in the Appendix AIII.2.

As can be seen in the frequency list, there are some *c*-type perturbation allowed transitions and some transitions which are neither *a*-, *b*-, nor *c*-type. It is not a surprise because the quantum numbers K_a and K_c have no meaning for the symmetry of the rotational transitions apart from the (00) species. In all other species, the K_a, K_c quantum numbers just indicate the order of energy in analogy to the

asymmetric top energy level. One interesting point is that though the value of the dipole moment in the *a*-direction is almost zero, we could still observe the (00) component of one *a*-type transition, $4_{14} \leftarrow 3_{13}$, with its hyperfine structure.

IV. RESULTS OF THE FITS

A total of 315 rotational transitions with 1009 hyperfine components were assigned and fitted using the *XIAM* and the *BELGI-C_s-2Tops-hyperfine* codes, treating two methyl internal rotations and a weakly coupling quadrupole nucleus. While the *XIAM* fit gives a root-mean-square (rms) deviation of 399.8 kHz, the *BELGI-C_s-2Tops-hyperfine* fit offers a satisfactory rms deviation of 4.2 kHz. The coverage of the data and the quality of the fits are shown in Table 1. The molecular parameters from the *XIAM* fit and the results from *ab inito* calculation at the MP2/6-311++G(d,p) level of theory are given in Table 2. For comparison, parameters from the *BELGI-C_s-2Tops-hyperfine* fit which have been transformed into the PAM system are also listed in Table 2. The *BELGI-C_s-2Tops-hyperfine* parameters in the quasi-PAM system are shown in Table 3.

Table 1. Overview of the data set coverage and fit qualities for 45DMTA.

Γ^a	$(\sigma_1\sigma_2)$	$N_{hf}{}^b$	$N_t{}^c$	rms^d	$J_{max}{}^e$	$K_{max}{}^f$
A	(00)	214	68	2.9	9	7
E_1	(10)	209	66	6.3	8	6
E_2	(01)	212	68	4.0	9	6
E_3	(12)	180	58	3.5	7	6
E_4	(11)	194	55	3.5	7	5
XIAM fit		1009	315	399.8	9	7
BELGI fit		1009	315	4.2	9	7

[a] Symmetry species of the lines in each row.
[b] Number of hyperfine components in the torsional data group.
[c] Number of torsional components in each data group.
[d] Root-mean-square deviation of each data group in kHz.
[e] Largest J and K_a values in each data group.

Table 2. Molecular parameters of 45DMTA referred to the inertial principal axis system (PAM) obtained by the programs *XIAM* and *BELGI-C_s-2Tops-hyperfine* as well as from *ab initio* calculation at the MP2/6-311++G(d,p) level of theory.

Parameter[a]	Unit	*XIAM*	*BELGI*	*ab initio*[b]
A	GHz	3.187379(11)	3.10317(73)	3.177
B	GHz	2.457116(11)	2.462464(91)	2.448
C	GHz	1.4116299(57)	1.41137155(90)	1.407
D_J	kHz	–0.348(83)	0.0953(27)	0.1220
D_{JK}	kHz	2.52(29)		0.4159
D_K	kHz	–2.01(37)		-0.1047
d_1	kHz	0.093(40)		-0.04370
d_2	kHz	–0.094(16)		-0.002793
$V_{3,1}$	cm^{-1}	61.697(19)	71.007(38)	27.2
ρ_1	unitless	0.015900[c]	0.015744(11)	0.0154618
$F_{0,1}$	GHz	160[d]	161.3(12)	160
F_1	GHz	162.580[c]	161.2419[d]	162.9108
$\angle(i_1,a)$	°	108.9544(7)	109.149(24)	106.98
$\angle(i_1,b)$	°	18.9544(7)	19.149(24)	16.98
$\angle(i_1,c)$	°	90[e]	90[e]	89.98
$D_{pi2J,1}$	kHz	63.7(25)		
$D_{pi2K,1}$	MHz	–0.5882(46)		
$D_{pi2-,1}$	kHz	140.7(19)		
$V_{3,2}$	cm^{-1}	126.543(13)	131.524(69)	64.3
ρ_2	unitless	0.019891[c]	0.018990(23)	0.0194656
$F_{0,2}$	GHz	160[d]	163.23(21)	160
F_2	GHz	163.251[c]	160.7439[d]	163.089986
$\angle(i_2,a)$	°	175.0838(40)	175.661(13)	176.64
$\angle(i_2,b)$	°	94.9162(40)	94.339(13)	93.36
$\angle(i_2,c)$	°	90[e]	90[e]	89.99
$D_{pi2J,2}$	kHz	45.3(57)		
$D_{pi2K,2}$	MHz	–0.671(11)		
$D_{pi2-,2}$	kHz	90.2(42)		
F_{12}	GHz	0.8630[c]	0.0435(99)	0.88
V_{cc}	cm^{-1}	–4.765(12)	–5.294(12)	5.5
V_{ss}	cm^{-1}		–13.14(20)	
χ_{aa}	MHz	0.55(12)	0.5401(13)	0.8070
χ_{-}[f]	MHz	–5.71(16)	–5.6659(29)	−5.6724
χ_{ab}	MHz	–2.04(23)	–2.2358(24)	–2.1512
rms[g]	kHz	399.8	4.2	
N[h]		1009	1009	

[a] All parameters refer to the principal axis system. Watson's S reduction and I^r representation was used. [b] Centrifugal distortion constants obtained by anharmonic frequency calculation at the MP2/6-311++G(d,p) level of theory. The rotational constants of the vibrational ground state are A = 3.161 GHz, B = 2.432 GHz, and C = 1.399 GHz. NQCC values obtained at the B3PW91/6-311+(d,p)//MP2/6-311++G(d,p) level. [c] Derived parameters. [d] Fixed parameter. [e] Fixed due to symmetry. [f] $\chi_{-} = \chi_{bb} - \chi_{cc}$. [g] Root-mean-square deviation of the fit. [h] Number of hyperfine components.

With program *XIAM*, the rotational constants, the centrifugal distortion constants, and the nuclear quadrupole coupling constants can be obtained. The internal rotation parameters which are the V_3 hindering potentials, the angles between the internal rotation axes and the principal *a*-axis, the higher order parameters D_{pi2K}, D_{pi2J} and D_{pi2-} (for definition, see Ref.[41]) were also determined from the fit. A fit without any top-top coupling parameters was performed first, where the rms deviation was about 4.2 MHz. Since the 2D-PES, given in section 2.1.3, indicated possible couplings between the two methyl groups, we attempted to reduce the rms deviation by including the top-top coupling parameter V_{cc}, multiplying the cosine terms of the two tops. The rms decreases by approximately 10 times to 399.8 kHz. However, the parameters are highly correlated. All attempts to reduce the rms deviation by fitting another top-top coupling parameter including the sine terms, V_{ss}, were not successful. We note that the sign of D_J should be positive, which is confirmed by the results of the *BELGI* fit given in Tables 2 and 3. Because of the large rms deviation, the deduced centrifugal distortion constants are not physically meaningful. The D_J constant is contaminated by the internal rotation effects which are insufficiently described with *XIAM* and becomes an effective parameter which no longer presents the effect of centrifugal distortion.

Using the same data set the *BELGI-C_s-2Tops-hyperfine* code floated 37 parameters, which are the three rotational constants *A, B, C*, five quartic centrifugal distortion constants, the NQCCs χ_{aa}, χ_{bb}, and χ_{ab} in Eq. (1), the r_1 and r_2 parameters multiplying the off-diagonal $P_x p_2$ and $P_x p_1$ terms, respectively, the potential barrier heights for each top V_{31} and V_{32}, the rotation-torsion coupling term q_1 and q_2 (which are related to the ρ_1 and ρ_2 constants). Fifteen higher order terms were also determined representing the rotation-torsion interaction beyond the rigid top-rigid frame model, and finally five terms corresponding to the top-top interaction (V_{12cc}, V_{12ss}, F_{12}, B_{12}, r_{12P}). At the beginning, we also tried to fit the two reduced internal rotational constants F_1 and F_2, but the rms deviation of the fit did not significantly decrease and the parameters were highly correlated, as it is often the case when the data set only contains transitions from the ground torsional state. The F_1 and F_2 parameters were then fixed to values obtained when they were floated. We note that $F_g = \frac{F_{0g}}{r_g}$ with $r_g = 1 - I_g\left(\frac{\lambda_{ga}^2}{I_a} + \frac{\lambda_{gb}^2}{I_b}\right)$. The rms deviation of the *BELGI-C_s-2Tops-hyperfine* fit is 4.2 kHz, which is almost the measurement accuracy.

Table 3. Molecular parameters of 45DMTA referred to the quasi-PAM axis system obtained by the program *BELGI-C_s-2Tops-hyperfine*.

Operator[a]	Par.[b]	Program[c]	Unit	Value[d]
P_z^2	A	*OA*	GHz	3.16755(72)
P_x^2	B	*B*	GHz	2.496028(75)
P_y^2	C	*C*	GHz	1.41137155(90)
$-P^4$	Δ_J	*DJ*	kHz	0.0953(27)
$-P^2P_z^2$	Δ_{JK}	*DJK*	kHz	1.047(32)
$-P_z^4$	Δ_K	*DK*	kHz	–5.051(46)
$-2P^2\left(P_x^2-P_y^2\right)$	δ_J	*ODELN*	kHz	0.0322(13)
$-\left\{P_z^2,\left(P_x^2-P_y^2\right)\right\}$	δ_K	*ODELK*	kHz	0.2172(38)
$(1/2)(1-cos\alpha_1)$	$V_{3,1}$	*V31*	cm^{-1}	71.007(38)
$(1/2)(1-cos\alpha_1)\{P_z,P_x\}$	$V_{3,1AB}$	*V31AB*	MHz	–14.558 (77)
p_1^2	f_1	*F1*	GHz	161.2419[e]
$p_1^2P^2$	f_{1J}	*F1J*	MHz	–1.1211(54)
P_zp_1	q_1	*Q1*	GHz	2.1144(21)
$P_z^3p_1$	q_{1K}	*Q1K*	MHz	–0.03949(20)
P_xp_1	r_1	*R1*	GHz	–4.6166(36)
$(1/2)\{P_z^2,P_x\}p_1$	r_{1K}	*R1K*	MHz	0.02734(23)
$p_1^2P_x^2$	B_1	*B1*	MHz	0.830(23)
$p_1^2P_y^2$	C_1	*C1*	MHz	0.9544(55)
$(1/2)(1-cos\alpha_2)$	$V_{3,2}$	*V32*	cm^{-1}	131.524(69)
$(1/2)(1-cos\alpha_2)\,P^2$	$V_{3,2J}$	*V32J*	MHz	–4.956 (77)
$(1/2)(1-cos\alpha_2)\,P_z^2$	$V_{3,2K}$	*V32K*	MHz	198.6(14)
$(1/2)(1-cos\alpha_2)\{P_z,P_x\}$	$V_{3,2AB}$	*V32AB*	MHz	5.10(25)
$(1/2)(1-cos\alpha_2)\left(P_x^2-P_y^2\right)$	$V_{3,2BC}$	*V32BC*	MHz	–6.423(76)
p_2^2	f_2 [e]	*F2*	GHz	160.7439
$p_2^2P_z^2$	f_{2K}	*F2K*	MHz	8.299(66)
P_zp_2	q_2	*Q2*	GHz	6.0878(75)
$P_z^3p_2$	q_{2K}	*Q2K*	MHz	0.4181(32)
P_xp_2	r_2	*R2*	GHz	0.46744(72)
$(1/2)\{P_z^2,P_x\}p_2$	r_{2K}	*R2K*	MHz	0.2741(28)
$p_2^2P_x^2$	B_2	*B2*	MHz	–0.3179(92)
$p_2^2P^2P_z^2$	Δ_{2JK}	*DEL2JK*	kHz	–0.278(11)
$sin3\alpha_1 sin3\alpha_2$	V_{12S}	*V12S*	cm^{-1}	–13.14(20)
$(1-cos3\alpha_1)(1-cos3\alpha_2)$	V_{12C}	*V12C*	cm^{-1}	–5.294(12)
p_1p_2	f_{12}	*F12*	GHz	0.087(20)
$p_1p_2(p_1+p_2)P_x$	r_{12P}	*R12P*	MHz	–4.666(74)
$p_1p_2P_x^2$	B_{12}	*B12*	MHz	–0.0700(47)
	$2\chi_{aa}$ [f]	*XAA*	MHz	0.6137(13)
	$2\chi_{bb}$ [f]	*XBB*	MHz	–3.1766(13)
	$2\chi_{ab}$ [f]	*XAB*	MHz	–2.1716(24)
	rms[g]		kHz	4.2
	N[h]			1009

[a] Operator which the parameter multiplies in the program. α_1 and α_2 correspond to the 5- and the 4-methyl groups, respectively. {u, v} is the anti-commutator uv + vu. [b] Notation of Eq. (6) and Table 3 of Ref.[32], except for *A*, *B*, and *C*, where the prime was removed. [c] Notation used in the program input and output. [d] Value of the parameter obtained from the final least-squares fit, with one standard uncertainty given in parentheses. [e] Fixed to values

obtained in a previous fit. [f] Hyperfine energies were calculated using Eq. (1) of Refs.[30,34]. [g] Root-mean-square deviation of the fit. [h] Number of hyperfine components.

V. DISCUSSION

A. Quality of the fits

The fit given as Fit *XIAM* in Table 2 has a rms deviation of 399.8 kHz, which is 100 times the estimated measurement accuracy of 4.0 kHz. This can be explained by the relatively low hindering potentials of both methyl groups and the rather significant coupling between the two tops. Similar deviations have been found in many one-top problems with similar barrier heights treated by the program *XIAM*, i.a. ethyl acetate[42] (101.606(23) cm^{-1}, 85.3 kHz), allyl acetate[43] (98.093(12) cm^{-1}, 54.0 kHz), and vinyl acetate[44] (151.492(34) cm^{-1}, 92.3 kHz). If top-top coupling is present, as in the case of pinacolone[45], the rms deviation determined by *XIAM* is even worse (121.532(57) cm^{-1}, 1155.8 kHz).

We notice that the rms value can be reduced from 399.8 kHz to about 350 kHz by fitting F_{12}. However, this rms value is still not comparable to the measurement accuracy. Thus, we decided to keep this parameter as a derived parameter rather than floating it in the *XIAM* fit since it is correlated with other parameters in the fit. The *XIAM* fit presented in Table 2 follows a model considering two molecular subunits (the top and the frame) with fixed geometries and fixed dihedral angles describing the orientation of these subunits within the molecule. Indeed, very few higher order terms in *XIAM* allow for distortion from this rigid frame-rigid top model. Therefore, the value of F_{12} derived from the *XIAM* fit fairly matches the one calculated at the MP2/6-311++G(d,p) level of theory which also corresponds to a rigid frame-rigid top model. On the other hand, the F_{12} value fitted by *BELGI-C_s-2Tops-hyperfine* has a value of 0.0435(99) GHz which is 20 times smaller than the value from the *XIAM* fit. This is probably due to the different approach used in the *BELGI-2Tops-hyperfine* code, where F_{12} is an effective parameter with a different meaning compared to that from the rigid top-rigid rotor model. Fifteen higher order terms have to be used in the *BELGI-C_s-2Tops-hyperfine* code in order to achieve the measurement accuracy. Those higher order terms allow for various distortion and Coriolis effects.

B. Geometry parameters

The rotational constants obtained from the *XIAM* fit differ from the values calculated at the MP2/6-311++G(d,p) level of theory by –0.33% for *A*, –0.37% for *B*, and –0.33% for *C* (with respect to the *XIAM* values). This result matches well with our expectation for the level of theory in use. Since the rotational constants from the *XIAM* fit are deduced from the vibrational ground state and the results obtained from the *ab initio* calculations refer to the molecular equilibrium values, they are not directly comparable. The rotational constants in the vibrational ground state obtained from anharmonic frequency calculations given in the footnote of Table 2 are not in better agreement with the experimental values with deviations of –0.82% for *A*, –1.02 % for *B* and –0.89% for *C*. In general, the rotational constants are predicted well with various combinations of method and basis set (see Table S-3 in the Supplementary Material). The MP2/6-311++G(d,p) level of theory yielded good results for 45DMTA and is therefore recommended for substituted thiazoles. Results from calculations using the more cost-efficient Truhlar's method or B3LYP method are also satisfactory.

While the *B* and *C* constants determined from *XIAM* and *BELGI-C_s-2Tops-hyperfine* are essentially similar with deviation of only 0.22% and –0.02%, respectively, the A rotational constants differ by –2.64% (with respect to the *XIAM* values). Due to symmetry, the *C* constant should be the same in *XIAM* and *BELGI-C_s-2Tops-hyperfine*. The small deviation of –0.02% for the *C* constant can be explained by the contamination from higher order terms. The significant difference on the *A* rotational constant between the *XIAM* and the *BELGI*-family codes has been frequently observed in previous work[17,46,47]. The centrifugal distortion constants are not well-determined in the *XIAM* fit (probably because of the limitation on the maximum *J* and *K* values accessible in our experiments and the large rms deviation of the fit) and those from *BELGI-C_s-2Tops-hyperfine* in the quasi-PAM system are not comparable with the values calculated using anharmonic frequency calculations.

The conjugated π electron system in thiazoles and oxazoles causes the planarity of the molecules, which is directly associated with the aromaticity. In the cases of thiazole[3] and oxazole[48], the inertial defect $\Delta_c = I_c - I_a - I_b$ is almost zero with a value of 0.074 and 0.056 uÅ^2, respectively, where I_a, I_b, I_c are the principal moments of inertia. In the cases of mono-methyl substituted derivatives, we obtained inertial defects close to 3.2 uÅ^2 caused by two out-of-plane hydrogen atoms, which are, e.g., –3.059, –3.092, and –3.077 uÅ^2 for n-methylthiazole[4-6] (n = 2 (**1**), 4 (**2**), 5 (**3**), respectively, for molecule

numbering see Figure 1) as well as –3.127, –3.100, and –3.121 uÅ^2 for n-methyloxazole[7,8] (n = 2 (**5**), 4 (**6**), 5 (**7**), respectively). In 45DMTA, there are two methyl substitutions with two pairs of out-of-plane hydrogen atoms, leading to an inertial defect of 6.4 uÅ^2. This is similar to the values of –6.275, –6.280, –6.469, and –6.508 uÅ^2 found for 2,5-dimethylthiophene[10], 2,5-dimethylfuran[11], and *trans* and *cis*-2-acetyl-5-methylfuran[26], respectively, which are also aromatic five-membered rings possessing two methyl groups.

C. ^{14}N nuclear quadrupole coupling constants

The experimentally deduced ^{14}N NQCCs from both *XIAM* and *BELGI* fits are in very good agreement. Calculated values obtained using the combination B3PW91/6-311+G(d,p)//MP2/6-311++G(d,p) recommended for formamides possessing conjugated π-electron systems[23] are sufficiently accurate for the assignment. This combination also yielded satisfactory results for some other aromatic rings such as benzonitrile[49] and 2-methylpyrrole[50]. However, in this particular case of 45DMTA, values from calculations using the traditional combination B3PW91/6-311+G(df,pd)//MP2/6-311++G(d,p), which performs better for aliphatic formamides, are slightly closer to the experimental values.

In thiazole, monomethyl thiazoles, and 45DMTA, the principal *c*-axis is perpendicular to the ring plane. Therefore, it is collinear with one principal axis of the coupling tensor, enabling direct comparison of the χ_{cc} components. A summary of the ^{14}N coupling constants χ_{cc} is also presented in Figure 1. The value of 2.41 MHz found for thiazole[3] (**1**) is essentially the same as that of 2.390 MHz for 2-methylthiazole[4] (**2**), indicating that methylation effect on χ_{cc} can be almost neglected (for molecule numbering see Figure 1). Comparison of the χ_{cc} value for different nitrogen containing heterocycles and their mono-methyl derivatives confirms this conclusion[50]. Surprisingly, in 4- (**3**) and 5-methylthiazole (**4**), the value of χ_{cc} increases significantly to 2.539 and 2.711 MHz, respectively. The χ_{cc} value found in 45DMTA (**5**) lies in between the values of χ_{cc} in 4-methylthiazole (**3**) and 5-methylthiazole (**4**). Obviously, the +I effect of methyl groups[51] play a significant role for the π electron distribution within the ring, which also contributes to the unexpected low barriers to internal rotation of the methyl groups and the different electronic surrounding of the nitrogen nucleus. This might also explain the better

performance of the B3PW91/6-311+G(df,pd)//MP2/6-311++G(d,p) over the B3PW91/6-311+G(d,p)//MP2/6-311++G(d,p) combination.

D. Methyl torsional barriers

As can be seen in Figure 1, the barriers to internal rotation of 357.55(14) cm^{-1} and 332.02(81) cm^{-1} found for the methyl groups in 4- (**3**)[5] and 5- methylthiazole (**4**)[6], respectively, are very similar. In the case of 45DMTA (**5**), we expected higher values of this parameter due to sterical hindrance, as previously observed in aromatic six-membered rings such as 3,4-dimethylbenzaldehyde[18], 3,4-dimethylanisole[38], and *o*-xylene[52] (about 500 cm^{-1} in all cases). Surprisingly, the experimentally deduced barrier height decreases drastically to 61.697(19) cm^{-1} for the 5-methyl and 126.543(13) cm^{-1} for the 4-methyl group. A similar situation has been observed in 2,3-dimethylanisole[53], where the barrier height of the *o*-methyl group featuring the highest sterical hindrance is only about 27 cm^{-1}, while the value for its neighboring *m*-methyl group is 518.7(12) cm^{-1}. In a work on methyl substituted naphthalenes, *Schnitzler et al.* reported that the barrier of the methyl internal rotation in 1-methylnaphthalene is so high, that the torsional splittings are not resolvable in the spectrum[54]. This usually corresponds to a value of approximately 1000 cm^{-1} or higher value of the barrier to internal rotation. If a methyl group is added in the close proximity, as in the case of 1,2-dimethylnaphthalene, the barrier height of the 1-methyl group decreases remarkably to 306.96(25) cm^{-1}, while the value of the 2-methyl group increases from 227.12(42) cm^{-1} (found for 2-methylnaphthalene[54]) to 437.95(75) cm^{-1}. We believe that the low torsional barriers observed for the two methyl groups of 45DMTA as well as for the 1-methyl group of 1,2-dimethylnaphthalene can be explained similarly as for the *o*-methyl group of 2,3-dimethylanisole. Following the atom numbering in Figure 2, and assuming that the electronic environment of the C_5 atom and its methyl group would be exactly the same as the one around the N_3 atom, the local frame symmetry of the 4-methyl group would be C_{2v} and therefore, the leading term in the expansion of the potential function would no longer be V_3 but V_6. In reality, the C_5 atom and its methyl group have a different electronic environment compared to the N_3 atom. Thus, the frame symmetry is slightly out-of-balance, resulting in a small V_3 contribution.

The same explanation can also be applied for the 5-methyl group. The higher barrier found for the 4-methyl group compared to that of the 5-methyl group, can be due to the fact that the electronic surrounding for one carbon atom with an attached methyl group is more similar to that for a sulfur atom than that for a nitrogen atom. The closer one is to a C_{2v} symmetry, the lower the barrier will be.

Quantum chemical calculations at all levels of theory in use result in a V_3 potential barrier lower for the 5-methyl group than for the 4-methyl group (see Figure 3). This is in agreement with the experimental results. However, the value of this parameter for each top varies strongly depending on the level of theory (for the 4-methyl group between 16 and 272 cm^{-1} and for the 5-methyl group between 24 and 174 cm^{-1}). Currently, attempts to find a level of theory which yields sufficiently accurate V_3 potential value to satisfy the experimental data are still not successful, and predicting the barriers to internal rotation remains a difficult task.

The V_6 contribution in the potential barrier of the 5-methyl group could not be determined with the current data set. Therefore, the significant contribution of over 50% found in calculations at the MP2/6-311++G(d,p) level cannot be validated experimentally.

While the barrier to internal rotation of 126.543(13) cm^{-1} of the 4-methyl group deduced from the *XIAM* fit is in agreement with the value of 131.524(69) cm^{-1} from *BELGI-2Tops-C_s-hyperfine*, the value of the 5-methyl group differs by approximately 10 cm^{-1} (see Table 2). The differences might be caused by effects absorbed into the torsional barriers which are accounted for by the high order parameters fitted in *BELGI-C_s-2Tops-hyperfine* but not treated in *XIAM*.

E. Top-top coupling

The value of the top-top potential coupling constant V_{12c}, multiplying the $(1 - \cos 3\alpha_1)(1 - \cos 3\alpha_2)$ operator, is –4.765(12) cm^{-1} and –5.294(12) cm^{-1} in the *XIAM* and *BELGI-C_s-2Tops-hyperfine* fits respectively, i.e. about 7 % of the $V_{3,1}$ potential barrier height for the 5-methyl group and close to the value of –3.5 cm^{-1} found for methyl acetate[19]. The value found for the closely related constant V_{12s}, multiplying $\sin 3\alpha_1 \cdot \sin 3\alpha_2$, is –13.14(20) cm^{-1}, larger than that of V_{12c}.

The value and sign of V_{12c} obtained from the *XIAM* fit agrees well with those of the *BELGI* fit, while V_{12s} cannot be determined by *XIAM*. Table 2 and 3 show that the effects associated with this top-top torsional mode coupling near the equilibrium configuration are actually larger in 45DMTA than in methyl acetate[19], since the difference $|V_{3,1} - V_{3,2}|$ is about 61.5 cm^{-1}, while V_{12s} is only about −13 cm^{-1}.

VI. CONCLUSION

The microwave spectrum of 45DMTA with five torsional species and ^{14}N quadrupole hyperfine splittings were recorded under molecular jet conditions and successfully assigned assisted by quantum chemistry. In total, 97 rotational transitions with 315 torsional and 1009 quadrupole hyperfine components were identified and highly accurate molecular parameters were determined using the programs *XIAM* und *BELGI-C_S-2Tops-hyperfine*. While the fitting procedure was a challenge for *XIAM*, *BELGI-C_S-2Tops-hyperfine* could reduce the rms deviation by a factor of approximately 100 times down to 4.2 kHz, a value close to the measurement accuracy. In contrast to the intermediate barriers found for the respective monomethyl derivatives (357.6 cm^{-1} for 4-methylthiazole and 332.0 cm^{-1} for 5-methylthiazole) and in spite of steric hindrance, the torsional barriers of both methyl groups in 45DMTA are low (126.543(13) cm^{-1} for the 4-methyl group and 61.697(19) cm^{-1} for the 5-methyl group). This is most probably due to potential coupling between the two methyl groups arising from motions with an anti-geared character. Methylation at the fourth and/or fifth position(s) significantly influence(s) the π electron distribution within the ring, resulting in different electronic surroundings for the nitrogen nucleus and higher values of the χ_{cc} component of the quadrupole tensor.

APPENDIX

See the Appendix section AIII.2 for nuclear coordinates of 45DMTA at the MP2/6-311++G(d,p) level of theory (Table S-I), Fourier coefficients of fitted potential curves for 4- and 5-methyl groups (Table S-IIa, S-IIb, respectively), the rotational constants at various levels of theory along with their deviations compared to the experimentally deduced values (Table S-III), coefficients of the 2D-PESs (Table S-IV) as well as frequency list in Table S-IV.

ACKOWLEDGMENTS

We thank Dr. Alexandra Welzel for the results from her Ph.D. thesis entitled “Bau einer heizbaren Ultraschalldüse zur mikrowellenspektroskopischen Untersuchung schwerflüchtiger Substanzen im Molekularstrahl” at the RWTH Aachen University. V.V. thanks the Fonds der Chemischen Industrie (FCI) and T.N. the Université de Paris for a Ph.D. fellowship. Simulations were performed with computing resources granted by JARA-HPC from the RWTH Aachen University under the project jara0124. This work is supported by the Agence Nationale de la Recherche ANR (project ID ANR-18-CE29-0011).

NOTE

It should be mentioned that the Fig. 2 is not correct. In fact, the projections of H_{11} and H_{12} atoms are exactly the same. They are slightly different in the Fig. 2 due to a mistake while we made the figure.

REFERENCES

[1] M.J. Wilbym P.J. Hutchinson, *CNS Drug Rev.* **10**, 281, (2004).

[2]E. B.-Partida, B. V.-Salas, E. V.-Salas, G.P.-Cortéz, N. Nedev, J. Nanomater. (2019) Article ID 5287632.

[3]L. Nygaard, E. Asmussen, J.H. Høg, R.C. Maheshwari, C.H. Nielsen, I.B. Petersen, J. R.-Andersen, G.O. Sørensen, *J. Mol. Struct.* **8**, 225 (1971).

[4]J.-U. Grabow, H. Hartwig, N. Heineking, W. Jäger, H. Mäder, H.W. Nicolaisen, W. Stahl, *J. Mol. Struct.* **612**, 349 (2002).

[5]W. Jäger, H. Mäder, *Z. Naturforsch.* **42a**, 1405 (1987).

[6]W. Jäger, H. Mäder, *J. Mol. Struct.* **190**, 295 (1988).

[7]E. Fliege, *Z. Naturforsch.* **45a**, 911 (1990).

[8]E. Fliege, H. Dreizler, M. Meyer, K. Iqbal, J. Sheridan, *Z. Naturforsch.* **41a**, 623 (1986).

[9]V.M. Gaware, N.S. Dighe, S.R. Pattan, H.V. Shinde, D.S. Musmade, P.A. Chavan, P. Patel, *Pharm. Lett.* **2**, 35 (2010) .

[10]V. Van, W. Stahl, H.V.L. Nguyen, *Phys. Chem. Chem. Phys.* **17**, 32111 (2015).

[11]V. Van, J. Bruckhuisen, W. Stahl, V. Ilyushin, H.V.L. Nguyen, *J. Mol. Spectrosc.* **343**, 121 (2018).

[12]H. Hartwig, H. Dreizler, *Z. Naturforsch.* **51a**, 923 (1996).

[13]R. Kannengießer, M.J. Lach, W. Stahl, H.V.L. Nguyen, *ChemPhysChem* **16**, 1906 (2015).

[14]K. Eibl, R. Kannengießer, W. Stahl, H.V.L. Nguyen, I. Kleiner, *Mol. Phys.* **114**, 3483 (2016).

[15]L. Ferres, W. Stahl, I. Kleiner, H.V.L. Nguyen, *J. Mol. Spectrosc.* **343**, 44 (2018).

[16]H.V.L. Nguyen, I. Kleiner, S.T. Shipman, Y. Mae, K. Hirose, S. Hatanaka, K. Kobayashi, *J. Mol. Spectrosc.* **299**, 17 (2014).

[17]H.V.L. Nguyen, V. Van, W. Stahl, I. Kleiner, *J. Chem. Phys.* **140**, 214303 (2014).

[18]M. Tudorie, I. Kleiner, M. Jahn, J.-U. Grabow, M. Goubet, O. J. Pirali, *Phys. Chem. A* **117**, 13636 (2013).

[19]M. Tudorie, I. Kleiner, J.T. Hougen, S. Melandri, L.W. Sutikdja, W. Stahl, *J. Mol. Spectrosc.* **269**, 211 (2011).

[20]R. Ditchfield, W.J. Hehre, J.A. Pople, *J. Chem. Phys.* **54**, 724 (1971).

[21]T.H. Dunning Jr., *J. Chem. Phys.* **90**, 1007 (1989).

[22]Gaussian 09 (Revision A.02), M.J. Frisch, G.W. Trucks, H.B. Schlegel, G.E. Scuseria, M.A. Robb, J.R. Cheeseman, G. Scalmani, V. Barone, B. Mennucci, G.A. Petersson, H. Nakatsuji, M. Caricato, X. Li, H.P. Hratchian, A.F. Izmaylov, J. Bloino, G. Zheng, J.L. Sonnenberg, M. Hada, M. Ehara, K. Toyota, R. Fukuda, J. Hasegawa, M. Ishida, T. Nakajima, Y.Honda, O. Kitao, H. Nakai, T. Vreven, J.A. Montgomery Jr, J.E. Peralta, F. Ogliaro, M. Bearpark, J.J. Heyd, E. Brothers, K.N. Kudin, V.N. Staroverov, R. Kobayashi, J. Normand, K. Raghavachari, A. Rendell, J.C. Burant, S.S. Iyengar, J. Tomasi, M. Cossi, N. Rega, J.M. Millam, M. Klene, J.E. Knox, J.B. Cross, V. Bakken, C. Adamo, J. Jaramillo, R. Gomperts, R.E. Stratmann, O. Yazyev, A.J. Austin, R. Cammi, C. Pomelli, J.W. Ochterski, R.L. Martin, K. Morokuma, V.G. Zakrzewski, G.A. Voth, P. Salvador, J.J. Dannenberg, S. Dapprich, A.D. Daniels, O. Farkas, J.B. Foresman, J.V. Ortiz, J. Cioslowski, D.J. Fox, Gaussian, Inc., Wallingford CT, 2009.

[23]R. Kannengießer, W. Stahl, H.V.L. Nguyen, W.C. Bailey, *J. Mol. Spectrosc.* **317**, 50 (2015).

[24]W.C. Bailey, *Chem. Phys.* **252**, 57 (2000).

[25]A. Jabri, V. Van, H.V.L. Nguyen, W. Stahl, I. Kleiner, *ChemPhysChem* **17**, 2660 (2016).

[26]V. Van, W. Stahl, H.V.L. Nguyen, *ChemPhysChem* **17**, 3223 (2016).

[27]R. Kannengießer, S. Klahm, H.V.L. Nguyen, A. Lüchow, W. Stahl, *J. Chem. Phys.* **141**, 204308 (2014).

[28]Y. Zhao, D.G. Truhlar, *Theor. Chem. Acc.* **120**, 215 (2008).

[29]H.B. Schlegel, *J. Comput. Chem.* **3**, 214 (1982).

[30]R.D. Suenram, G.Y. Golubiatnikov, I.I. Leonov, J.T. Hougen, J. Ortigoso, I. Kleiner, G.T. Fraser, *J. Mol. Spectrosc.* **208**, 188 (2001).

[31]R. Kannengießer, W. Stahl, H.V.L. Nguyen, I. Kleiner, *J. Phys. Chem. A* **120**, 3992 (2016).

[32]N. Ohashi, J.T. Hougen, R.D. Suenram, F.J. Lovas, Y. Kawashima, M. Fujitake, J. Pykad, *J. Mol. Spectrosc.* **227**, 28 (2004).

[33]E. Herbst, J.K. Messer, F.C. De Lucia, P. Helminger, *J. Mol. Spectrosc.* **108**, 42 (1984).

[34]C.H. Townes, A.L. Schawlow, Microwave Spectroscopy, McGraw–Hill, New York (1955).

[35]W.H. Press, S.A. Teukolsky, W.T. Vetterling, B.P. Fannery, Numerical Recipes – The Art of Scientific Computing, 3rd edition, Cambridge University Press (2007).

[36]H. Dreizler, *Z. Naturforsch.* **16a**, 1354 (1961).

[37]P. R. Bunker, P. Jensen, Molecular Symmetry and Spectroscopy, 2nd ed., NRC Research Press: Ottawa, Ontario, Canada, 2006.

[38]L. Ferres, J. Cheung, W. Stahl, H.V.L. Nguyen, *J. Phys. Chem. A* **123**, 3497 (2019).

[39]L. Ferres, W. Stahl, H.V.L. Nguyen, *J. Chem. Phys.* **151**, 104310 (2019).

[40]J.-U. Grabow, W. Stahl, H. Dreizler, *Rev. Sci. Instrum.* **67**, 4072 (1996).

[41]L. Ferres, W. Stahl, H.V.L. Nguyen, *J. Chem. Phys.* **148**, 124304 (2018).

[42]D. Jelisavac, D.C. Cortés-Gómez, H.V.L. Nguyen, L.W. Sutikdja, W. Stahl, I. Kleiner, *J. Mol. Spectrosc.* **257**, 111 (2009).

[43]H.V.L. Nguyen, H. Mouhib, W. Stahl, I. Kleiner, *Mol. Phys.* **108**, 763 (2010).

[44]H.V.L. Nguyen, A. Jabri, V. Van, W. Stahl, *J. Phys. Chem. A* **118**, 12130 (2014).

[45]Y. Zhao, H.V.L. Nguyen, W. Stahl, J.T. Hougen, *J. Mol. Spectrosc.* **318**, 91 (2015).

[46]M. Andresen, I. Kleiner, M. Schwell, W. Stahl, H.V.L. Nguyen, *ChemPhysChem* **20**, 2063 (2019).

[47]K. Eibl, W. Stahl, I. Kleiner, H.V.L. Nguyen, *J. Chem. Phys.* **149**, 144306 (2018).

[48]A. Kumar, J. Sheridan, O.L. Stiefvater, *Z. Naturforsch.* **33a**, 145 (1978).

[49]J.B. Graneek, W.C. Bailey, M. Schnell, *Phys. Chem. Chem. Phys.* **20**, 22210 (2018).

[50]T. Nguyen, C. Dindic, W. Stahl, H.V.L. Nguyen, I. Kleiner, *Mol. Phys.* **118**, 1668572 (2020).

[51]R.F. Daley, Organic Chemistry, Part 1 of 3, Edition 1.3, Daley Press (2013).

[52]H.D. Rudolph, K. Walzer, I. Krutzik, *J. Mol. Spectrosc.* **47**, 314 (1973).

[53]L. Ferres, K.-N. Truong, W. Stahl, H.V.L. Nguyen, *ChemPhysChem* **19**, 1781 (2018).

[54]E.G. Schnitzler, B.L.M. Zenchyzen, W. Jäger, *ApJ* **805**, 141 (2015).

PART IV: NITROGEN AROMATIC RINGS WITH ONE ROTOR AND TWO ^{14}N NUCLEI

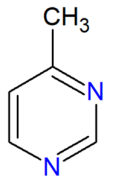

4-methylpyrimidine

To model the microwave spectra of molecules which contain one rotor and two weakly nuclei quadrupole coupling originating from ^{14}N, a new code called *TW21* was written, new features were implemented into the *WS18* code as well as in the *BELGI-2N* code. The detailed description of the *TW21* code will be given in the first chapter of this part. The new code was tested for three molecules mentioned in Part I of this chapter, which are 2-methylthiazole, 2-methylpyrrole and 3-methylpyrrole, revealing high-accuracy molecular parameters that are in very good agreement with the ones obtained using *BELGI* codes. The flexibility in choosing the $v_{t_{max}}$ and k_{max} allowed us to analyze quantitatively the *rms* deviations as a function of $v_{t_{max}}$. In the fitting process of microwave data presently available, which involves rather low *J* and occurs only within the torsional ground state $v_t = 0$, The results showed, that the interactions among v_t states are minor compared to that of adding additional rotation-torsion terms into the Hamiltonian.

As the first applied molecular system, the microwave spectrum of 4-methylpyrimidine (4MPY) was recorded using the molecular jet Fourier transform microwave spectrometer operating in the frequency range of 2-26.5 GHz. With the aids of quantum chemistry, we successfully assigned the microwave spectrum of 4MPY, fully understood the fine structure of A-E splittings arising from internal rotation of the methyl group as well as the rather complicated pattern of hyperfine splittings due to two ^{14}N nuclei. Three codes, *WS18*, *TW21* and *BELGI-2N*, were used and enabled us to reproduce the experimental data within the measurement accuracy. They provide very high accuracy molecular parameters which will be of great help for further studies (at higher frequency, e.g., THz, IR, etc., involving higher *J* values) with the chosen molecule.

Chapter IV.1: The TW21 code – a new code to model the spectra of molecules with one rotor in the presence of up to two ^{14}N nuclei

I. INTRODUCTION

Thorough the fitting processes with the molecules investigated in this thesis, we found that the *BELGI* code often gives satisfactory *rms* deviations. Especially in cases of lower barrier heights, these *rms* were much closer to experimental accuracy than with the *XIAM* code, sometimes a factor of 200 times better is found (see Chapter II.1 and III.2). Nevertheless, the *BELGI* code does require much more time (not only the computer time but also human time to find the correct starting set of parameters) compared to the *XIAM* approach, especially when higher *J* values are involved. The underlying reasons are: (i) *BELGI* allows users to float higher order parameters than *XIAM* and (ii) *BELGI* takes into account the first nine torsional states of the ground vibrational state while the *XIAM* code only considers the ground torsional state with $v_t = 0$. Some studies[1,2] suggested that the main reason of the *XIAM* code failing to reproduce the experimental data within the measurement accuracy is, that in the *XIAM* approach there are just a few higher order terms beyond the rigid top-rigid frame available. Those studies[1,2] also mentioned that the interactions among v_t states play a minor role in reducing the *rms* deviation in the fitting process but lacking of a detailed analysis on regard of this aspect. While it remains unclear which of the effects, either adding additional terms into the Hamiltonian or the interactions among v_t states, is important, it is certain that when increasing the truncation of the matrix elements (increasing v_t) will have a huge impact on the computational time of the program, directly relate to the time-consumption in the fitting process. This motivates us (i) analyze the contributions of the two effects above mentioned, how they affect the quality of the fits and (ii) to study how we can find a good compromise between offering satisfactory *rms* deviations but at the same time not require more time than necessary.

In this chapter, we will introduce our newly written code called *TW21* which employed the rho-axis-system, modelling the rotational transitions of molecules containing one rotor with up to two ^{14}N nuclei. We first will report how this new code *TW21* was tested on three molecules already studied in my thesis (2-methylthiazole, 2-methylpyrrole, 3-methylpyrrole, see Part II). Then we will present in details our

suggestions to optimize the size of the Hamiltonian matrix for the best *rms* at the least of the computational time requirement.

II. HAMILTONIAN

The *TW21* program is written to model the spectra of one rotor molecules with C_s point group of the frame symmetry in the presence of up to two weakly coupled nuclear quadrupoles. The Hamiltonian consists of three parts, the overall rotation $\mathbf{H_r}$, the torsional part $\mathbf{H_t}$, the centrifugal distortional terms $\mathbf{H_{cd}}$ as well as the Coriolis-like interaction terms. The Hamiltonian is setup exclusively in the rho-axis-system (see also Eqn. (72) in Part I).

$$\mathbf{H} = \mathbf{H_t} + \mathbf{H_r} + \mathbf{H_{cd}} + \mathbf{H_{rt}} \tag{1}$$

with

$$\mathbf{H_t} = A\mathbf{P_z^2} + F(\mathbf{p_\alpha} - \rho_z\mathbf{P_z})^2 + V_3\frac{1}{2}(\mathbf{1} - \mathbf{cos3\alpha}) \tag{2}$$

$$\mathbf{H_r} = B\mathbf{P}_x^2 + C\mathbf{P}_y^2 + D_{ab}\left(\mathbf{P}_x\mathbf{P}_y + \mathbf{P}_y\mathbf{P_x}\right) \tag{3}$$

$$\begin{aligned}\mathbf{H_{cd}} = &-\Delta_J\mathbf{P^4} - \Delta_{JK}\mathbf{P^2P_z^2} - \Delta_K\mathbf{P_z^4} - 2\delta_J\mathbf{P^2}\left(\mathbf{P_x^2} - \mathbf{P_y^2}\right)\\ &- \delta_K\left[\mathbf{P_z^2}\left(\mathbf{P_x^2} - \mathbf{P_y^2}\right) + \left(\mathbf{P_x^2} - \mathbf{P_y^2}\right)\mathbf{P_z^2}\right] - D_J\mathbf{P^4} - D_{JK}\mathbf{P^2P_z^2} - D_K\mathbf{P_z^4}\\ &+ d_1\mathbf{P^2}(\mathbf{P_+^2} - \mathbf{P_-^2}) + d_2(\mathbf{P_+^4} - \mathbf{P_-^4})\end{aligned} \tag{4}$$

$$\begin{aligned}\mathbf{H_{rt}} = &G_v\mathbf{P^2P_\alpha^2} + c_1\left(\mathbf{P_x^2} - \mathbf{P_y^2}\right)\mathbf{P_\alpha^2} + F_v(\mathbf{1} - \mathbf{cos3\alpha})\mathbf{P^2} + k_5(\mathbf{1} - \mathbf{cos3\alpha})\mathbf{P_z^2} +\\ &c_2(\mathbf{1} - \mathbf{cos3\alpha})\left(\mathbf{P_x^2} - \mathbf{P_y^2}\right) + d_{ab}(\mathbf{1} - \mathbf{cos3\alpha})\{\mathbf{P_z}, \mathbf{P_y}\} + k_1\mathbf{P_\alpha P_z^3} + k_2\mathbf{P^2P_\alpha^2} +\\ &c_4\{\mathbf{P_\alpha P_z}, \mathbf{P_x^2} - \mathbf{P_y^2}\} + \Delta_{ab}\mathbf{P_\alpha^2}\{\mathbf{P_z}, \mathbf{P_x}\}\end{aligned} \tag{5}$$

where A, B, C are the rotational constants, the reduced rotational constant F. $\mathbf{P_x}$, $\mathbf{P_y}$, $\mathbf{P_z}$ are the Cartesian components of the overall angular momentum, $\mathbf{p_\alpha}$ is the torsional angular momentum, the torsional potential V_3 and the torsional angle α. The two set of parameters (Δ_J, Δ_{JK}, Δ_K, δ_J, δ_K) and (D_J, D_{JK}, D_K, d_1, d_2) are the five quartic centrifugal distortion constants correspond with the Watson's A and Watson's S, respectively. We note that in the following, to ease the understanding of readers, some equations in Part I are repeated.

The torsional Hamiltonian can also be written as

$$\mathbf{H_t} = A\mathbf{P_z^2} + F\mathbf{P_\alpha^2} - 2F\rho_z\mathbf{P_\alpha P_z} + F\rho^2\mathbf{P_z^2} + \mathrm{V}_3\frac{\mathbf{1}}{\mathbf{2}}(\mathbf{1} - \mathbf{cos3\alpha}) \quad (6)$$

$$\mathbf{H_t} = F\mathbf{P_\alpha^2} - 2F\rho\mathbf{P_\alpha P_z} + (A + F\rho^2)\mathbf{P_z^2} + V_3\frac{\mathbf{1}}{\mathbf{2}}(\mathbf{1} - \mathbf{cos3\alpha}) \quad (7)$$

$$\mathbf{H_t} = F\mathbf{P_\alpha^2} + R\mathbf{P_\alpha P_z} + A_1\mathbf{P_z^2} + \mathrm{V}_3\frac{\mathbf{1}}{\mathbf{2}}(\mathbf{1} - \mathbf{cos3\alpha}) \quad (8)$$

Here we defined two new parameters call R and A_1 with

$$R = -2F\rho \text{ and } A_1 = A + F\rho^2 \quad (9)$$

Clearly, the Hamiltonian in the *TW21* code is similar to what has been implemented in the *BELGI* code[3] (see Table 1, Part I) and *RAM36*[4] code but with some modification in the way the torsional Hamiltonian ($\mathbf{H_t}$) is defined. We used the fact that (i) the basis functions correspond to different σ do not mix for a threefold symmetry internal problem and (ii) because $[\mathbf{H_t}, \mathbf{P_z}] = 0$, basis functions of different K do not mix either (*Herbst et al*.[5]). That enables us to regroup also the term $A\mathbf{P_z^2}$ to our torsional Hamiltonian in Eqn. (7). By regrouping the terms this way, the correlation among parameters significantly decreased as discussed in Ref. 4.

III. STRUCTURE OF THE PROGRAM

The general structure of the *TW21* code is given in Fig. 1 and details of each steps will be given in the following sub-sections.

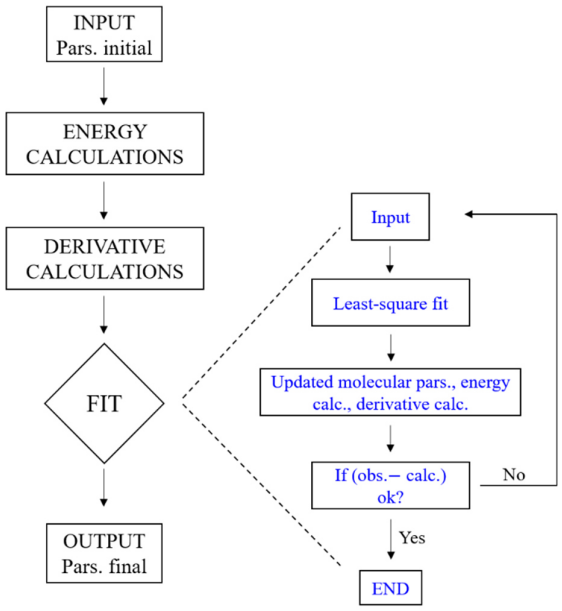

FIG. 1. The general algorithm of the code *TW21* showing how the initial parameters (Pars.) are least-squared fit.

A. INPUT / OUTPUT

The input file has three blocks with the keywords given in capital: CTRLPAR (Control parameters), MOLECULAR PARAMETERS and TRANSITIONS blocks.

1. INPUT

a. Block CTRLPAR

The CTRLPAR block contains parameters such as:

- "*pamin*": which can be set as 1 or 0. In order to ease the calculations of the initial parameters, we offer in the code the possibility to transform the values from PAM to RAM. If *pamin* is set to 1, the program will take the values initialized as PAM values (A_{PAM}, B_{PAM}, etc.) convert them to their values in the RAM system in the first fit cycle. If *pamin* is set to 0, the program will start directly with the RAM parameters. The advantage of this setting, which is not the case for the *BELGI* code or other internal rotation codes, is that it allows to use directly the parameters from quantum chemical calculation. The converting procedure is implemented as follows.

$$X = \begin{pmatrix} A & 0 \\ 0 & B \end{pmatrix},\ Y = \begin{pmatrix} B_z & D_{xz} \\ D_{xz} & B_x \end{pmatrix},\ T = \begin{pmatrix} cos\theta_{\mathrm{RAM}} & sin\theta_{\mathrm{RAM}} \\ -sin\theta_{\mathrm{RAM}} & cos\theta_{\mathrm{RAM}} \end{pmatrix} \tag{10}$$

where X, Y present the molecular parameters in the PAM, RAM system, respectively and T is transformation matrix. Therefore,

$$Y = T^{-1}XT. \tag{11}$$

By multiplying those metrices, the obtaining relations are (see also Eqn. (77-80), Part I):

$$B_z = Acos\theta_{\mathrm{RAM}}{}^2 + Bsin\theta_{\mathrm{RAM}}{}^2 \tag{12}$$

$$B_x = Asin\theta_{\mathrm{RAM}}{}^2 + Bcos\theta_{\mathrm{RAM}}{}^2 \tag{13}$$

$$D_{xz} = (A - B)cos\theta_{\mathrm{RAM}}sin\theta_{\mathrm{RAM}} \tag{14}$$

The value of angle θ_{RAM} is determined by

$$cos\theta_{\mathrm{RAM}} = \frac{\lambda_a A}{F_0 \rho} \tag{15}$$

with

$$\rho = 1 - I_\alpha \left(\frac{\lambda_a^2}{I_a} + \frac{\lambda_b^2}{I_b}\right), \lambda_a = cos(i,a),\ \lambda_b = cos(i,b). \tag{16}$$

- "*ncycl*": defines how many fit cycles the program should calculate.
- "*kmax*": defines the size of the truncation matrix in the first step diagonalization.
- "*vmax*": defines the size of the truncation matrix in the second step diagonalization.
- "*Jmax*": Maximum value of *J* from experimental data

b. Block MOLECULAR PARAMETERS

The block MOLECULAR PARAMETERS contains all molecular parameters. Each parameter will be defined with 3 characters: name, value, unit, and fit or fix.

- "*name*": name of parameters.
- "*value*": value of parameters.
- "*unit*": users freely choose among units, e.g., GHz, MHz, kHz, deg.
- "*fit or fix*": there are three modes. 1 stands for fit, 0 stands for fix, and 8 if program uses PAM parameters for initialization.

c. Block TRANSITIONS

Three types of molecules correspond with different format of TRANSITIONS block:

		Upper level			Lower level			Upper level		Lower level		Obs. Freq.
• Without ^{14}N	σ	J	K_a	K_c	J	K_a	K_c					f
• With one ^{14}N	σ	J	K_a	K_c	J	K_a	K_c	F		F		f
• With two ^{14}N	σ	J	K_a	K_c	J	K_a	K_c	F	F_1	F	F_1	f

with σ = 0/1 where 0 stands for non-degenerate species (A) and 1 stands for double-degenerate species E. J, K_a, K_c are the symmetric top rotational quantum numbers. The quantum numbers F and F_1 are defined in section II.3, Part I earlier and f is observed frequency. It is however important that after the last transition there must be an empty line in order to give sign for program to stop.

2. OUTPUT

The format of the output is similar to the one used for the input. The output contains three blocks:

- CTRLPAR: rewrite the parameters which users initialize in the input
- MOLECULAR PARAMETERS: Rewrite the initial values as in the input and update the fit RAM parameters.
- TRANSITIONS: After each cycle, all transitions are rewritten along with their residuals and after each block of transitions, we can find the updated molecular parameters and the correlation matrix.

B. ENERGY CALCULATIONS

In the *TW21* code, we followed the two-step diagonalization proposed by Herbst *et al.*[5] and then also applied in *BELGI*[3] (see Part I) as well as the *RAM36*[4] programs. A pre-diagonalization of the torsional Hamiltonian $\mathbf{H_t}$ is carried out in the basis set consisting of free rotor torsional eigenfunction $|\sigma k\rangle$ of $\mathbf{p_\alpha} = -\partial/\partial\alpha$ and eigenfunctions $|K\rangle$ of $\mathbf{P_a}$:

$$|K\sigma k\rangle = \frac{1}{\sqrt{2\pi}}|K\rangle e^{i(3k+\sigma)\alpha} \quad (17)$$

with $\sigma = 0, \pm 1$ (corresponding with the A and E states, respectively) and *k* is an integer value.

The torsional Hamiltonian matrix elements are calculated for each σ and *K* values, containing diagonal as well as off-diagonal matrix elements connected by ± 1 and ± 2 units in *k*. After diagonalization, the torsional eigenfunctions are

$$|Kv_t\sigma\rangle = \frac{1}{\sqrt{2\pi}}|K\rangle \sum_{k=-k_{max}}^{k_{max}} A_{3k+\sigma}^{K,v_t} e^{i(3k+\sigma)\alpha} \quad (18)$$

where k_{max} is an integer value which determined the truncation of the Hamiltonian matrix, v_t is the torsional vibrational quantum number and the eigenvector elements $A_{3k+\sigma}^{K,v_t}$.

In the second step, the energy eigenvalues correspond to the Hamiltonian ($\mathbf{H_r} + \mathbf{H_{cd}} + \mathbf{H_{rt}}$) are calculated in the basis of $|JK\rangle \cdot |Kv_t\sigma\rangle$. Here, $|JK\rangle$ is the symmetric top functions with J is the total angular momentum. Several examples of calculations for the Hamiltonian matrix elements in the second step are presented in the following. In the second step, the Hamiltonian is truncated at a certain $v_{t_{max}}$. It should be noted that only real matrices are allowed.

For the first step diagonalization, mathematically speaking, k_{max} should be infinite, but in fact values of $k_{max} = 8$ with *ntop*[6] program and 10 with the *BELGI*[3], *RAM36*[4] and the program written by *Herbst et al.*[5] were found to provide sufficient accuracy. For the second step diagonalization, the *BELGI*[3] and *RAM36*[4] codes consider the nine first torsional state $v_{t_{max}} = 8$ and the *XIAM* program considers just one torsional state $v_{t_{max}} = 0$. As already mentioned, through several investigated molecular systems studied in my thesis, the *BELGI* has advantage over *XIAM* code in reducing the *rms* deviations, but often it takes much more computational time than necessary to run the code. In our approach, we let the k_{max} and $v_{t_{max}}$ being read from the input. It allows the users to test the best compromise between accuracy and computational time. Essentially, during the assignment process, a fast approach ($v_{t_{max}} = 0$) is preferred but when it comes to the final stage of the fitting process, one wants the fit as accurate as possible (increasing $v_{t_{max}}$). Some examples demonstrated this procedure will be explained in details later on.

1. Matrix elements

Here, we will give two examples of how to calculate the matrix element for the parameters k_l associated with the operator $\mathbf{P_z^3 P_\alpha}$, and for c_l associated with the operator $\left(\mathbf{P_x^2} - \mathbf{P_y^2}\right)\mathbf{P_\alpha^2}$.

- $\mathbf{P_z^3 P_\alpha}$

$$\langle v_t' K'\sigma|\langle JK'|\mathbf{P_z^3 P_\alpha}|JK\rangle|v_t K\sigma\rangle$$

$$= \sum_{v_t'',K''} \langle v_t' K'\sigma|\langle JK'|\mathbf{P_z^3}|JK''\rangle|v_t'' K''\sigma\rangle \cdot \langle v_t'' K''\sigma|\langle JK''|\mathbf{P_\alpha}|JK\rangle|v_t K\sigma\rangle \tag{19}$$

$$= \sum_{v_t'',K''} \langle v_t' K'\sigma|v_t'' K''\sigma\rangle \cdot \langle J,K'|\mathbf{P_z^3}|J,K''\rangle \cdot \langle v_t'' K''\sigma|\mathbf{P_\alpha}|v_t K\sigma\rangle \cdot \langle JK''|JK\rangle \tag{20}$$

$$= \sum_{v_t'',K''} \langle v_t' K'\sigma|v_t'' K''\sigma\rangle \cdot K^3\langle JK'|JK''\rangle \cdot \langle v_t'' K''\sigma|\mathbf{P_\alpha}|v_t'' K''\sigma\rangle \cdot \langle JK''|JK\rangle \tag{21}$$

Because $\langle JK'|JK''\rangle = \delta_{K',K''}$ and $\langle JK''|JK\rangle = \delta_{K,K''}$, therefore

$$\langle v_t' K'\sigma|\langle JK'|\mathbf{P_z^3 P_\alpha}|JK\rangle|v_t K\sigma\rangle = K^3\langle v_t'' K''\sigma|\mathbf{P_\alpha}|v_t K\sigma\rangle\delta_{K',K} \tag{22}$$

here $\langle v_t'' K''\sigma|\mathbf{P_\alpha}|v_t K\sigma\rangle$ is obtained via similarity transformation of $\mathbf{P_\alpha}$ with the eigenvector matrix of the first step diagonalization.

- $\left(\mathbf{P_x^2} - \mathbf{P_y^2}\right)\mathbf{P_\alpha^2}$

We have: $\mathbf{P_+} = \mathbf{P_x} + i\mathbf{P_y}$ and $\mathbf{P_-} = \mathbf{P_x} - i\mathbf{P_y}$, therefore

$$\mathbf{P_+^2} = \mathbf{P_x^2} + \mathrm{i}\mathbf{P_x P_y} + \mathrm{i}\mathbf{P_y P_x} - \mathbf{P_y^2} \tag{23}$$

$$\mathbf{P_-^2} = \mathbf{P_x^2} - \mathrm{i}\mathbf{P_x P_y} - \mathrm{i}\mathbf{P_y P_x} - \mathbf{P_y^2} \tag{24}$$

$$\mathbf{P_x^2} - \mathbf{P_y^2} = \frac{1}{2}(\mathbf{P_+^2} + \mathbf{P_-^2}) \tag{25}$$

Thus, we have: $\left(\mathbf{P_x^2} - \mathbf{P_y^2}\right)\mathbf{P_\alpha^2} = \mathbf{P_+^2 P_\alpha^2} + \mathbf{P_-^2 P_\alpha^2} = \mathbf{H_1} + \mathbf{H_2}$.

According to the matrix multiplication rule: $(\mathbf{H_1})_{\mathbf{ij}} = \sum_{\mathbf{k}}\left(\mathbf{P_+^2}\right)_{\mathbf{ik}}(\mathbf{P_\alpha^2})_{\mathbf{kj}}$, thus

$$\langle v_t' K'\sigma|\langle JK'|\mathbf{H_1}|JK\rangle|v_t K\sigma\rangle$$

$$= \sum_{v_t'',K''} \langle v_t' K'\sigma|\langle JK'|\mathbf{P_+^2}|JK''\rangle|v_t'' K''\sigma\rangle \cdot \langle v_t'' K''\sigma|\langle JK''|\mathbf{P_\alpha^2}|JK\rangle|v_t K\sigma\rangle \tag{26}$$

$$= \sum_{v_t'',K''} \langle v_t' K'\sigma | v_t'' K''\sigma\rangle \cdot \langle J,K'|\mathbf{P_+^2}|J,K''\rangle \cdot \langle JK''|JK\rangle \cdot \langle v_t'' K''\sigma|\mathbf{P_\alpha^2}|v_t K\sigma\rangle \quad (27)$$

$$= \sum_{v_t'',K''} \langle v_t' K'\sigma | v_t'' K''\sigma\rangle \cdot \langle J,K'|\mathbf{P_+^2}|J,K''\rangle \cdot \delta_{K,K''} \cdot \langle v_t'' K''\sigma|\mathbf{P_\alpha^2}|v_t K\sigma\rangle \quad (28)$$

$$= \sqrt{J(J+1)-K(K-1)}\sqrt{J(J+1)-(K-1)(K-2)} \cdot \delta_{K,K-2} \cdot \sum_{v_t''} \langle v_t'(K-2)\sigma | v_t'' K\sigma\rangle \cdot \langle v_t'' K''\sigma|\mathbf{P_\alpha^2}|v_t K\sigma\rangle. \quad (29)$$

Similar for $(\mathbf{H_2})_{\mathbf{ij}} = \sum_{\mathbf{k}} \left(\mathbf{P_-^2}\right)_{\mathbf{ik}} (\mathbf{P_\alpha^2})_{\mathbf{kj}}$, we have

$$\langle v_t' K'\sigma | \langle JK'|\mathbf{H_2}|JK\rangle | v_t K\sigma\rangle$$

$$= \sqrt{J(J+1)-K(K+1)}\sqrt{J(J+1)-(K+1)(K+2)} \cdot \delta_{K,K+2} \cdot \sum_{v_t''} \langle v_t'(K+2)\sigma | v_t'' K\sigma\rangle \cdot \langle v_t'' K''\sigma|\mathbf{P_\alpha^2}|v_t K\sigma\rangle. \quad (30)$$

Thus, the matrix elements associated with the operator $\left(\mathbf{P_x^2} - \mathbf{P_y^2}\right)\mathbf{P_\alpha^2}$ is the sum of Eqn. (22) + Eqn. (23). Other calculations are carried out in similar ways and will not be repeated.

2. Transition's notation

In the *TW21* code, the transitions' labelling scheme after the second diagonalization is based on the energy ordering. For a given *J* block, we associate each energy level with the two determined rotational labels K_a, K_c of the usual asymmetric rotor. The details of the process are referred to Fig.3 in Part I and can be easily formulated into equations as follows:

$$\begin{gathered} 0 \le J \le J_{max} \\ 1 \le i \le 2J+1 \\ K_{a_i} = i/2 \\ K_{c_i} = (2J+2-i)/2 \end{gathered} \quad (31)$$

with *i* takes integer values only.

The choice of this notation has the advantage that: (i) it is easy to program and unique, (ii) it is the same as what is done in *XIAM*[7], *RAM36*[4], enabling for direct exchange data set among those programs and (iii) it avoids the problem arising from using the eigenvector composition scheme when there is no dominant eigenvector basis component as described in section 4.1.8 in Ref.[8].

C. DERIVATIVES NEEDED FOR THE FIT

The easiest way to calculate the derivatives $\partial E/\partial Y$ (with Y is the floated molecular parameter in a fit) is to express the energy E as the linear function of Y. That way will enable to obtain analytical solutions for the derivative calculations. For example, from Eqn. (8), we will have for the torsional energies:

$$E_t = F\langle \mathbf{P_\alpha^2} \rangle + R\langle \mathbf{P_\alpha P_z} \rangle + A_1\langle \mathbf{P_z^2} \rangle + V_3 \langle \frac{\mathbf{1}}{\mathbf{2}}(\mathbf{1} - \mathbf{cos3\alpha}) \rangle \tag{32}$$

Thus, the derivations will have the form:

$$\frac{\partial E_t}{\partial F} = \langle \mathbf{P_\alpha^2} \rangle \tag{33}$$

$$\frac{\partial E_t}{\partial R} = \langle \mathbf{P_\alpha P_z} \rangle \tag{34}$$

$$\frac{\partial E_t}{\partial A_1} = \langle \mathbf{P_z^2} \rangle \tag{35}$$

$$\frac{\partial E_t}{\partial V_3} = \langle \frac{\mathbf{1}}{\mathbf{2}}(\mathbf{1} - \mathbf{cos3\alpha}) \rangle \tag{36}$$

The derivatives of E_t were calculated in a similar way for all other parameters as well which we will not detail here.

D. FIT

The fitting process is based on the nonlinear least-squares method. After each cycle of fitting, the molecular parameters are updated and the energies as well as derivatives of all transitions are calculated by using the updated parameters. The fitting process stops after the number of fitting cycles defined by the *ncycl* parameter.

IV. CHECKING OF THE *TW21* CODE

The program *TW21* has been applied for a total of four molecules which are: 2-methylthiazole (2MTA), 2-methylpyrrole (2MP), 3-methylpyrrole (3MP) and 4-methylpyrrimidine (4MPY). The first three molecules, which were already studied in Part II, serving as the first tests of our code. They belong to the group of molecules which contain one methyl group and one ^{14}N whereas the last one (4MPY) has

one rotor CH_3 and two ^{14}N nuclei. The obtaining results for the three first molecules will be discussed in the following of this chapter and the result on 4MPY will be reported in Chapter IV.2.

A. Results of the fits for 2MTA, 2MP and 3MP

The three whole data sets, which were already fitted using the programs *XIAM* and *BELGI-C_s-hyperfine* with the results reported in Chapter II.1 for 2MTA, Chapter II.2 for 2MP and Chapter II.3 for 3MP, were refitted using the *TW21* code. The nuclear quadrupole coupling effect due to one ^{14}N is treated by the first order approximation following the Eqn. (31-34) in the Theory chapter (Part I). The resulting molecular parameters are summarized in Table I, Table II and Table III for 2MTA, 2MP and 3MP, respectively. For comparison purpose, the molecular parameters obtaining with the *BELGI-C_s-hyperfine* code are also presented.

Table I. Molecular parameters of 2-methylthiazole in the rho-axis-system obtaining with the *BELGI-C_s-hyperfine* (under column *BELGI*) and with the *TW21* codes.

Par.[a]	Unit	*BELGI*	*TW21*
A_1	MHz	-	5498.727(56)
A	MHz	5318.408(48)	5138.409(56)[b]
B	MHz	3269.2857(64)	3269.2854(61)
C	MHz	2051.5081(15)	2051.5080(14)
D_{ab}	MHz	102.256(68)	102.260(65)
R	GHz	-	–10.89314(30)
Δ_J	kHz	0.23763(54)	0.23763(51)
Δ_{JK}	kHz	0.9768(28)	0.9768(27)
Δ_K	kHz	–2.978(14)	–2.977(13)
δ_J	kHz	0.07742(24)	0.07742(23)
δ_K	kHz	0.7517(27)	0.7515(26)
χ_{aa}	MHz	1.4725(34)	0.7363(16)
χ_{bb}	MHz	–6.2528(31)[c]	–3.835141(19)
χ_{ab}	MHz	–4.232(21)[c]	–2.1181(97)
V_3	cm^{-1}	34.2535(12)	34.25354(57)
ρ	unitless	0.03310670(95)	0.033102(51)[b]
F_0		-	159[d]
F	GHz	164.516[e]	164.516[b]
Δ_{ab}	MHz	–1.110(23)	–1.111(22)
F_v	MHz	1.6234(67)	1.6238(64)
k_5	MHz	31.971(78)	31.969(75)
c_2	MHz	0.4666(53)	0.2334(25)
d_{ab}	MHz	–3.192(61)	–3.195(58)
k_1	MHz	–0.10274(62)	–0.10272(59)
c_4	kHz	4.82(21)	4.81(20)
N_A / N_E / N_q[f]		93/83/531	93/83/531
rms[g]	kHz	3.2	3.0

[a] All parameters refer to the rho axis system. Statistical uncertainties are shown as one standard uncertainty in the last digit.

[b] Derived parameters.

[c] There is a factor of two difference compared to the implementation in *BELGI-C_s-hyperfine* code.

[d] Fixed to the value from *ab initio* calculation (see Chapter II.1).

[e] Fixed to the value from *XIAM* fit (see Chapter II.1).

[f] Number of A and E species transitions as well as hyperfine components.

[g] Root-mean-square deviation of the fit.

Table II. Molecular parameters of 2-methylpyrrole in the rho-axis-system obtaining with the *BELGI-C_s-hyperfine* (under column *BELGI*) and with the *TW21* codes.

Par.[a]	Unit	*BELGI*	*TW21*
		-	9048.638(27)
A	MHz	8568.696(23)	8568.646(27)[b]
B	MHz	3433.887(29)	3433.888(28)
C	MHz	2489.1935(69)	2489.1935(68)
D_{ab}	MHz	73.64(87)	73.66(85)
R	GHz	-	−17.90763(30)
Δ_J	kHz	0.2391 (11)	0.2391(11)
Δ_K	kHz	0.736(17)	0.736(17)
Δ_{JK}	kHz	1.3174 (56)	1.3174(55)
δ_J	kHz	0.06585(43)	0.06585(42)
δ_K	kHz	1.000(10)	1.000(10)
χ_{aa}	MHz	2.6683(22)[c]	1.3342(11)
χ_{bb}	MHz	3.0258(22)[c]	1.5128(20)
V_3	cm^{-1}	278.9946(13)	278.99442(62)
ρ	unitless	0.0536021(93)	0.053602(19)[b]
F_0		-	158[d]
F	cm^{-1}	167.042[e]	167.042[b]
F_v	MHz	−0.920(61)	−0.926(32)
Rms[f]	kHz	3.1	3.1
$N_A/N_E/N_q$[g]		62/67/359	62/67/359

[a] All parameters refer to the rho axis system. Watson's A and I^r representation are used. Statistical uncertainties are shown as one standard uncertainty in the last digit.

[b] Derived parameters.

[c] There is a factor of two difference compared to the implementation in *BELGI-C_s-hyperfine* code.

[d] Fixed to the calculated value with *ab initio* calculation (Chapter II.2).

[e] Fixed to the value obtained from *XIAM* fit (Chapter II.2).

[f] Root-mean-square deviation of the fit.

[g] Number of A and E species transitions as well as hyperfine components.

Table III. Molecular parameters of 3-methylpyrrole in the rho-axis-system obtaining with the *BELGI-C_s-hyperfine* (under column *BELGI*) and with the *TW21* codes.

Par.[a]	Unit	Fit *BELGI*	*TW21*
A_1	MHz	-	9118.580(14)
A	MHz	8631.0585(40)	8631.059(14)[b]
B	MHz	3341.8407(43)	3341.8436(42)
C	MHz	2445.5916(45)	2445.5887(44)
D_{ab}		0[c]	0[fix]
R	GHz	-	−18.05399(24)
Δ_J	kHz	0.2191(27)	0.2191(26)
Δ_{JK}	kHz	1.586(10)	1.586(10)
Δ_K	kHz	0.525(14)	0.525(13)
δ_J	kHz	0.0608(78)	0.0608(76)
δ_K	kHz	1.129(17)	1.128(17)
F_0	GHz	-	158[d]
F	GHz	167.130[e]	167.145[b]
V_3	cm^{-1}	245.14101(89)	245.16843(43)
ρ		0.05400716(72)	0.05407(15)[b]
G_v	MHz	0.05832(93)	0.05832(90)
c_1	MHz	0.01200(22)	0.01167(21)
χ_{aa}	MHz	1.41345(12)[b]	1.4135(12)
χ_{bb}	MHz	1.37535(12)[b]	1.3753(20)
Rms[g]	kHz	2.9	2.9
$N_A/N_E/N_q$[h]		36/53/264	36/53/264

[a] All parameters refer to the rho-axis-system. Statistical uncertainties are given as one standard uncertainty in the last digit. Watson's A reduction and I^r representation were used.

[b] Derived parameters.

[c] Fixed to zero (see text Chapter II.3).

[d] Fixed to the calculated value (Chapter II.3).

[e] Fixed to the value of *XIAM*.

[g] Root-mean-square deviation of the fit.

[h] Number of A and E species rotational transitions as well as number of the hyperfine components.

Clearly, the *TW21* code is able to fit the microwave spectra of 2MTA, 2MP and 3MP to measurement accuracy, the *rms* deviations are comparable to that of *BELGI-C_s-hyperfine* code for 2MP, 3MP and even a little better for 2MTA. Because both programs employ the same method (RAM), the molecular parameters agree within their errors. Comparison made on the nuclear quadrupole coupling constants should be carried out with caution since in *BELGI-C_s-hyperfine*, there is a factor of two difference compared to the definition which is implemented in *TW21* code. Note that in our published results for the 3MP molecule we already took this factor of two into consideration for the *BELGI* fit.

B. Accuracy and computational time

To study whether or not the interactions between torsional states play a major role in the obtaining accuracy of the final fit, we performed fits with different values of $v_{t_{max}}$. The *rms* deviations and computational time for each fit are presented as functions of $v_{t_{max}}$ for 2MTA and 3MP in Fig. 2 and Fig. 3, respectively. We note that k_{max} was set to 10 and all fits were done in the same computer Intel® Core™ i7-8565U CPU 1.80 GHz, 2001 MHz, 4 Cores, 8 Logical Processors.

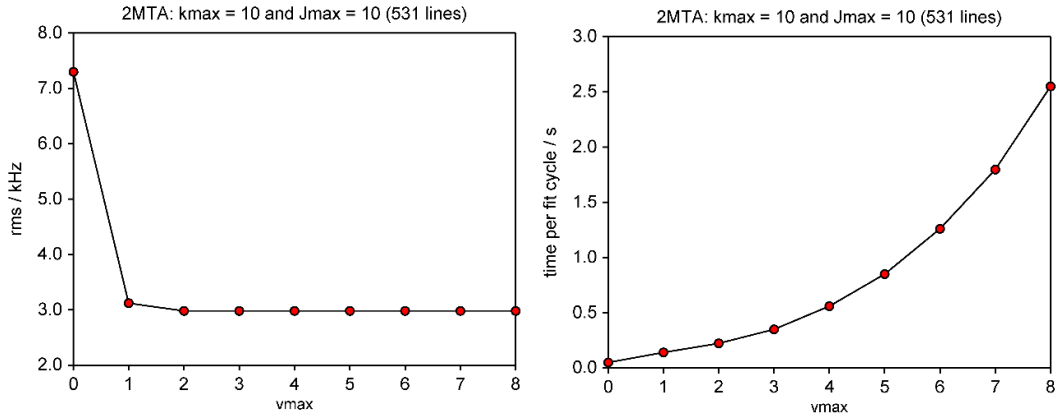

FIG. 2. The root-mean-square deviation (left-side) and computational time (right-side) are depicted as functions of $v_{t_{max}}$ for 2MTA.

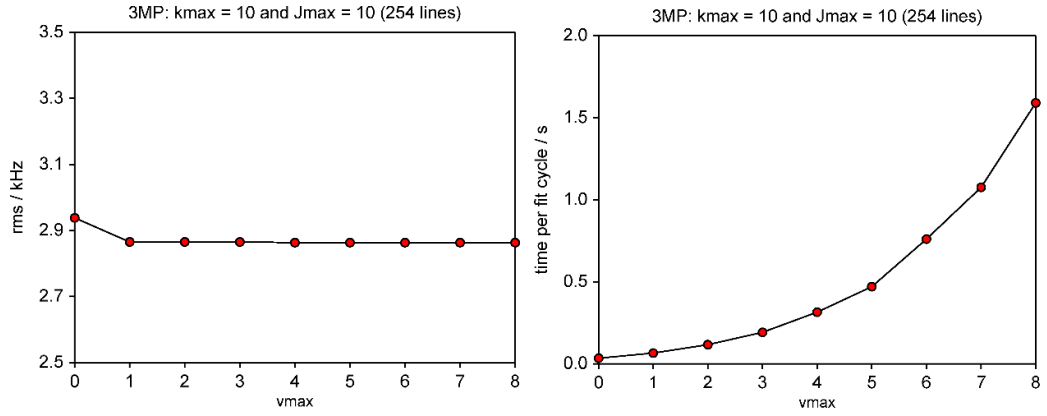

FIG. 3. The root-mean-square deviation (left-side) and computational time (right-side) are depicted as functions of $v_{t_{max}}$ for 3MP.

In the case of 2MTA (Fig. 2), the *rms* deviations do not change if $v_{t_{max}} \geq 2$ but the computational time increases exponentially while $v_{t_{max}}$ increases. The best compromise occurs when we set $v_{t_{max}} = 2$. In

the case of 3MP (Fig. 3), the same trend applies and the best $v_{t_{max}}$ is 1. Clearly, while barrier gets lower as in case of 2MTA, we will need to set $v_{t_{max}}$ at higher value. Nevertheless, for fitting the microwave spectra of the ground vibrational state (often with *J* values lower than 15), setting $v_{t_{max}} = 8$ would take us more time than the actual need.

As we discussed in Chapter II.1 for 2MTA, by adding torsion-rotation terms, the *rms* deviation significantly decreased (from 443 kHz to 3.2 kHz) whereas increasing $v_{t_{max}}$ from 0 to 2 improves the *rms* deviation to about 4 kHz. It shows the that, for fitting the rotational transitions at low *J*, in the case of the molecules we studied, the interactions between $v_{t_{max}}$ plays a minor role compared to that of adding torsion-rotation parameters. Therefore, we encourage users to use $v_{t_{max}} = 0$ for assigning purpose because it is fast and provides enough accuracy and increase $v_{t_{max}}$ slowly at the final state of fitting process to obtain the best *rms* deviations.

REFERENCES

[1]L. Ferres, W. Stahl, H.V.L. Nguyen, *J. Chem. Phys.* **148**, 124304 (2018).

[2]S. Herbers, H.V.L. Nguyen, *J. Mol. Spectrosc.* **370**, 111289 (2020).

[3]J. T. Hougen, I. Kleiner, M. Godefroid, *J. Mol. Spectrosc.* **163**, 559 (1994).

[4]V.V. Ilyushin, Z. Kisiel, L. Pszczólkowski, H. Mäder, J.T. Hougen, *J. Mol. Spectrosc.* **259**, 26 (2010).

[5]E. Herbst, J. K. Messer, F.C. De Lucia, P. Helminger, *J.Mol. Spectrosc.* **108**, 42 (1984).

[6]L. Ferres, W. Stahl, H.V.L. Nguyen, *J. Chem. Phys.* **151**, 104310 (2019).

[7]H. Hartwig and H. Dreizler, *Z. Naturforsch.* **51a**, 923 (1996).

[8]I. Kleiner, *J. Mol. Spectrosc.* **260**, 1 (2010).

Chapter IV.2: The rotational signature of 4-methylpyrimidine

I. INTRODUCTION

The experimental and theoretical advancements in microwave spectroscopy during the last decade gave rise to more complicated studies with chemical or biochemical importance e.g., rotational characterization of sugars, high-energy tautomeric species[1,2,3], investigation of molecule with up to four large amplitude motions[4] and analyzing hyperfine structure with up to four ^{14}N quadrupole nuclei[2,3].

In fact, many experimental molecular investigations have been carried out at different levels of details depending on the existence of relevant theoretical models and programs. Rigid molecules which contain up to nine ^{14}N atoms can be treated using *SPFIT* and *SPECAT* codes[5]. When a molecule contains an internal methyl rotor together with the presence of not more than one ^{14}N atom, its microwave spectrum can be modelled using *XIAM*[6], *BELGI* in its hyperfine version[7] and *RAM36* programs[8]. Prior to my thesis, to the best of my knowledge, no internal rotor program using a global approach could deal with the compounds which contain one methyl group and two ^{14}N nuclei. However, this class of molecule recently attracted attention with a number of experimental spectroscopic investigations on 2-methylpyrimidine[9], 5-methylpyrimidine[10] and very recently on the four isomers of methylimidazole[11]. As the first applied system to test the codes that we developed, in the local approach (*WS18* code) and in the global approach (*TW21* and *BELGI-2N* codes), we report in this chapter our results on the microwave spectrum for the 4-methylpyrimidine (4MPY) molecule.

II. QUANTUM CHEMICAL CALCULATIONS

A. Geometry optimizations

We performed the geometry optimizations of 4MPY with the GAMESS package[12] using two different methods: The B3LYP density functional theory[13] and the second-order Møller-Plesset MP2[14] in combination with the Pople basis set 6-31G, 6-311G, 6-311G++(d,p) and the only Dunning basis set cc-pVDZ. The resulting rotational constants (*A*, *B*, *C*) as well as the angle between the *a*-axis and the *i*-

internal axis along with the dipole moment components are given in Table I together with the level at which calculations were performed.

Table I. Rotational constants *A*, *B*, *C* (in MHz), deviations of the rotational constants compared to the experimental ones *ΔA*, *ΔB*, *ΔC* (in %), angle between the principal *a* axis and the internal rotor axis *i* (in degree) and dipole moment components (in Debye) obtained by optimization of the molecular geometry of 4MPY at various levels of theory.

	A	*ΔA*	*B*	*ΔB*	*C*	*ΔC*	*∠(i,a)*	μ_a	μ_b	μ_c
MP2										
6-31G	5809.3	–3.68	2568.4	–2.96	1801.1	–3.19	179.2	–1.82	–2.19	0.00
6-311G	5841.3	–3.15	2588.0	–2.21	1813.8	–2.51	179.0	–1.77	–2.22	0.05
6-311+G(d,p)	6047.4	0.26	2650.1	0.13	1863.8	0.18	179.5	–1.76	–2.11	0.00
6-311++G(d,p)	6047.1	0.26	2650.1	0.13	1863.8	0.18	179.5	–1.76	–2.12	0.00
cc-pVDZ	5970.4	–1.01	2612.6	–1.29	1838.3	–1.19	179.6	–1.53	–1.81	0.00
B3LYP										
6-31G	5794.8	–3.92	2574.0	–2.74	1803.0	–3.09	179.2	–1.95	–2.01	–0.05
6-311G	5808.1	–3.70	2583.8	–2.37	1809.0	–2.76	179.2	–1.90	–1.84	–0.05
6-311+G(d,p)	5939.3	–1.53	2618.0	–1.08	1838.5	–1.18	179.5	–1.85	–1.97	–0.01
6-311++G(d,p)	5939.1	–1.53	2618.0	–1.08	1838.5	–1.18	179.5	–1.84	–1.99	–0.01
cc-pVDZ	5888.1	–2.37	2591.3	–2.09	1820.7	–2.14	179.6	–1.63	–1.63	–0.05
Experimental										
	6031.3		2646.6		1860.5		0.9			

All calculations yielded only one stable conformer. With the MP2 methods, only the calculation using the basis set 6-311G yielded one non-planar molecular structure, all other calculations resulted in a planar conformer. However, all calculations carried out with the B3LYP method yielded non-planar structures. The closest to a planar conformer is observed with the most expensive basis set 6-311++G(d,p). A visualization of the equilibrium geometries obtained at different level of theory are presented in Fig. 1.

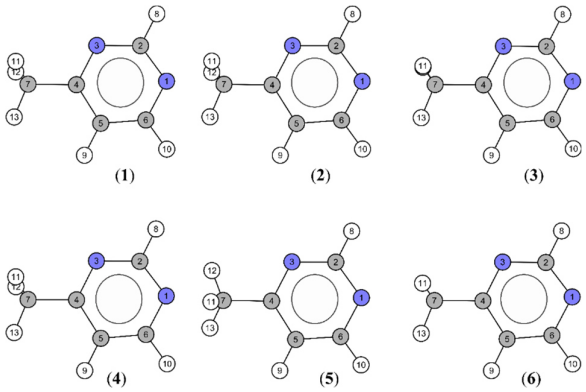

FIG. 1. Geometry optimizations at equilibrium obtained with various levels of theory: (**1**) B3LYP/6-31G, (**2**) B3LYP/6-311G, (**3**) B3LYP/6-311++G(d,p), (**4**) B3LYP/cc-pVDZ, (**5**) MP2/6-311G, (**6**) MP2/cc-pVDZ. The N atoms are presented in blue; C atoms are given in grey and H atoms in white. In (**6**), the hydrogen atom H_{12} is located behind H_{11}. The equilibrium geometry optimizations at MP2/6-31G as well as MP2/6-311++G(d,p) look the same as in (**6**).

B. Torsional potential of the methyl group

The potential energy curves of 4MPY were generated by rotating the dihedral angle $\alpha = \angle(H_{11},C_7,C_4,N_3)$ in step of 1° with all other geometry parameters are optimized at the MP2 as well as B3LYP levels, using the Pople basis set 6-311G as well as the Dunning basis set cc-pVDZ. Fig. 2 presents the two potential curves resulting from MP2 method whereas Fig. 3 depicts the two potential curves obtaining with B3LYP methods. The Fourier coefficient is given in Table S-II Appendix AIV.2.

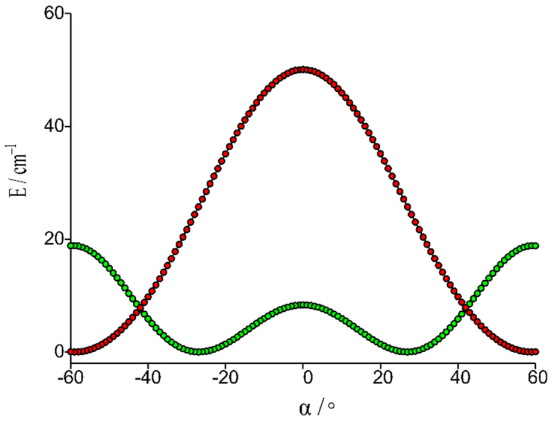

FIG. 2. Potential energy curves of 4-methylpyrrimidine (in cm^{-1}) obtained by varying the dihedral angle $\alpha = \angle(H_{11},C_7,C_4,N_3)$ in step of 1° while all other parameters were optimized at the MP2/cc-pVDZ (red dots) and the MP2/6-311G (green dots). The energies are transferred to cm^{-1} relative to the lowest energies accordingly.

The values of V_3 of the methyl group are determined to be 50.40 and 10.12 cm^{-1} with the cc-pVDZ and the 6-311G basis sets, respectively. While the potential cure obtained with the cc-pVDZ basis set shows a normal three-fold sinus function with negligible contribution of all higher-order terms, the potential curve with the 6-311G basis set shows a dominant V_6 contribution of 13.36 cm^{-1}.

In contrary to a three-fold or six-fold sinus diagram, the diagram obtaining with the B3LYP looks surprising for a methyl symmetric top. The barrier height $\Delta E = E_2 - E_1$ are found to be approximately 27 cm^{-1} and 10 cm^{-1} with the B3LYP/6-311G and B3LYP/cc-pVDZ basis sets, respectively. It is clearly seen that there are some local minima, e.g., at –40° or 40°, etc. The underlying reason might be that the methyl group is attached to a local frame which is not symmetric. One side of the methyl group is a nitrogen atom while the other side is a carbon atom. Each time one of the hydrogens of the methyl group is staggered to the nitrogen atom, it finds a local minimum. In the Fig. S-I in the Appendix, the geometry structures at local minima are also presented. The calculated data points are given in Table S-III in the Appendix AIV.2.

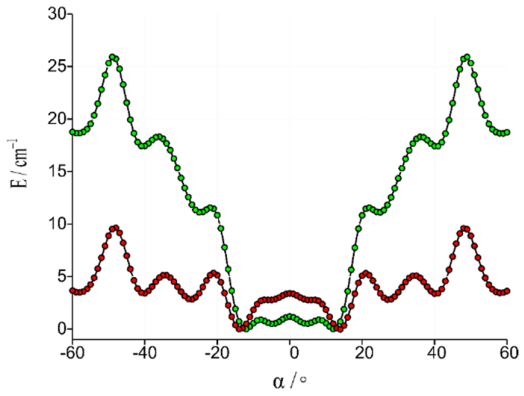

FIG. 3. Potential energy curves of 4-methylpyrrimidine (in cm^{-1}) obtained by varying the dihedral angle $\alpha = \angle(H_{11},C_7,C_4,N_3)$ in step of 1° while all other parameters were optimized at the B3LYP/cc-pVDZ (red dots) and the B3LYP/6-311G (green dots). The energies are transferred to cm^{-1} relative to the lowest energies.

It should also be mentioned that all input parameters are set in the default mode of GAMESS except the OPTTOL (gradient convergence tolerance) was set to 10^{-5}. More details in the input parameters of GAMESS are referred to GAMESS User's Guide - Input Description (spec.org).

C. ^{14}N nuclear quadrupole coupling constants

Using the molecular structure optimized at the MP2 level of theory at various basis sets, e.g., 6-31G, 6-311++G(d,p), cc-pVDZ, from which all planar structures were yielded as mentioned above, the calculation of the electric field gradient (EFG) at the B3PW91/6-311+G(d,p) level of theory was

performed. The calibration factor eQ/h = –4.5580 MHz/a.u. given by Bailey[15] was used to calculate the quadrupole coupling tensor. The results are summarized in Table III. Note that the χ_{ac} and χ_{bc} are 0 due to symmetry.

Table III. Nuclear quadrupole coupling constants (in MHz) of ^{14}N in 4MPY calculated at the B3PW91/6-311+G(d,p) level of theory while all other geometry parameters are optimized at various levels of theory.

	χ_{aa}	χ_{bb}	χ_{cc}	χ_{ab}
		Atom N_1		
B3PW91/6-311+G(d,p)//MP2/6-31G	–4.5930	1.6791	2.9139	–0.3854
B3PW91/6-311+G(d,p)// MP2/6-311++G(d,p)	–4.5975	1.5110	3.0865	–0.4670
B3PW91/6-311+G(d,p)// MP2/cc-pVDZ	–4.5081	1.5262	2.9819	–0.5033
		Atom N_3		
B3PW91/6-311+G(d,p)//MP2/6-31G	–0.0410	–2.7815	2.8225	2.8675
B3PW91/6-311+G(d,p)// MP2/6-311++G(d,p)	–0.1272	–2.8618	2.9890	2.7922
B3PW91/6-311+G(d,p)// MP2/cc-pVDZ	–0.0792	–2.8115	2.8907	2.7629

III. EXPERIMENTAL

A. Measurements

A pulsed supersonic jet Fourier transform microwave spectrometer in Aachen operating in the frequency from 2 to 26.5 GHz[16] was used to carry out the experimental data. The substance, commercially available 4-methylpyrimidine, was purchased from Sigma-Aldrich, Germany with a stated purity of over 97% and was used without any further purification. The substance was put in a small piece of pipe cleaner which is then kept at the nozzle exit. Helium was used as carried gas at the backing pressure of about 200 kPa. The mixture of about 1-2% substance with carried gas was flowed into the cavity. The supersonic jet is aligned coaxially with the resonator. Therefore, each rotational transition is split into two components due to the Doppler effect. The arithmetic mean of these two components is the rest frequency. The obtaining data in time domain was Fourier transformed to retrieved the spectrum. A GPS-disciplined rubidium frequency standard was used as reference of frequency measurement which is estimated to be better than 2 kHz.

B. Spectral assignment

At first, a broadband scan with a step width of 500 kHz was recorded in the frequency range from 10.0 to 14.3 GHz and was used to make the first torsional-rotation assignments in which the hyperfine structures were neglected. The spectrum of 4MPY was primarily assigned with the program *XIAM*[6]. Using the calculated molecular parameters, e.g., the rotational constants, the angles between the principal *a*-axis and the internal axis calculated at the MP2/cc-pVDZ level of theory, we first created a prediction for the A species only, using *XIAM* in its rigid mode. After trials and errors, some intense components of the A species for the $J'_{K'aK'c} \leftarrow J_{KaKc}$ transitions such as $4_{13} \leftarrow 3_{22}$, $3_{03} \leftarrow 2_{12}$, $2_{20} \leftarrow 2_{11}$, $5_{14} \leftarrow 5_{15}$, etc., were identified. The linear combinations of the rotational constants $B_K = A - 0.5(B + C)$, $B_J = 0.5(B + C)$, $B_- = 0.5(B - C)$ were fitted. Using those parameters, we were then able to identify all the A lines species in the broadband scan. After excluding from the survey spectrum all the already identified transitions, we started to search for E lines. A systematic series of predictions were performed using the rotational constants obtained from the fit of the A species alone, including values for the angles between the *a*-axis and the *i* internal axis $\angle(i,a)$ and with values of the potential V_3 varrying in step of 10 cm^{-1} ranging from 5-100 cm^{-1}. After some trials, we were able to identify some E components for the transitions $1_{10} \leftarrow 0_{00}$, $2_{12} \leftarrow 1_{01}$, $3_{22} \leftarrow 3_{13}$, $5_{23} \leftarrow 5_{14}$, etc. Regardless the hyperfine structure which we ignored at that stage in the 4MPY's spectrum, we put the assigned lines into a *XIAM* fit which yielded a *rms* of approximately 1.0 MHz. The molecular parameters from this fit enable us to find all lines left in the frequency range of our spectrometer.

IV. RESULTS AND DISCUSSIONS

A. Results of the fits

After the first step of assignment which was carried out using the *XIAM* program, separate fits for A and E species were then performed with the *WS18* code to analyze the complex spectra originating from two ^{14}N nuclei. It should be noted that some transitions spread out in the range of about 4 MHz in width and can contain up to 20 hyperfine patterns or even more. A closer look of the spectrum of 4MPY is presented in Fig. 4. Transitions with *J* up to 9 were measured. In total, 1299 lines we assigned 526 lines for A species and 773 lines for E species with a *rms* of 3.1 kHz and 2.4 kHz for each torsional species,

respectively. These satisfactory *rms* give us confidence that the assignments were correct. The resultant molecular parameters of the separate fits using *WS18* are summarized in Table IV.

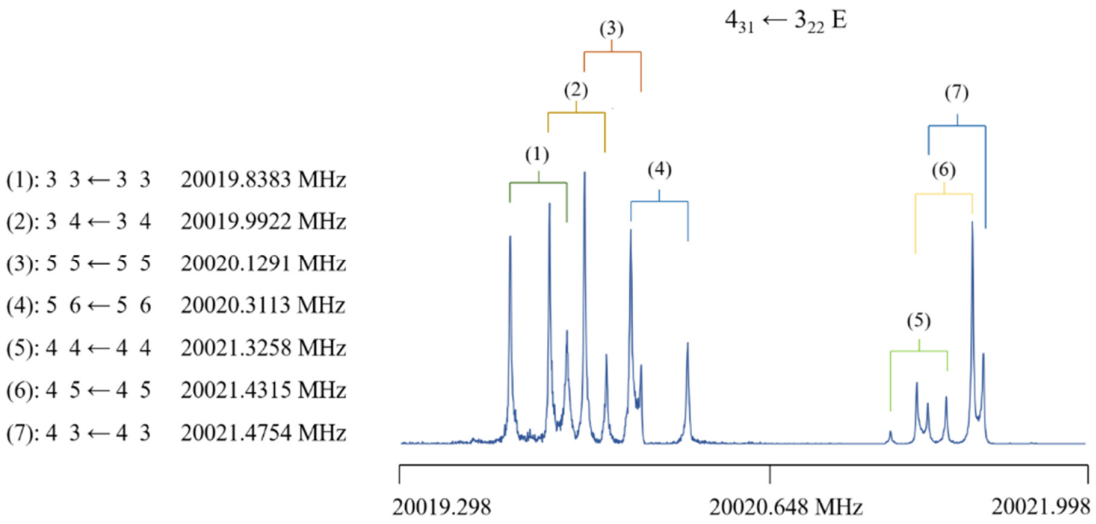

FIG. 4. The $4_{31} \leftarrow 3_{22}$ transition of the E species of 4MPY with its hyperfine components given as $F' F_1' \leftarrow F F_1$. The splittings indicated by brackets are due to Doppler effect.

Table IV: The obtained molecular parameters for 4MPY using the *WS18* fit for each separate A and E species.

Par.	Unit	A species	E species
A	MHz	6102.36526(12)	5996.58078(11)
B	MHz	2646.372443(47)	2646.324622(42)
C	MHz	1860.577539(39)	1860.674918(35)
Δ_J	kHz	0.13900(80)	0.1401(68)
Δ_{JK}	kHz	0.3025(31)	0.4389(35)
Δ_K	kHz	29.534(18)	–9.744(18)
δ_J	kHz	0.4425(16)	0.04486(28)
δ_K	kHz	0.1932(23)	–0.3601(50)
r	MHz	-	12.1788(89)
q	GHz	-	1.7591801(24)
q_K	MHz	-	–2.102646(83)
q_J	kHz	-	0.5326(62)
q_{KK}	kHz	-	0.9220(70)
$\chi_{aa}(N_1)$	MHz	–4.57904(62)	–4.57945(43)
$\chi_{bb}-\chi_{cc}(N_1)$	MHz	–1.7869(13)	–1.7856(12)
$\chi_{aa}(N_3)$	MHz	–0.20747(88)	–0.20419(77)
$\chi_{bb}-\chi_{cc}(N_3)$	MHz	–5.9876(12)	–5.9817(15)
$\chi_{ab}(N_3)$	MHz	-	–2.13(20)
N		526	773
rms	kHz	3.0	2.4

[a] All parameters refer to the principal axis system. Watson's A reduction and I^r representation were used. Single standard errors in the unit of the last digits are given in parentheses.

[b] Number of hyperfine components.

[c] Root-mean-square deviation of the fit.

We note that all parameters in the separate fits (see Table IV) are effective and do not represent the real (geometry) parameters. Consequently, the whole data set (except three lines which showed relatively large observed-calculated residuals) were refitted using the two codes *TW21* and *BELGI-2N* resulting in *rms* of 2.7 kHz and 3.8 kHz, respectively. The molecular parameters obtained from the global fits are presented in Table V. The frequencies are given in Table S-IV.

Table V. Molecular parameters of 4MPY in RAM obtained from fits with *TW21* as well as *BELGI-2N* programs.

Par.[a]	Unit	Operator	*TW21*	*BELGI*
$A_1 = A + F\rho^2$	MHz	$\mathbf{P_z^2}$	6268.2570(40)	-
A	MHz	$\mathbf{P_z^2}$	6031.176(24)[b]	6031.1780(56)
B	MHz	$\mathbf{P_x^2}$	2646.727(40)	2646.7295(57)
C	MHz	$\mathbf{P_y^2}$	1860.521(40)	1860.5227(56)
D_{ab}	GHz	$\mathbf{\{P_z, P_y\}}$	0.023157(19)	0.023164(26)
$R = -2F\rho$	GHz	$\mathbf{P_\alpha P_z}$	–12.446231(10)	-
ρ	unitless		0.0380968(10)[b]	0.0380968(43)
F_0	GHz		157[c]	-
F	GHz	$\mathbf{P_\alpha^2}$	164.3500[b]	164.3500[c]
V_3	cm^{-1}	$(1/2)(\mathbf{1-\cos 3\alpha})$	94.390920(19)	94.391728(53)
Δ_J	kHz	$\mathbf{-P^4}$	0.14026(70)	0.14029(99)
Δ_{JK}	kHz	$\mathbf{-P^2P_z^2}$	0.2976(31)	0.2980(44)
Δ_K	kHz	$\mathbf{-P_z^4}$	0.876(17)	0.868(24)
δ_J	kHz	$\mathbf{-2P^2(P_z^2 - P_x^2)}$	0.04443(18)	0.04434(26)
δ_K	kHz	$\mathbf{-\{P_z^2, (P_z^2 - P_x^2)\}}$	0.4192(29)	0.4212(40)
G_v	MHz	$\mathbf{P^2P_\alpha^2}$	0.02187(55)	0.02161(77)
F_v	MHz	$\mathbf{(1-\cos 3\alpha)P^2}$	–0.2912(73)	–0.295(10)
c_2	MHz	$\mathbf{(1-\cos 3\alpha)(P_y^2 - P_x^2)}$	–0.14712(36)	–0.14744(51)
χ_{aa} (N_1)	MHz		–4.57958(49)	–4.5802(20)
$\chi_{bb} - \chi_{cc}$ (N_1)	MHz		–1.7866(12)	–1.7686(74)
χ_{aa} (N_3)	MHz		–0.2366(39)	–0.2420(55)
$\chi_{bb} - \chi_{cc}$ (N_3)	MHz		–5.9552(38)	–5.951(64)
χ_{ab} (N_3)	MHz		2.30(27)	2.49(37)
N[d]			1296	1296
rms[e]	kHz		2.7	3.8

[a] All parameters are referred to the rho-axis-system. Statistical uncertainties are given as one standard uncertainty in the last digit. Watson's A reduction and I^r representation were used. $\mathbf{P_x, P_y, P_z}$ are the components of the overall rotation angular momentum, $\mathbf{P_\alpha}$ is the angular momentum conjugate to the internal rotation angle α. {u, v} is the anti-commutator uv + vu.

[b] Derived parameters.

[c] Fixed parameters.

[d] Number of lines.

[e] Root-mean-square of the fits.

Because the *TW21* and *BELGI-2N* codes both employed the rho-axis-system, the parameters can be directly compared to each other. We can see that all the parameters are in excellent agreement. For a better understanding of their physical meaning, some of the parameters are converted to the principal axis system. The results are given in Table VI, the experimentally derived values are given along with their calculated values from *ab initio* at MP2/cc-pVDZ level of theory.

Table VI. Molecular parameters of 4MPY in the principal axis system obtained from the fits with the *TW21* as well as the *BELGI-2N* programs given along with *ab initio* calculated values at the MP2/cc-pVDZ level of theory.

Par.[a]	Unit	*TW21*	*BELGI*	*Ab initio*
A	MHz	6031.334(24)	6031.3365(56)	5970.4
B	MHz	2646.5688(40)	2646.5709(57)	2612.6
C	MHz	1860.5208(40)	1860.5227(56)	1838.3
F_0	MHz	157[b]	-	157
$\angle(i,a)$	°	179.10671(72)	179.1064(10)	179.62
V_3	cm^{-1}	94.390920(19)	94.391728(99)	50.34
		N_1		
χ_{aa}	MHz	–4.57917(48)	–4.5800(20)	–4.5081
χ_{bb}	MHz	1.3961(12)	1.4056(27)	1.5262
χ_{cc}	MHz	3.1830(12)	3.096(11)	2.9819
χ_{ab}	MHz	-	-	–0.5033
		N_3		
χ_{aa}	MHz	–0.2052(53)	–0.2080(75)	–0.0792
χ_{bb}	MHz	–2.8907(52)	–2.8884(74)	–2.8115
χ_{cc}	MHz	3.0960(37)	3.0960(37)	2.8907
χ_{ab}	MHz	2.28(26)	2.47(37)	2.7629
N		1296	1296	
rms	kHz	2.7	3.8	

[a] All parameters are referred to the inertial principal axis system. Statistical uncertainties are given as one standard uncertainty in the last digit. Watson's A reduction was used.

[b] Fixed to the calculated value at the MP2/cc-pVDZ level of theory.

B. Discussions

1. Geometry parameters

Results on rotational constants *A*, *B*, *C* obtained from the two fits *TW21* as well as *BELGI-2N* are in very good agreement. The most-time consuming calculation carried out at the MP2/6-311++G(d,p) level of theory gives the most satisfactory results. All other calculations underestimated the value of *A*, *B*, *C* and in case of 4MPY, we can observe a trend that the bigger the basis set, the closer the predicted rotational constants.

Moran et al.[17] reported that non-planar equilibrium structures had been found for benzene and arenes[17]. They also reported that diffuse functions on hydrogen (denoted by ++ augmentation) are problematic for this issue. For example, in their calculation, a basis set with diffuse function only on the heavy atom, e.g., 6-311+G(d,p) leads to smoothly planar equilibrium structure, whereas a basis set with diffuse function on both, heavy atom and hydrogen atom, e.g., 6-311++G(d,p) leads to non-planar structure. This is however not the case for 4MPY since the results used MP2/6-311++G(d,p) are essentially the same as MP2/6-311+G(d,p). And this is also true with the B3LYP method. However, for 4MPY, the method seems to play a crucial role as the results from all the B3LYP calculations yielded non-planar conformers while planar equilibrium structure is dominantly found using MP2 method.

2. Nuclear quadrupole coupling constants

In general, all the calculated values at different levels of theory yielded results in good agreement with the experimental ones. The results from MP2/6-311++G(d,p) are slightly closer to experimental values compared to others.

The nuclear quadrupole coupling hyperfine constants deduced from the fits with *TW21*, *BELGI-2N* and their calculated values at MP2/cc-pVDZ//B3PW91/6-311++G(d,p) model are summarized in Table VI. An exceptional large deviation is found for the χ_{aa} component of atom N_3. A similar observation on χ_{aa} for atom N_{15} of 2-nitrobenzenitrile was reported by *Graneek et al.*[18]. The remaining components of the nuclear quadrupole hyperfine tensor are in good agreement with the calculated ones (in their absolute values).

If the inertial principal *a*- or *b*-axis would align with the nuclear coupling tensor, the value of χ_{ab} would vanish since it is associated with the expectation value of $\{P_a, P_b\}$. Also, as we saw in the previous chapters, when the barrier to internal rotation is high, χ_{ab} cannot be deduced experimentally. In the case of 4MPY, we were able to determine from the experimental data the value of χ_{ab} for the N_3 atom. However, the signs of χ_{ab} are not consistent. The obtained values from *TW21* and *BELGI-2N* code (Table VI) are both positive while the *WS18* code results in a negative value (Table V).

Spoerel et al.[19] reported that whereas the spectral analysis only provides the magnitude of the single tensor element, it does allow us to determine the sign of the product $\chi_{ab}\chi_{bc}\chi_{ac}$. The authors also pointed out that the signs of the single tensor elements do change when the inertia principal axis system is rotated. That means it is only possible to determine the sign of each off-diagonal term alone when the orientation of the molecule in fix-space is known. For example, if one changes the value of $\angle(i,a)$ to $\angle(i,a) \mp 180°$ in the *XIAM* input, the *rms* and values of all parameters will stay unchanged, except the χ_{ab} will have opposite sign. In case of *WS18* code, changing the signs of *q* or *r* will also lead to the changes in sign of χ_{ab}. This is a great advantage when an off-diagonal term in the nuclear quadrupole coupling tensor is determined since by comparing the experimentally deduced with the calculated one, we can know exactly the orientation of the molecule in our theoretical fits. In our case, obviously the orientations in the fix-space of the 4MPY in the *WS18* fit is different compared to the ones in the *TW21* as well as in *BELGI-2N*.

3. Torsional barrier of the methyl group

The value of the V_3 potential to the methyl internal rotation deduced experimentally is accurately determined to be 94.390920(19) and 94.391728(99) cm^{-1} with *TW21* and *BELGI* codes, respectively. Those values are in excellent agreement as expected since the two codes employed the same coordinate system, use the same data set and float the same set of parameters. The values of potential barrier obtained from quantum chemical calculations range from 5 to 50 cm^{-1} which is by factor of 2 to 20 times different with respect to the experimental value. With such a relatively low barrier, initial spectral

assignments were quite challenging. In case of 4MPY, the result of calculation at MP2/cc-pVDZ level of theory is still in the closest with the experimental deduced value.

In Fig. 5, the determined value of torsional barrier to methyl internal rotation of 4MPY (**2**) is compared with two other isomers of pyrimidine 2-methylpyrrimidine[9] (**1**) and 5-methylpyrimidine[10] (**3**).

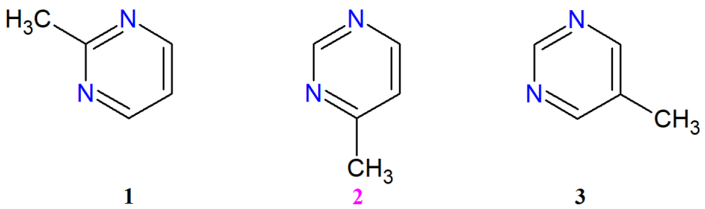

	1	**2**	**3**
V_3 / cm^{-1}	-	94.39	-
V_6 / cm^{-1}	1.56	-	4.09

FIG. 5. Barrier to methyl internal rotation of mono-methylated pyrimidine derivatives: (**1**) 2-methylpyrimidine[9], (**2**) 4-methylpyrimidine (present study), (**3**) 5-methylpyrimidine[10].

The barrier of the methyl group strongly depends on the position where the methyl group is attached to the ring. Similar to what we already mentioned in the discussion sections of the 2-methylpyrrole and 3-methylpyrrole molecules (Chapter II.2 and II.3, respectively), if a methyl group is attached to a symmetric molecular frame, it will result in a V_6 potential, as observed in e.g., 2-methylpyrimidine[9] and 5-methylpyrimidine[10]. In cases a methyl group is attached to an asymmetric frame symmetry, a V_3 potential is found as for 4MPY. However, lower barriers are in general observed for methylated pyrimidine (six-membered rings) compared to methylated pyrrole (five-membered rings).

4. Performance of the new code TW21

While *XIAM* fixed $v_{t_{max}}$ at 0 in the second step diagonalization, *BELGI*[20] and *RAM36*[8] codes fixed $v_{t_{max}}$ at 8. This choice affects the computational time of each code as in the second step where we need to diagonalize the Hamiltonian matrix with a size of $(2J+1)\cdot(v_{t_{max}}+1)$. The larger the matrix's size, the more computational time is required. Moreover, as reported by *Ferres et al.*[18] (*i*) the *XIAM*

program allows a limited number of fitted parameters and (*ii*) it neglects the interactions among v_t states. This finally raised the question whether or not the implementation of more higher order terms beyond the rigid frame – rigid top model would be sufficient to model the spectra of molecules exhibiting internal rotation with the *XIAM* program and decrease the root-mean-square deviation, or if the truncation to v_{tmax} at 0 in the second step diagonalization also plays a role. *Ferres et al.* also pointed out, that the deviations with *aixPAM* code[21] (which uses a direct diagonalization in one step) are just 4 kHz different from *XIAM*, indicating that the matrices' truncations do not have a significant effect on the accuracy of the fit. To quantitatively determine which value of $v_{t_{max}}$ is suitable to give the best computational time but also to offer enough accuracy (close to experimental one), we decided to make the value of $v_{t_{max}}$ accessible via the input, thereby the users can selectively choose the size of the matrices.

In the Fig. 6, the computational time per fit cycle in second is depicted as function of v_{max} (left side) and in the right-hand side, the *rms* in kHz of the fit is plotted as function of v_{max} for the case of 4MPY. This test is similar to the ones already performed for 2MTA and 3MP in Chapter IV.1. It should be mentioned that the same set of data and the same set of parameters were used in all fits. All fits were performed using the PC Intel® Core™ i7-8565U CPU @ 1.8GHz, 2001 MHz, 4 cores, k_{max} (the truncation of the first diagonalization step) is kept fixed at 10.

Clearly, $v_{t_{max}} = 0$ does not offer enough accuracy whereas $v_{t_{max}} = 8$ requires too much time than the actual need. For the case of our fitted microwave dataset for the 4MPY molecule, $v_{t_{max}} = 1$ is the best choice for the compromise between speed and *rms*. The truncation of the matrix made a difference of about 4 kHz, which is the same effect reported by *Ferres et al.*[21]. This effect may vary depending on the investigated molecules and the dataset involved. It should also be mentioned that the value of k_{max} is kept fixed at 10 in *BELGI* whereas it is changeable via input with *XIAM* program and *TW21*. The choice of k_{max} plays a minor role in the speed of the program as the size of the matrix is $(2k_{max} + 1)$ and the cut off at $k_{max} = 8$ is normally sufficient in most cases.

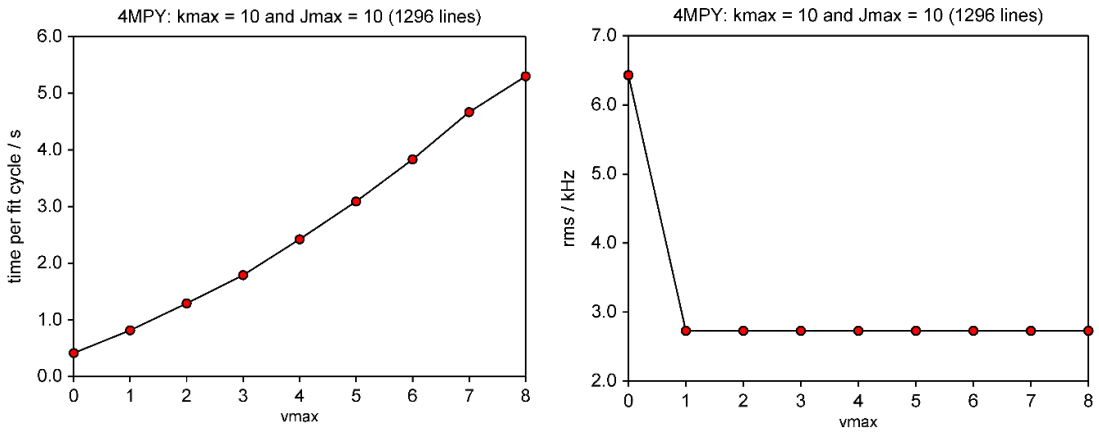

FIG. 6. Left side: The diagram of the time computational require per fit cycle (s) as function of $v_{t_{max}}$. Right side: The diagram of the *rms* given in kHz as a function of $v_{t_{max}}$.

V. CONCLUSION

In this study, we successfully assigned the rotational spectrum of 4-methylpyrimidine recorded under molecular jet conditions with the complementary from quantum chemical calculations. Within the scope of this work, both local and global approaches were developed and employed to fit within experimental accuracy of a few kHz the complex spectra originating from the combination of one internal rotation together with two weakly nuclear quadrupoles coupling. The molecular parameters achieved with high accuracy using the *WS18*, *TW21* as well as *BELGI-2N* codes provide useful information for further study on 4-methylpyrimidine. The sign of the off-diagonal nuclear quadrupole coupling tensor are discussed.

APPENDIX

See the Appendix section AIV.2 for nuclear coordinates of 4MPY at various levels of theory (Table S-I), the Fourier coefficient of potential energy curve in Fig.2 (Table S-II), the potential curves together with illustrations of the geometry optimizations at the minima Fig. S-I, the calculated data points for potential energy curves at the 6-311G level of theory using MP2 and B3LYP method (Table S-III) and the frequency list in Table S-IV.

REFERENCES

[1]J.L. Alonso, I. Pena, J.C. Lopez, V. Vaquero, *Angew. Chem. Int. Ed.* **48,** 6141 (2009).

[2]J.L. Alonso, V. Vaquero, I. Peña, J. C. López, S. Mata, W. Caminati, *Angew. Chem. Int. Ed.* **52**, 2331 (2013).

[3]L.B. Favero, I. Uriarte, L. Spada, P. Ecija, C. Calabrese, W. Caminati, E. J. Cocinero, *J. Phys. Chem. Lett.* **7**, 1187 (2016).

[4]V. Van, W. Stahl, A.R. Philipps, H.V.L. Nguyen, The internal rotation of four methyl groups in Tetramethylthiophene, *HRMS*, *24th Colloquium*, Dijon, France, 24-28 Aug (2015).

[5] H. Pickett, *J. Mol. Spectros.* **148**, 371 (1991). See also http://spec.jpl.nasa.gov/ for downloading and instruction of the program.

[6]H. Hartwig, H. Dreizler, *Z. Naturforsch.* **51a**, 923 (1996).

[7]R. Kannengießß, W. Stahl, H. V. L. Nguyen, I. Kleiner, *J. Phys. Chem. A* **120**, 3992 (2016).

[8]V. V. Ilyushin, Z. Kisiel, L. Pszczólkowski, H. Mäder, J. T. Hougen, *J. Mol. Spectrosc.* **259**, 26 (2010).

[9]W. Caminati, G. Cazzoli, D. Troiano, *Chem. Phys. Letters.* **43**, 65 (1976).

[10]W. Caminati, G. Cazzoli, A.M. Mirri, *Chem. Phys. Letters.* **31**, 104 (1975).

[11]E. Gougoula, C. Medcraft, M. Heitkämper, N. R. Walker, *J. Chem. Phys.* **151**, 144301 (2019).

[12]M.W. Schmidt, K.K. Baldridge, J.A. Boatz, S.T. Elbert, M.S. Gordon, J.H. Jensen, S. Koseki, N. Matsunaga, K.A. Nguyen, S.J. Su, T.L. Windus, M. Dupuis, J.A. Montgomery, *J. Comput. Chem.* **14**, 1347 (1993).

[13]C.T. Lee, W.T. Yang, R.G. Paar, *Phys. Rev. B.* **37**, 785 (1988).

[14]C. Møller, M.S. Plesset, *Phys. Rev.* **46**, 618 (1934).

[15]W.C. Bailey, http://nqcc.wcbailey.net/.

[16]J.-U. Grabow, W. Stahl, H. Dreizler, *Rev. Sci. Instrum.* **67**, 4072 (1996).

[17]D. Moran, A.C. Simmonett, F. E. Leach, W.D. Allen, P v.R. Scheleyer, H.F. Schaefer, *J. Am. Chem. Soc.***128**, 29 (2006).

[18]J.B. Graneek, W.C. Bailey, M. Schnell, *Phys. Chem. Chem. Phys.* **20**, 22210 (2018).

[19]U. Spoerel, H. Dreiler, W. Stahl, *Z. Naturforsch.* **49a**, 645-646 (1994).

[20]J.T. Hougen, I. Kleiner, M. Godefroid, *J. Mol. Spectrosc.* **163**, 559 (1994).

[21]L. Ferres, W. Stahl, H.V.L. Nguyen, *J. Chem. Phys.* **148**, 124304 (2018).

CONCLUSION

Using the combination of molecular jet Fourier transform microwave spectroscopy, quantum chemical calculations and spectral modelling, in total six nitrogen containing aromatic rings which are 2-methylpyrrole (2MP), 3-methylpyrrole (3MP), 2-methylthiazole (2MTA), 2,5-dimethylpyrrole (25DMP), 4,5-dimethylthiazole (45DMTA), 4-methylpyrimidine (4MPY), were investigated within this thesis. The targeted molecules show internal rotation(s) in the presence of one or two weakly quadrupole hyperfine couplings arising from ^{14}N nuclei. Geometry parameters, e.g., rotational constants, centrifugal distortion constants, nuclear quadrupole constants, etc., as well as dynamic parameters such as barrier to internal rotation(s) are determined with high accuracy. They are used as benchmark for quantum chemical calculations. They can also be served as an excellent starting point for further spectroscopic investigations in the gas phase in other spectral domain (millimeter-wave, sub-millimeter-wave, terahertz, far-infrared or infrared) and finally they are of good use for astrophysical search.

Quantum chemical calculations were performed at various levels of theory, the results show that with sufficient large basis set, the geometry parameters (the rotational constants A, B, C) can be predicted within 2% deviations from the experimentally derived constants and thus serving as a good tool for guiding the spectral assignments. In addition, our work showed that predicting the barrier to internal rotation of V_3 remains challenging. The calculated barriers to internal rotation(s) with deviations of about 10% from the experimental values are usually found. The 2D potential energy surface(s) is a good tool to study possible coupling in case there are several internal rotations undergoing within the molecule(s). Finally, the Bailey's method still proved its predictive power in calculating the nuclear quadrupole coupling. Usually, the predicted nuclear quadrupole coupling constants are in excellent agreement with the experimental deduced ones, easing the spectral assignment process.

The rotational transitions can be analyzed for each symmetry species separately ("local" approach) using the *WS18* code. In difficult cases, such as high barrier in combination with hyperfine coupling (as found in our present work with the 25DMP molecule, Chapter III.1), the hyperfine patterns overlap with the torsional splittings, it is an excellent tool for assigning spectra. Generally, the *WS18* code is useful in all cases since it will help us to make sure that the assignment is correct before going on with the fitting

process. The microwave spectra of all the studied molecules were fitted using the so-called "global" approach, implemented in the *XIAM* and the *BELGI*-family codes and the results are compared. Often the *BELGI*-family code shows great advantages over *XIAM* code in reducing the *rms* deviations. In cases of low barrier such as 2MTA (Chapter II.1) or 45DMTA (Chapter III.2), a factor of about 200 times improvement is found. Nevertheless, the *XIAM* approach is extremely fast because it neglects interactions between torsional v_t states whereas the *BELGI* codes which takes into account the first nine torsional states, showing a slower computational speed, especially for molecule with two tops and when transitions with high *J* values involved.

Prior to this work, it remains unclear whether the interactions among v_t states play a major role in reducing the *rms* deviations or if this advantage was mostly due to the lack of higher-order torsion-rotation terms missing in *XIAM* or both effects contribute significant influences. Within the course of this thesis, a new code *TW21* was written and tested for 2MTA, 2MP, 3MP molecules. Then we applied to fit the microwave spectrum of the 4MPY. The obtaining results prove that including the interactions between different v_t states have a minor effect on substantially decreasing the *rms* whereas the effect of adding additional rotation-torsion terms play a major role. That explains why *BELGI* succeeded to model the microwave spectra of molecules with low barriers while *XIAM* often experiences difficulties. Also, the *TW21* code enables to find out which value of $v_{t_{max}}$ is the best suited for a given molecule and dataset, allowing to fit with enough accuracy at the least of time requirement. The flexibility for users being able to choose $v_{t_{max}}$ and k_{max} should also be applied for programs in future, especially for programs with deal with multiple internal rotations in a molecule, which require large matrix to be diagonalized.

For the first time, the combination of one internal rotation and two weakly nuclear quadrupoles coupling of ^{14}N nuclei has been successfully modelled using both, local (*WS18*) and global approaches (*BELGI-2N*, *TW21*). The developments of those codes will allow future investigations on similar compounds and provide proper tools for fitting processes. And therefore, they will allow for deeper understanding about the molecular geometry, the internal dynamics as well as the chemical bonds at the sites of ^{14}N nuclei in those molecules.

The results obtaining from my thesis investigations were compared with other compounds already studied in the literature, demonstrating the trend of an increasing internal rotation barrier for compounds with the same ring but with diffirent skeleton atom substituted by S, N, and O. The steric effects as well as the electronic distribution within the ring also play important role in the resulting barrier height. By studying the electronic configurations within those studied rings, the nuclear quadrupole coupling constants along the *c*-direction of the inertial principal axis are classified into two classes, one with positive signs and the other with negative signs.

Those results extend the understanding about nitrogen containing aromatic rings, especially five-membered rings and they satisfy our aims which was to provide accurate molecular parameters for investigated systems, as well as to produce line lists with high accuracy. Our theoretical models and codes dealing with internal rotation and hyperfine structure were successful in assigning and fitting within experimental accuracy the observed frequencies. In turn, this allowed us to understand which effects play an important role in the resulting barrier height for each molecule. Nevertheless, no rule for predicting the barrier(s) to internal rotation of five- and six-membered heterocyclics has been found yet. To facilitate this finding, future investigations are necessary. We suggest future investigations on those following rings (see Fig. 1).

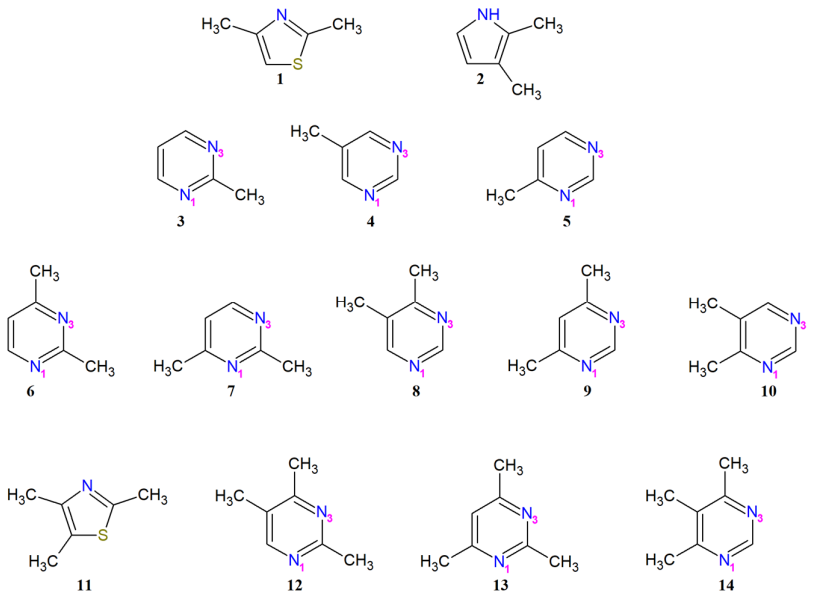

FIG. 1. Suggested molecules for future investigations: (**1**) 2,4-dimethylthiazole, (**2**) 2,3-dimethylpyrrole, (**3**) 2-methylpyrimidine, (**4**) 5-methylpyrimidine, (**5**) 6-methylpyrimidine, (**6**) 2,4-dimethylpyrimidine, (**7**) 2,6-

dimethylpyrimidine, (**8**) 4,5-dimethylpyrimidine, (**9**) 4,6-dimethylpyrimidine, (**10**) 5,6-dimethylpyrimidine, (**11**) 2,4,5-trimethylthiazole, (**12**) 2,4,5-trimethylpyrimidine, (**13**) 2,4,6-trimethylpyrimidine, (**14**) 4,5,6-trimethylpyrimidine.

The suggested investigations (**1**, **2**, **11**) will further extend the knowledge in five-membered systems connecting with the current thesis, direct comparison can be made and therefore possibly confirming further the steric and electronic effects on the obtaining V_3 values. Our thesis has also opened the door for studying other molecules, with one internal rotor and two ^{14}N nuclei (**3**, **4**, **5**), belonging to the same family as 4MPY. Those intensive investigations (if successful) will systematically enhance our understanding on which effects play major roles on that family. All of them will enlarge the data base for nuclear quadrupole coupling constants, thus provide chance to calculate more accurately the constants *eqQ*. Coupled large amplitude motions of two (**6**, **7**, **8**, **9**, **10**) or three internal rotors (**12**, **13**, **14**) can also be investigated but will have to rely intensively on the development of internal rotation theoretical models and codes which will require new appropriate Hamiltonian and therefore, pushing the edge of our knowledge.

APPENDIX

AII.1: The microwave spectrum of 2-methylthiazole: ^{14}N nuclear quadrupole coupling and methyl internal rotation

Table S-I: Nuclear coordinates in the principal inertial axes of 2-methylthiazole calculated with the B3LYP, HF, and MP2 methods at the Pople 6-311++G(d,p) basis set. The atoms are numbered according to Figure 1.

	B3LYP/6–311++G(d,p) α = 60°			HF/6–311++G(d,p) α = 60°		
	a / Å	*b* / Å	*c* / Å	*a* / Å	*b* / Å	*c* / Å
S_1	–0.288279	–1.172143	–0.000011	–0.281745	–1.160566	0.000028
C_2	0.798117	0.217711	–0.000403	0.784628	0.216808	0.000081
N_3	0.180925	1.360727	–0.000172	0.183843	1.341032	0.000104
C_4	–1.186462	1.201717	0.000191	–1.185884	1.184283	–0.000058
C_5	–1.637067	–0.081920	0.000067	–1.631219	–0.077971	–0.000064
C_6	2.286042	0.054797	0.000167	2.275377	0.060646	–0.000103
H_7	2.742154	1.044748	–0.004154	2.725824	1.043741	–0.001139
H_8	2.629003	–0.485883	0.886631	2.607070	–0.481881	0.879018
H_9	2.629319	–0.494931	–0.880455	2.607039	–0.483658	–0.878158
H_{10}	–1.818751	2.079220	0.000277	–1.806431	2.058689	–0.000154
H_{11}	–2.653536	–0.442641	0.000168	–2.642053	–0.428316	–0.000194
	MP2/6–311++G(d,p) α = 32.9°			MP2/6–311++G(d,p) α = 60°		
	a / Å	*b* / Å	*c* / Å	*a* / Å	*b* / Å	*c* / Å
S_1	–0.274723	–1.161612	–0.004888	–0.275444	–1.162162	–0.000207
C_2	0.786409	0.208399	–0.020977	0.787212	0.207969	–0.001211
N_3	0.166292	1.370398	–0.012000	0.166618	1.370251	–0.000568
C_4	–1.192110	1.195334	0.006625	–1.192174	1.195750	0.000378
C_5	–1.623929	–0.111788	0.015632	–1.624376	–0.110638	0.000669
C_6	2.275216	0.062395	0.016710	2.276449	0.062443	0.000868
H_7	2.723795	0.931983	–0.466533	2.712115	1.062473	–0.009412
H_8	2.634934	0.017695	1.048955	2.625473	–0.465265	0.892742
H_9	2.603916	–0.841668	–0.501231	2.626575	–0.484323	–0.878957
H_{10}	–1.843499	2.061020	0.008521	–1.844444	2.060739	0.000595
H_{11}	–2.638546	–0.484945	0.017879	–2.638924	–0.484147	0.001123

Table S-II: Data points of the potential energy curves for the methyl torsion of 2-methylthiazole given in Figure 2 obtained by varying the dihedral angle $\alpha = \angle(S_1,C_2,C_6,H_9)$ in a grid of 10° (2° around stationary points) while all other molecular parameters were optimized at the B3LYP/6-311++G(d,p), HF/6-311++G(d,p), and MP2(ae)/6-311++G(d,p) levels of theory. The energy values are given in Hartree.

α	B3LYP	HF	MP2(ae)
0	–608.453587567	–606.405615457	–607.49677112582
2	–608.453588521	–606.405617394	–607.49677230800
10	–608.453610984	–606.405662330	–607.49679865699
20	–608.453670474	–606.405783897	–607.49685884350
30	–608.453738656	–606.405933817	–607.49690178821
40	–608.453791533	–606.406063786	–607.49688881270
50	–608.453819258	–606.406145213	–607.49682922387
58	–608.453826686	–606.406170894	–607.49679214460
60	–608.453827254	–606.406171821	–607.49678871527
62	–608.453826818	–606.406170968	–607.49679042611
70	–608.453819982	–606.406145661	–607.49682300076
80	–608.453793408	–606.406064977	–607.49688498172
90	–608.453741612	–606.405936246	–607.49690342797
100	–608.453673913	–606.405787896	–607.49686278687
110	–608.453613709	–606.405666381	–607.49680164066
118	–608.453589265	–606.405618422	–607.49677260602
120	–608.453587631	–606.405615566	–607.49677119167
122	–608.453587897	–606.405616206	–607.49677180072
130	–608.453607376	–606.405655074	–607.49679647026
140	–608.453664732	–606.405770761	–607.49685681612
150	–608.453733467	–606.405920341	–607.49690121305
160	–608.453789149	–606.406055797	–607.49688920898
170	–608.453818922	–606.406143093	–607.49682810491
178	–608.453826651	–606.406170803	–607.49679120603
180	–608.453827055	–606.406172018	–607.49678947405
182	–608.453826671	–606.406170753	–607.49679122408
190	–608.453818895	–606.406143092	–607.49682837210
200	–608.453789110	–606.406055795	–607.49688957066
210	–608.453733422	–606.405920327	–607.49690156282
220	–608.453664504	–606.405770483	–607.49685655474
230	–608.453607314	–606.405655049	–607.49679646986
238	–608.453587830	–606.405616194	–607.49677168640
240	–608.453587539	–606.405615562	–607.49677115770
242	–608.453589129	–606.405618585	–607.49677303627
250	–608.453613660	–606.405666367	–607.49680158794
260	–608.453673860	–606.405787887	–607.49686306132

270	–608.453741552	–606.405936241	–607.49690335858
280	–608.453793347	–606.406064971	–607.49688500769
290	–608.453819903	–606.406145631	–607.49682288952
298	–608.453826792	–606.406170970	–607.49679033045
300	–608.453826955	–606.406171910	–607.49678957105
302	–608.453826914	–606.406170730	–607.49679218123
310	–608.453819244	–606.406145187	–607.49682917542
320	–608.453791570	–606.406063838	–607.49688910038
330	–608.453738702	–606.405933893	–607.49690175185
340	–608.453670528	–606.405783969	–607.49685881550
350	–608.453611037	–606.405662378	–607.49679864685
358	–608.453588494	–606.405617303	–607.49677219293
360	–608.453587567	–606.405615457	–607.49677112582

Table S-III: Observed frequencies ($\nu_{obs.}$) of the A and E species of 2-methylthiazole. $\nu_{calc.}$ are the calculated frequencies; $\nu_{obs.}-\nu_{calc.}$ values as obtained after a fit with the program *XIAM* and *BELGI-C_1-hyperfine*. J, K_a, K_c are the asymmetric top rotational quantum numbers of the lower energy level; J', K_a', K_c' are those of the upper energy level. F is the total angular momentum in the coupled basis with $F = J + I$.

$J'K_a'K_c'F'$	J K_a K_c F	Sym	$\nu_{obs.}$	$\nu_{obs.} - \nu_{calc.}$	$\nu_{obs.} - \nu_{calc.}$
Upper level	Lower level		GHz	*BELGI*/MHz	*XIAM*/MHz
1 1 1 2	0 0 0 1	A	7.542783	0.000	–0.0145
0	1	A	7.544099	–0.002	0.0298
1	1	A	7.541904	–0.000	–0.0457
2 0 2 3	1 1 1 2	A	8.036110	–0.006	–0.1354
1	0	A	8.033915	–0.000	–0.1891
2	1	A	8.035829	–0.001	–0.0769
2 1 2 2	1 0 1 2	A	11.646717	0.001	–0.0368
3	2	A	11.647483	–0.001	–0.0378
1	1	A	11.647749	–0.000	–0.0660
2	1	A	11.646554	–0.000	–0.0679
1	0	A	11.648153	–0.001	0.0082
2 2 0 2	1 1 1 2	A	20.114700	0.001	–0.1159
3	2	A	20.114515	–0.003	–0.0967
1	1	A	20.115294	–0.002	–0.0520
2	1	A	20.115582	0.004	–0.0817
1	0	A	20.113100	0.001	–0.1266
2 2 1 3	1 1 0 2	A	18.523204	0.004	–0.0351
1	1	A	18.522581	0.002	–0.0208
2	1	A	18.522313	0.004	–0.0689
1	0	A	18.524372	0.001	–0.0194
2 2 0 1	2 1 1 2	A	7.048960	0.000	0.0576

			2				3	A	7.050185	0.002	0.0566
			3				3	A	7.050008	0.006	0.0839
			2				2	A	7.049245	0.004	0.0250
			1				1	A	7.050426	0.002	0.1107
2	2	1	1	2	1	2	2	A	10.314465	0.001	0.0265
			2				3	A	10.313429	0.002	–0.0226
			3				2	A	10.314376	0.008	0.0161
			3				3	A	10.313604	0.004	0.0111
			2				2	A	10.314197	0.002	–0.0216
			1				1	A	10.313271	0.002	0.0257
3	1	2	4	3	0	3	4	A	7.883331	0.000	–0.1160
			3				3	A	7.884768	–0.001	–0.0927
			2				2	A	7.882827	–0.001	–0.1252
3	1	3	4	2	0	2	3	A	15.314391	0.000	–0.0530
			3				2	A	15.313724	0.000	–0.0713
			2				1	A	15.314585	–0.002	–0.0442
			2				2	A	15.314868	–0.001	–0.0788
			3				3	A	15.313550	0.007	–0.0410
3	0	3	4	2	1	2	3	A	13.247979	–0.003	–0.1436
			3				2	A	13.248176	–0.002	–0.1268
			2				1	A	13.247753	–0.002	–0.1488
			2				2	A	13.248947	–0.003	–0.1479
			3				3	A	13.247409	–0.001	–0.1268
3	1	2	4	2	2	1	3	A	10.817706	–0.007	–0.2706
			2				1	A	10.817309	–0.005	–0.2996
3	2	1	4	2	1	2	3	A	27.966403	0.002	–0.2091
			3				2	A	27.967921	–0.000	–0.1915
			2				1	A	27.965711	–0.000	–0.2184
			2				2	A	27.966904	–0.002	–0.2185
			3				3	A	27.967152	–0.001	–0.1935
3	2	2	4	2	1	1	3	A	22.627870	0.001	–0.0494
			3				2	A	22.626928	0.000	–0.0830
			2				1	A	22.628391	–0.001	–0.0330
3	3	0	4	2	2	1	3	A	30.396181	0.001	–0.1391
			3				2	A	30.396286	0.001	–0.1438
			2				1	A	30.396108	–0.000	–0.1446
3	3	1	4	2	2	0	3	A	29.940614	–0.001	–0.1161
			2				1	A	29.940763	0.003	–0.1117
3	2	2	4	3	1	3	4	A	12.342869	0.007	–0.0315
			3				3	A	12.343714	0.003	–0.0395
			2				2	A	12.342567	0.002	–0.0349
			3				4	A	12.342869	0.007	–0.0315
			4				3	A	12.343714	0.003	–0.0395
3	3	0	4	3	2	1	4	A	12.743374	–0.005	0.0731
			3				3	A	12.742553	–0.005	0.0171

			2				2	A	12.743667	0.001	0.0984
3	3	1	4	3	2	2	4	A	14.362757	0.010	0.0221
			3				3	A	14.362621	0.002	–0.0249
			5				2	A	14.362795	0.003	0.0290
4	0	4	5	3	1	3	4	A	17.992344	0.002	–0.1375
			4				3	A	17.992331	–0.001	–0.1366
			3				2	A	17.992266	0.000	–0.1399
			4				4	A	17.991484	0.000	–0.1306
			3				3	A	17.993409	–0.002	–0.1484
4	1	4	5	3	0	3	4	A	18.946654	0.001	–0.0781
			4				3	A	18.946264	0.000	–0.0880
			3				2	A	18.946700	–0.000	–0.0754
4	1	3	5	3	2	2	4	A	17.552256	–0.007	–0.2886
			4				4	A	17.552883	–0.005	–0.2507
			3				3	A	17.552094	–0.008	–0.2991
4	3	1	5	3	2	2	4	A	36.726398	0.002	–0.1929
			4				3	A	36.726766	–0.004	–0.1991
			3				2	A	36.726297	–0.003	–0.1977
4	3	2	5	3	2	1	4	A	34.517568	0.001	–0.0978
			4				3	A	34.516961	–0.001	–0.1248
			3				2	A	34.517791	–0.002	–0.0920
4	1	3	5	4	0	4	5	A	11.902784	0.001	–0.1796
			4				4	A	11.904265	–0.001	–0.1546
			3				3	A	11.902401	–0.001	–0.1881
4	2	2	5	4	1	3	5	A	7.708394	0.000	–0.0138
			4				4	A	7.708783	–0.001	–0.0147
			3				3	A	7.708292	–0.001	–0.0156
4	2	3	5	4	1	4	5	A	15.047664	0.001	–0.0820
			4				4	A	15.048608	0.002	–0.0752
			3				3	A	15.047421	0.000	–0.0840
4	3	1	5	4	2	2	5	A	11.465738	–0.002	0.0995
			4				4	A	11.465095	–0.003	0.0613
			3				3	A	11.465906	0.002	0.1120
4	4	1	5	4	3	2	5	A	19.328932	–0.002	–0.0920
			4				4	A	19.328619	–0.003	–0.1313
			3				3	A	19.329010	–0.005	–0.0843
5	1	5	5	4	0	4	4	A	22.767163	0.000	–0.1110
			4				3	A	22.767374	0.003	–0.1031
5	0	5	6	4	1	4	5	A	22.391111	0.000	–0.1394
			5				4	A	22.391037	–0.000	–0.1390
			4				3	A	22.391075	0.000	–0.1389
5	1	4	6	4	2	3	5	A	23.849890	0.004	–0.2541
			4				3	A	23.849823	–0.001	–0.2622
5	2	3	6	4	3	2	5	A	18.630724	–0.009	–0.3456
			4				3	A	18.630552	–0.004	–0.3502

5	2	4	6	4	1	3	5	A	29.181100	–0.001	–0.0442
			5				4	A	29.180369	0.010	–0.0541
			4				3	A	29.181284	–0.001	–0.0386
5	3	2	6	4	3	1	5	A	28.577526	0.001	–0.2240
			5				4	A	28.577897	–0.001	–0.2043
			4				3	A	28.577472	0.004	–0.2264
5	3	3	4	4	2	2	3	A	38.243930	–0.002	–0.0531
			6				5	A	38.243723	–0.001	–0.0589
5	1	4	6	5	0	5	6	A	16.506440	0.002	–0.1998
			4				4	A	16.506169	–0.001	–0.2073
5	2	3	6	5	1	4	6	A	10.022519	0.001	–0.0836
			5				5	A	10.023294	–0.000	–0.0720
			4				4	A	10.022360	0.001	–0.0871
5	2	4	6	5	1	5	6	A	18.316510	0.000	–0.1166
			5				5	A	18.317461	–0.001	–0.1077
			4				4	A	18.316316	0.000	–0.1186
5	3	2	6	5	0	5	6	A	36.987334	–0.001	–0.2024
			5				5	A	36.989115	–0.003	–0.1883
			4				4	A	36.986972	0.001	–0.2045
5	3	2	6	5	2	3	6	A	10.458379	0.000	0.0850
			5				5	A	10.458067	–0.002	0.0628
			4				4	A	10.458440	–0.002	0.0869
5	3	3	6	5	2	4	6	A	16.771013	–0.004	–0.0325
			4				4	A	16.770934	–0.006	–0.0341
5	4	2	6	5	3	3	6	A	19.464101	–0.009	–0.0827
			4				4	A	19.464144	0.005	–0.0634
5	4	1	6	5	3	2	6	A	17.778644	–0.002	–0.0129
			5				5	A	17.778060	–0.003	–0.0496
			4				4	A	17.778759	–0.006	–0.0094
6	0	6	7	5	0	5	6	A	26.712636	0.002	–0.1309
			6				5	A	26.712521	0.001	–0.1329
			5				4	A	26.712614	–0.003	–0.1356
6	0	6	7	5	1	5	6	A	26.612368	0.002	–0.1411
			6				5	A	26.612286	0.001	–0.1430
			5				4	A	26.612342	–0.000	–0.1432
6	1	6	7	5	0	5	6	A	26.746606	0.002	–0.1265
			6				5	A	26.746481	0.002	–0.1286
			5				4	A	26.746585	–0.004	–0.1320
6	1	6	7	5	1	5	6	A	26.646338	0.002	–0.1368
			6				5	A	26.646245	–0.000	–0.1396
			5				4	A	26.646312	–0.002	–0.1406
6	1	5	7	5	2	4	6	A	29.413656	0.002	–0.2082
			6				5	A	29.413716	–0.000	–0.2036
			5				4	A	29.413635	–0.005	–0.2153
6	2	5	7	5	1	4	6	A	32.225241	0.001	–0.0574

			6				5	A	32.224710	0.000	–0.0712
			5				4	A	32.225340	0.000	–0.0545
6	2	4	7	5	2	3	6	A	35.098429	0.005	–0.1522
			6				5	A	35.098304	0.001	–0.1567
			5				4	A	35.098472	–0.009	–0.1649
6	2	5	7	5	2	4	6	A	30.314899	–0.002	–0.1549
			6				5	A	30.314767	–0.001	–0.1536
6	2	5	7	5	3	2	6	A	11.744343	–0.001	–0.0588
6	4	3	7	5	4	2	6	A	33.072462	0.002	–0.1492
			6				5	A	33.072636	0.002	–0.1318
			5				4	A	33.072430	–0.005	–0.1593
6	1	5	7	6	0	6	7	A	21.117799	0.001	–0.1827
			5				5	A	21.117611	–0.002	–0.1887
6	2	5	7	6	1	6	7	A	21.985075	0.001	–0.1307
			6				6	A	21.985984	–0.001	–0.1206
			5				5	A	21.984920	–0.001	–0.1339
6	3	3	7	6	2	4	7	A	10.499671	0.001	0.0452
			6				6	A	10.499750	0.001	0.0394
6	2	4	7	6	1	5	7	A	13.796950	0.002	–0.1250
			5				5	A	13.796782	0.001	–0.1290
6	3	4	7	6	2	5	7	A	19.009793	0.001	–0.0427
			6				6	A	19.010309	–0.001	–0.0430
			5				5	A	19.009702	–0.003	–0.0465
6	4	2	7	6	3	3	7	A	16.126043	–0.001	0.0283
			6				6	A	16.125469	–0.003	–0.0025
			5				5	A	16.126136	–0.005	0.0296
6	5	1	7	6	4	2	7	A	24.021119	0.002	–0.2941
			6				6	A	24.020738	0.000	–0.3246
			5				5	A	24.021180	–0.001	–0.2923
7	0	7	8	6	0	6	7	A	30.792528	0.001	–0.1430
			7				6	A	30.792446	–0.000	–0.1450
			6				5	A	30.792508	–0.003	–0.1461
7	0	7	8	6	1	6	7	A	30.758560	0.002	–0.1453
			7				6	A	30.758487	0.000	–0.1483
			6				5	A	30.758536	–0.003	–0.1508
7	1	7	8	6	0	6	7	A	30.803517	0.004	–0.1381
			7				6	A	30.803428	–0.001	–0.1442
			6				5	A	30.803494	–0.003	–0.1447
7	1	7	8	6	1	6	7	A	30.769548	0.005	–0.1414
			7				6	A	30.769469	–0.001	–0.1475
			6				5	A	30.769523	–0.002	–0.1483
7	1	6	8	6	2	5	7	A	34.301975	0.001	–0.1633
			7				6	A	34.301917	0.003	–0.1596
7	2	6	8	6	1	5	7	A	35.577679	0.000	–0.0789
			7				6	A	35.577343	–0.001	–0.0873

			6				5	A	35.577729	0.003	–0.0742
7	2	5	8	6	3	4	7	A	33.825485	0.003	–0.2257
			7				6	A	33.825907	0.002	–0.2067
			6				5	A	33.825436	0.008	–0.2227
7	2	5	8	7	1	6	8	A	18.533302	0.002	–0.1061
			6				7	A	18.533155	–0.000	–0.1116
7	3	4	8	7	2	5	8	A	12.098329	0.001	0.0253
			7				7	A	12.098767	0.001	0.0311
			6				6	A	12.098263	–0.001	0.0217
7	3	5	8	7	2	6	8	A	21.909334	0.001	–0.0368
			7				7	A	21.909932	–0.002	–0.0337
			6				6	A	21.909245	–0.001	–0.0400
7	4	4	8	7	3	5	8	A	21.083125	–0.003	–0.0350
			7				7	A	21.083304	–0.002	–0.0406
7	4	3	8	7	3	4	8	A	14.434506	–0.001	0.0390
			7				7	A	14.434104	–0.002	0.0181
			6				6	A	14.434563	–0.002	0.0410
7	5	3	8	7	4	4	8	A	24.446656	–0.003	–0.2585
			7				7	A	24.446510	–0.001	–0.2745
			6				6	A	24.446692	0.011	–0.2412
8	0	8	9	7	0	7	8	A	34.887641	–0.002	–0.1515
			8				7	A	34.887588	0.007	–0.1437
			7				6	A	34.887624	–0.004	–0.1536
8	0	8	9	7	1	7	8	A	34.876660	0.003	–0.1484
			8				7	A	34.876601	0.002	–0.1495
			7				6	A	34.876637	–0.005	–0.1560
8	1	8	9	7	0	7	8	A	34.891082	0.003	–0.1464
			8				7	A	34.891019	0.002	–0.1478
			7				6	A	34.891061	–0.004	–0.1526
8	1	7	9	7	1	6	8	A	39.138435	–0.003	–0.1026
			8				7	A	39.138258	0.002	–0.1011
			7				6	A	39.138456	0.001	–0.0981
8	1	8	9	7	1	7	8	A	34.880096	0.002	–0.1483
			8				7	A	34.880035	0.001	–0.1506
			7				6	A	34.880076	–0.003	–0.1531
8	1	7	9	7	2	6	8	A	38.763983	0.003	–0.1247
			8				7	A	38.763876	–0.002	–0.1304
8	2	7	9	7	1	6	8	A	39.281228	0.001	–0.0872
			8				7	A	39.281015	–0.001	–0.0935
			7				6	A	39.281253	0.005	–0.0823
8	3	5	9	7	4	4	8	A	34.682114	0.011	–0.0145
			8				7	A	34.682815	0.007	0.0116
			7				6	A	34.682029	0.008	–0.0214
8	4	5	9	7	5	2	8	A	19.567367	–0.009	0.2080
			8				7	A	19.567525	0.004	0.2443

8	1	7	9	8	0	8	9	A	29.779287	0.001	–0.0967
			8				8	A	29.780086	–0.001	–0.0873
			7				7	A	29.779182	–0.003	–0.1023
8	2	6	9	8	1	7	9	A	23.501576	0.001	–0.0381
			8				8	A	23.502458	–0.000	–0.0232
			7				7	A	23.501462	–0.001	–0.0429
8	2	7	9	8	1	8	9	A	29.918639	0.000	–0.0864
			8				8	A	29.919407	–0.004	–0.0805
			7				7	A	29.918538	–0.004	–0.0914
8	3	5	9	8	2	6	9	A	15.409010	0.002	0.0724
			8				8	A	15.409712	0.001	0.0860
			7				7	A	15.408921	0.001	0.0701
8	4	4	9	8	3	5	9	A	13.593069	–0.002	0.0547
			8				8	A	13.592962	–0.000	0.0477
			7				7	A	13.593087	0.002	0.0601
8	4	5	9	8	3	6	9	A	22.887996	0.000	0.0160
			8				8	A	22.888306	–0.000	0.0152
			7				7	A	22.887957	0.000	0.0161
8	5	4	8	8	4	5	8	A	24.655875	0.003	–0.1983
			7				7	A	24.655917	–0.004	–0.1922
9	4	5	10	8	5	4	9	A	32.792311	–0.005	0.4799
			9				8	A	32.793079	–0.005	0.5146
			8				7	A	32.792229	–0.007	0.4746
9	1	8	10	9	0	9	10	A	33.945846	0.000	–0.0310
			9				9	A	33.946561	0.000	–0.0214
			8				8	A	33.945766	0.000	–0.0321
9	2	8	10	9	1	9	10	A	33.996120	0.002	–0.0252
			9				9	A	33.996826	0.003	–0.0153
			8				8	A	33.996040	0.001	–0.0274
9	3	7	10	9	2	8	10	A	29.113854	0.003	0.0651
			9				9	A	29.114475	–0.001	0.0696
			8				8	A	29.113781	–0.000	0.0610
2	0	2	2	1	0	1	2	E	10.3706281	0.001	–0.0310
			3				2	E	10.3709649	0.003	0.1510
			2				1	E	10.3708370	0.001	0.0387
2	1	2	2	1	0	1	2	E	11.603870	–0.001	0.0141
			3				2	E	11.604499	0.000	–0.0389
			1				1	E	11.605054	–0.003	–0.0020
			2				1	E	11.604078	–0.002	0.0830
			1				0	E	11.604532	–0.001	–0.1763
2	2	1	2	1	1	1	1	E	19.8099135	0.001	0.5154
			3				2	E	19.8098072	0.001	0.5856
			1				1	E	19.8093832	0.000	0.4601

			1				0	E	19.8099636	–0.003	0.7182
2	2	1	1	2	1	1	2	E	8.3952448	0.000	0.7930
			2				3	E	8.3965060	–0.003	0.9960
			3				2	E	8.3954367	0.003	0.8153
			3				3	E	8.3961702	0.002	0.9657
			2				2	E	8.3957746	0.000	0.8478
			1				1	E	8.3963868	0.001	1.0279
2	2	1	1	2	1	2	2	E	11.836088	–0.001	1.2759
			2				3	E	11.835987	–0.004	1.3819
			3				2	E	11.836278	–0.001	1.2962
			3				3	E	11.835650	–0.001	1.3503
			2				2	E	11.836616	–0.004	1.3288
			1				1	E	11.835112	–0.000	1.3608
3	0	3	3	2	1	2	2	E	13.4999857	0.002	0.1667
			2				2	E	13.5008074	0.002	0.2766
3	1	2	4	2	0	2	3	E	22.0366772	–0.001	0.1649
			3				2	E	22.0376820	–0.003	0.3287
			2				1	E	22.0362542	–0.003	0.0680
3	1	2	4	2	1	2	3	E	20.8031424	0.000	0.3541
			3				2	E	20.8044408	–0.000	0.2842
			2				1	E	20.8025584	0.000	0.3892
3	1	2	4	2	2	1	3	E	8.9674931	0.002	–0.9955
			3				2	E	8.9678274	0.006	–1.0420
			2				1	E	8.9674475	0.001	–0.9706
			3				3	E	8.9681613	–0.001	–1.0135
3	1	3	4	2	0	2	3	E	15.3353666	–0.001	0.1000
			3				2	E	15.3349046	–0.002	0.2711
			2				2	E	15.3359806	–0.001	0.2834
			2				1	E	15.3354583	–0.002	0.0018
			3				3	E	15.3345675	–0.003	0.0888
3	2	1	4	2	1	1	3	E	25.0232522	0.001	0.6979
			2				1	E	25.0234401	–0.001	0.7520
			3				2	E	25.0231390	0.001	0.6245
3	2	1	4	2	1	2	3	E	28.4627333	–0.000	1.0838
			3				2	E	28.4639806	–0.002	1.1058
			2				1	E	28.4621671	–0.000	1.0866
3	2	2	4	2	1	2	3	E	24.4116826	0.001	0.3938
			3				2	E	24.4123659	–0.000	0.4374
			2				1	E	24.4113096	–0.004	0.3848
3	2	2	4	2	1	1	3	E	20.9722012	0.002	0.0075
			3				2	E	20.9715232	0.002	–0.0449
			2				1	E	20.9725832	–0.004	0.0508
			3				3	E	20.9722549	–0.000	0.1036
3	3	1	4	2	2	1	3	E	30.3653416	0.002	–0.2983
			3				2	E	30.3652268	0.001	–0.3383

			2				1	E	30.3654508	0.002	–0.2780
3	1	2	4	3	0	3	4	E	7.3031764	–0.002	0.0523
			3				3	E	7.3044556	–0.002	0.1180
			2				2	E	7.3027266	–0.004	0.0272
3	2	1	4	3	1	2	4	E	7.6595913	–0.000	0.7301
			3				3	E	7.6595398	–0.002	0.8215
			2				2	E	7.6596092	0.000	0.6980
			2				3	E	7.6587017	–0.002	0.7169
			3				2	E	7.6604463	–0.001	0.8016
			3				4	E	7.6602071	–0.005	0.8026
			4				3	E	7.6589232	0.002	0.7482
3	2	1	4	3	1	3	4	E	14.3609010	–0.001	0.7942
			3				3	E	14.3623173	–0.003	0.8792
			2				2	E	14.3604035	–0.003	0.7626
3	2	2	4	3	1	3	4	E	10.3098486	–0.002	0.1024
			3				3	E	10.3107025	–0.001	0.2107
			2				2	E	10.3095459	–0.006	0.0607
3	3	1	4	3	2	1	4	E	13.7382571	0.001	–0.0330
			3				3	E	13.7378639	0.001	–0.1135
			2				2	E	13.7383956	0.002	–0.0039
			3				2	E	13.7387025	0.002	–0.0084
4	0	4	5	3	1	3	4	E	18.0996070	–0.001	0.1713
			4				3	E	18.0995543	0.013	0.1610
			3				2	E	18.0995413	–0.010	0.1679
			4				4	E	18.0987432	–0.001	0.1379
			3				3	E	18.1006289	0.002	0.1917
4	1	4	5	3	0	3	4	E	18.9332551	–0.001	0.1840
			4				3	E	18.9329242	–0.001	0.2497
			3				2	E	18.9332819	–0.002	0.1577
			4				4	E	18.9323130	–0.004	0.1658
			3				3	E	18.9341052	–0.001	0.2692
4	1	3	5	3	2	1	4	E	14.9931109	0.011	–0.5808
			4				3	E	14.9929358	–0.003	–0.7495
			3				2	E	14.9932010	0.002	–0.5428
4	1	3	5	3	2	2	4	E	19.0441541	0.003	0.1017
			4				3	E	19.0445574	0.002	–0.0742
			3				2	E	19.0440586	0.006	0.1591
4	2	2	5	3	3	1	4	E	9.1635745	–0.002	–0.3869
			4				3	E	9.1642470	–0.001	–0.2914
			3				2	E	9.1634248	0.000	–0.4096
4	3	1	5	3	2	1	4	E	35.7413749	0.003	–0.2868
			4				3	E	35.7411990	0.004	–0.3372
			3				2	E	35.7414784	0.004	–0.2660
4	3	2	5	3	2	2	4	E	34.0102550	–0.005	2.1959
			4				3	E	34.0102125	–0.000	2.1483

			3				2	E	34.0102768	–0.000	2.2229
4	1	3	5	4	0	4	5	E	11.2543953	0.002	0.0324
			4				4	E	11.2557175	0.000	–0.0126
			3				3	E	11.2540519	–0.001	0.0406
4	2	2	5	4	1	3	5	E	7.9087297	–0.003	0.1700
			3				3	E	7.9086162	–0.003	0.1261
			4				4	E	7.9091692	–0.003	0.3386
4	2	3	5	4	1	4	5	E	13.6780080	0.001	0.1652
			3				3	E	13.6777465	–0.002	0.1448
			4				4	E	13.6790121	0.001	0.2319
4	3	1	5	4	2	2	5	E	12.8395424	0.003	0.1321
			3				3	E	12.8396572	0.001	0.1466
			4				4	E	12.8390862	0.003	0.0659
			4				3	E	12.8402184	0.004	0.1827
5	0	5	6	4	1	4	5	E	22.4297107	0.000	0.1632
			5				4	E	22.4296166	0.000	0.1621
			4				3	E	22.4296819	0.002	0.1648
5	1	4	6	4	1	3	5	E	27.2477490	0.000	0.1578
			4				3	E	27.2478331	0.002	0.1501
5	1	4	6	4	2	2	5	E	19.3390165	0.000	–0.0150
			5				4	E	19.3382954	0.004	–0.1551
5	1	4	6	4	2	3	5	E	24.5923582	0.003	0.0039
			5				4	E	24.5924665	0.001	–0.1010
			4				3	E	24.5923341	–0.002	0.0225
5	1	5	6	4	0	4	5	E	22.7405964	0.001	0.2039
			5				4	E	22.7404013	–0.000	0.2241
			4				3	E	22.7405872	–0.002	0.1952
5	2	3	6	4	2	2	5	E	29.2127084	0.001	–0.1055
			5				4	E	29.2127479	0.003	–0.1653
5	2	4	6	4	1	3	5	E	28.7727895	0.001	0.3957
			5				4	E	28.7722308	–0.000	0.4873
			4				6	E	28.7729257	–0.001	0.3708
5	2	3	6	4	3	1	5	E	16.3731675	–0.001	–0.2362
			5				4	E	16.3736591	–0.002	–0.2338
			4				3	E	16.3730891	–0.002	–0.2372
5	1	4	6	5	0	5	6	E	15.8406538	0.002	0.0043
			4				4	E	15.8404041	–0.001	0.0079
			5				5	E	15.8418613	0.001	–0.0320
5	2	3	5	5	1	4	5	E	9.8744506	–0.002	–0.0121
			6				6	E	9.8736898	–0.002	–0.0927
			4				4	E	9.8735326	–0.004	–0.1113
5	2	4	6	5	1	5	6	E	17.286588	0.001	0.2238
			5				5	E	17.2875475	0.001	0.2512
			4				4	E	17.2863868	–0.004	0.2125
5	3	2	6	5	2	3	6	E	11.5592451	0.003	–0.1551

			4				4	E	11.5592994	0.003	–0.1601
			5				5	E	11.5589758	0.003	–0.1332
5	3	2	6	5	2	4	6	E	19.9078949	0.002	–0.4851
			4				4	E	19.9077379	0.001	–0.4935
			5				5	E	19.9086593	0.000	–0.4500
5	4	1	6	5	3	2	6	E	18.4228651	–0.005	–1.7553
			4				4	E	18.4229323	–0.007	–1.7469
			5				5	E	18.4225270	–0.006	–1.8047
6	0	6	7	5	0	5	6	E	26.6939064	0.003	0.1916
			6				5	E	26.6937904	0.000	0.1953
			5				4	E	26.6938839	–0.003	0.1844
6	0	6	7	5	1	5	6	E	26.6148007	0.002	0.1739
			6				5	E	26.6147093	–0.000	0.1735
			5				4	E	26.6147757	–0.001	0.1700
6	1	6	7	5	0	5	6	E	26.7191329	0.002	0.1993
			6				5	E	26.7190119	0.001	0.2062
6	1	6	7	5	1	5	6	E	26.6400316	0.006	0.1860
			6				5	E	26.6399291	–0.001	0.1827
			5				4	E	26.6400039	–0.001	0.1780
6	1	5	7	5	2	4	6	E	29.7330378	0.002	–0.0810
			6				5	E	29.7330072	–0.007	–0.1272
6	2	4	6	5	2	3	5	E	34.8700526	0.001	0.1240
			7				6	E	34.8701917	0.002	0.1815
			5				4	E	34.8702412	–0.004	0.1856
6	2	5	6	5	3	2	5	E	10.5242131	–0.000	0.5421
6	2	5	7	5	1	4	6	E	31.9580717	–0.000	0.3409
			6				5	E	31.9576395	0.000	0.3968
			5				4	E	31.9581515	0.000	0.3304
6	4	2	7	5	4	1	6	E	33.2250750	0.009	–0.4482
			6				5	E	33.2252344	0.002	–0.4373
			5				4	E	33.2250445	–0.005	–0.4650
6	1	5	7	6	0	6	7	E	20.4048256	0.002	–0.0306
			6				6	E	20.4058510	–0.001	–0.0440
			5				5	E	20.4046485	–0.002	–0.0323
6	2	4	7	6	1	5	7	E	13.4857977	–0.008	–0.0736
			5				5	E	13.4856521	0.002	–0.0633
6	2	5	7	6	1	6	7	E	21.0795940	0.001	0.1473
			6				6	E	21.0804901	0.001	0.1599
			5				5	E	21.0794403	–0.001	0.1427
6	3	3	6	6	2	4	6	E	11.0374490	0.004	–0.5621
			5				5	E	11.0373031	0.004	–0.6769
			6				7	E	11.0382432	–0.001	–0.5933
			6				5	E	11.0383855	0.007	–0.5904
			7				7	E	11.0373228	0.003	–0.6617
6	3	3	6	6	2	5	6	E	23.8243102	–0.000	–0.8496

			5				5	E	23.8229285	–0.001	–0.9299
			7				7	E	23.8231308	0.002	–0.9156
6	3	4	6	6	2	5	6	E	17.2457308	0.006	1.3784
			5				5	E	17.2449938	0.005	1.3214
			7				7	E	17.2451023	0.007	1.3317
7	0	7	8	6	0	6	7	E	30.7676948	0.005	0.1876
			7				6	E	30.7676093	0.001	0.1866
			6				5	E	30.7676635	–0.010	0.1721
7	0	7	8	6	1	6	7	E	30.7424654	0.003	0.1770
			7				6	E	30.7423884	–0.000	0.1763
			6				5	E	30.7424416	–0.003	0.1704
7	1	7	8	6	0	6	7	E	30.7753940	0.003	0.1901
			7				6	E	30.7753061	–0.001	0.1889
			6				5	E	30.7753710	–0.003	0.1826
7	1	7	8	6	1	6	7	E	30.7501711	0.008	0.1860
			7				6	E	30.7500866	–0.000	0.1800
			6				5	E	30.7501392	–0.007	0.1710
7	1	6	7	6	2	5	6	E	34.4055772	–0.001	–0.1192
			6				5	E	34.4056742	–0.004	–0.1101
7	2	6	8	6	1	5	7	E	35.3832503	–0.001	0.1851
			7				6	E	35.3829636	–0.000	0.2078
7	2	6	6	6	1	5	5	E	35.3832971	0.008	0.1897
7	1	6	8	7	0	7	8	E	24.7428011	0.000	–0.1361
			7				7	E	24.7436787	–0.000	–0.1359
			6				6	E	24.7426718	–0.002	–0.1389
7	2	5	8	7	1	6	8	E	18.1278798	–0.002	0.0207
			6				6	E	18.1277441	–0.005	0.0213
7	3	4	8	7	2	5	8	E	12.2680121	0.003	–0.7123
			7				7	E	12.2684862	0.005	–0.6306
			6				6	E	12.2679455	0.004	–0.7224
7	3	5	8	7	2	6	8	E	20.6838815	0.006	1.0227
			6				6	E	20.6837862	0.005	1.0173
7	4	3	8	7	3	4	8	E	15.5760715	0.000	–2.5272
			7				7	E	15.5757070	–0.002	–2.5390
			6				6	E	15.5761206	–0.003	–2.5290
8	0	8	9	7	1	7	8	E	34.8510595	0.003	0.1717
			8				7	E	34.8509979	0.002	0.1718
			7				6	E	34.8510365	–0.005	0.1634
8	1	8	9	7	0	7	8	E	34.8610276	–0.007	0.1662
			8				7	E	34.8609734	0.001	0.1765
			7				6	E	34.8610160	–0.004	0.1688
8	1	7	9	7	1	6	8	E	39.0335477	–0.004	–0.0612
			8				7	E	39.0333846	0.002	–0.0499
8	1	8	9	7	1	7	8	E	34.8533374	0.003	0.1727
			8				7	E	34.8532771	0.003	0.1747

			7				6	E	34.8533148	–0.005	0.1646
8	1	7	9	7	2	6	8	E	38.7559707	0.003	–0.1613
			8				7	E	38.7558520	–0.002	–0.1691
8	2	7	9	7	1	6	8	E	39.1341659	–0.005	–0.0112
			8				7	E	39.1339808	–0.002	0.0000
8	2	7	9	7	2	6	8	E	38.8565902	0.003	–0.1099
			8				7	E	38.8564552	0.001	–0.1121
8	1	7	8	8	0	8	8	E	28.9183666	–0.001	–0.3620
8	2	6	9	8	1	7	9	E	22.9794524	–0.003	0.0932
			8				8	E	22.9802710	–0.004	0.0806
			7				7	E	22.9793481	–0.005	0.0936
8	3	6	9	8	2	7	9	E	24.3474994	0.005	0.7219
			8				8	E	24.3481387	0.003	0.7334
			7				7	E	24.3474142	0.000	0.7158
10	4	6	9	10	3	7	9	E	17.1997558	–0.002	–0.9813
			11				11	E	17.1998075	–0.001	–0.9773
			10				10	E	17.2003155	–0.001	–0.9439

AII.2: ^{14}N nuclear quadrupole coupling and methyl internal rotation in the microwave spectrum of 2-methylpyrrole

Figure S-I: The torsional potential function of the methyl group with respect to the molecular frame calculated at the MP2/cc-pVDZ level of theory.

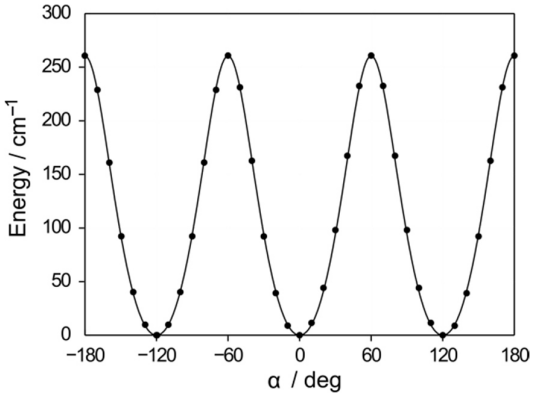

Table S-I: Nuclear coordinates in the principal intertial axes of the only conformer of 2-methylpyrrole calculated at the MP2/cc-pVDZ level of theory. The atoms are numbered according to Figure 1.

	a / Å	b / Å	c / Å
N_1	–0.085811	–1.049748	–0.000076
C_2	0.700766	0.083144	–0.000091
C_3	–0.169483	1.175320	0.000021
C_4	–1.506230	0.673096	–0.000048
C_5	–1.422986	–0.718098	0.000129
C_6	2.197636	0.011310	0.000065
H_7	0.139736	2.221227	0.000042
H_8	–2.428647	1.253920	–0.000096
H_9	–2.196151	–1.485240	0.000180
H_{10}	0.273653	–1.997580	–0.000227
H_{11}	2.614881	1.029946	–0.001070
H_{12}	2.586889	–0.510927	–0.892053
H_{13}	2.586832	–0.508935	0.893372

Table S–II: Rotational constants of 2–methylpyrrole in MHz optimized with various combinations of methods and basis sets and their deviations to the experimental values (obs. – calc.) in MHz.

Basis set	*A*	Δ*A*	*B*	Δ*B*	*C*	Δ*C*
MP2						
6–31G(d,p)	8583.8	–24.9	3433.2	–0.7	2490.3	–1.4
6–31+G(d,p)	8559.7	–0.7	3425.3	7.2	2484.2	4.6
6–31++G(d,p)	8558.5	0.5	3425.3	7.2	2484.1	4.7
6–311G(d,p)	8547.1	11.9	3424.4	8.1	2483.0	5.9
6–311+G(d,p)	8536.0	22.9	3417.4	15.1	2478.4	10.5
6–311++G(d,p)	8533.9	25.0	3419.1	13.4	2479.1	9.8
6–311G(df,pd)	8600.2	–41.3	3445.3	–12.8	2498.3	–9.4
6–311+G(df,pd)	8589.2	–30.3	3440.6	–8.1	2494.9	–6.0
6–311++G(df,pd)	8588.5	–29.6	3440.4	–7.9	2494.8	–5.9
6–311G(3df,3pd)	8616.9	–57.9	3448.4	–15.9	2501.1	–12.2
6–311+G(3df,3pd)	8610.8	–51.8	3445.9	–13.4	2499.3	–10.4
6–311++G(3df,3pd)	8610.7	–51.8	3445.9	–13.4	2499.3	–10.4
cc–pVDZ	8462.7	96.2	3398.5	34.0	2462.7	26.1
cc–pVTZ	8607.6	–48.6	3446.9	–14.4	2499.5	–10.6
aug–cc–pVDZ	8442.8	116.2	3386.2	46.3	2454.6	34.3
aug–cc–pVTZ	8600.7	–41.7	3443.0	–10.4	2496.9	–8.0
B3LYP–D3						
6–31G(d,p)	8577.3	–18.4	3425.0	7.5	2485.6	3.3
6–31+G(d,p)	8557.5	1.4	3417.7	14.8	2480.3	8.6
6–31++G(d,p)	8557.5	1.4	3417.7	14.8	2480.2	8.6
6–311G(d,p)	8600.0	–41.0	3430.0	2.6	2490.1	–1.2
6–311+G(d,p)	8594.5	–35.6	3427.0	5.5	2488.1	0.8
6–311++G(d,p)	8594.3	–35.3	3427.0	5.5	2488.1	0.8
6–311G(df,pd)	8627.4	–68.4	3441.1	–8.6	2498.2	–9.3
6–311+G(df,pd)	8622.5	–63.6	3438.3	–5.8	2496.3	–7.4
6–311++G(df,pd)	8622.4	–63.4	3438.3	–5.8	2496.3	–7.4
6–311G(3df,3pd)	8643.8	–84.9	3445.2	–12.7	2501.6	–12.7
6–311+G(3df,3pd)	8639.1	–80.2	3443.7	–11.2	2500.4	–11.6
6–311++G(3df,3pd)	8639.1	–80.1	3443.8	–11.2	2500.4	–11.6
cc–pVDZ	8535.3	23.6	3415.7	16.8	2477.7	11.2
cc–pVTZ	8639.7	–80.7	3444.5	–11.9	2500.9	–12.0
aug–cc–pVDZ	8539.9	19.1	3413.9	18.7	2477.0	11.8
aug–cc–pVTZ	8638.6	–79.6	3443.2	–10.7	2500.1	–11.2
B3LYP–D3BJ						
6–31G(d,p)	8578.4	–19.4	3425.7	6.8	2486.1	2.8
6–31+G(d,p)	8558.7	0.3	3418.6	13.9	2480.8	8.1
6–31++G(d,p)	8558.7	0.3	3418.6	14.0	2480.8	8.1
6–311G(d,p)	8600.6	–41.7	3430.5	2.0	2490.4	–1.6
6–311+G(d,p)	8595.2	–36.3	3427.6	4.9	2488.5	0.4
6–311++G(d,p)	8595.0	–36.0	3427.6	4.9	2488.5	0.4
6–311G(df,pd)	8627.6	–68.6	3441.5	–9.0	2498.4	–9.5
6–311+G(df,pd)	8622.8	–63.9	3438.7	–6.2	2496.6	–7.7
6–311++G(df,pd)	8622.7	–63.8	3438.8	–6.3	2496.6	–7.7
6–311G(3df,3pd)	8643.9	–84.9	3445.5	–13.0	2501.8	–12.9

6–311+G(3df,3pd)	8639.2	–80.3	3444.1	–11.6	2500.6	–11.8
6–311++G(3df,3pd)	8639.2	–80.2	3444.1	–11.6	2500.6	–11.8
cc–pVDZ	8536.5	22.4	3416.6	15.9	2478.3	10.6
cc–pVTZ	8639.7	–80.8	3444.8	–12.3	2501.0	–12.2
aug–cc–pVDZ	8541.1	17.9	3414.8	17.7	2477.6	11.2
aug–cc–pVTZ	8638.7	–79.7	3443.5	–11.0	2500.3	–11.4
M06–2X						
6–31G(d,p)	8627.0	–68.0	3444.3	–11.8	2500.0	–11.1
6–31+G(d,p)	8610.1	–51.1	3438.0	–5.5	2495.4	–6.5
6–31++G(d,p)	8610.0	–51.1	3438.0	–5.5	2495.4	–6.5
6–311G(d,p)	8640.5	–81.5	3447.5	–14.9	2502.8	–13.9
6–311+G(d,p)	8636.1	–77.2	3444.8	–12.3	2501.0	–12.1
6–311++G(d,p)	8635.9	–76.9	3444.8	–12.3	2501.0	–12.1
6–311G(df,pd)	8662.8	–103.8	3456.2	–23.7	2509.2	–20.3
6–311+G(df,pd)	8659.6	–100.6	3453.7	–21.2	2507.6	–18.7
6–311++G(df,pd)	8659.5	–100.5	3453.8	–21.3	2507.6	–18.7
6–311G(3df,3pd)	8681.4	–122.4	3460.5	–28.0	2512.8	–24.0
6–311+G(3df,3pd)	8677.1	–118.2	3459.2	–26.7	2511.8	–22.9
6–311++G(3df,3pd)	8677.1	–118.1	3459.2	–26.7	2511.8	–22.9
cc–pVDZ	8590.8	–31.9	3437.8	–5.3	2494.0	–5.1
cc–pVTZ	8675.4	–116.4	3459.9	–27.4	2512.0	–23.1
aug–cc–pVDZ	8596.0	–37.1	3435.1	–2.6	2492.9	–4.1
aug–cc–pVTZ	8676.0	–117.0	3459.1	–26.6	2511.7	–22.8
CCSD						
6–311++G(d,p)	8549.4	9.6	3413.6	18.9	2477.6	11.3
Experiment	8559.0		3432.5		2488.9	

Table S–III: Fourier expansion of the potential energy curve given in Figure 2. The potential is expanded as $V(\alpha) = \sum_{i=0}^{4} a_i f_i$.

i	f_i	a_i / Hartree	a_i / cm^{-1}
0	1	–248.7111746	
1	cos 3α	–0.0005815	–127.62
2	cos 6α	0.0000824	18.08
3	cos 9α	–0.0000120	–2.63
4	cos 12α	0.0000026	0.57

Table S–IV: Observed frequencies ($\nu_{obs.}$) of the A and E species of 2–methylpyrrole. $\nu_{calc.}$ are the calculated frequencies; $\nu_{obs.}-\nu_{calc.}$ values as obtained after a fit with the program *XIAM* and *BELGI–C_1–hyperfine*. J, K_a, K_c are the asymmetric top rotational quantum numbers of the lower energy level; J', K_a', K_c' are those of the upper energy level. F is the total angular momentum in the coupled basis with $F = J + I$.

J'	K_a'	K_c'	F'	J	K_a	K_c	F		$\nu_{obs.}$	$\nu_{obs.} - \nu_{calc.}$	$\nu_{obs.} - \nu_{calc.}$
upper level				lower level					GHz	*XIAM/kHz*	*BELGI/kHz*
1	0	1	2	0	0	0	1	A	5.9215622	–0.6	–1
			1				1	A	5.9219639	0.8	1
			0				1	A	5.9209619	–0.3	0
1	1	1	2	0	0	0	1	A	11.0664614	3.8	2
			1				1	A	11.0669150	3.8	2
1	1	0	1	1	0	1	1	A	6.0872114	0.8	–1
			1				2	A	6.0876131	2.1	1
			2				1	A	6.0880626	–2.0	–4
			1				0	A	6.0882182	6.7	5
			2				2	A	6.0884609	–4.1	–6
			0				1	A	6.0893467	1.1	0
2	0	2	1	1	0	1	1	A	11.7242889	0.9	1
			3				2	A	11.7249889	0.0	0
2	0	2	1	1	1	1	1	A	6.5793379	–2.0	0
			3				2	A	6.5800848	–9.2	–8
			2				1	A	6.5801852	3.9	6
			1				0	A	6.5804746	0.7	2
			2				2	A	6.5806344	–0.5	1
2	1	2	1	1	0	1	1	A	16.0437585	2.9	2
			3				2	A	16.0446669	2.6	1
			1				0	A	16.0447521	–4.4	–5
			2				1	A	16.0451868	7.9	7
			2				2	A	16.0455827	3.5	2
2	1	1	1	1	1	0	0	A	12.7855514	–1.7	–2
			3				2	A	12.7865669	2.9	3
			2				1	A	12.7869319	–0.1	0
			1				1	A	12.7876864	–1.6	–1
2	1	2	3	1	0	1	2	A	16.0446664	2.1	1
			1				0	A	16.0447528	–3.7	–5
			2				1	A	16.0451808	1.9	1
2	1	2	1	1	1	1	1	A	10.8988079	0.4	1
			3				2	A	10.8997640	–5.4	–5
			1				0	A	10.8999374	–4.1	–4
			2				1	A	10.9002331	2.3	3
2	2	0	3	1	1	1	2	A	29.2829526	3.3	1
			1				0	A	29.2839295	–0.7	–3
2	1	1	2	2	0	2	2	A	7.1490157	2.5	1
			3				2	A	7.1495014	2.2	1
			2				3	A	7.1495587	4.6	3
			1				2	A	7.1497737	4.5	3
			2				1	A	7.1498582	3.5	2
			3				3	A	7.1500407	0.6	–1
2	1	1	3	2	1	2	3	A	2.8303613	–3.4	–3
			1				1	A	2.8311512	8.1	8
2	2	0	2	2	1	1	2	A	15.5527633	3.1	0
			3				3	A	15.5528272	12.1	9

2	2	1	2	2	1	2	2	A	18.2636043	4.2	1
			1				2	A	18.2642732	5.9	3
			3				3	A	18.2649431	–0.9	–4
			1				1	A	18.2656943	3.7	1
3	0	3	3	2	0	2	3	A	17.3045095	–0.6	0
			4				3	A	17.3037873	1.2	1
			2				1	A	17.3038288	–4.4	–4
			3				2	A	17.3039681	–1.1	–1
3	0	3	3	2	1	2	2	A	12.9839208	1.0	2
			4				3	A	12.9841102	–0.5	1
			2				1	A	12.9843613	–4.3	–3
			3				3	A	12.9848328	–1.9	0
			4				3	A	16.2799984	0.7	1
3	1	3	2	2	1	2	1	A	16.2801211	–2.2	–2
3	1	3	2	2	0	2	2	A	20.5987487	–0.8	–2
			2				1	A	20.5995884	–2.5	–4
			4				3	A	20.5996755	2.4	1
3	1	2	2	2	1	1	1	A	19.1005943	–4.7	–4
			4				3	A	19.1007452	–0.4	0
			3				2	A	19.1008783	–0.7	0
			2				2	A	19.1013539	–1.1	–1
3	2	1	3	2	1	2	2	A	36.6077911	4.4	3
			4				3	A	36.6089850	4.2	3
			2				1	A	36.6095901	3.3	2
3	2	1	2	2	2	0	1	A	18.2255977	–0.4	1
			4				3	A	18.2258084	7.5	9
			3				2	A	18.2260642	1.5	3
3	2	2	3	2	2	1	2	A	17.7651652	–0.8	0
			4				3	A	17.7647403	3.2	4
			2				2	A	17.7651664	0.4	1
3	1	2	4	3	0	3	4	A	8.9470014	1.8	1
			2				2	A	8.9473791	2.7	2
3	1	2	4	3	1	3	4	A	5.6511112	–1.4	–1
3	2	1	4	3	1	2	4	A	14.6778738	3.4	1
			3				3	A	14.6779487	4.8	3
3	2	2	3	3	1	3	3	A	19.7485952	5.3	3
			4				4	A	19.7496800	–3.3	–6
			2				2	A	19.7500643	–1.8	–4
4	0	4	5	3	0	3	4	A	22.6013795	–0.3	0
			3				2	A	22.6013965	2.2	2
			4				3	A	22.6015858	1.0	1
4	0	4	4	3	1	3	3	A	19.3053278	–0.5	1
			5				4	A	19.3054915	–1.3	0
			3				2	A	19.3056340	–2.6	–2
4	1	4	3	3	0	3	2	A	24.8845984	2.6	2
			5				4	A	24.8846556	1.9	1
			4				3	A	24.8851420	2.0	1
4	1	4	5	3	1	3	4	A	21.5887676	0.9	1
			3				2	A	21.5888393	1.1	1
			4				3	A	21.5888831	–0.5	0
4	2	3	5	3	1	2	4	A	37.6926361	3.1	1
			4				4	A	37.6928310	–11.9	–14
4	2	3	3	3	2	2	2	A	23.5940024	–5.9	–5
			5				4	A	23.5940625	0.2	1
			4				3	A	23.5942718	–0.4	0
4	1	3	4	4	0	4	4	A	11.6511236	0.3	0
			5				5	A	11.6522994	0.5	0
			3				3	A	11.6526063	5.1	5
4	1	3	5	4	1	4	5	A	9.3690241	–0.9	0

			3				3	A	9.3693966	–3.1	–3
4	2	2	3	4	1	3	3	A	14.0497212	3.6	3
4	2	3	4	4	1	4	4	A	21.7539823	3.8	2
			5				5	A	21.7549803	1.3	–1
			3				3	A	21.7552327	–3.5	–5
4	3	1	4	4	2	2	4	A	26.8564682	0.4	1
5	0	5	6	4	0	4	5	A	27.6543188	–1.3	–2
			4				3	A	27.6543355	5.1	5
			5				4	A	27.6545133	–0.1	0
5	1	5	6	4	0	4	5	A	29.1036910	1.2	0
			5				4	A	29.1040673	1.7	1
5	1	4	6	4	1	3	5	A	31.3472048	–2.2	–2
			5				4	A	31.3473261	0.6	1
5	1	4	5	4	2	3	4	A	18.9609039	–11.1	–8
			6				5	A	18.9612467	–6.4	–3
			4				3	A	18.9613339	0.7	4
5	2	4	4	4	2	3	3	A	29.3455818	–7.9	–8
			6				5	A	29.3456096	2.7	3
			5				4	A	29.3457477	1.1	2
5	3	2	6	4	3	1	5	A	30.1153746	–5.6	–2
			5				4	A	30.1155025	–5.2	–2
5	3	3	4	4	3	2	3	A	29.9254375	0.0	3
			6				5	A	29.9254795	–6.3	–4
			5				4	A	29.9256563	–4.0	–1
5	4	2	4	4	4	1	3	A	29.8699581	–3.6	1
			6				5	A	29.8700529	–8.6	–4
5	1	4	6	5	0	5	6	A	15.3451857	–0.1	0
			4				4	A	15.3454369	–3.6	–3
5	3	3	5	5	2	4	5	A	29.0348453	–4.2	0
			6				6	A	29.0352591	–5.4	–1
			4				4	A	29.0353453	–3.8	1
5	4	1	5	5	3	2	5	A	38.8212130	–19.2	–7
			6				6	A	38.8214359	–6.6	5
6	0	6	7	5	0	5	6	A	32.5715403	–2.4	–3
			5				4	A	32.5715621	7.0	7
			6				5	A	32.5717037	2.3	2
6	1	5	7	5	1	4	6	A	37.1542108	–1.7	–1
			6				5	A	37.1543597	2.5	3
6	1	5	6	5	2	4	5	A	26.7695238	–1.9	1
			7				6	A	26.7698557	–2.9	0
			5				4	A	26.7699273	0.3	3
6	3	3	7	5	3	2	6	A	36.4368250	–10.8	–6
6	3	4	5	5	3	3	4	A	35.9516781	–11.7	–9
			7				6	A	35.9517103	0.8	4
			6				5	A	35.9518071	–5.4	–2
6	1	5	5	6	0	6	5	A	19.9280733	4.3	5
6	2	4	6	6	1	5	6	A	14.7821022	–9.8	–5
			7				7	A	14.7824686	–3.4	1
			5				5	A	14.7825275	–5.2	–1
6	2	5	6	6	1	6	6	A	27.3028895	1.4	0
			7				7	A	27.3038116	–0.4	–2
			5				5	A	27.3039726	4.6	3
7	1	7	8	6	0	6	7	A	37.9361210	2.9	2
			7				6	A	37.9362967	1.2	1
7	0	7	8	6	0	6	7	A	37.4546812	–2.3	–3
			6				5	A	37.4547035	5.9	5
			7				6	A	37.4548040	–0.3	–1
7	0	7	8	6	1	6	7	A	36.5971821	3.5	3
7	2	5	8	7	1	6	8	A	16.5974653	–12.3	–3

			6				6	A	16.5975413	–13.2	–3
7	3	5	8	7	2	6	8	A	31.3772644	–14.4	–3
			6				6	A	31.3773285	–15.8	–4
9	1	8	9	9	0	9	9	A	36.1896636	5.4	1
			10				10	A	36.1906659	7.1	3
			8				8	A	36.1907747	4.0	0
1	1	0	2	0	0	0	1	E	12.0136497	2.3	1
			1				1	E	12.0128176	3.5	2
1	1	1	0	0	0	0	1	E	11.0386530	–5.0	–1
			2				1	E	11.0393045	–3.0	1
			1				1	E	11.0397367	–3.7	0
1	1	0	1	1	0	1	2	E	6.0912491	–2.2	–3
			2				1	E	6.0916844	0.2	–1
			2				2	E	6.0920857	1.1	0
			0				1	E	6.0929346	0.4	–1
			1				0	E	6.0918562	4.4	4
2	0	2	3	1	1	1	2	E	6.6069947	5.0	0
			2				2	E	6.6075341	3.3	–1
			2				1	E	6.6070912	–6.7	–11
			1				0	E	6.6073447	6.2	1
			1				1	E	6.6062654	9.3	5
2	1	1	3	1	1	0	2	E	12.7763648	–0.6	1
			2				1	E	12.7767142	–1.1	0
			1				1	E	12.7774667	–0.6	1
2	1	2	3	1	0	1	2	E	16.0277141	–0.9	1
			2				2	E	16.0286240	–3.4	–1
			2				1	E	16.0282215	–5.5	–3
			1				1	E	16.0268009	–6.9	–5
2	1	2	3	1	1	1	2	E	10.9099728	2.4	0
			2				1	E	10.9104506	0.8	–1
2	2	1	2	1	1	1	1	E	28.9552700	–8.2	–5
			1				0	E	28.9570896	–5.5	–3
2	1	1	2	2	0	2	2	E	7.1426921	1.0	2
			3				2	E	7.1431731	–1.5	–1
			2				3	E	7.1432334	1.1	2
			1				2	E	7.1434499	6.8	7
			2				1	E	7.1435352	2.3	3
			3				3	E	7.1437161	0.4	1
2	2	1	2	2	1	1	3	E	15.2049965	–9.2	–3
			3				3	E	15.2054749	–3.0	4
			3				2	E	15.2059538	–7.6	–1
			1				2	E	15.2062173	–6.4	0
			2				1	E	15.2047228	–14.4	–8
			1				1	E	15.2054616	–10.1	–3
2	2	0	2	2	1	1	1	E	15.7007284	6.5	5
			2				3	E	15.7009914	0.9	0
			2				2	E	15.7014665	–7.4	–9
			1				1	E	15.7014934	–3.0	–4
2	2	0	2	2	1	2	2	E	18.5408173	4.2	1
			3				2	E	18.5413146	3.6	1
			1				2	E	18.5415916	4.0	1
			2				3	E	18.5417291	3.6	0
			3				3	E	18.5422267	3.3	0
			1				1	E	18.5430106	3.7	1
2	2	1	2	2	1	2	2	E	18.0448215	–6.8	–2
			3				2	E	18.0452962	–4.4	1
			3				3	E	18.0462060	–6.9	–2
3	0	3	2	2	0	2	2	E	17.3020486	–0.2	–1
			4				3	E	17.3028448	1.3	1

			2				1	E	17.3028897	–0.9	–1
			3				2	E	17.3030267	–0.2	–1
3	0	3	3	2	1	2	2	E	12.9996790	4.1	1
			4				3	E	12.9998654	2.6	–1
			2				1	E	13.0001211	5.0	2
			3				3	E	13.0005889	1.6	–2
3	1	2	2	2	1	1	1	E	19.0978269	–0.8	–1
			4				3	E	19.0979732	0.0	0
			3				2	E	19.0981048	0.0	0
			2				2	E	19.0985794	–0.3	0
3	1	3	2	2	0	2	2	E	20.5845188	–0.1	1
			2				1	E	20.5853553	–5.4	–4
			4				3	E	20.5854422	–0.3	1
			3				2	E	20.5859927	–1.6	0
3	1	3	4	2	1	2	3	E	16.2824633	1.5	0
			2				1	E	16.2825869	0.7	0
			3				2	E	16.2826435	1.2	0
3	2	1	4	2	1	1	3	E	33.8248267	–0.6	0
			4				3	E	36.6655674	5.1	4
3	2	1	2	2	2	0	1	E	18.1231500	1.2	3
			4				3	E	18.1233361	–2.8	–1
			3				2	E	18.1235872	–2.6	–1
3	2	2	2	2	2	1	1	E	17.8678996	4.3	2
			4				3	E	17.8681498	3.6	2
			3				2	E	17.8685895	3.7	2
3	1	2	3	3	0	3	3	E	8.9377687	–0.3	1
			4				4	E	8.9388448	–0.6	1
3	2	1	4	3	1	2	4	E	14.7268537	–0.4	0
			3				3	E	14.7269570	–1.9	–1
3	2	1	4	3	1	3	4	E	20.3831011	0.6	0
			2				2	E	20.3835696	0.2	0
3	2	2	3	3	1	3	3	E	19.6307677	–4.1	0
			4				4	E	19.6318930	–4.3	0
			2				2	E	19.6322857	–5.6	–2
4	0	4	5	3	0	3	4	E	22.5994180	–0.2	–1
			3				2	E	22.5994349	2.1	2
			4				3	E	22.5996245	1.1	0
4	0	4	4	3	1	3	3	E	19.3166586	2.6	0
			5				4	E	19.3168217	2.5	0
			3				2	E	19.3169644	1.8	–1
4	1	4	3	3	0	3	2	E	24.8719621	–1.6	0
			5				4	E	24.8720215	0.2	1
			4				3	E	24.8725078	0.8	2
4	1	4	5	3	1	3	4	E	21.5894238	1.5	1
			3				2	E	21.5894949	1.4	0
			4				3	E	21.5895406	0.9	0
4	1	3	3	3	1	2	2	E	25.3049649	–0.1	0
			5				4	E	25.3050256	0.8	1
			4				3	E	25.3051262	–4.3	–5
4	1	3	4	3	2	1	3	E	10.5781730	1.4	1
4	1	3	4	3	2	2	3	E	11.3291661	5.7	1
			5				4	E	11.3293800	6.2	1
			3				2	E	11.3294278	2.1	–3
4	2	2	3	3	2	1	2	E	24.6269345	–7.6	–6
			5				4	E	24.6269646	1.6	3
4	2	3	3	3	2	2	2	E	23.6471499	3.7	2
			5				4	E	23.6472120	2.7	1
			4				3	E	23.6474440	1.5	0
4	1	3	5	4	0	4	5	E	11.6444502	–1.8	0

			3				3	E	11.6447460	–8.3	–7
4	1	3	5	4	1	4	5	E	9.3718484	–0.5	–1
			3				3	E	9.3722205	–2.9	–3
4	2	2	3	4	1	3	3	E	14.0487909	–3.7	–1
5	1	4	6	4	1	3	5	E	31.3451985	2.4	2
			5				4	E	31.3453144	–0.3	–1
5	1	4	5	4	2	3	4	E	19.0270350	2.5	–1
			6				5	E	19.0273631	2.4	–1
			4				3	E	19.0274463	8.0	4
5	2	3	5	4	2	2	4	E	31.2786252	4.4	6
			6				5	E	31.2786695	–2.5	–1
5	3	2	4	4	3	1	3	E	30.0395541	3.6	5
			6				5	E	30.0395878	–4.8	–4
			5				4	E	30.0397285	–3.7	–3
5	3	3	4	4	3	2	3	E	30.0029986	4.0	6
			6				5	E	30.0030383	–2.9	–1
			5				4	E	30.0032046	1.3	4
5	1	4	5	5	0	5	5	E	15.3369332	–2.9	–1
			6				6	E	15.3381843	–2.4	0
6	0	6	7	5	0	5	6	E	32.5682859	–0.7	–2
			5				4	E	32.5683041	5.1	4
			6				5	E	32.5684463	1.1	0
6	0	6	6	5	1	5	5	E	31.1269069	3.1	1
			7				6	E	31.1269292	2.2	0
			5				4	E	31.1269776	1.2	–1
6	1	5	5	5	1	4	4	E	37.1509169	3.1	3
			7				6	E	37.1509425	–0.2	–1
			6				5	E	37.1510887	1.0	1
6	2	4	6	5	2	3	5	E	37.9348475	5.0	7
			5				4	E	37.9348747	0.3	2
6	1	5	6	5	2	4	5	E	26.8148129	3.1	0
			7				6	E	26.8151402	1.0	–2
			5				4	E	26.8152102	3.3	0
6	2	5	7	5	2	4	6	E	35.0092238	3.1	2
			6				5	E	35.0093366	0.9	0
6	3	3	5	5	3	2	4	E	36.3290782	6.5	1
			6				5	E	36.3291147	16.5	11
6	3	4	7	5	3	3	6	E	36.0623221	–5.9	4
			6				5	E	36.0624243	–10.6	–1
			5				4	E	36.0622891	–17.7	–8
6	1	5	6	6	0	6	6	E	19.9195752	–3.5	–1
			5				5	E	19.9210573	1.1	4
6	2	4	6	6	1	5	6	E	14.7658373	–6.8	–1
			7				7	E	14.7661991	–5.3	1
			5				5	E	14.7662597	–5.5	1
6	2	5	6	6	1	6	6	E	27.2620270	–4.2	–1
6	3	4	6	6	2	5	6	E	29.7969105	28.5	1
			7				7	E	29.7973628	34.3	7
			5				5	E	29.7974395	35.6	8
7	0	7	8	6	0	6	7	E	37.4514790	–1.6	–3
			6				5	E	37.4515017	6.9	6
			7				6	E	37.4516016	0.3	–1
7	0	7	8	6	1	6	7	E	36.5995071	–5.3	–8
7	1	7	6	6	0	6	5	E	37.9293543	–4.1	–4
			7				6	E	37.9295296	0.4	0
7	1	7	8	6	1	6	7	E	37.0773846	0.5	–1
			7				6	E	37.0774537	–2.2	–4
7	1	6	7	6	2	5	6	E	34.4667283	1.5	–1
			8				7	E	34.4670010	2.3	0

			6				5	E	34.4670488	–0.5	–3
7	2	6	7	7	1	7	7	E	30.7415978	–3.3	–1
			8				8	E	30.7424922	–2.5	0
			6				6	E	30.7426186	–4.9	–2
7	3	5	7	7	2	6	7	E	31.2639705	12.9	0
			8				8	E	31.2644356	13.9	1
			6				6	E	31.2645015	12.9	0
8	1	7	9	8	0	8	9	E	30.6392461	–2.6	–1
			7				7	E	30.6393892	0.1	2
8	2	7	8	8	1	8	8	E	34.6070781	–2.4	–1
			9				9	E	34.6079384	–0.7	1
			7				7	E	34.6080456	–1.7	0
9	1	8	9	9	0	9	9	E	36.1698095	–0.3	0
			10				10	E	36.1708091	–0.3	0
			8				8	E	36.1709167	–4.4	–4
9	2	8	9	9	1	9	9	E	38.7822475	–0.1	0
			10				10	E	38.7830666	0.0	0
			8				8	E	38.7831583	0.2	0

AII.3: ^{14}N Nuclear quadrupole coupling and methyl internal rotation in 3-methylpyrrole investigated by microwave spectroscopy

Table S-I: Nuclear coordinates in the principal inertial axes of 3-methylpyrrole calculated at the MP2/cc-pVDZ level of theory. The atoms are numbered according to Figure 1.

	a / Å	*b* / Å	*c* / Å
N_1	0.101161	1.097164	–0.000034
C_2	–0.731506	–0.008265	–0.000289
C_3	0.110677	–1.150889	–0.000059
C_4	1.421745	–0.713681	0.000037
C_5	1.396755	0.653579	0.000094
C_6	–2.226266	0.012097	0.000135
H_7	–0.204689	2.147878	–0.000104
H_8	1.778605	–2.180913	0.000179
H_9	2.350144	–1.256604	0.000254
H_{10}	2.208560	1.243954	–0.000068
H_{11}	–2.630789	–0.490713	0.878264
H_{12}	–2.631582	–0.487695	–0.879404
H_{13}	–2.599873	1.034786	0.002073

Figure S-II: The torsional potential function of the methyl group with respect to the molecular frame calculated at the MP2/cc-pVDZ level of theory.

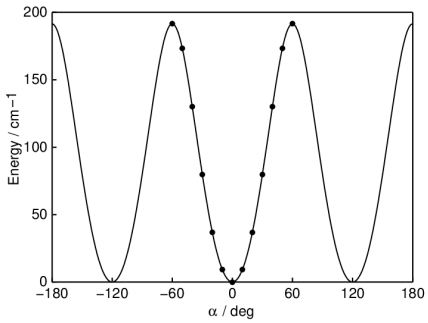

Table S-III: Fourier expansion of the potential energy curve given in Figure S2. The potential is expanded as $V(\alpha) = \sum_{i=0}^{5} a_i f_i$. Note that $V_{3i} = 2 \cdot a_i$.

i	f_i	a_i / Hartree	a_i / cm^{-1}
0	1	–248.7094793	
1	cos 3α	–0.0004323	–94.88
2	cos 6α	0.0000363	7.96
3	cos 9α	–0.0000041	–0.90
4	cos 12α	0.0000013	0.29

Table S-IV: Observed frequencies ($\nu_{obs.}$) of the A and E species of 3-methylpyrrole. $\nu_{calc.}$ are the calculated frequencies; $\nu_{obs.}-\nu_{calc.}$ values as obtained after a fit with the programs *XIAM* and *BELGI-C_s-hyperfine*. J, K_a, K_c are the asymmetric top rotational quantum numbers of the lower energy level; J', K_a', K_c' are those of the upper energy level. F is the total angular momentum in the coupled basis with $F = J + I$.

J'	K_a'	K_c'	F'	J	K_a	K_c	F		$\nu_{obs.}$	$\nu_{obs.} - \nu_{calc.}$	$\nu_{obs.} - \nu_{calc.}$
upper level				lower level					GHz	*XIAM* / MHz	*BELGI* / MHz
1	1	1	0	0	0	0	1	A	11.0894561	–0.0062	–0.001
			2				1	A	11.0900782	–0.0017	0.002
			1				1	A	11.0904876	–0.0041	–0.001
1	1	0	1	1	0	1	2	A	6.1977500	0.0017	0.003
			2				1	A	6.1981622	0.0022	0.003
			1				0	A	6.1983872	0.0018	0.004
2	1	1	3	1	1	0	2	A	12.4719750	–0.0011	0.005
			2				1	A	12.4723634	–0.0081	–0.002
			1				1	A	12.4730481	–0.0096	–0.004
2	1	2	1	1	0	1	1	A	15.9808595	–0.0017	0.004
			3				2	A	15.9817788	–0.0050	0.001
			1				0	A	15.9819141	–0.0090	–0.002
			2				1	A	15.9822375	–0.0178	–0.012
2	1	2	1	1	1	1	1	A	10.6786550	–0.0034	0.002
			3				2	A	10.6795672	–0.0009	0.004
			1				0	A	10.6796836	–0.0042	0.000
			2				1	A	10.6800468	–0.0058	0.000
2	1	1	3	2	0	2	3	A	7.1990188	–0.0053	–0.004
			1				1	A	7.1995779	0.0007	0.002
2	1	1	2	2	1	2	3	A	2.6883320	–0.0039	–0.002
			3				3	A	2.6887765	–0.0005	0.000
3	0	3	4	2	0	2	3	A	16.9556686	–0.0052	0.001
			2				1	A	16.9557219	–0.0076	–0.001
			3				2	A	16.9558322	–0.0078	–0.002
3	1	2	2	2	1	1	1	A	18.6384199	–0.0075	–0.001
			4				3	A	18.6385612	–0.0048	0.002
			3				2	A	18.6386962	–0.0068	0.000
			2				2	A	18.6391062	–0.0074	–0.002
3	1	2	3	3	1	3	4	A	5.3693409	–0.0051	–0.003
3	1	3	4	2	1	2	3	A	15.9576882	–0.0047	0.002
			2				1	A	15.9578070	–0.0068	–0.001
			3				2	A	15.9578684	–0.0055	0.001
			3				3	A	15.9587634	–0.0067	0.000
3	2	1	2	2	2	0	1	A	17.7714974	–0.0168	–0.010
			4				3	A	17.7717288	–0.0063	0.001

			3				2	A	17.7720311	–0.0097	–0.002
3	2	2	2	2	2	1	1	A	17.3633824	–0.0092	–0.003
			4				3	A	17.3636371	–0.0074	–0.001
			3				2	A	17.3640912	–0.0084	–0.001
3	1	2	2	3	1	3	2	A	5.3701350	0.0014	0.002
3	2	2	3	3	1	3	3	A	20.0001041	–0.0061	–0.002
			4				4	A	20.0011815	–0.0059	–0.002
			2				2	A	20.0015592	–0.0052	–0.001
4	0	4	5	3	0	3	4	A	22.1840759	–0.0054	0.000
			3				2	A	22.1840971	–0.0027	0.003
			4				3	A	22.1842645	–0.0051	0.000
4	0	4	4	3	1	3	3	A	18.6716425	–0.0042	0.001
			5				4	A	18.6718104	–0.0046	0.000
			3				2	A	18.6719538	–0.0046	0.000
4	1	4	3	3	0	3	2	A	24.6839692	–0.0060	0.001
			5				4	A	24.6840232	–0.0062	0.000
			4				3	A	24.6844950	–0.0056	0.000
4	1	3	5	3	2	2	4	A	10.0793908	–0.0129	–0.010
			4				3	A	10.0791916	–0.0092	–0.006
4	2	3	3	3	2	2	2	A	23.0701382	–0.0065	–0.001
			5				4	A	23.0701954	–0.0053	0.000
			4				3	A	23.0704158	–0.0027	0.003
4	3	2	3	3	3	1	2	A	23.3388709	–0.0082	–0.002
			4				3	A	23.3394036	–0.0089	–0.001
4	2	2	3	3	2	1	2	A	24.0372934	0.0019	0.008
			5				4	A	24.0373220	–0.0030	0.003
			4				3	A	24.0373579	–0.0076	–0.001
4	1	3	5	4	0	4	5	A	11.4087757	–0.0003	0.002
			3				3	A	11.4090625	0.0006	0.002
4	1	3	4	4	1	4	4	A	8.9074327	–0.0005	0.001
			5				5	A	8.9088268	–0.0011	0.000
			3				3	A	8.9091875	0.0009	0.002
4	2	2	5	4	1	3	5	A	14.4703013	–0.0076	–0.004
5	1	4	5	4	2	3	4	A	17.6491077	0.0039	0.002
			6				5	A	17.6494183	0.0014	–0.001
			4				3	A	17.6494973	0.0050	0.002
5	1	4	6	5	0	5	6	A	14.8710526	0.0012	0.002
			4				4	A	14.8712940	0.0009	0.001
5	1	4	6	5	1	5	6	A	13.2334896	0.0009	0.000
			4				4	A	13.2337723	0.0029	0.002
5	2	3	6	5	1	4	6	A	14.2960116	–0.0066	–0.001
			4				4	A	14.2960359	–0.0120	–0.007
			5				5	A	14.2958566	–0.0157	–0.011
5	2	4	6	5	1	5	6	A	24.2920737	–0.0046	–0.002
			4				4	A	24.2922606	–0.0060	–0.003
6	1	5	6	6	0	6	6	A	19.2091273	0.0029	0.000
			7				7	A	19.2103407	0.0049	0.001
			5				5	A	19.2105419	0.0016	–0.002
6	2	4	6	6	1	5	6	A	14.8739777	–0.0061	0.000
			7				7	A	14.8742877	–0.0047	0.001
			5				5	A	14.8743368	–0.0077	–0.002
6	2	4	6	6	2	5	6	A	5.9196998	–0.0004	0.001
			7				7	A	5.9204436	–0.0000	0.000
			5				5	A	5.9205698	0.0007	0.001
6	5	2	5	7	4	3	6	A	10.3573436	–0.0138	0.003
7	2	5	7	7	1	6	7	A	16.3928109	–0.0051	0.000
			8				8	A	16.3932813	–0.0044	0.001
			6				6	A	16.3933491	–0.0044	0.001
8	2	6	8	8	1	7	8	A	18.9791695	–0.0015	0.000

			9				9	A	18.9797844	–0.0022	–0.001
			7				7	A	18.9798638	–0.0003	0.001
1	1	0	1	0	0	0	1	E	12.0087124	0.0094	0.004
			2				1	E	12.0094934	0.0080	0.003
			0				1	E	12.0106650	0.0057	0.001
1	1	1	2	0	0	0	1	E	11.0281890	–0.0097	0.001
			1				1	E	11.0285462	–0.0102	0.000
1	1	1	2	1	0	1	1	E	5.2398956	–0.0069	0.002
			2				2	E	5.2403169	–0.0104	0.000
			1				2	E	5.2406744	–0.0105	–0.001
2	0	2	1	1	1	1	1	E	6.2301897	0.0083	–0.001
			3				2	E	6.2308586	0.0114	0.002
			2				1	E	6.2310522	0.0080	0.000
			1				0	E	6.2310867	0.0109	0.000
			2				2	E	6.2314097	0.0079	–0.001
2	1	1	1	1	1	0	0	E	12.4433201	–0.0036	0.002
			2				2	E	12.4438154	–0.0073	–0.001
			3				2	E	12.4442517	–0.0049	0.001
2	1	2	3	1	0	1	2	E	15.9476409	–0.0030	0.002
			2				1	E	15.9481072	–0.0009	0.003
2	1	2	3	1	1	1	2	E	10.7073244	0.0078	0.003
			2				1	E	10.7078532	0.0052	0.001
			2				2	E	10.7082104	0.0048	0.000
2	1	1	2	2	0	2	2	E	7.1937098	0.0022	0.002
			3				2	E	7.1941461	0.0047	0.004
			2				3	E	7.1942604	–0.0018	–0.001
			1				2	E	7.1943859	0.0034	0.002
			3				3	E	7.1946975	0.0014	0.001
2	1	1	2	2	1	2	3	E	2.7177939	0.0011	–0.003
			3				3	E	2.7182297	0.0030	–0.002
			2				1	E	2.7182924	0.0057	0.002
2	2	1	2	2	1	2	2	E	18.2035096	–0.0041	0.000
			3				2	E	18.2040069	–0.0059	–0.002
			1				2	E	18.2042804	–0.0098	–0.005
			2				3	E	18.2043944	–0.0083	–0.005
			3				3	E	18.2048939	–0.0079	–0.003
			1				1	E	18.2056687	–0.0043	0.001
2	2	0	2	2	1	1	1	E	16.2846199	0.0120	0.001
			2				3	E	16.2848600	0.0110	0.000
			2				2	E	16.2852941	0.0113	–0.001
			3				3	E	16.2853718	0.0123	0.002
			1				1	E	16.2854034	0.0012	–0.008
			3				2	E	16.2858062	0.0128	0.002
			1				2	E	16.2860884	0.0113	0.001
2	2	0	2	2	1	2	2	E	19.0022050	0.0184	0.003
			3				2	E	19.0027134	0.0162	0.001
			1				2	E	19.0029980	0.0171	0.003
			2				3	E	19.0030924	0.0168	0.001
			3				3	E	19.0036018	0.0156	0.001
			1				1	E	19.0043818	0.0180	0.004
2	2	1	2	2	1	1	1	E	15.4859247	–0.0103	–0.002
			2				3	E	15.4861648	–0.0112	–0.003
			2				2	E	15.4865991	–0.0108	–0.003
			3				3	E	15.4866645	–0.0107	–0.002
3	0	3	2	2	0	2	2	E	16.9534827	0.0027	0.000
			4				3	E	16.9542894	0.0023	0.001
			2				1	E	16.9543439	0.0011	0.000
			3				2	E	16.9544557	0.0019	0.001
3	0	3	2	2	1	2	2	E	12.4766818	0.0055	–0.001

			3				2	E	12.4776554	0.0053	0.000
			4				3	E	12.4778238	0.0061	0.000
			2				1	E	12.4780652	0.0061	0.000
3	1	3	2	2	0	2	2	E	20.4403701	0.0008	0.002
			2				1	E	20.4412299	–0.0022	0.000
			4				3	E	20.4413014	0.0011	0.003
			3				2	E	20.4418217	0.0007	0.002
			3				3	E	20.4423751	–0.0006	0.001
3	1	2	4	2	1	1	3	E	18.6310219	–0.0015	–0.001
			3				2	E	18.6311546	–0.0006	0.000
			2				2	E	18.6315630	–0.0000	0.000
3	1	2	3	2	2	1	2	E	3.1445528	0.0075	0.001
3	1	3	4	2	1	2	3	E	15.9648352	0.0043	0.001
			2				1	E	15.9649515	0.0031	0.000
			3				2	E	15.9650199	0.0026	0.000
3	2	1	2	2	2	0	1	E	17.6379894	–0.0066	–0.006
			4				3	E	17.6382133	0.0006	0.002
			3				2	E	17.6385300	–0.0019	0.000
3	2	1	4	2	2	1	3	E	18.4369208	0.0238	0.005
			3				2	E	18.4372250	0.0201	0.003
			2				2	E	18.4374844	0.0212	0.004
3	2	2	2	2	2	1	1	E	17.4983638	0.0028	0.000
			3				3	E	17.4985635	0.0036	0.001
			4				3	E	17.4986232	0.0052	0.003
			3				2	E	17.4990612	0.0021	0.001
3	1	2	3	3	0	3	3	E	8.8704080	–0.0009	0.001
			4				4	E	8.8714322	–0.0002	0.002
			2				2	E	8.8717909	0.0003	0.002
3	1	2	3	3	1	3	4	E	5.3841116	–0.0055	–0.005
			4				4	E	5.3844181	–0.0011	–0.002
3	2	1	2	3	1	2	2	E	15.2925222	0.0122	0.002
			4				4	E	15.2925598	0.0110	0.001
			3				3	E	15.2926706	0.0110	0.000
3	2	2	2	3	1	2	2	E	14.3541766	–0.0077	–0.001
			4				4	E	14.3542632	–0.0065	0.000
			3				3	E	14.3545075	–0.0063	–0.001
3	2	2	3	3	1	3	3	E	19.7375497	–0.0058	–0.001
			4				4	E	19.7386897	0.0008	0.006
			2				2	E	19.7390798	–0.0058	–0.001
4	0	4	3	3	0	3	3	E	22.1801678	0.0052	0.000
			5				4	E	22.1811219	0.0040	–0.001
			4				3	E	22.1813112	0.0046	0.000
4	0	4	4	3	1	3	3	E	18.6939455	0.0061	–0.001
			5				4	E	18.6941117	0.0069	–0.001
			3				2	E	18.6942539	0.0068	–0.001
4	1	3	3	3	1	2	2	E	24.7071308	0.0033	–0.001
			5				4	E	24.7071849	0.0036	0.000
			4				3	E	24.7072850	0.0035	0.000
4	1	4	3	3	0	3	2	E	24.6611006	0.0026	0.000
			5				4	E	24.6611554	0.0036	0.001
			4				3	E	24.6616254	0.0037	0.001
4	1	4	5	3	1	3	4	E	21.1741443	0.0056	0.000
			3				2	E	21.1742140	0.0053	0.000
			4				3	E	21.1742594	0.0049	0.000
4	1	3	4	3	2	2	3	E	10.3527783	0.0106	0.002
			5				4	E	10.3529220	0.0104	0.000
			3				2	E	10.3529501	0.0069	–0.003
4	2	3	3	3	2	1	2	E	22.2497110	–0.0077	0.000
			5				4	E	22.2498260	–0.0091	–0.001

			4				3	E	22.2502101	–0.0088	–0.001
4	2	3	3	3	2	2	3	E	23.1881243	0.0015	–0.007
			4				3	E	23.1883732	0.0085	0.001
4	3	1	3	3	3	0	2	E	23.3611442	0.0052	0.001
			5				4	E	23.3612976	0.0059	0.002
			4				3	E	23.3616642	0.0033	0.000
4	3	2	3	3	3	1	2	E	23.3635918	0.0049	0.002
			5				4	E	23.3637461	0.0063	0.004
			4				3	E	23.3641123	0.0032	0.001
4	1	3	5	4	0	4	5	E	11.3974940	–0.0017	0.001
			3				3	E	11.3977814	–0.0003	0.003
4	1	3	4	4	1	4	4	E	8.9160668	–0.0019	–0.001
			5				5	E	8.9174608	–0.0010	0.000
			3				3	E	8.9178210	0.0009	0.001
4	2	2	5	4	1	3	5	E	14.5072946	0.0109	0.005
4	2	3	3	4	1	3	3	E	12.8350985	–0.0027	–0.001
			5				5	E	12.8352016	–0.0010	0.001
			4				4	E	12.8355964	–0.0006	0.000
4	2	3	4	4	1	4	4	E	21.7516642	–0.0014	0.001
			5				5	E	21.7526605	–0.0039	–0.002
			3				3	E	21.7529220	0.0007	0.003
5	0	5	5	4	1	4	4	E	24.6933570	0.0097	–0.003
			6				5	E	24.6934543	0.0081	–0.005
			4				3	E	24.6935390	0.0090	–0.004
5	1	4	5	4	2	3	4	E	17.8012239	0.0085	–0.004
			6				5	E	17.8015103	0.0082	–0.005
			4				3	E	17.8015825	0.0117	–0.001
5	1	4	6	5	0	5	6	E	14.8607187	–0.0017	0.001
			4				4	E	14.8609612	–0.0009	0.001
5	1	4	6	5	1	5	6	E	13.2382151	–0.0028	–0.003
			4				4	E	13.2384986	0.0003	0.000
5	2	3	5	5	1	4	5	E	14.2884458	0.0048	0.002
			6				6	E	14.2885845	0.0040	0.001
			4				4	E	14.2886118	0.0029	0.000
6	2	4	6	5	3	2	5	E	10.0149930	0.0522	0.010
			7				6	E	10.0151786	0.0532	0.010
			5				4	E	10.0152035	0.0500	0.006
6	2	4	6	5	3	3	5	E	11.1993310	–0.0707	–0.002
			7				6	E	11.1995267	–0.0683	–0.001
			5				4	E	11.1995498	–0.0751	–0.008
6	2	4	6	6	1	5	6	E	14.8542811	0.0034	0.002
			7				7	E	14.8545893	0.0040	0.003
			5				5	E	14.8546397	0.0025	0.001
7	2	5	7	7	1	6	7	E	16.3737408	0.0034	0.002
			8				8	E	16.3742113	0.0034	0.001
			6				6	E	16.3742795	0.0038	0.002
7	2	5	7	7	2	6	7	E	9.5933765	–0.0008	–0.004
			8				8	E	9.5942338	0.0097	0.006
			6				6	E	9.5943393	–0.0069	–0.010
8	2	6	8	8	1	7	8	E	18.9663856	0.0043	–0.001
			9				9	E	18.9670047	0.0065	0.001
			7				7	E	18.9670818	0.0059	0.000

AIII.1: Local versus global approaches to treat two equivalent methyl internal rotations and ^{14}N nuclear quadrupole coupling of 2,5-dimethylpyrrole

Table S-I. Nuclear coordinates in the principal inertial axes of 2,5-dimethylpyrrole calculated at the MP2/cc-pVDZ level of theory. The atoms are numbered according to Fig. 1.

	a /Å	*b* /Å	*c* /Å
N_1	0.000035	0.828587	−0.000082
C_2	1.140181	0.049411	0.000038
C_3	0.714151	−1.279657	−0.000116
C_4	−0.714237	−1.279613	0.000053
C_5	−1.140165	0.049437	−0.000102
C_6	2.512975	0.648650	0.000103
C_7	−2.512979	0.648714	0.000058
H_8	0.000071	1.843068	−0.000442
H_9	1.373890	−2.148264	0.000131
H_{10}	−1.373980	−2.148243	0.000257
H_{11}	2.693582	1.272752	0.893677
H_{12}	2.691606	1.276869	−0.891018
H_{13}	3.265139	−0.155078	−0.002676
H_{14}	−2.691231	1.276629	0.891409
H_{15}	−3.265295	−0.154970	0.002831
H_{16}	−2.693397	1.272893	−0.893445

Table S-II. Coefficients of the two-dimensional Fourier expansion for the potential energy surfaces calculated with the MP2/cc-pVDZ level of theory as illustrated in Fig. 4 **a**, **b**, **c**. Due to symmetry, only data points in the range from $\alpha_1 = -60°$ to 60° and $\alpha_2 = -60°$ to 60° are needed. The potential is expanded as $\boldsymbol{V(\alpha_1, \alpha_2) = \sum_i f_i V_i}$. Max. dev. stands for maximum deviations between the fitted values (depicted in the figures) and the calculated values from *ab initio* calculations.

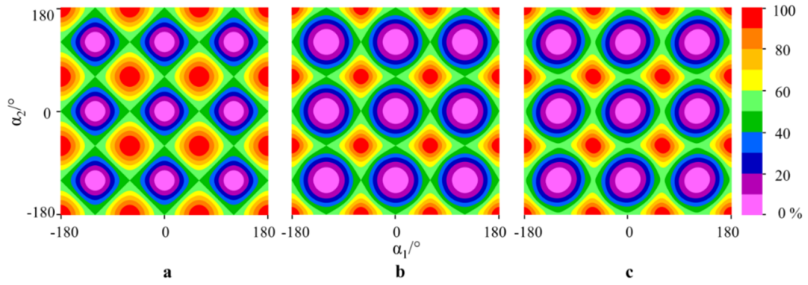

		a	b	c
i	f_i	V_i / Hartree	V_i / Hartree	V_i / Hartree
1	1	−287.896560835	−287.8965762	−287.8965763
2	$\cos(3\alpha_1) + \cos(3\alpha_2)$	−0.000654670	−0.0006393	−0.0006402
3	$\cos(6\alpha_1) + \cos(6\alpha_2)$		0.0000970	0.0000970
4	$\cos(9\alpha_1) + \cos(9\alpha_2)$		−0.0000182	−0.0000182
5	$\cos(3\alpha_1)\cos(3\alpha_2)$			−0.0000120
6	$\sin(3\alpha_1)\sin(3\alpha_2)$			−0.0000679
	Max. dev. (%)	10.0	2.8	1.1

Table S-III. Character table G_{36} of the molecular symmetry includes the spin statistical weights of 25DMP.

G_{36}			E	a^{-1}	ab	ab^{-1}	P	bP	Q	aQ	R	
Equiv. rot.[a]			R^0	R^0	R^0	R^0	R_b^0	R_b^0	R_a^0	R_a^0	R_c^0	
S1[b]	S2[c]	S3[d]	1[f]	4	2	2	3	6	3	6	9	wt
(00)·A_1	A_1	A_1A_1	1	1	1	1	1	1	1	1	1	216
(00)·B_1	A_2	A_2A_1	1	1	1	1	−1	−1	1	1	−1	168
(00)·A_2	A_3	A_1A_2	1	1	1	1	1	1	−1	−1	−1	216
(00)·B_2	A_4	A_2A_2	1	1	1	1	−1	−1	−1	−1	1	168
(12)·A′	E_1	E A_1	2	−1	2	−1	0	0	2	−1	0	96
(12)·A″	E_2	E A_2	2	−1	2	−1	0	0	−2	1	0	96
(11)·A	E_3	A_1E	2	−1	−1	2	2	−1	0	0	0	120
(11)·B	E_4	A_2E	2	−1	−1	2	−2	1	0	0	0	72
(01)·A	G	EE	4	1	−2	−2	0	0	0	0	0	384

a = (11 12 13); b = (14 15 16); R = (12 13)(15 16)*

P = (11 14)(12 16)(13 15)(9 10)(2 5)(3 4)

Q = (11 14)(12 15)(13 16)(9 10)(2 5)(3 4)*

[a] Equivalent rotations of the four-group.

[b] Symmetry labels based on the semi-direct product.[1]

[c] Symmetry labels following Ref. [2].

[d] Symmetry labels as written based on the direct product.[3]

[f] Number of elements in each class

[g] Spin statistical weight.

References

[1] G. S. Ezra, Symmetry Properties of Molecules, Lecture Notes in Chemistry 28, Springer-Verlag, Berlin, Heidelberg, New York, 1982.

[2] P. R. Bunker and P. Jensen, Molecular Symmetry and Spectroscopy, NRC Research Press, Ottawa, Ontario, Canada, 2006.

[3] H. Dreizler, Z. Naturforsch., 1961, 16a, 1354.

Table S-IV. Observed frequencies ($\nu_{obs.}$) of the 4 torsional species of 2,5-dimethylpyrrole. The names of the torsional species are given in column ***sym***. $\nu_{calc.}$ are the calculated frequencies; $\nu_{obs.}-\nu_{calc.}$ values (given in kHz) as obtained after a fit with the programs *WS18*, *XIAM* and *BELGI-C_{2v}-2Tops-hyperfine*. ***J***, ***K_a***, ***K_c*** are the asymmetric top rotational quantum numbers of the lower energy level; ***J'***, ***K_a'***, ***K_c'*** are those of the upper energy level. *F* is the total angular momentum in the coupled basis with $F = J + I$, ***F'*** corresponds to upper level, ***F*** corresponds to lower level.

J'	***K_a'***	***K_c'***	***J***	***K_a***	***K_c***	***F'***	***F***	***sym***	$\nu_{obs.}$	$\nu_{obs.} - \nu_{calc.}$	$\nu_{obs.} - \nu_{calc.}$	$\nu_{obs.} - \nu_{calc.}$
upper level			lower level						*GHz*	*WS18*	*XIAM*	*BELGI*
1	1	1	0	0	0	0	1	(00)	7.850898	−2	0.1	0
1	1	1	0	0	0	2	1	(00)	7.851644	1	1.4	1
1	1	1	0	0	0	1	1	(00)	7.852135	−3	−3.7	−4
1	1	0	1	0	1	1	0	(00)	4.737367	−7	−7.1	−8
2	1	2	1	0	1	2	2	(00)	10.966801	−3	−3.2	−3
2	1	2	1	0	1	2	1	(00)	10.966406	−1	−0.7	−1
2	1	2	1	0	1	2	2	(00)	10.966801	−3	−3.3	−3
2	1	2	1	0	1	2	1	(00)	10.966414	8	8.2	8
2	2	0	1	1	1	2	1	(00)	20.934995	2	3.2	1
2	2	0	1	1	1	2	2	(00)	20.935486	−3	−2.4	−5
2	2	0	1	1	1	1	1	(00)	20.935775	5	5.0	3
2	2	0	1	1	1	3	2	(00)	20.935986	−2	−2.4	−4
2	2	1	1	1	0	2	2	(00)	20.440364	1	1.1	0
2	2	1	1	1	0	3	2	(00)	20.440792	3	2.0	1
2	2	1	1	1	0	2	1	(00)	20.441265	10	7.7	6
2	2	0	2	1	1	2	3	(00)	12.867403	0	−2.8	−4
2	2	0	2	1	1	1	1	(00)	12.867888	2	−1.4	−2
2	2	0	2	1	1	3	3	(00)	12.867896	−8	−11.0	−12
2	2	0	2	1	1	2	2	(00)	12.867927	−8	−11.3	−13
3	0	3	2	1	2	3	2	(00)	6.730023	−1	2.1	3
3	0	3	2	1	2	4	3	(00)	6.730345	−5	−2.9	−2
3	2	2	2	1	1	2	1	(00)	23.554693	−2	−1.6	−2
3	2	2	2	1	1	4	3	(00)	23.554991	2	1.2	1
3	2	2	2	1	1	3	2	(00)	23.555520	0	−1.7	−2
3	2	1	3	1	2	3	2	(00)	12.339742	6	5.7	5
3	2	1	3	1	2	2	2	(00)	12.339985	−5	−5.9	−7
3	2	1	3	1	2	4	4	(00)	12.340074	4	3.3	2
3	2	1	3	1	2	3	3	(00)	12.340291	−5	−6.3	−8
4	0	4	3	1	3	4	3	(00)	10.675581	−3	−1.5	−1
4	0	4	3	1	3	5	4	(00)	10.675919	−2	−1.4	−1
4	0	4	3	1	3	3	2	(00)	10.676112	0	−0.1	0
4	2	2	4	1	3	3	3	(00)	11.807907	2	4.6	3
4	2	2	4	1	3	5	5	(00)	11.807953	−3	−0.7	−2
4	2	2	4	1	3	4	4	(00)	11.808158	1	3.3	2
5	0	5	4	1	4	5	4	(00)	14.586956	−1	−2.8	−2
5	0	5	4	1	4	6	5	(00)	14.587227	0	−3.0	−2
5	0	5	4	1	4	4	3	(00)	14.587349	1	−2.1	−2
5	2	3	5	1	4	5	5	(00)	11.399767	−2	3.9	1
6	0	6	5	1	5	6	5	(00)	18.394872	1	−3.3	−2
6	0	6	5	1	5	7	6	(00)	18.395057	0	−4.2	−3
6	0	6	5	1	5	5	4	(00)	18.395135	1	−3.1	−2
7	0	7	6	1	6	7	6	(00)	22.062666	1	−1.2	0
7	0	7	6	1	6	8	7	(00)	22.062772	−1	−3.9	−3
7	0	7	6	1	6	6	5	(00)	22.062822	0	−3.5	−3
1	1	1	0	0	0	0	1	(01)	7.843639	−1	−1.8	0
1	1	1	0	0	0	2	1	(01)	7.844366	1	−0.4	1
2	2	0	1	1	0	2	2	(01)	20.535909	−3	6.3	−1
2	2	0	1	1	0	3	2	(01)	20.536382	0	8.5	1
2	2	0	1	1	0	2	1	(01)	20.536797	4	12.1	4
2	2	0	1	1	0	1	1	(01)	20.537522	−2	5.1	−2

2	2	0	1	1	0	1	0	(01)	20.535323	1	10.1	2
2	2	0	1	1	1	2	1	(01)	21.004131	−1	11.6	1
2	2	0	1	1	1	2	2	(01)	21.004616	0	12.9	2
2	2	0	1	1	1	3	2	(01)	21.005084	−2	10.0	−1
2	1	2	1	0	1	3	2	(01)	10.961458	1	−0.2	1
2	1	2	1	0	1	1	0	(01)	10.961521	−1	−2.4	−1
2	2	1	1	1	0	1	0	(01)	20.352998	1	−8.6	2
2	2	1	1	1	0	2	2	(01)	20.353608	−2	−11.3	0
2	2	1	1	1	0	3	2	(01)	20.354067	1	−9.5	2
2	2	1	1	1	0	2	1	(01)	20.354494	3	−7.7	3
2	2	1	1	1	1	2	1	(01)	20.821829	0	−6.9	1
2	2	1	1	1	1	3	2	(01)	20.822767	−1	−9.0	−1
2	2	1	1	1	1	1	0	(01)	20.823750	3	−5.0	3
2	1	1	2	0	2	2	2	(01)	5.230125	−1	2.0	1
2	1	1	2	0	2	2	1	(01)	5.230908	4	5.9	5
2	1	1	2	0	2	1	2	(01)	5.230949	−2	1.0	0
2	1	1	2	0	2	3	3	(01)	5.231154	−2	0.2	−1
2	1	1	2	0	2	1	1	(01)	5.231731	3	4.3	3
2	2	0	2	1	1	2	1	(01)	12.930646	4	14.0	6
2	2	0	2	1	1	2	3	(01)	12.930939	3	12.9	5
2	2	0	2	1	1	2	2	(01)	12.931469	2	11.7	4
2	2	1	2	1	1	3	3	(01)	12.749094	5	−5.3	6
2	2	1	2	1	1	2	2	(01)	12.749159	−5	−14.5	−4
2	2	1	2	1	2	2	2	(01)	14.130288	0	−5.9	3
2	2	1	2	1	2	3	2	(01)	14.130751	7	0.2	9
2	2	1	2	1	2	1	2	(01)	14.130996	−2	−9.0	0
2	2	1	2	1	2	2	3	(01)	14.131244	−1	−7.1	2
2	2	1	2	1	2	3	3	(01)	14.131697	−3	−10.6	−2
2	2	1	2	1	2	1	1	(01)	14.132485	0	−8.5	1
3	1	3	2	0	2	4	3	(01)	13.860499	1	−0.9	0
3	1	3	2	0	2	3	2	(01)	13.861125	1	−1.5	0
3	1	3	2	0	2	2	1	(01)	13.860374	−8	−9.4	−8
3	2	1	3	1	2	4	4	(01)	12.368335	3	9.0	4
3	2	1	3	1	2	3	3	(01)	12.368584	−3	3.3	−2
3	3	0	3	2	1	3	3	(01)	22.466450	3	1.4	4
3	3	0	3	2	1	4	4	(01)	22.466859	−4	−6.2	−3
3	3	1	3	2	2	3	3	(01)	22.448400	1	5.7	2
3	3	1	3	2	2	4	4	(01)	22.448945	−2	2.0	−2
4	1	4	3	0	3	3	2	(01)	16.588876	1	−1.6	0
4	1	4	3	0	3	5	4	(01)	16.588970	0	−2.3	−1
4	1	4	3	0	3	4	3	(01)	16.589570	0	−2.4	−1
4	0	4	3	1	3	4	3	(01)	10.678607	1	0.0	0
4	0	4	3	1	3	5	4	(01)	10.678943	−1	−1.6	−2
4	0	4	3	1	3	3	2	(01)	10.679137	2	0.7	0
4	2	2	4	1	3	5	5	(01)	11.814057	0	3.0	0
4	2	2	4	1	3	3	3	(01)	11.814001	−2	0.5	−2
4	3	1	4	2	2	4	4	(01)	22.247700	2	3.2	3
4	3	1	4	2	2	5	5	(01)	22.247786	−4	−3.0	−3
5	0	5	4	1	4	5	4	(01)	14.589330	−1	−1.4	−2
5	0	5	4	1	4	6	5	(01)	14.589601	−1	−1.5	−2
5	0	5	4	1	4	4	3	(01)	14.589723	1	−0.2	0
5	1	5	4	0	4	4	3	(01)	19.216183	−2	−4.8	−3
5	1	5	4	0	4	6	5	(01)	19.216251	1	−1.7	0
5	1	5	4	0	4	5	4	(01)	19.216774	0	−2.6	−1
5	1	4	4	2	3	5	4	(01)	7.576386	3	6.5	1
5	1	4	4	2	3	6	5	(01)	7.576833	−1	2.3	−4
5	1	4	5	0	5	6	6	(01)	8.845258	0	4.6	3
5	1	4	5	0	5	4	4	(01)	8.845506	0	4.5	2
5	2	3	5	1	4	4	4	(01)	11.398050	−7	−5.9	−9
5	2	3	5	1	4	6	6	(01)	11.398076	2	3.2	0
5	2	3	5	1	4	5	5	(01)	11.398162	1	2.7	0
5	2	4	5	1	5	6	6	(01)	17.074647	−2	0.6	5
5	2	4	5	1	5	4	4	(01)	17.074848	−2	0.3	4
5	3	3	5	2	3	6	6	(01)	21.539404	−1	−7.7	3
5	3	3	5	2	3	5	5	(01)	21.539531	0	−6.3	5
5	3	2	5	2	4	5	5	(01)	22.983592	0	7.4	−2
5	3	2	5	2	4	6	6	(01)	22.983966	−1	5.9	−3
5	3	2	5	2	4	4	4	(01)	22.984044	2	8.2	−1

5	3	2	5	2	3	6	6	(01)	21.809493	1	2.9	3
5	3	2	5	2	3	5	5	(01)	21.809614	1	3.4	4
5	3	3	5	2	4	5	5	(01)	22.713509	−1	−2.9	−2
5	3	3	5	2	4	6	6	(01)	22.713879	0	−2.9	−1
5	3	3	5	2	4	4	4	(01)	22.713956	2	−0.7	1
6	1	6	5	0	5	5	4	(01)	21.821597	3	0.8	2
6	1	6	5	0	5	7	6	(01)	21.821632	0	−2.4	−1
6	1	6	5	0	5	6	5	(01)	21.822056	1	−2.0	−1
6	0	6	5	1	5	6	5	(01)	18.396670	0	−0.7	−1
6	0	6	5	1	5	7	6	(01)	18.396854	−1	−1.7	−2
6	0	6	5	1	5	5	4	(01)	18.396932	0	−0.6	−1
7	0	7	6	1	6	7	6	(01)	22.063928	0	−0.1	0
7	0	7	6	1	6	8	7	(01)	22.064036	0	−0.5	0
7	0	7	6	1	6	6	5	(01)	22.064086	−1	−0.9	−1
7	1	6	7	0	7	8	8	(01)	13.513548	1	5.4	9
7	1	6	7	0	7	6	6	(01)	13.513740	0	4.1	8
7	3	4	7	2	5	8	8	(01)	20.247846	0	1.1	6
7	3	4	7	2	5	7	7	(01)	20.248166	1	1.6	6
7	3	5	7	2	6	7	7	(01)	23.549718	0	−2.4	−4
7	3	5	7	2	6	8	8	(01)	23.550104	1	−1.5	−4
7	3	5	7	2	6	6	6	(01)	23.550158	0	−3.4	−5
8	1	7	7	2	6	8	7	(01)	21.815083	−1	−0.7	−2
8	1	7	7	2	6	9	8	(01)	21.815519	0	−0.5	−2
8	1	7	7	2	6	7	6	(01)	21.815585	1	0.8	−1
2	1	2	1	0	1	1	1	(11)	10.959072	1	1.8	1
2	1	2	1	0	1	1	2	(11)	10.959468	−2	−1.0	−1
2	1	2	1	0	1	3	2	(11)	10.960003	1	1.9	2
2	1	2	1	0	1	1	0	(11)	10.960068	2	1.8	2
2	2	0	1	1	1	2	1	(11)	20.917350	5	6.2	4
2	2	0	1	1	1	2	2	(11)	20.917838	−4	−2.2	−4
2	2	0	1	1	1	3	2	(11)	20.918344	1	2.5	1
2	2	1	1	1	0	1	0	(11)	20.422084	−1	−2.7	−4
2	2	1	1	1	0	2	2	(11)	20.422765	−1	−0.3	−1
2	2	1	1	1	0	3	2	(11)	20.423194	1	1.8	1
2	2	1	1	1	0	2	1	(11)	20.423663	1	2.9	2
2	2	1	1	1	0	1	1	(11)	20.424327	3	3.8	3
2	2	1	2	1	2	2	2	(11)	14.193669	0	3.1	0
2	1	1	2	0	2	3	3	(11)	5.226832	−2	1.0	−1
2	2	1	2	1	2	3	2	(11)	14.194097	2	2.7	1
2	2	1	2	1	2	1	2	(11)	14.194332	−1	0.1	−2
2	2	1	2	1	2	2	3	(11)	14.194625	−4	−1.6	−3
2	2	1	2	1	2	3	3	(11)	14.195055	0	2.1	1
3	1	3	2	0	2	2	1	(11)	13.858258	−5	−3.7	−4
3	1	3	2	0	2	4	3	(11)	13.858381	1	2.8	2
3	1	3	2	0	2	3	2	(11)	13.859008	−1	2.4	2
3	2	1	3	1	2	2	2	(11)	12.322999	−6	−8.3	−8
3	2	1	3	1	2	4	4	(11)	12.323088	3	1.1	1
3	2	1	3	1	2	3	3	(11)	12.323313	1	0.4	1
3	2	2	3	1	3	3	3	(11)	14.904690	0	1.1	−1
3	2	2	3	1	3	4	4	(11)	14.905817	0	1.4	0
3	2	2	3	1	3	2	2	(11)	14.906212	−1	1.2	0
4	1	4	3	0	3	3	2	(11)	16.586578	−1	1.3	0
4	1	4	3	0	3	5	4	(11)	16.586676	1	4.0	3
4	1	4	3	0	3	4	3	(11)	16.587276	0	3.8	3
4	0	4	3	1	3	4	3	(11)	10.680117	0	−3.8	−2
4	0	4	3	1	3	5	4	(11)	10.680456	−1	−3.1	−2
4	0	4	3	1	3	3	2	(11)	10.680649	1	−0.9	1
4	0	4	3	1	3	4	4	(11)	10.681245	−1	−3.6	−2
4	2	2	4	1	3	3	3	(11)	11.791474	0	−0.5	−1
4	2	2	4	1	3	5	5	(11)	11.791526	1	0.2	−1
4	2	2	4	1	3	4	4	(11)	11.791728	2	2.0	1
5	0	5	4	1	4	5	4	(11)	14.590796	0	−2.6	−1
5	0	5	4	1	4	6	5	(11)	14.591066	−1	−3.1	−2
5	0	5	4	1	4	4	3	(11)	14.591188	0	−1.7	0
5	1	5	4	0	4	4	3	(11)	19.213919	0	4.0	3
5	1	5	4	0	4	6	5	(11)	19.213986	2	6.2	5
5	1	5	4	0	4	5	4	(11)	19.214508	0	4.6	4

5	2	3	5	1	4	4	4	(11)	11.384116	−7	−5.1	−9
5	2	3	5	1	4	6	6	(11)	11.384142	2	4.4	1
5	2	3	5	1	4	5	5	(11)	11.384225	2	4.5	1
5	2	4	5	1	5	5	5	(11)	17.070780	2	−1.2	0
5	2	4	5	1	5	6	6	(11)	17.071770	1	−0.8	1
5	2	4	5	1	5	4	4	(11)	17.071970	−1	−2.8	−1
6	0	6	5	1	5	6	5	(11)	18.397885	0	−0.8	1
6	0	6	5	1	5	7	6	(11)	18.398069	−1	−1.7	0
6	0	6	5	1	5	5	4	(11)	18.398147	0	−0.6	1
7	0	7	6	1	6	7	6	(11)	22.064813	1	1.7	3
7	0	7	6	1	6	8	7	(11)	22.064921	0	1.2	2
7	0	7	6	1	6	6	5	(11)	22.064969	−1	−0.1	1
1	1	0	0	0	0	1	1	(12)	8.321774	1	1.1	1
1	1	0	0	0	0	2	1	(12)	8.322620	1	0.8	0
1	1	1	0	0	0	0	1	(12)	7.828206	1	−0.5	0
1	1	1	0	0	0	2	1	(12)	7.828881	4	1.1	2
1	1	1	0	0	0	1	1	(12)	7.829324	−1	−5.2	−5
1	1	0	1	0	1	2	1	(12)	4.748288	−3	−3.6	−4
1	1	0	1	0	1	1	0	(12)	4.748441	−2	0.3	0
1	1	0	1	0	1	2	2	(12)	4.748691	0	0.6	0
1	1	0	1	0	1	1	1	(12)	4.747439	−5	−5.3	−6
1	1	0	1	0	1	1	2	(12)	4.747845	1	1.6	1
2	1	2	1	0	1	3	2	(12)	10.954166	2	0.6	1
2	1	2	1	0	1	1	0	(12)	10.954231	−2	−2.1	−1
2	1	2	1	0	1	2	1	(12)	10.954716	−2	−4.1	−4
2	1	2	1	0	1	2	2	(12)	10.955118	2	0.0	1
2	2	0	1	1	1	2	1	(12)	21.096392	2	−1.6	3
2	2	0	1	1	1	2	2	(12)	21.096836	−1	−5.7	−1
2	2	0	1	1	1	3	2	(12)	21.097305	0	−4.0	1
2	2	1	1	1	0	3	2	(12)	20.244231	3	6.2	1
2	2	1	1	1	0	2	1	(12)	20.244612	−2	0.8	−5
2	2	1	1	1	0	1	1	(12)	20.245327	−4	0.0	−5
2	2	1	1	1	1	2	1	(12)	20.737065	3	10.2	4
2	2	1	1	1	1	3	2	(12)	20.737972	1	7.6	1
2	2	0	1	1	0	1	0	(12)	20.602550	−2	−8.2	−3
2	2	0	1	1	0	2	2	(12)	20.603095	1	−6.9	−1
2	2	0	1	1	0	3	2	(12)	20.603564	2	−5.1	1
2	2	0	1	1	0	2	1	(12)	20.603939	−2	−10.5	−5
2	2	0	2	1	1	3	3	(12)	13.006961	2	−2.6	3
2	2	0	2	1	1	2	2	(12)	13.007012	−4	−10.9	−5
2	2	0	2	1	2	2	2	(12)	14.396669	1	−5.5	−1
2	2	0	2	1	2	3	2	(12)	14.397138	2	−3.2	2
2	2	0	2	1	2	1	2	(12)	14.397393	−3	−7.8	−3
2	2	0	2	1	2	2	3	(12)	14.397622	2	−4.7	0
2	2	0	2	1	2	3	3	(12)	14.398088	0	−5.9	−1
2	2	1	2	1	2	2	2	(12)	14.037342	1	5.4	−1
2	2	1	2	1	2	3	2	(12)	14.037804	2	7.5	1
2	2	1	2	1	2	1	2	(12)	14.038057	−2	4.7	−2
2	2	1	2	1	2	2	3	(12)	14.038294	0	4.9	−2
2	2	1	2	1	2	3	3	(12)	14.038756	1	6.4	0
3	1	3	2	0	2	2	2	(12)	13.854501	−2	−3.6	−3
3	1	3	2	0	2	2	1	(12)	13.855278	−5	−5.2	−4
3	1	3	2	0	2	4	3	(12)	13.855400	2	1.4	2
3	2	2	2	1	1	2	1	(12)	23.420242	−4	2.2	−2
3	2	2	2	1	1	3	2	(12)	23.420991	2	5.5	1
3	2	1	3	1	2	4	4	(12)	12.431322	0	−3.6	1
3	2	1	3	1	2	3	3	(12)	12.431599	1	−4.6	0
3	2	2	3	1	2	4	4	(12)	12.034727	−1	6.2	3
3	2	2	3	1	2	3	3	(12)	12.035087	0	5.5	2
4	0	4	3	1	3	4	3	(12)	10.683136	−2	−0.6	−2
4	0	4	3	1	3	5	4	(12)	10.683473	0	0.3	−1
4	0	4	3	1	3	3	2	(12)	10.683665	1	1.2	0
4	1	4	3	0	3	3	2	(12)	16.584732	2	2.8	4
4	1	4	3	0	3	5	4	(12)	16.584826	1	2.0	3
4	1	4	3	0	3	4	3	(12)	16.585425	1	1.3	2
4	2	2	4	1	3	3	3	(12)	11.844521	−1	−2.7	0
4	2	2	4	1	3	5	5	(12)	11.844580	−1	−2.5	0

4	2	2	4	1	3	4	4	(12)	11.844812	1	−1.4	1
5	0	5	4	1	4	5	4	(12)	14.592607	−1	0.4	0
5	0	5	4	1	4	6	5	(12)	14.592877	0	0.3	−1
5	0	5	4	1	4	4	3	(12)	14.592999	1	1.6	1
5	1	5	4	0	4	4	3	(12)	19.212645	−2	0.6	2
5	1	5	4	0	4	6	5	(12)	19.212712	1	3.1	4
5	1	5	4	0	4	5	4	(12)	19.213234	0	2.1	3
5	2	3	5	1	4	6	6	(12)	11.408367	1	0.2	0
5	2	3	5	1	4	5	5	(12)	11.408461	0	−0.6	−1
6	0	6	5	1	5	6	5	(12)	18.399046	0	2.0	1
6	0	6	5	1	5	7	6	(12)	18.399228	−2	0.0	−1
6	0	6	5	1	5	5	4	(12)	18.399307	0	2.1	1
6	1	6	5	0	5	5	4	(12)	21.818579	3	7.0	8
6	1	6	5	0	5	7	6	(12)	21.818614	0	3.4	4
6	1	6	5	0	5	6	5	(12)	21.819038	1	4.3	5
7	0	7	6	1	6	7	6	(12)	22.065568	0	3.6	3
7	0	7	6	1	6	8	7	(12)	22.065676	0	3.0	2
7	0	7	6	1	6	6	5	(12)	22.065724	−1	2.1	1
7	2	5	7	1	6	7	7	(12)	11.438549	−3	−3.7	−12
7	2	5	7	1	6	8	8	(12)	11.438789	0	−0.8	−10
7	2	5	7	1	6	6	6	(12)	11.438820	−3	−3.8	−13
7	2	6	7	1	7	7	7	(12)	20.228107	2	−8.0	6

AIII.2: Couple large amplitude motions: The effects of two methyl internal rotations and ^{14}N quadrupole coupling in 4,5-dimethylthiazole investigated by microwave spectroscopy

Table S-I. Nuclear coordinates in the principal inertial axes of 4,5-dimethylthiazole calculated at the MP2/6-311++G(d,p) level of theory. The atoms are numbered according to Fig. 2.

	a /Å	b /Å	c /Å
S_1	1.509874	0.318035	0.000084
C_2	1.076626	−1.347444	0.000000
N_3	−0.215591	−1.588311	−0.000013
C_4	−0.927700	−0.408767	−0.000150
C_5	−0.160704	0.746268	−0.000337
H_6	1.835438	−2.121034	−0.000045
C_7	−2.425419	−0.496627	0.000133
H_8	−2.893258	0.489828	−0.000661
H_9	−2.768837	−1.043367	−0.882938
H_{10}	−2.768576	−1.041611	0.884402
C_{11}	−0.598942	2.181310	0.000067
H_{12}	−0.227921	2.712565	−0.881858
H_{13}	−1.688918	2.240540	−0.007752
H_{14}	−0.240625	2.708325	0.889793

Table S-IIa: Fourier expansion of the potential energy curves of the 4-methyl group given in Fig. 3 calculated at the with the methods MP2, B3LYP, M06-2X, and CCSD and the basis set 6-311++G(d,p) obtained by varying the dihedral angle $\alpha_2 = \angle(N_3,C_4,C_7,H_8)$ in 2° steps, corresponding to the internal rotations of the 4-methyl group. The potential is expanded as $V(\alpha_2) = a_0 + \sum_{n=1}^{3} a_n \cos(3n\alpha_2)$.

	MP2		B3LYP		M06-2X		CCSD	
	Hartree	cm^{-1}	Hartree	cm^{-1}	Hartree	cm^{-1}	Hartree	cm^{-1}
a_0	−646.481472247		−647.779985711		−647.632511307		−646.524991784	
a_1	0.000143666	31.5	0.000377227	82.8	0.000223919	49.1	0.000361813	79.4
a_2	0.000006338	1.4	−0.000002006	−0.4	−0.000026485	−5.8	0.000011846	2.6
a_3			0.000003019	0.7	0.000002936	0.6	−0.000004495	−1.0

Table S-IIb. Fourier expansion of the potential energy curves given in Fig. 3 calculated at the with the methods MP2, B3LYP, M06-2X, and CCSD and the basis set 6-311++G(d,p) obtained by varying the dihedral angle $\alpha_1 = \angle(S_1,C_5,C_{11},H_{12})$ in 2° steps, corresponding to the internal rotations of the 5-methyl group. The potential is expanded as $V(\alpha_1) = a_0 + \sum_{n=1}^{3} a_n \cos(3n\alpha_1)$.

	MP2		B3LYP		M06-2X		CCSD	
	Hartree	cm^{-1}	Hartree	cm^{-1}	Hartree	cm^{-1}	Hartree	cm^{-1}
a_0	−646.481563019		−647.780093017		−647.632619440		−646.525173884	
a_1	0.000038045	8.3	0.000291360	63.9	0.000160933	35.3	0.000197150	43.3
a_2	0.000041341	9.1	0.000012421	2.7			0.000029499	6.5
a_3	−0.000006766	−1.5					−0.000005158	−1.1

Table S-III. The rotational constants A, B, and C in GHz, the deviations (Dev.) between the experimental and calculated rotational constants in MHz, the angles between the internal rotor axis and the principal axes of inertia $\angle(i_1,a)$, $\angle(i_1,b)$, $\angle(i_1,c)$ of the 5-methyl rotor, the angles between the internal rotor axis and the principal axes of inertia $\angle(i_2,a)$, $\angle(i_2,b)$, $\angle(i_2,c)$ of the 4-methyl rotor in degree, the barriers to internal rotation $V_{3,1}$ of the 5-methyl rotor, and $V_{3,2}$ of the 4-methyl rotor in cm^{-1} calculated using various methods and basis sets. Harmonic frequency calculations were carried out to verify the nature of the stationary points.

Method/Basis set	A	Dev.	B	Dev.	C	Dev.	$\angle(i_1,a)$	$\angle(i_1,b)$	$\angle(i_1,c)$	$\angle(i_2,a)$	$\angle(i_2,b)$	$\angle(i_2,c)$	$V_{3,1}/cm^{-1}$	$V_{3,2}/cm^{-1}$
CCSD/cc-pVDZ	3.131	56	2.416	42	1.388	24	106.15	16.15	89.99	176.53	93.47	90.00		
MP2/cc-pVTZ	3.195	−8	2.466	−9	1.416	−4	107.23	17.23	89.99	176.56	93.44	90.00	73.5	43.0
MP2/cc-pVDZ	3.143	44	2.427	30	1.394	18	106.24	16.24	89.98	177.27	92.73	90.00	20.1	40.4
MP2/6-311++G(3df,2pd)	3.203	−16	2.473	−16	1.420	−9	107.54	17.54	89.60	176.40	93.60	89.90		
MP2/6-311++G(d,p)	3.176	11	2.448	9	1.407	4	106.98	16.98	89.98	176.64	93.36	89.99	27.2	63.0
MP2/6-311+G(d,p)	3.185	2	2.447	10	1.408	3	108.46	18.47	89.26	176.10	93.89	89.77	64.2	24.1
MP2/6-311G(d,p)	3.184	3	2.451	7	1.409	2	107.44	17.46	89.27	176.66	93.34	89.97	15.9	34.9
MP2/6-31++G(d,p)	3.185	2	2.445	13	1.407	4	107.98	18.00	89.23	176.21	93.79	90.14	63.1	
MP2/6-31+G(d,p)	3.185	2	2.445	12	1.408	4	107.90	17.93	89.05	176.23	93.77	90.14	60.7	
MP2/6-31G(d,p)	3.185	2	2.450	8	1.409	3	107.18	17.20	89.26	176.56	93.44	89.89	50.1	47.0
M06-2X/cc-pvqz	3.210	−23	2.478	−20	1.423	−11	107.44	17.44	90.00	175.57	94.43	90.00	113.1	66.5
M06-2X/cc-pVTZ	3.205	−18	2.473	−16	1.420	−9	107.33	17.33	90.00	175.64	94.36	90.00	101.1	69.3
M06-2X/cc-pVDZ	3.178	9	2.452	6	1.408	3	106.96	16.96	89.99	176.14	93.86	90.00	92.7	92.2
M06-2X/6-311++G(3df,2pd)	3.208	−21	2.478	−20	1.423	−11	107.32	17.32	89.99	175.65	94.35	90.01	98.6	53.5
M06-2X/6-311++G(d,p)	3.189	−2	2.461	−3	1.413	−2	106.81	16.81	89.99	175.92	94.08	90.00	103.2	72.4
M06-2X/6-311+G(d,p)	3.189	−2	2.461	−3	1.413	−2	106.83	16.83	89.99	175.91	94.09	90.00	98.6	68.3
M06-2X/6-311G(d,p)	3.190	−3	2.462	−4	1.414	−2	106.71	16.71	89.99	176.06	93.94	90.00	64.5	71.5
M06-2X/6-31++G(d,p)	3.183	4	2.455	3	1.410	1	106.91	16.91	89.99	175.99	94.01	90.00	109.8	88.1
M06-2X/6-31+G(d,p)	3.183	4	2.455	3	1.410	1	106.91	16.91	89.99	175.99	94.01	90.00	109.4	87.5
M06-2X/6-31G(d,p)	3.185	2	2.457	1	1.411	0	106.93	16.93	89.99	176.03	93.97	90.00	94.0	109.1
B3LYP/cc-pVQZ	3.187	0	2.457	0	1.412	0	107.27	17.27	89.99	175.60	94.40	90.00	153.6	98.3
B3LYP/cc-pVTZ	3.182	5	2.452	6	1.409	3	107.16	17.16	89.99	175.65	94.35	90.00	147.4	105.7

B3LYP/cc-pVDZ	3.148	39	2.426	32	1.394	18	106.83	16.83	89.99	176.15	93.85	90.00	119.7	121.5
B3LYP/6-311++G(3df,2pd)	3.189	−2	2.459	−1	1.412	−1	107.35	17.35	89.99	175.59	94.41	90.00	149.7	91.5
B3LYP/6-311++G(d,p)	3.166	21	2.437	20	1.401	11	107.02	17.02	89.99	175.77	94.23	89.99	168.0	127.0
B3LYP/6-311+G(d,p)	3.166	21	2.437	20	1.401	11	107.02	17.02	89.99	175.77	94.23	89.99	164.9	124.0
B3LYP/6-311G(d,p)	3.167	20	2.439	18	1.402	10	106.84	16.84	89.99	175.98	94.02	90.00	129.8	135.2
B3LYP/6-31++G(d,p)	3.156	32	2.430	28	1.397	15	106.89	16.89	89.99	175.95	94.05	90.00	162.7	141.1
B3LYP/6-31+G(d,p)	3.155	32	2.430	28	1.397	15	106.88	16.88	89.99	175.95	94.05	90.00	162.6	141.7
B3LYP/6-31G(d,p)	3.158	29	2.432	25	1.398	14	106.92	16.92	89.99	176.00	94.00	90.00	149.0	167.0
HF/6-311++G(3df,2pd)	3.212	−25	2.491	−33	1.427	−16	106.98	16.98	89.99	174.61	95.39	90.00	264.2	152.9
HF/6-311++G(d,p)	3.193	−6	2.473	−15	1.418	−6	106.63	16.63	89.99	174.77	95.23	90.00	271.6	174.1
HF/6-311+G(d,p)	3.193	−6	2.473	−15	1.418	−6	106.64	16.64	89.99	174.77	95.23	90.00	266.8	170.4
HF/6-311G(d,p)	3.196	−9	2.475	−17	1.419	−7	106.57	16.57	89.99	174.89	95.11	90.00	237.4	164.9
HF/6-31++G(d,p)	3.192	−5	2.470	−12	1.417	−5	106.59	16.59	89.99	174.90	95.10	89.99	241.0	166.3
HF/6-31+G(d,p)	3.192	−5	2.470	−13	1.417	−5	106.58	16.58	89.99	174.90	95.10	89.99	237.7	162.2
HF/6-31G(d,p)	3.194	−7	2.472	−14	1.418	−6	106.63	16.63	89.99	174.90	95.10	89.99	220.2	167.9
Experiment	**3.187**		**2.457**		**1.412**		**108.95**	**18.95**	**90.00[b]**	**175.08**	**94.92**	**90.00[b]**	**61.7**	**126.5**

Table S-IV. Coefficients of the two-dimensional Fourier expansion for the potential energy surfacess calculated with the MP2, B3LYP, M06-2X, and CCSD methods and the basis set 6-311++G(d,p) given in Figure 4. Due to symmetry, only data points in the range from $\alpha_1 = 0°$ to 120° and $\alpha_2 = 0°$ to 120° are needed. The potential is expanded as $\boldsymbol{V(\alpha_1, \alpha_2) = \sum_{i=1}^{13} V_i f_i}$.

		MP2	B3LYP	M06-2X	CCSD
i	f_i	V_i/Hartree	V_i/Hartree	V_i/Hartree	V_i/Hartree
1	1	−646.481423123	−647.779753852	−647.632331306	−646.524833279
2	$\cos(3\alpha_1)$	−0.000044684	−0.000247766	−0.000187156	−0.000209613
3	$\cos(3\alpha_2)$	−0.000164881	−0.000339366	−0.000262191	−0.000372103
4	$\cos(6\alpha_1)$	0.000048167	0.000016274		0.000043379
5	$\cos(6\alpha_2)$	0.000025073		−0.000015810	0.000022584
6	$\cos(3\alpha_1)\cos(3\alpha_2)$	0.000025286	−0.000040561	0.000037313	0.000028470
7	$\sin(3\alpha_1)\sin(3\alpha_2)$	−0.000034950	0.000096390	0.000008074	−0.000025703
8	$\cos(3\alpha_1)\cos(6\alpha_2)$	−0.000014472		−0.000011094	−0.000013389
9	$\sin(3\alpha_1)\sin(6\alpha_2)$	0.000011994		0.000009230	0.000009719
10	$\cos(3\alpha_2)\cos(6\alpha_1)$	−0.000019570			−0.000016253
11	$\sin(3\alpha_2)\sin(6\alpha_1)$	0.000014361			0.000010676
12	$\cos(6\alpha_1)\cos(6\alpha_2)$	0.000015745			0.000013547
13	$\sin(6\alpha_1)\sin(6\alpha_2)$	−0.000013875			−0.000011694

Table S-V. Observed frequencies ($\nu_{obs.}$) of the five torsional species (under column ***sym***) of 4,5-dimethylthiazole. $\nu_{calc.}$ are the calculated frequencies; $\nu_{obs.}-\nu_{calc.}$ values as obtained after a fit with the program *XIAM* and *BELGI-C_s-2Tops-hyperfine*. *J*, K_a, K_c are the symmetric top rotational quantum numbers of the lower energy level; *J'*, K_a', K_c' are those of the upper energy level. *F* is the total angular momentum in the coupled basis with *F* = *J* + *I*. *F'* corresponds to the upper level, *F* to the lower level.

	J'	***K_a'***	***K_c'***	***J***	***K_a***	***K_c***	***F'***	***F***	***sym***	$\nu_{obs.}$	$\nu_{obs.} - \nu_{calc.}$	$\nu_{obs.} - \nu_{calc.}$
	upper level			lower level						*GHz*	*XIAM/MHz*	*BELGI/MHz*
1.	1	1	0	0	0	0	2	1	(11)	6.5569272	0.7825	–0.001
							1	1	(11)	6.5571524	0.7652	0.000
							0	1	(11)	6.5565896	0.8075	–0.001
2.	1	1	1	0	0	0	1	1	(00)	4.6115016	0.0155	–0.001
							2	1	(00)	4.6124583	0.0233	0.001
							0	1	(00)	4.6138913	0.0312	0.002
							1	1	(10)	4.5227074	0.0431	–0.003
							2	1	(10)	4.5231790	0.0220	–0.001
							0	1	(10)	4.5238818	–0.0148	–0.002
							1	1	(01)	4.4388953	–0.0652	–0.001
							2	1	(01)	4.4396839	–0.0526	0.003
							0	1	(01)	4.4408602	–0.0414	0.002
							1	1	(11)	4.3606419	–0.0765	0.001
							2	1	(11)	4.3607130	–0.1166	0.001
							0	1	(11)	4.3608177	–0.1792	–0.001

								1	1	(12)	4.5883111	–0.0328	0.000
								2	1	(12)	4.5891849	–0.0346	0.000
								0	1	(12)	4.5904940	–0.0394	–0.001
3.	2	0	2		1	1	1	1	0	(00)	6.4411400	–0.0024	–0.001
								2	2	(00)	6.4418469	0.0229	0.001
								2	1	(00)	6.4427997	0.0268	–0.001
								1	0	(10)	5.7638451	–0.1401	–0.004
								3	2	(10)	5.7644538	–0.1763	–0.004
								2	1	(10)	5.7647537	–0.1982	–0.003
								1	1	(10)	5.7650249	–0.1926	0.002
								1	0	(01)	6.5936547	0.0275	0.000
								2	2	(01)	6.5940852	0.0554	0.000
								3	2	(01)	6.5945661	0.0460	0.001
								2	1	(01)	6.5948710	0.0652	0.001
								1	1	(01)	6.5956156	0.0473	–0.001
								2	2	(11)	5.8510467	–0.5147	–0.001
								2	1	(11)	5.8511185	–0.5541	–0.001
								3	2	(11)	5.8513355	–0.5050	0.001
								1	0	(11)	5.8513873	–0.4407	0.001
								1	1	(11)	5.8515641	–0.5424	–0.001
								1	0	(12)	5.7146498	–0.2724	0.003
								3	2	(12)	5.7159240	–0.2728	0.002
								2	1	(12)	5.7167317	–0.2693	0.000
4.	2	1	2		1	0	1	2	1	(10)	7.7544814	0.1433	–0.004
								2	2	(10)	7.7545444	0.1384	0.001
								3	2	(10)	7.7553233	0.1323	0.001
								1	1	(10)	7.7556944	0.1352	–0.003
								1	0	(10)	7.7558427	0.1124	0.000
								2	1	(01)	7.3607702	0.0052	0.001
								2	2	(01)	7.3609755	0.0183	0.000
								3	2	(01)	7.3617709	0.0155	0.003
								1	1	(01)	7.3620030	–0.0035	0.001
								1	0	(01)	7.3625194	0.0302	0.002
								2	2	(11)	7.7214575	0.3203	0.002
								2	1	(11)	7.7216108	0.3424	0.002
								3	2	(11)	7.7222140	0.3130	0.001
								1	0	(11)	7.7224046	0.2746	0.000
								1	1	(11)	7.7227884	0.3317	0.001
								2	1	(12)	7.7562905	0.1636	0.001
								2	2	(12)	7.7565422	0.1632	–0.003
								3	2	(12)	7.7573398	0.1609	0.000
								1	1	(12)	7.7575257	0.1545	0.000
								1	0	(12)	7.7581634	0.1610	–0.001
5.	2	1	1		1	1	1	1	0	(10)	9.6655662	–0.0404	–0.001
								1	1	(10)	9.6667391	–0.0998	–0.002
								2	1	(10)	9.6670886	–0.1026	0.000
								3	2	(10)	9.6663946	–0.0774	–0.001
								1	0	(11)	9.7524925	–0.0802	0.003
								1	1	(11)	9.7526743	–0.1768	0.006
								2	1	(11)	9.7528779	–0.1875	0.001
								3	2	(11)	9.7526743	–0.1421	0.003
								1	0	(12)	9.5703414	–0.0127	0.003

							1	1	(12)	9.5725238	–0.0198	0.001
							2	1	(12)	9.5729748	–0.0210	0.001
							3	2	(12)	9.5718134	–0.0161	0.003
6.	2	2	0		1	1	0	1	0	(10)	12.2205147	–0.1932	–0.001
								2	1	(10)	12.2196511	–0.2099	0.002
								3	2	(10)	12.2199574	–0.1905	0.001
								1	1	(01)	12.0010377	0.1480	0.001
								2	1	(01)	12.0013918	0.1345	0.002
								3	2	(01)	12.0017433	0.1388	0.002
								2	2	(01)	12.0019691	0.1281	0.001
								1	0	(01)	12.0024823	0.1342	–0.001
								1	0	(11)	12.6089040	0.6328	–0.001
								2	1	(11)	12.6082262	0.6228	0.001
								2	2	(11)	12.6084482	0.6023	–0.002
								3	2	(11)	12.6085277	0.6416	0.001
7.	2	2	0		1	1	1	1	0	(00)	12.6734678	0.0660	–0.004
								1	1	(00)	12.6758608	0.0850	0.001
								2	1	(00)	12.6765903	0.0711	0.003
								2	2	(00)	12.6756328	0.0624	0.000
								3	2	(00)	12.6751669	0.0746	0.002
								1	0	(10)	14.0423481	–0.0430	0.001
								3	2	(10)	14.0431123	–0.0948	0.003
								2	1	(10)	14.0436848	–0.1530	0.002
								1	0	(01)	13.3772098	0.3126	–0.003
								3	2	(01)	13.3785157	0.3222	0.000
								2	1	(01)	13.3795257	0.3198	–0.002
								2	2	(01)	13.3787426	0.3127	0.000
								1	1	(01)	13.3791727	0.3344	–0.002
								2	1	(11)	14.8047327	1.4605	–0.005
								3	2	(11)	14.8047433	1.5421	0.001
								3	2	(12)	13.5143091	0.5977	0.001
								2	1	(12)	13.5158165	0.5799	–0.002
8.	2	2	1		1	1	0	1	0	(00)	11.0149570	0.0517	0.001
								1	1	(00)	11.0130318	0.0626	–0.002
								2	1	(00)	11.0127247	0.0467	0.001
								2	2	(00)	11.0134906	0.0381	–0.001
								3	2	(00)	11.0136953	0.0558	0.004
								1	0	(10)	10.1742940	0.0357	–0.007
								1	1	(10)	10.1732668	0.0698	–0.006
								2	1	(10)	10.1742383	0.1211	–0.004
								2	2	(10)	10.1746463	0.1042	–0.007
								3	2	(10)	10.1740275	0.0769	–0.003
								1	0	(01)	10.2388627	–0.2586	0.002
								1	1	(01)	10.2374144	–0.2486	0.000
								2	1	(01)	10.2374909	–0.2671	0.003
								2	2	(01)	10.2380663	–0.2754	0.000
								3	2	(01)	10.2380219	–0.2586	0.003
								1	0	(11)	9.4757252	–0.7507	0.000
								1	1	(11)	9.4751662	–0.7046	0.002
								2	1	(11)	9.4767014	–0.6400	0.003
								2	2	(11)	9.4769229	–0.6610	0.000
								3	2	(11)	9.4759389	–0.6996	0.002

							1	0	(12)	10.5933990	–0.3865	0.001
							1	1	(12)	10.5918502	–0.3771	–0.001
							2	1	(12)	10.5917488	–0.3709	0.002
							2	2	(12)	10.5923642	–0.3789	–0.001
							3	2	(12)	10.5924351	–0.3772	0.003
9.	2	2	1		1	1	3	2	(10)	11.9971778	0.1680	–0.005
							2	1	(10)	11.9982650	0.1709	–0.010
							1	0	(10)	11.9961251	0.1836	–0.007
							3	2	(01)	11.6147938	–0.0757	0.001
							1	0	(01)	11.6135887	–0.0818	–0.001
10.	2	2	0		2	1	3	3	(01)	6.5723101	0.2805	–0.001
							2	2	(01)	6.5733163	0.2520	–0.014
							1	1	(01)	6.5717439	0.2888	–0.001
11.	2	2	1		2	1	3	3	(00)	5.3666971	0.0414	–0.004
							3	2	(00)	5.3675235	0.0380	–0.002
							2	3	(00)	5.3664951	0.0265	–0.007
							2	2	(00)	5.3673250	0.0266	–0.001
							2	1	(00)	5.3660462	0.0385	0.002
							1	2	(00)	5.3676318	0.0422	–0.004
							1	1	(00)	5.3663547	0.0559	0.000
							3	3	(01)	4.8085897	–0.1159	0.001
							2	2	(01)	4.8094293	–0.1357	0.001
							1	1	(01)	4.8081214	–0.1069	–0.001
12.	3	0	3		2	1	2	1	(00)	9.6848636	0.0085	–0.001
							2	2	(00)	9.6861458	0.0000	0.000
							3	2	(00)	9.6849355	0.0137	0.000
							3	3	(00)	9.6841109	0.0189	0.000
							4	3	(00)	9.6850102	0.0115	0.002
							2	1	(10)	9.3974315	–0.0349	–0.006
							2	2	(10)	9.3986434	–0.0441	–0.006
							3	2	(10)	9.3976904	–0.0359	–0.006
							3	3	(10)	9.3969120	–0.0293	–0.005
							4	3	(10)	9.3976174	–0.0360	–0.006
							2	1	(01)	9.7187725	0.0179	–0.002
							2	2	(01)	9.7200088	0.0126	0.002
							3	2	(01)	9.7187908	0.0266	0.003
							3	3	(01)	9.7179968	0.0307	0.001
							4	3	(01)	9.7189004	0.0218	0.002
							2	1	(11)	9.4261294	–0.1357	0.000
							2	2	(11)	9.4273076	–0.1458	–0.001
							3	2	(11)	9.4262865	–0.1445	–0.004
							3	3	(11)	9.4255317	–0.1354	–0.001
							4	3	(11)	9.4262865	–0.1380	0.000
							2	1	(12)	9.3865954	–0.0738	0.000
							2	2	(12)	9.3878316	–0.0819	0.000
							3	2	(12)	9.3869303	–0.0708	0.000
							3	3	(12)	9.3861354	–0.0659	–0.001
							4	3	(12)	9.3868040	–0.0731	0.001
13.	3	1	3		2	0	2	2	(00)	10.0177155	0.0083	–0.001
							3	2	(00)	10.0164012	0.0202	–0.001
							3	3	(00)	10.0159341	0.0312	0.000
							4	3	(00)	10.0169077	0.0224	0.000

							2	1	(10)	10.3341390	0.1505	–0.001
							2	2	(10)	10.3344069	0.1527	0.000
							3	2	(10)	10.3331679	0.1629	0.001
							3	3	(10)	10.3329936	0.1596	–0.002
							4	3	(10)	10.3339141	0.1547	0.000
							2	1	(01)	9.9822271	0.0217	0.005
							2	2	(01)	9.9829684	0.0005	–0.001
							3	2	(01)	9.9816647	0.0146	0.002
							3	3	(01)	9.9811829	0.0231	0.000
							4	3	(01)	9.9821519	0.0160	0.001
							2	1	(11)	10.3104719	0.3415	–0.001
							2	2	(11)	10.3109183	0.3540	0.000
							3	2	(11)	10.3096617	0.3630	0.001
							3	3	(11)	10.3093735	0.3539	0.000
							4	3	(11)	10.3103059	0.3488	0.000
							2	1	(12)	10.3281498	0.2034	–0.001
							2	2	(12)	10.3282484	0.1914	–0.002
							3	2	(12)	10.3270295	0.2038	0.000
							4	3	(12)	10.3278692	0.2027	0.000
14.	3	1	2		2	1	2	2	1	(10)	14.9145384	–0.0525	–0.004
								4	3	(10)	14.9151602	–0.0530	0.000
								3	2	(10)	14.9164670	–0.0630	–0.002
								3	2	(11)	14.9267244	–0.2175	–0.001
								2	1	(12)	14.8757305	–0.1758	0.002
								4	3	(12)	14.8763883	–0.1763	0.004
								3	2	(12)	14.8777951	–0.1807	0.002
15.	3	1	3		2	1	1	4	3	(10)	6.4319749	0.0574	–0.001
								3	2	(10)	6.4308337	0.0680	–0.001
								2	1	(10)	6.4324213	0.0542	–0.001
								4	3	(11)	6.4089687	–0.0125	0.000
								3	2	(11)	6.4079008	–0.0052	–0.001
								2	1	(11)	6.4093685	–0.0173	–0.001
								4	3	(12)	6.4719798	–0.0539	–0.002
								3	2	(12)	6.4707860	–0.0448	–0.001
								2	1	(12)	6.4724586	–0.0558	0.000
16.	3	1	3		2	1	2	4	3	(00)	9.7508797	0.0162	0.001
								3	2	(00)	9.7507347	0.0238	0.006
								4	3	(01)	9.7705118	0.0196	0.000
								2	1	(01)	9.7704131	0.0226	0.003
								3	2	(01)	9.7703378	0.0236	0.001
17.	3	1	2		2	2	0	4	3	(01)	9.3661025	–0.2150	0.004
								3	2	(01)	9.3665596	–0.1958	0.005
								2	1	(01)	9.3659905	–0.2221	0.005
18.	3	1	2		2	2	1	2	1	(01)	11.1296143	0.1750	0.006
								4	3	(01)	11.1298236	0.1821	0.002
								3	2	(01)	11.1304602	0.2056	0.003
								3	2	(11)	9.7787739	–0.6128	0.000
								4	3	(11)	9.7793211	–0.5621	0.001
								2	1	(11)	9.7797152	–0.5361	0.001
								2	1	(12)	9.0752361	–0.2258	0.003
								4	3	(12)	9.0754880	–0.2262	0.003
								3	2	(12)	9.0761682	–0.2265	0.002

19.	3	2	2		2	1	1		2	1	(00)	13.8376232	0.0536	–0.001
									2	2	(00)	13.8360312	0.0435	–0.001
									3	2	(00)	13.8360312	0.0435	–0.001
									3	3	(00)	13.8370545	0.0500	–0.001
									4	3	(00)	13.8370545	0.0500	–0.001
									2	1	(10)	13.8678000	0.1807	0.001
									3	2	(10)	13.8674837	0.1922	0.001
									4	3	(10)	13.8676848	0.1849	0.002
									4	3	(01)	13.5278678	–0.0890	0.004
									2	1	(01)	13.5283806	–0.0890	0.000
									3	2	(11)	13.6927579	0.3628	0.005
									2	1	(12)	13.9357406	0.0296	–0.001
									3	2	(12)	13.9351686	0.0324	0.000
									4	3	(12)	13.9355493	0.0315	0.001
20.	3	2	1		2	2	1		2	1	(10)	14.8075627	–0.3394	–0.008
									2	2	(10)	14.8066016	–0.3803	0.000
									3	2	(10)	14.8072197	–0.3770	0.009
									4	3	(10)	14.8073772	–0.3557	–0.005
									3	2	(11)	15.3974596	0.1271	0.003
									4	3	(11)	15.3981971	0.1725	0.004
									2	1	(11)	15.3986564	0.1953	0.003
									2	1	(12)	14.3188982	0.3015	0.003
									3	2	(12)	14.3197636	0.2956	0.003
									4	3	(12)	14.3191336	0.3005	0.004
21.	3	2	2		2	2	1		4	3	(01)	12.0218104	0.1304	0.003
									3	2	(01)	12.0218696	0.1431	0.002
22.	3	3	1		2	1	1		2	1	(10)	20.0466403	0.4031	–0.018
									4	3	(10)	20.0468256	0.4231	–0.011
									3	2	(10)	20.0474638	0.4561	–0.014
									2	1	(11)	19.1110751	0.1461	–0.004
									4	3	(11)	19.1114070	0.1641	0.000
									3	2	(11)	19.1124225	0.2019	–0.001
									4	3	(12)	20.9232701	–0.5000	0.001
									3	2	(12)	20.9232831	–0.4850	0.003
									2	1	(12)	20.9233223	–0.5081	–0.002
23.	3	3	0		2	2	0		2	1	(10)	18.4552286	–0.5722	0.002
									3	2	(10)	18.4547360	–0.5809	–0.002
									4	3	(10)	18.4550839	–0.5706	0.000
									3	2	(01)	18.3987604	0.0604	–0.004
									2	1	(01)	18.3990777	0.0717	0.004
									2	1	(11)	18.8742103	0.3387	0.001
									3	2	(11)	18.8739450	0.3411	0.002
									4	3	(11)	18.8741547	0.3463	0.003
									2	1	(12)	17.7920109	0.3136	–0.002
									3	2	(12)	17.7912688	0.2944	–0.002
									4	3	(12)	17.7917225	0.3115	–0.001

24.	3	3	0	2	2	1	2	1	(00)	18.5127104	0.0725	0.000
							3	2	(00)	18.5132306	0.0724	0.000
							4	3	(00)	18.5128758	0.0745	0.000
							3	2	(10)	20.5001494	–0.9112	0.004
							4	3	(10)	20.5010177	–0.8341	0.007
							2	1	(10)	20.5014493	–0.8012	0.008
							2	1	(12)	19.0730927	0.9442	–0.003
							4	3	(12)	19.0731960	0.9348	–0.002
							3	2	(12)	19.0734442	0.9008	–0.004
25.	3	3	1	2	2	0	2	1	(00)	17.6572657	0.0595	–0.002
							3	2	(00)	17.6564199	0.0547	–0.001
							4	3	(00)	17.6569815	0.0660	0.005
							3	2	(10)	15.6708690	0.5079	–0.014
							3	2	(01)	15.8562064	–0.5496	0.002
							4	3	(01)	15.8563885	–0.5411	0.004
							2	1	(01)	15.8564951	–0.5438	0.000
							2	1	(11)	14.0588923	–1.5529	0.001
							4	3	(11)	14.0593475	–1.5106	0.011
							3	2	(11)	14.0605662	–1.4476	0.003
							2	2	(12)	16.9800305	–1.1069	0.002
							3	2	(12)	16.9804400	–1.0874	0.005
							4	3	(12)	16.9807749	–1.1134	0.004
							2	1	(12)	16.9810205	–1.1272	0.002
							3	3	(12)	16.9810725	–1.1045	0.001
26.	3	3	1	2	2	1	4	3	(10)	17.7160434	0.1788	–0.007
							3	2	(10)	17.7162825	0.1776	–0.008
							4	3	(01)	17.6201083	–0.1453	0.001
							2	1	(01)	17.6201183	–0.1473	0.001
							4	3	(11)	17.1919271	–0.1786	0.001
							2	1	(11)	17.1920710	–0.1696	0.000
							3	2	(11)	17.1920909	–0.1849	0.001
							2	1	(12)	18.2621030	–0.4959	0.001
							4	3	(12)	18.2622479	–0.4905	0.003
							3	2	(12)	18.2626158	–0.4806	0.003
27.	3	1	2	3	0	3	2	2	(00)	6.1788509	0.0552	0.013
							4	4	(00)	6.1793942	0.0394	–0.002
							3	3	(00)	6.1809947	0.0425	0.002
							2	2	(10)	5.5171055	–0.0191	0.000
							4	4	(10)	5.5175366	–0.0232	–0.001
							3	3	(10)	5.5187728	–0.0308	0.000
							2	2	(11)	5.4988216	–0.0608	–0.001
							4	4	(11)	5.4992415	–0.0631	0.001
							3	3	(11)	5.5004345	–0.0763	0.000
							2	2	(12)	5.4891348	–0.1023	0.002
							4	4	(12)	5.4895843	–0.1032	0.003

28.	3	2	2	3	1	3	2	2	(00)	7.2703322	0.0678	–0.001
							4	4	(00)	7.2706764	0.0682	0.002
							3	3	(00)	7.2716478	0.0572	0.000
							2	2	(01)	7.0595054	–0.0086	–0.003
							4	4	(01)	7.0598850	–0.0084	0.000
							3	3	(01)	7.0609587	–0.0186	–0.001
							2	2	(11)	7.2834171	0.3580	0.000
							4	4	(11)	7.2837904	0.3605	0.001
							3	3	(11)	7.2848513	0.3623	0.000
							2	2	(12)	7.4632825	0.0859	0.000
							4	4	(12)	7.4635698	0.0857	0.003
							3	3	(12)	7.4643819	0.0765	0.001
29.	3	3	1	3	2	2	4	4	(00)	6.6022526	0.0404	0.007
							3	3	(00)	6.6021625	0.0225	0.004
							2	2	(00)	6.6022847	0.0471	0.008
30.	4	0	4	3	1	3	3	2	(00)	12.6359232	0.0065	0.001
							3	3	(00)	12.6372352	–0.0077	–0.001
							4	3	(00)	12.6358345	0.0064	0.000
							4	4	(00)	12.6348605	0.0148	0.000
							5	4	(00)	12.6359771	0.0060	0.001
							3	2	(10)	12.5546818	0.0359	–0.002
							3	3	(10)	12.5559220	0.0270	–0.002
							4	3	(10)	12.5546270	0.0381	–0.001
							4	4	(10)	12.5537068	0.0433	–0.002
							5	4	(10)	12.5547377	0.0352	–0.002
							3	2	(01)	12.6395447	0.0080	0.002
							3	3	(01)	12.6408512	–0.0033	0.003
							4	3	(01)	12.6394453	0.0076	0.001
							4	4	(01)	12.6384773	0.0158	0.000
							5	4	(01)	12.6395962	0.0077	0.002
							3	2	(11)	12.5608328	0.0352	0.001
							3	3	(11)	12.5620890	0.0258	–0.001
							4	3	(11)	12.5607694	0.0367	0.001
							4	4	(11)	12.5598364	0.0411	0.000
							5	4	(11)	12.5608881	0.0345	0.000
							3	2	(12)	12.5486838	0.0336	0.000
							3	3	(12)	12.5499033	0.0217	–0.001
							4	3	(12)	12.5486281	0.0346	0.000
							4	4	(12)	12.5477230	0.0416	–0.001
							5	4	(12)	12.5487391	0.0331	0.000
31.	4	1	4	3	0	3	3	2	(00)	12.7152106	0.0138	0.000
							3	3	(00)	12.7164220	0.0011	0.000
							4	3	(00)	12.7150033	0.0138	0.000
							4	4	(00)	12.7141046	0.0219	–0.001
							5	4	(00)	12.7152348	0.0135	0.000
							3	2	(10)	12.8321012	0.1147	0.000
							3	3	(10)	12.8330549	0.1072	0.000
							4	3	(10)	12.8317024	0.1175	0.000
							4	4	(10)	12.8309965	0.1237	0.000
							5	4	(10)	12.8320734	0.1165	0.001
							3	2	(01)	12.7014800	0.0082	0.002

							3	3	(01)	12.7026976	–0.0061	0.001
							4	3	(01)	12.7012800	0.0067	0.001
							4	4	(01)	12.7003764	0.0157	0.000
							5	4	(01)	12.7015053	0.0068	0.001
							3	2	(11)	12.8171065	0.2224	0.004
							3	3	(11)	12.8181199	0.2134	–0.001
							4	3	(11)	12.8167519	0.2240	0.001
							4	4	(11)	12.8159961	0.2256	–0.001
							5	4	(11)	12.8170857	0.2186	0.000
							3	2	(12)	12.8247540	0.1307	–0.003
							3	3	(12)	12.8256559	0.1202	–0.001
							4	3	(12)	12.8243194	0.1325	–0.001
							4	4	(12)	12.8236515	0.1404	–0.002
							5	4	(12)	12.8247156	0.1317	–0.001
32.	4	1	4		3	1	3	5	4	(00)	12.6493650	0.0084	0.001
								4	3	(00)	12.6492105	0.0101	0.001
								3	2	(00)	12.6493138	0.0083	0.000
								5	4	(01)	12.6498928	0.0079	0.002
								4	3	(01)	12.6497324	0.0091	0.002
								3	2	(01)	12.6498426	0.0067	0.000
33.	4	1	3		3	2	2	3	2	(00)	14.6137728	–0.0255	0.009
								3	3	(00)	14.6137728	–0.0255	0.009
								4	3	(00)	14.6139731	–0.0284	–0.003
								4	4	(00)	14.6139731	–0.0284	–0.003
								5	4	(00)	14.6138041	–0.0358	–0.003
								3	2	(10)	13.5586006	–0.1423	–0.014
								4	3	(10)	13.5590580	–0.1454	–0.010
								5	4	(10)	13.5586947	–0.1411	–0.011
								4	3	(01)	14.8244231	0.0540	0.001
								5	4	(01)	14.8243825	0.0471	0.002
								3	2	(11)	13.7073608	–0.4238	0.000
								4	3	(11)	13.7075739	–0.4425	–0.003
								5	4	(11)	13.7073935	–0.4295	–0.001
								3	2	(12)	13.4954786	–0.2436	–0.002
								4	3	(12)	13.4961646	–0.2360	0.000
								5	4	(12)	13.4956284	–0.2393	0.002
34.	4	2	3		3	1	2	3	2	(00)	16.1916534	0.0314	–0.002
								4	3	(00)	16.1905740	0.0260	–0.002
								5	4	(00)	16.1913822	0.0309	–0.001
								3	2	(10)	16.8803991	0.1900	0.000
								4	3	(10)	16.8795261	0.2009	0.003
								5	4	(10)	16.8801841	0.1951	0.004
								3	2	(01)	16.0456109	–0.0116	–0.002
								4	3	(01)	16.0445814	–0.0189	–0.004
								5	4	(01)	16.0453574	–0.0061	0.005
								3	2	(11)	16.7977765	0.5576	–0.001
								4	3	(11)	16.7970335	0.5745	0.001
								5	4	(11)	16.7975935	0.5632	0.001
								3	2	(12)	16.8752496	0.2332	–0.001
								4	3	(12)	16.8742469	0.2339	–0.001
								5	4	(12)	16.8749995	0.2335	–0.001

35.	4	2	2	3	2	2	3	2	(10)	19.4664396	–0.1518	–0.006
							4	3	(10)	19.4670447	–0.1594	–0.004
							5	4	(10)	19.4665655	–0.1498	–0.002
							3	2	(11)	19.5960448	–0.0289	–0.002
							4	3	(11)	19.5964299	–0.0431	0.000
							5	4	(11)	19.5961165	–0.0298	0.001
							3	2	(12)	19.3360662	–0.0444	0.002
							4	3	(12)	19.3368885	–0.0446	0.002
							5	4	(12)	19.3362422	–0.0433	0.003
36.	4	2	2	3	3	0	5	4	(01)	12.2617883	–0.1528	0.003
							3	2	(01)	12.2615100	–0.1616	0.001
37.	4	2	2	3	3	1	4	3	(00)	13.4852103	–0.0033	0.000
38.	4	3	1	3	2	2	4	3	(00)	24.2907442	0.0789	–0.003
							4	4	(00)	24.2907442	0.0789	–0.003
							5	4	(00)	24.2898251	0.0768	–0.006
39.	4	3	2	3	2	1	3	2	(00)	20.6055824	0.0703	0.003
							4	3	(00)	20.6044079	0.0569	–0.001
							5	4	(00)	20.6052586	0.0653	0.000
							5	4	(10)	19.5861192	0.6656	0.011
							4	3	(10)	19.5861515	0.6769	0.009
							3	2	(01)	19.6779818	–0.3778	0.000
							4	3	(01)	19.6772166	–0.3861	0.000
							5	4	(01)	19.6777506	–0.3805	–0.001
							3	2	(11)	18.9173329	0.2984	–0.005
							5	4	(11)	18.9174228	0.3037	–0.004
							4	3	(11)	18.9178594	0.3196	–0.004
40.	4	3	1	3	3	1	4	3	(10)	19.9539645	–1.3751	–0.004
							5	4	(10)	19.9542342	–1.3333	–0.004
							3	2	(10)	19.9543857	–1.3175	–0.003
							4	3	(11)	21.5665600	0.8159	0.002
							5	4	(11)	21.5673679	0.8639	0.003
							3	2	(11)	21.5676813	0.8784	0.003
							3	2	(12)	18.5743740	0.8355	0.004
							5	4	(12)	18.5744831	0.8296	0.003
							4	3	(12)	18.5750183	0.8129	0.002
41.	4	4	0	3	3	0	4	3	(10)	24.8743762	–0.8587	–0.004
							5	4	(10)	24.8745103	–0.8566	–0.001
							4	3	(01)	24.7840156	–0.0180	0.008
							5	4	(01)	24.7841186	–0.0141	0.009
							3	2	(01)	24.7841446	–0.0178	0.006
							4	3	(11)	25.2250179	0.0499	0.000
							3	2	(11)	25.2251085	0.0513	0.005
							3	2	(12)	24.1864627	0.3469	–0.004
							4	3	(12)	24.1858448	0.3335	–0.003
							5	4	(12)	24.1863248	0.3483	–0.002
42.	4	4	0	3	3	1	4	3	(00)	24.6304535	0.0407	–0.001
							5	4	(00)	24.6303972	0.0443	0.001
							4	3	(12)	24.9966750	1.7167	–0.008
							5	4	(12)	24.9972727	1.7734	–0.007
43.	4	4	1	3	3	1	3	2	(10)	23.7969168	0.1402	–0.010
							4	3	(10)	23.7965519	0.1265	–0.011

							5	4	(10)	23.7967793	0.1360	–0.009
							4	3	(01)	23.9141754	–0.2249	–0.004
							5	4	(01)	23.9142823	–0.2209	–0.002
							3	2	(01)	23.9143116	–0.2238	–0.004
							3	2	(11)	23.0933398	–0.9478	0.003
							5	4	(11)	23.0931567	–0.9509	0.005
							4	3	(11)	23.0928516	–0.9585	0.005
							3	2	(12)	24.3247284	–0.8903	0.000
							4	3	(12)	24.3249221	–0.8792	0.002
							5	4	(12)	24.3247484	–0.8862	0.003
44.	4	1	3		4	0	4	3	3	(00)	9.2481755	0.0295	0.001
								4	4	(00)	9.2497924	0.0284	0.003
								5	5	(00)	9.2485093	0.0323	0.004
								3	3	(10)	8.4393051	–0.0441	–0.002
								5	5	(10)	8.4396713	–0.0443	–0.001
								4	4	(10)	8.4410879	–0.0524	–0.001
								4	4	(01)	9.2459430	0.0342	0.006
								5	5	(01)	9.2446791	0.0389	0.008
								3	3	(11)	8.4299440	–0.1020	–0.002
								5	5	(11)	8.4302963	–0.1030	0.000
								4	4	(11)	8.4316573	–0.1154	–0.002
								3	3	(12)	8.4100811	–0.1875	0.002
								5	5	(12)	8.4104588	–0.1870	0.004
								4	4	(12)	8.4119194	–0.1932	0.002
45.	4	2	2		4	0	4	5	5	(10)	14.3475352	–0.0599	0.002
								4	4	(10)	14.3490719	–0.0691	0.002
								3	3	(10)	14.3471421	–0.0556	0.004
46.	4	2	2		4	1	3	3	3	(00)	5.4721635	0.0384	–0.002
								5	5	(00)	5.4724167	0.0407	0.000
								4	4	(00)	5.4733931	0.0410	0.000
								5	5	(10)	5.9078631	–0.0165	0.001
								4	4	(10)	5.9079815	–0.0192	0.001
								3	3	(01)	5.5780298	0.1383	0.000
								5	5	(01)	5.5782814	0.1408	0.003
								4	4	(01)	5.5792491	0.1398	0.001
								5	5	(11)	5.8887222	0.3988	0.002
								4	4	(11)	5.8888550	0.3984	0.001
								3	3	(12)	5.8405850	0.1966	0.001
								5	5	(12)	5.8406148	0.1969	0.003
								4	4	(12)	5.8407234	0.1909	0.001
47.	4	2	3		4	1	4	3	3	(00)	9.6552819	0.0610	0.000
								4	4	(00)	9.6565668	0.0560	0.001
								5	5	(00)	9.6555412	0.0565	–0.004
								3	3	(10)	9.5654089	0.0618	0.006
								5	5	(10)	9.5656508	0.0588	0.005
								4	4	(10)	9.5665963	0.0523	0.003
								3	3	(01)	9.5630955	0.0317	0.004
								4	4	(01)	9.5644073	0.0249	0.004
								5	5	(01)	9.5633656	0.0321	0.006
								3	3	(11)	9.4794963	0.2791	–0.001
								5	5	(11)	9.4797477	0.2800	0.001
								4	4	(11)	9.4807158	0.2739	0.000

							3	3	(12)	9.5396280	–0.0021	0.001
							5	5	(12)	9.5398683	–0.0013	0.003
							4	4	(12)	9.5407914	–0.0093	0.001
48.	4	3	1		4	2	2	3	3	(10)	6.6667936	–0.9362	–0.009
								5	5	(10)	6.6668077	–0.9470	–0.018
								4	4	(10)	6.6668991	–0.9527	–0.015
								5	5	(01)	4.6982909	0.3033	0.000
								3	3	(01)	4.6983911	0.3046	–0.001
								4	4	(11)	7.3898001	0.7035	0.002
								5	5	(11)	7.3899013	0.7119	0.003
								3	3	(11)	7.3899216	0.7084	–0.003
								5	5	(12)	6.2259622	0.3419	0.001
								4	4	(12)	6.2262411	0.3370	0.000
49.	4	3	2		4	2	3	3	3	(00)	7.8749078	0.0813	0.000
								4	4	(00)	7.8753616	0.0686	–0.002
								5	5	(00)	7.8750008	0.0789	0.000
								3	3	(10)	8.1201098	0.3847	0.003
								5	5	(10)	8.1202709	0.3893	0.006
								4	4	(10)	8.1208834	0.3933	0.004
								3	3	(01)	7.2776922	–0.1091	–0.001
								5	5	(01)	7.2778353	–0.1096	0.001
								3	3	(11)	7.7384988	0.4734	–0.001
								5	5	(11)	7.7387053	0.4751	–0.002
								4	4	(11)	7.7395125	0.4859	–0.001
								3	3	(12)	8.3423180	0.0615	–0.001
								5	5	(12)	8.3424045	0.0611	0.000
								4	4	(12)	8.3427390	0.0575	0.001
50.	4	4	1		4	3	2	4	4	(00)	8.2330937	–0.0216	–0.001
								5	5	(00)	8.2334535	–0.0063	0.001
51.	5	0	5		4	1	4	4	3	(00)	15.4890102	–0.0019	0.002
								4	4	(00)	15.4904268	–0.0167	0.000
								5	4	(00)	15.4889257	–0.0037	0.000
								5	5	(00)	15.4877960	0.0052	–0.001
								6	5	(00)	15.4890446	–0.0040	0.000
								4	3	(10)	15.4667561	0.0608	0.000
								4	4	(10)	15.4681080	0.0499	0.000
								5	4	(10)	15.4666619	0.0607	–0.001
								5	5	(10)	15.4655853	0.0682	–0.002
								6	5	(10)	15.4667871	0.0596	–0.001
								4	3	(01)	15.4852307	–0.0042	0.004
								4	4	(01)	15.4866465	–0.0188	0.002
								5	4	(01)	15.4851445	–0.0058	0.002
								5	5	(01)	15.4840150	0.0025	0.000
								6	5	(01)	15.4852643	–0.0068	0.002
								4	3	(11)	15.4645594	0.0879	0.001
								4	4	(11)	15.4659270	0.0769	0.000
								5	4	(11)	15.4644683	0.0880	0.000
								5	5	(11)	15.4633792	0.0955	0.000
								6	5	(11)	15.4645913	0.0865	0.000
								4	3	(12)	15.4608883	0.0634	0.000
								4	4	(12)	15.4622240	0.0504	–0.002
								5	4	(12)	15.4607897	0.0636	–0.001

							5	5	(12)	15.4597264	0.0732	0.000
							6	5	(12)	15.4609187	0.0629	–0.001
52.	5	1	5		4	0	4	4	3	(00)	15.5048528	0.0023	0.002
								4	4	(00)	15.5062533	–0.0120	0.001
								5	4	(00)	15.5047489	0.0002	0.000
								5	5	(00)	15.5036319	0.0086	–0.002
								6	5	(00)	15.5048827	–0.0005	0.000
								4	3	(10)	15.5285932	0.0855	–0.002
								4	4	(10)	15.5298899	0.0760	–0.001
								5	4	(10)	15.5284354	0.0880	–0.001
								5	5	(10)	15.5274042	0.0958	–0.001
								6	5	(10)	15.5286141	0.0874	0.000
								4	3	(01)	15.4973796	–0.0044	0.003
								4	4	(01)	15.4987822	–0.0187	0.001
								5	4	(01)	15.4972786	–0.0053	0.002
								5	5	(01)	15.4961597	0.0028	0.000
								6	5	(01)	15.4974111	–0.0060	0.001
								5	4	(11)	15.5202382	0.1437	0.001
								5	5	(11)	15.5191846	0.1484	–0.001
								6	5	(11)	15.5204044	0.1404	0.000
53.	5	1	4		4	2	3	4	3	(00)	18.0162002	–0.0621	0.004
								5	4	(00)	18.0160582	–0.0617	0.001
								6	5	(00)	18.0161769	–0.0663	–0.001
								4	3	(10)	17.5488715	–0.0768	–0.010
								5	4	(10)	17.5489614	–0.0680	–0.002
								6	5	(10)	17.5488992	–0.0687	–0.002
								4	3	(01)	18.0637084	–0.0362	–0.002
								5	4	(01)	18.0635283	–0.0320	0.000
								6	5	(01)	18.0636834	–0.0340	0.000
								4	3	(11)	17.6003997	–0.1501	–0.002
								5	4	(11)	17.6004220	–0.1477	0.002
								6	5	(11)	17.6004103	–0.1483	0.000
								4	3	(12)	17.5294694	–0.0953	0.001
								5	4	(12)	17.5295924	–0.0928	0.000
								6	5	(12)	17.5294968	–0.0946	0.001
54.	5	2	4		4	1	3	4	3	(00)	18.5501763	–0.0084	–0.001
								5	4	(00)	18.5496013	–0.0085	0.000
								6	5	(00)	18.5500719	–0.0083	–0.001
								4	3	(10)	19.1302341	0.1253	0.006
								5	4	(10)	19.1294069	0.1285	0.005
								6	5	(10)	19.1300764	0.1253	0.006
								4	3	(01)	18.4801800	–0.0340	–0.001
								5	4	(01)	18.4796311	–0.0370	–0.003
								6	5	(01)	18.4800789	–0.0364	–0.003
								4	3	(11)	19.0635090	0.4838	0.001
								5	4	(11)	19.0627646	0.4925	0.001
								6	5	(11)	19.0633692	0.4855	0.001
								4	3	(12)	19.1089301	0.1956	–0.002
								5	4	(12)	19.1080369	0.1965	–0.001
								6	5	(12)	19.1087591	0.1956	–0.002
55.	5	2	4		4	2	2	6	5	(10)	13.2222132	0.1417	0.004
								5	4	(10)	13.2214258	0.1481	0.005

							4	3	(10)	13.2224001	0.1398	0.003
							6	5	(12)	13.2681451	–0.0006	–0.003
							5	4	(12)	13.2673111	0.0032	–0.004
							4	3	(12)	13.2683454	–0.0007	–0.003
56.	5	3	3		4	2	2	5	4	(00)	22.8778326	0.0316	0.000
								4	3	(10)	23.1782759	0.3527	0.012
								5	4	(10)	23.1779447	0.3561	0.010
								6	5	(10)	23.1781955	0.3515	0.010
								4	3	(11)	22.9624632	0.5523	–0.003
								5	4	(11)	22.9622790	0.5622	–0.002
								6	5	(11)	22.9624136	0.5554	–0.002
								4	3	(12)	23.2399502	0.0507	–0.005
								5	4	(12)	23.2394863	0.0527	–0.003
								6	5	(12)	23.2398484	0.0524	–0.003
57.	5	1	4		5	0	5	4	4	(00)	12.1824707	–0.0004	0.000
								6	6	(00)	12.1826751	–0.0042	–0.003
								5	5	(00)	12.1836980	–0.0033	0.002
								4	4	(10)	11.6475281	–0.0720	0.000
								6	6	(10)	11.6477605	–0.0718	0.001
								5	5	(10)	11.6488935	–0.0788	0.000
								4	4	(01)	12.1415708	–0.0027	–0.004
								6	6	(01)	12.1417794	–0.0004	–0.001
								5	5	(01)	12.1427870	–0.0053	–0.002
								4	4	(11)	11.6153396	0.0441	–0.001
								6	6	(11)	11.6155688	0.0472	0.003
								5	5	(11)	11.6166679	0.0366	–0.001
								4	4	(12)	11.6082094	–0.1606	0.002
								6	6	(12)	11.6084456	–0.1596	0.004
58.	5	2	4		5	1	5	4	4	(00)	12.2934997	0.0195	–0.002
								6	6	(00)	12.2936941	0.0201	–0.001
								5	5	(00)	12.2946423	0.0172	0.000
								4	4	(10)	12.0409441	–0.0062	0.004
								6	6	(10)	12.0411338	–0.0062	0.005
								5	5	(10)	12.0420591	–0.0123	0.004
								4	4	(01)	12.2271454	0.0014	–0.005
								6	6	(01)	12.2273418	0.0034	–0.002
								5	5	(01)	12.2282912	–0.0017	–0.003
								4	4	(11)	11.9730696	0.2403	–0.002
								6	6	(11)	11.9732603	0.2413	0.000
								5	5	(11)	11.9741848	0.2345	–0.001
								6	6	(12)	11.9974719	–0.0802	0.003
								5	5	(12)	11.9983942	–0.0877	0.001
59.	5	3	3		5	2	4	6	6	(00)	9.8010298	0.0863	0.001
								5	5	(00)	9.8016223	0.0790	–0.002
								4	4	(00)	9.8009002	0.0789	–0.007
								6	6	(01)	9.5724492	–0.0050	–0.001
								5	5	(01)	9.5731171	–0.0100	–0.002
								4	4	(01)	9.5723148	–0.0023	0.001
60.	5	4	1		5	3	2	6	6	(01)	6.7566058	0.1417	0.002
								5	5	(01)	6.7559050	0.1305	0.001
								4	4	(01)	6.7567474	0.1428	0.001

61.	5	4	2	5	3	3	6	6	(00)	8.8974024	0.0936	0.003
							4	4	(10)	8.6718024	1.0551	0.010
							6	6	(10)	8.6719171	1.0591	0.011
							5	5	(10)	8.6724713	1.0698	0.010
							4	4	(01)	7.7615212	–0.2692	–0.003
							6	6	(01)	7.7615461	–0.2702	–0.003
							5	5	(01)	7.7616645	–0.2788	–0.003
							4	4	(11)	7.8839960	0.2432	–0.008
							6	6	(11)	7.8841450	0.2463	–0.008
							5	5	(11)	7.8848755	0.2604	–0.007
62.	5	5	0	5	4	1	6	6	(00)	9.5313210	–0.0883	0.006
63.	6	0	6	5	1	5	5	4	(00)	18.3179390	–0.0177	0.001
							5	5	(00)	18.3194415	–0.0318	–0.001
							6	5	(00)	18.3178768	–0.0178	0.001
							6	6	(00)	18.3166253	–0.0093	–0.002
							7	6	(00)	18.3179669	–0.0184	0.000
							5	4	(10)	18.3062469	0.0644	0.000
							5	5	(10)	18.3077011	0.0521	–0.001
							6	5	(10)	18.3061715	0.0643	0.000
							6	6	(10)	18.3049616	0.0728	–0.001
							7	6	(10)	18.3062720	0.0640	0.000
							5	4	(01)	18.3124440	–0.0237	0.001
							6	5	(01)	18.3123814	–0.0239	0.001
							7	6	(01)	18.3124722	–0.0241	0.001
							5	4	(11)	18.3015202	0.0959	0.001
							6	5	(11)	18.3014481	0.0961	0.000
							7	6	(11)	18.3015455	0.0950	0.000
							5	4	(12)	18.3001691	0.0662	0.000
							6	5	(12)	18.3000901	0.0657	–0.001
							7	6	(12)	18.3001923	0.0646	–0.001
64.	6	1	6	5	0	5	5	4	(00)	18.3208102	–0.0161	0.001
							5	5	(00)	18.3223090	–0.0314	–0.001
							6	5	(00)	18.3207440	–0.0173	0.000
							6	6	(00)	18.3194953	–0.0082	–0.002
							7	6	(00)	18.3208371	–0.0174	0.000
							5	4	(10)	18.3182712	0.0732	0.000
							6	5	(10)	18.3181837	0.0721	–0.001
							7	6	(10)	18.3182945	0.0728	0.000
							5	4	(01)	18.3146060	–0.0230	0.001
							5	5	(01)	18.3161081	–0.0359	0.001
							6	5	(01)	18.3145407	–0.0236	0.001
							7	6	(01)	18.3146335	–0.0237	0.001
							6	5	(11)	18.3120697	0.1119	0.001
							7	6	(11)	18.3121715	0.1074	–0.002
							6	5	(12)	18.3117576	0.0719	–0.001
							5	4	(12)	18.3118514	0.0758	0.003
							7	6	(12)	18.3118700	0.0715	–0.001
65.	6	1	5	5	2	4	5	4	(00)	21.0248120	–0.0980	0.004
							6	5	(00)	21.0246138	–0.1010	0.000
							7	6	(00)	21.0247892	–0.1018	0.000
							5	4	(10)	20.8754975	–0.0717	0.004

							6	5	(10)	20.8753627	–0.0731	0.001
							7	6	(10)	20.8754829	–0.0756	0.000
							6	5	(01)	21.0239981	–0.0953	–0.004
							7	6	(01)	21.0241813	–0.0963	–0.003
							5	4	(11)	20.8821688	–0.0245	0.003
							6	5	(11)	20.8820228	–0.0252	0.001
							7	6	(11)	20.8821545	–0.0267	0.001
							5	4	(12)	20.8600559	–0.0576	0.002
							6	5	(12)	20.8599251	–0.0577	0.000
							7	6	(12)	20.8600431	–0.0599	–0.001
66.	6	2	5		5	1	4	5	4	(00)	21.1640304	–0.0692	–0.001
								6	5	(00)	21.1637306	–0.0676	0.000
								7	6	(00)	21.1639946	–0.0685	0.000
								5	4	(10)	21.3817273	0.0360	0.007
								6	5	(10)	21.3812696	0.0371	0.006
								7	6	(10)	21.3816624	0.0353	0.006
								5	4	(01)	21.1310993	–0.0885	–0.005
								6	5	(01)	21.1308098	–0.0869	–0.003
								5	4	(11)	21.3400632	0.2607	–0.001
								6	5	(11)	21.3396439	0.2646	0.000
								7	6	(11)	21.3400057	0.2610	–0.001
								5	4	(12)	21.3591303	0.0535	–0.002
								6	5	(12)	21.3586513	0.0536	–0.002
								7	6	(12)	21.3590620	0.0530	–0.002
67.	6	1	5		6	0	6	5	5	(00)	15.0003710	–0.0626	–0.001
								7	7	(00)	15.0005149	–0.0648	–0.002
								6	6	(00)	15.0013803	–0.0650	0.001
								5	5	(10)	14.6101918	–0.1451	0.005
								7	7	(10)	14.6103448	–0.1457	0.005
								6	6	(10)	14.6112493	–0.1507	0.005
								5	5	(01)	14.9389048	–0.0695	–0.007
								7	7	(01)	14.9390513	–0.0685	–0.006
								6	6	(01)	14.9399086	–0.0724	–0.006
								5	5	(11)	14.5537177	0.1194	0.000
								7	7	(11)	14.5538694	0.1197	0.001
								6	6	(11)	14.5547597	0.1134	0.000
								5	5	(12)	14.5571670	–0.2062	0.002
								7	7	(12)	14.5573226	–0.2048	0.004
								6	6	(12)	14.5582303	–0.2100	0.002
68.	6	2	4		6	1	5	7	7	(00)	11.7229800	–0.0521	0.001
								6	6	(00)	11.7238539	–0.0539	0.001
								5	5	(00)	11.7228256	–0.0587	–0.005
								7	7	(01)	11.7286245	–0.0164	0.002
								6	6	(01)	11.7294826	–0.0167	0.003
								5	5	(01)	11.7284814	–0.0146	0.003
69.	6	2	5		6	1	6	7	7	(00)	15.0258327	–0.0552	–0.003
								6	6	(00)	15.0266802	–0.0579	–0.002
								5	5	(00)	15.0256939	–0.0504	0.001
								7	7	(10)	14.7111279	–0.1099	0.007
								6	6	(10)	14.7119792	–0.1140	0.007
								5	5	(10)	14.7109878	–0.1056	0.010
								7	7	(01)	14.9582063	–0.0693	–0.010

							6	6	(01)	14.9590533	–0.0714	–0.009
							5	5	(01)	14.9580714	–0.0608	–0.002
							7	7	(11)	14.6433980	0.1958	0.000
							6	6	(11)	14.6442429	0.1901	–0.001
							5	5	(11)	14.6432554	0.1969	0.000
							7	7	(12)	14.6556373	–0.1784	0.003
							6	6	(12)	14.6564885	–0.1833	0.002
							5	5	(12)	14.6554938	–0.1773	0.003
70.	6	3	4		6	2	5	7	7	(00)	12.2038908	0.0398	0.001
								5	5	(00)	12.2037718	0.0344	–0.005
								7	7	(10)	12.0719759	0.1575	0.006
								6	6	(10)	12.0725808	0.1522	0.004
								5	5	(10)	12.0718694	0.1540	0.002
								7	7	(01)	12.1002047	0.0048	0.002
								6	6	(01)	12.1008928	0.0010	0.001
								5	5	(01)	12.1000849	0.0018	–0.001
								7	7	(11)	11.9758690	0.4619	–0.003
								6	6	(11)	11.9764923	0.4587	–0.003
								5	5	(11)	11.9757619	0.4606	–0.005
								7	7	(12)	12.0377552	0.0136	0.000
								6	6	(12)	12.0383472	0.0080	–0.001
								5	5	(12)	12.0376510	0.0103	–0.003
71.	6	4	3		6	3	4	5	5	(00)	10.2402409	0.1336	–0.002
								6	6	(00)	10.2405736	0.1275	–0.002
								7	7	(00)	10.2402893	0.1331	–0.001
								5	5	(10)	10.5439381	0.6566	0.016
								7	7	(10)	10.5440047	0.6588	0.018
								6	6	(10)	10.5443864	0.6594	0.017
								5	5	(01)	9.6470783	–0.0880	0.001
								7	7	(01)	9.6471540	–0.0866	0.003
								6	6	(01)	9.6475897	–0.0909	0.003
								6	6	(11)	10.1655075	0.5422	–0.004
72.	6	5	1		6	4	2	6	6	(11)	10.4013605	–0.3063	–0.006
								7	7	(11)	10.4017339	–0.2882	–0.006
								5	5	(11)	10.4017968	–0.2852	–0.006
73.	6	6	0		6	5	1	6	6	(11)	13.0513833	1.4079	–0.013
								7	7	(11)	13.0519446	1.4233	–0.013
								5	5	(11)	13.0520376	1.4241	–0.015
								6	6	(12)	11.7648348	1.5318	0.024
								5	5	(12)	11.7658060	1.5546	0.020
74.	6	6	1		6	5	2	7	7	(00)	12.2999871	–0.2678	0.004
								6	6	(00)	12.2995320	–0.2824	0.001
								5	5	(00)	12.3000560	–0.2733	–0.003
								7	7	(01)	11.4483956	–0.7372	–0.006
								6	6	(01)	11.4478385	–0.7573	–0.013
								5	5	(01)	11.4484776	–0.7458	–0.017
75.	7	0	7		6	1	6	6	5	(00)	21.1420148	–0.0409	–0.002
								7	6	(00)	21.1419709	–0.0384	0.000
								8	7	(00)	21.1420407	–0.0382	0.001
								6	5	(10)	21.1301521	0.0576	0.000
								7	6	(10)	21.1300967	0.0579	0.000
								8	7	(10)	21.1301735	0.0576	0.001

							6	5	(01)	21.1360886	–0.0465	–0.001
							7	6	(01)	21.1360430	–0.0457	0.000
							8	7	(01)	21.1361125	–0.0458	0.000
							7	6	(11)	21.1246524	0.0886	0.001
							6	5	(11)	21.1247046	0.0871	0.000
							8	7	(11)	21.1247277	0.0884	0.001
76.	7	1	7		6	0	6	7	6	(00)	21.1424600	–0.0378	0.000
								6	5	(00)	21.1425063	–0.0384	0.000
								8	7	(00)	21.1425299	–0.0379	0.000
								6	5	(10)	21.1323174	0.0600	0.000
								7	6	(10)	21.1322603	0.0603	0.000
								8	7	(10)	21.1323389	0.0604	0.001
								7	6	(11)	21.1265276	0.0920	0.000
								6	5	(11)	21.1265815	0.0907	0.000
								8	7	(11)	21.1266038	0.0915	0.000
								7	6	(12)	21.1260057	0.0585	–0.001
								6	5	(12)	21.1260642	0.0576	–0.002
								8	7	(12)	21.1260858	0.0585	–0.001
77.	7	1	6		6	2	5	6	5	(00)	23.8938442	–0.1514	0.002
								7	6	(00)	23.8936737	–0.1532	0.000
								8	7	(00)	23.8938304	–0.1547	–0.001
								6	5	(10)	23.8419300	–0.1060	0.008
								7	6	(10)	23.8417645	–0.1076	0.005
								8	7	(10)	23.8419166	–0.1087	0.005
								6	5	(01)	23.8802918	–0.1585	–0.005
								7	6	(01)	23.8801207	–0.1592	–0.006
								8	7	(01)	23.8802788	–0.1608	–0.007
								6	5	(12)	23.8251710	–0.0944	0.000
								7	6	(12)	23.8250037	–0.0956	–0.002
								8	7	(12)	23.8251581	–0.0962	–0.002
78.	7	2	6		6	1	5	6	5	(00)	23.9248416	–0.1371	0.002
								7	6	(00)	23.9246496	–0.1387	0.000
								8	7	(00)	23.9248233	–0.1418	–0.002
								6	5	(10)	23.9670603	–0.0469	0.015
								7	6	(10)	23.9668117	–0.0535	0.007
								8	7	(10)	23.9670310	–0.0545	0.007
								7	6	(01)	23.9034809	–0.1537	–0.006
								8	7	(01)	23.9036534	–0.1557	–0.007
								6	5	(01)	23.9036692	–0.1530	–0.005
								6	5	(11)	23.9425466	0.0891	0.001
								7	6	(11)	23.9423166	0.0889	–0.001
								8	7	(11)	23.9425256	0.0878	–0.001
79.	7	2	5		7	1	6	6	6	(00)	14.7186627	–0.1093	–0.003
								7	7	(00)	14.7194853	–0.1099	–0.001
								6	6	(10)	14.0402544	0.0589	–0.005
								8	8	(10)	14.0403747	0.0601	–0.003
								7	7	(10)	14.0411959	0.0560	–0.003
								6	6	(01)	14.6784031	–0.0859	–0.002
								8	8	(01)	14.6785095	–0.0820	0.002
								7	7	(01)	14.6792169	–0.0855	0.000
								6	6	(11)	14.0211373	0.2429	–0.003
								8	8	(11)	14.0212538	0.2440	–0.001

							7	7	(11)	14.0220484	0.2384	–0.002
							6	6	(12)	14.0002389	–0.0671	–0.001
							8	8	(12)	14.0003606	–0.0658	0.001
							7	7	(12)	14.0011916	–0.0696	0.000
80.	7	3	5		7	2	6	6	6	(00)	14.8564095	–0.0541	–0.003
								8	8	(00)	14.8565068	–0.0519	0.000
								7	7	(00)	14.8571631	–0.0550	–0.001
								6	6	(10)	14.5453645	0.0829	0.001
								8	8	(10)	14.5454584	0.0844	0.003
								7	7	(10)	14.5460943	0.0799	0.002
								6	6	(01)	14.7830201	–0.0647	–0.002
								8	8	(01)	14.7831186	–0.0618	0.001
								7	7	(01)	14.7837771	–0.0660	–0.001
								6	6	(11)	14.4726747	0.4236	–0.006
								8	8	(11)	14.4727690	0.4253	–0.004
								7	7	(11)	14.4734058	0.4206	–0.006
								6	6	(12)	14.4949404	–0.0568	–0.004
								8	8	(12)	14.4950344	–0.0551	–0.002
								7	7	(12)	14.4956698	–0.0592	–0.003
81.	7	3	4		7	2	5	7	7	(00)	10.8504470	–0.1375	0.007
								6	6	(10)	9.5830309	0.4873	–0.008
								8	8	(10)	9.5831258	0.4885	–0.007
								6	6	(11)	9.6088449	0.7016	–0.006
								8	8	(11)	9.6089384	0.7016	–0.006
								7	7	(11)	9.6095813	0.6965	–0.007
								6	6	(12)	9.5468701	0.2678	–0.005
								8	8	(12)	9.5469693	0.2692	–0.003
								7	7	(12)	9.5476441	0.2662	–0.005
82.	7	4	4		7	3	5	6	6	(00)	12.2341714	0.0912	–0.004
								8	8	(00)	12.2342383	0.0931	–0.002
								7	7	(00)	12.2346859	0.0899	–0.002
								6	6	(10)	12.3582054	0.3534	0.008
								8	8	(10)	12.3582614	0.3538	0.009
								7	7	(10)	12.3586436	0.3506	0.007
								6	6	(01)	12.0039005	–0.0095	0.003
								8	8	(01)	12.0039767	–0.0062	0.006
								7	7	(01)	12.0044776	–0.0104	0.005
								6	6	(11)	12.1815462	0.6129	–0.008
								8	8	(11)	12.1816091	0.6138	–0.007
								7	7	(11)	12.1820373	0.6123	–0.008
								6	6	(12)	12.3607541	0.0253	–0.008
								8	8	(12)	12.3608048	0.0259	–0.006
								7	7	(12)	12.3611471	0.0213	–0.008
83.	7	4	3		7	3	4	6	6	(00)	6.8232434	0.0655	–0.003
								8	8	(00)	6.8233040	0.0643	–0.005
								7	7	(00)	6.8237333	0.0655	–0.003
								7	7	(10)	9.2387564	–1.9431	–0.020
								8	8	(10)	9.2389390	–1.9376	–0.016
								6	6	(10)	9.2389576	–1.9446	–0.023
								6	6	(01)	7.0614320	0.4063	0.007
								8	8	(01)	7.0614914	0.4074	0.008
								7	7	(01)	7.0618960	0.4077	0.009

							7	7	(11)	9.3056992	–0.4732	–0.003
							8	8	(11)	9.3059295	–0.4718	0.000
							6	6	(11)	9.3059589	–0.4754	–0.004
							7	7	(12)	9.0397569	–0.6670	0.005
							8	8	(12)	9.0399276	–0.6601	0.009
							6	6	(12)	9.0399490	–0.6623	0.007
84.	7	5	2		7	4	3	7	7	(01)	7.9412275	0.4293	–0.002
								8	8	(01)	7.9417682	0.4384	–0.001
								6	6	(01)	7.9418442	0.4377	–0.002
								7	7	(11)	10.9023702	–2.9788	0.009
								8	8	(11)	10.9024420	–2.9709	0.008
								6	6	(11)	10.9024589	–2.9632	0.015
								6	6	(12)	8.7275666	–1.3117	0.005
								8	8	(12)	8.7275964	–1.3137	0.003
								7	7	(12)	8.7278144	–1.3166	0.004
85.	7	5	3		7	4	4	8	8	(01)	9.8956069	–0.2237	–0.003
								7	7	(01)	9.8957998	–0.2261	–0.001
86.	7	6	1		7	5	2	7	7	(00)	11.0123451	0.0913	0.003
								8	8	(10)	11.7879201	–1.1187	–0.002
								7	7	(10)	11.7872752	–1.1358	–0.003
								6	6	(10)	11.7880076	–1.1218	–0.007
								8	8	(01)	11.8819183	–0.3146	0.014
								7	7	(01)	11.8814077	–0.3278	0.011
								6	6	(01)	11.8819852	–0.3194	0.008
87.	7	6	2		7	5	3	8	8	(00)	12.1546007	0.0203	0.002
								7	7	(00)	12.1543055	0.0158	0.006
								6	6	(00)	12.1546512	0.0288	0.009
88.	8	0	8		7	1	7	8	7	(00)	23.9652566	–0.0630	0.000
								7	6	(00)	23.9652904	–0.0649	–0.001
								9	8	(00)	23.9653106	–0.0638	0.000
								7	6	(10)	23.9518282	0.0397	–0.003
								8	7	(10)	23.9517913	0.0447	0.002
								9	8	(10)	23.9518519	0.0454	0.003
								8	7	(01)	23.9591709	–0.0718	0.000
								7	6	(01)	23.9592023	–0.0761	–0.005
								9	8	(01)	23.9592271	–0.0704	0.001
89.	8	1	8		7	0	7	8	7	(00)	23.9653368	–0.0626	0.001
								7	6	(00)	23.9653702	–0.0650	–0.002
								9	8	(00)	23.9653913	–0.0630	0.001
								7	6	(10)	23.9521990	0.0403	–0.003
								8	7	(10)	23.9521615	0.0449	0.001
								9	8	(10)	23.9522226	0.0459	0.003
								7	6	(01)	23.9592613	–0.0751	–0.004
								9	8	(01)	23.9592830	–0.0725	–0.001
90.	8	3	5		8	2	6	9	9	(00)	14.1737915	–0.2145	0.003
								8	8	(00)	14.1744614	–0.2162	0.002
								7	7	(00)	14.1737030	–0.2185	–0.001
91.	8	4	4		8	3	5	9	9	(00)	9.6474136	–0.1969	0.003
								8	8	(00)	9.6481113	–0.1988	–0.001
								7	7	(00)	9.6473210	–0.2014	–0.002
92.	8	4	5		8	3	6	9	9	(00)	14.6854883	–0.0226	–0.002
								8	8	(00)	14.6859988	–0.0231	–0.001

							7	7	(00)	14.6854235	–0.0230	–0.003
							9	9	(10)	14.4971802	0.3042	–0.001
							8	8	(10)	14.4976357	0.3019	–0.001
							7	7	(10)	14.4971254	0.3070	0.002
							9	9	(01)	14.5775812	–0.0536	0.006
							8	8	(01)	14.5781063	–0.0545	0.006
							7	7	(01)	14.5775156	–0.0529	0.006
93.	8	5	4	8	4	5	9	9	(01)	11.9617876	–0.0690	0.007
							8	8	(01)	11.9621551	–0.0722	0.007
							7	7	(01)	11.9617416	–0.0683	0.008
94.	9	4	5	9	3	6	10	10	(00)	13.2033698	–0.4165	–0.001
							9	9	(00)	13.2040481	–0.4132	0.002
							8	8	(00)	13.2033005	–0.4103	0.006
95.	9	5	4	9	4	5	10	10	(00)	8.6037176	–0.0624	–0.004
							9	9	(00)	8.6041647	–0.0602	–0.002
							8	8	(00)	8.6036698	–0.0605	–0.002
96.	9	6	4	9	5	5	10	10	(00)	13.2045143	0.3670	–0.005
							9	9	(00)	13.2045890	0.3623	–0.006
							8	8	(00)	13.2045026	0.3642	–0.008
							10	10	(01)	12.0295918	–0.1665	0.006
							9	9	(01)	12.0298112	–0.1710	0.004
97.	9	7	2	9	6	3	10	10	(00)	12.2950474	0.5797	0.002
							9	9	(00)	12.2944723	0.5717	0.003
							8	8	(00)	12.2951029	0.5718	–0.006

AIV.2: The rotational signature of 4-methylpyrimidine

Table S-I: Nuclear coordinates in the principal inertial axes of 4-methylpyrimidine calculated with the B3LYP and MP2 methods at various basis sets. The atoms are numbered according to Fig. 1.

	MP2/6-31G			B3LYP/6-31G		
	A / Å	B / Å	C / Å	A / Å	B / Å	C / Å
N_1	1.861691	0.067995	−0.000150	1.858085	0.069047	−0.003379
C_2	1.053447	1.173080	−0.000037	1.049748	1.168392	−0.000832
N_3	−0.312403	1.178468	0.000152	−0.310715	1.178397	0.003895
C_4	−0.944284	−0.045246	0.000260	−0.943782	−0.041134	0.004262
C_5	−0.189218	−1.238699	0.000111	−0.189779	−1.241925	0.002969
C_6	1.215378	−1.141779	−0.000045	1.215864	−1.137599	−0.001111
C_7	−2.456173	−0.023406	−0.000207	−2.449102	−0.025106	−0.003179
H_8	1.547500	2.140352	−0.000060	1.555975	2.158534	−0.000751
H_9	−0.679402	−2.212454	0.000297	−0.695587	−2.233115	0.007606
H_{10}	1.852331	−2.024409	−0.000058	1.864924	−2.042630	−0.000607
H_{11}	−2.828649	0.514383	0.881958	−2.831926	0.684393	0.777050
H_{12}	−2.828758	0.500829	−0.890531	−2.831263	0.353975	−0.990612
H_{13}	−2.862228	−1.043791	0.007392	−2.879922	−1.044124	0.175046
	MP2/ 6-311G			MP2/ 6-311G		
	A / Å	B / Å	C / Å	A / Å	B / Å	C / Å
N_1	1.853346	0.063588	0.006168	1.853493	0.069628	−0.003502
C_2	1.055722	1.168387	0.001325	1.048776	1.169830	−0.000848
N_3	−0.307899	1.176790	−0.006195	−0.310840	1.174746	0.004110
C_4	−0.941157	−0.040641	−0.009288	−0.942694	−0.044041	0.004022
C_5	−0.191553	−1.232964	−0.005447	−0.188400	−1.240568	0.003068
C_6	1.206181	−1.142564	0.002209	1.213705	−1.137002	−0.001056
C_7	−2.447270	−0.021498	0.008010	−2.444663	−0.023636	−0.003133
H_8	1.550266	2.129719	0.000020	1.552586	2.157244	−0.000633
H_9	−0.685924	−2.200118	−0.011693	−0.691806	−2.230155	0.007360
H_{10}	1.841043	−2.021191	0.002938	1.866405	−2.035703	−0.000391
H_{11}	−2.827940	−0.060781	1.036094	−2.821584	0.694095	0.767459
H_{12}	−2.799003	0.907006	−0.447584	−2.823115	0.346590	−0.991711
H_{13}	−2.857314	−0.875778	−0.541400	−2.879682	−1.035667	0.185026

	MP2/6-311++G(d,p)			B3LYP/6-311++G(d,p)		
	A / Å	B / Å	C / Å	A / Å	B / Å	C / Å
N_1	1.829500	0.075385	−0.000001	1.838521	0.074661	−0.000468
C_2	1.024740	1.143768	−0.000001	1.032252	1.151335	−0.000078
N_3	−0.310714	1.153453	0.000001	−0.309163	1.160435	0.000557
C_4	−0.923239	−0.041890	0.000005	−0.931136	−0.040280	0.000519
C_5	−0.179274	−1.221398	0.000002	−0.182183	−1.231307	0.000369
C_6	1.206374	−1.108642	−0.000002	1.212552	−1.116099	−0.000144
C_7	−2.421933	−0.029475	−0.000002	−2.431869	−0.028161	−0.000442
H_8	1.511982	2.113001	−0.000001	1.535089	2.147795	−0.000122
H_9	−0.659703	−2.191727	−0.000003	−0.679013	−2.226660	0.001263
H_{10}	1.842255	−1.988102	0.000001	1.865049	−2.021574	0.000025
H_{11}	−2.784496	0.503664	0.879152	−2.811487	0.548091	0.883554
H_{12}	−2.784489	0.503382	−0.879332	−2.810439	0.507425	−0.910365
H_{13}	−2.828603	−1.039653	0.000152	−2.865184	−1.059593	0.021734
	MP2/ cc-pVDZ			MP2/ cc-pVDZ		
	A / Å	B / Å	C / Å	A / Å	B / Å	C / Å
N_1	1.845765	0.078844	−0.000001	−1.852553	−0.077524	−0.005865
C_2	1.026564	1.148825	−0.000001	−1.032465	−1.152064	−0.001328
N_3	−0.318075	1.162994	0.000001	0.316282	−1.169432	0.006742
C_4	−0.929735	−0.043482	0.000002	0.935016	0.039859	0.006629
C_5	−0.178010	−1.229320	0.000000	0.181596	1.237590	0.005255
C_6	1.217809	−1.112648	0.000000	−1.220325	1.117716	−0.001677
C_7	−2.436226	−0.033731	−0.000001	2.442557	0.031973	−0.004787
H_8	1.516787	2.129483	0.000001	−1.537191	−2.157334	−0.000655
H_9	−0.663038	−2.210103	0.000002	0.681740	2.239760	0.011838
H_{10}	1.858668	−2.002934	−0.000004	−1.876791	2.030640	−0.000877
H_{11}	−2.807376	0.504478	0.887308	2.826581	−0.784105	0.670207
H_{12}	−2.807371	0.504410	−0.887353	2.877415	1.024462	0.301661
H_{13}	−2.849835	−1.053951	0.000034	2.818894	−0.209869	−1.043087

Table S-II. Fourier expansion of the potential energy curve given in Fig. 2. The potential is expanded as $V(\alpha) = \sum_{i=0}^{5} a_i f_i$. Note that $V_{3i} = 2 \cdot a_i$.

		MP2/cc-pVDZ		MP2/6-311G	
i	f_i	a_i / Hartree	a_i / cm^{-1}	a_i / Hartree	a_i / cm^{-1}
0	1	–302.733961551		–302.350704704	
1	cos 3α	0.000114828	25.20	–0.000023073	–5.06
2	cos 6α	0.000007479	1.64	0.000030440	6.68
3	cos 9α	–0.000000423	–0.09	–0.000001285	–0.28
4	cos 12α	0.000000223	0.05	–0.000000029	0.01
5	cos 15α	–0.000000127	–0.03	-	-

Table S-III: Data points of the potential energy curves for the methyl torsional barrier of 4-methylpyrimidine given in Fig. 2 and Fig. 3, obtaining by varying the dihedral angle in a gid of 1° while all other molecular parameters were optimized at the B3LYP/6-311G as well as MP2/6-311G levels of theory. The energy values are in Hartree unit and angles α are given in degree.

α	MP2/6-311G	B3LYP/6-311G
−1	−302.3506987	−297.7316915850
−10	−302.3507095	−297.7316940958
−11	−302.3507114	−297.7316956325
−12	−302.3507135	−297.7316966627
−13	−302.3507156	−297.7316961731
−14	−302.3507180	−297.7316933676
−15	−302.3507202	−297.7316879145
−16	−302.3507223	−297.7316800754
−17	−302.3507245	−297.7316707182
−18	−302.3507265	−297.7316611837
−19	−302.3507284	−297.7316529744
−2	−302.3506990	−297.7316924739
−20	−302.3507302	−297.7316472658
−21	−302.3507317	−297.7316444456
−22	−302.3507332	−297.7316439984
−23	−302.3507344	−297.7316448333
−24	−302.3507353	−297.7316457848
−25	−302.3507360	−297.7316459765
−26	−302.3507364	−297.7316449634
−27	−302.3507365	−297.7316426968

−28	−302.3507364	−297.7316393991
−29	−302.3507359	−297.7316354170
−3	−302.3506996	−297.7316935023
−30	−302.3507351	−297.7316311072
−31	−302.3507340	−297.7316267734
−32	−302.3507325	−297.7316226665
−33	−302.3507307	−297.7316190168
−34	−302.3507286	−297.7316160673
−35	−302.3507262	−297.7316140670
−36	−302.3507233	−297.7316131986
−37	−302.3507204	−297.7316134677
−38	−302.3507172	−297.7316146139
−39	−302.3507135	−297.7316161058
−4	−302.3507005	−297.7316942190
−40	−302.3507098	−297.7316172320
−41	−302.3507059	−297.7316172434
−42	−302.3507019	−297.7316155135
−43	−302.3506978	−297.7316116866
−44	−302.3506936	−297.7316058086
−45	−302.3506893	−297.7315984191
−46	−302.3506848	−297.7315905747
−47	−302.3506807	−297.7315837337
−48	−302.3506767	−297.7315794062
−49	−302.3506727	−297.7315785804
−5	−302.3507015	−297.7316943276
−50	−302.3506690	−297.7315812413
−51	−302.3506656	−297.7315864213
−52	−302.3506624	−297.7315927209
−53	−302.3506595	−297.7315988561
−54	−302.3506570	−297.7316039530
−55	−302.3506549	−297.7316076291
−56	−302.3506532	−297.7316099171
−57	−302.3506519	−297.7316111178
−58	−302.3506510	−297.7316116022
−59	−302.3506507	−297.7316116177
−6	−302.3507027	−297.7316938361
−60	−302.3506507	−297.7316111662
−7	−302.3507041	−297.7316930902
−8	−302.3507058	−297.7316926351
−9	−302.3507076	−297.7316929431
0	−302.3506986	−297.7316912289

1	−302.3506987	−297.7316915646
10	−302.3507096	−297.7316940367
11	−302.3507116	−297.7316955660
12	−302.3507137	−297.7316966132
13	−302.3507158	−297.7316961659
14	−302.3507180	−297.7316934171
15	−302.3507202	−297.7316880283
16	−302.3507224	−297.7316802405
17	−302.3507245	−297.7316709073
18	−302.3507265	−297.7316613624
19	−302.3507284	−297.7316531099
2	−302.3506990	−297.7316924414
20	−302.3507302	−297.7316473442
21	−302.3507317	−297.7316444746
22	−302.3507332	−297.7316440025
23	−302.3507344	−297.7316448406
24	−302.3507353	−297.7316458156
25	−302.3507361	−297.7316460403
26	−302.3507364	−297.7316450602
27	−302.3507366	−297.7316428189
28	−302.3507364	−297.7316395359
29	−302.3507359	−297.7316355588
3	−302.3506996	−297.7316934698
30	−302.3507351	−297.7316312459
31	−302.3507339	−297.7316269045
32	−302.3507325	−297.7316227870
33	−302.3507307	−297.7316191239
34	−302.3507285	−297.7316161580
35	−302.3507261	−297.7316141381
36	−302.3507233	−297.7316132497
37	−302.3507203	−297.7316135028
38	−302.3507171	−297.7316146407
39	−302.3507136	−297.7316161366
4	−302.3507005	−297.7316941982
40	−302.3507099	−297.7316172798
41	−302.3507059	−297.7316173196
42	−302.3507019	−297.7316156246
43	−302.3506978	−297.7316118334
44	−302.3506936	−297.7316059839
45	−302.3506893	−297.7315986070
46	−302.3506851	−297.7315907519

47	−302.3506810	−297.7315838740
48	−302.3506770	−297.7315794895
49	−302.3506730	−297.7315786012
5	−302.3507015	−297.7316943228
50	−302.3506693	−297.7315812143
51	−302.3506658	−297.7315863718
52	−302.3506626	−297.7315926760
53	−302.3506597	−297.7315988328
54	−302.3506571	−297.7316039631
55	−302.3506550	−297.7316076732
56	−302.3506533	−297.7316099911
57	−302.3506520	−297.7316112151
58	−302.3506511	−297.7316117160
59	−302.3506507	−297.7316117440
6	−302.3507028	−297.7316938439
60	−302.3506508	−297.7316113031
7	−302.3507043	−297.7316930975
8	−302.3507059	−297.7316926275
9	−302.3507077	−297.7316929086

Fig. S-I: Potential energy curves of 4-methylpyrrimidine (in cm^{-1}) obtained by varying the dihedral angle $\alpha = \angle(H_{11},C_7,C_4,N_3)$ in step of 1° while all other parameters were optimized at the B3LYP/cc-pVDZ (red dots) and the B3LYP/6-311G (green dots) together with the geometry optimizations at minima. The energies are transferred to cm^{-1} relative to the lowest energies.

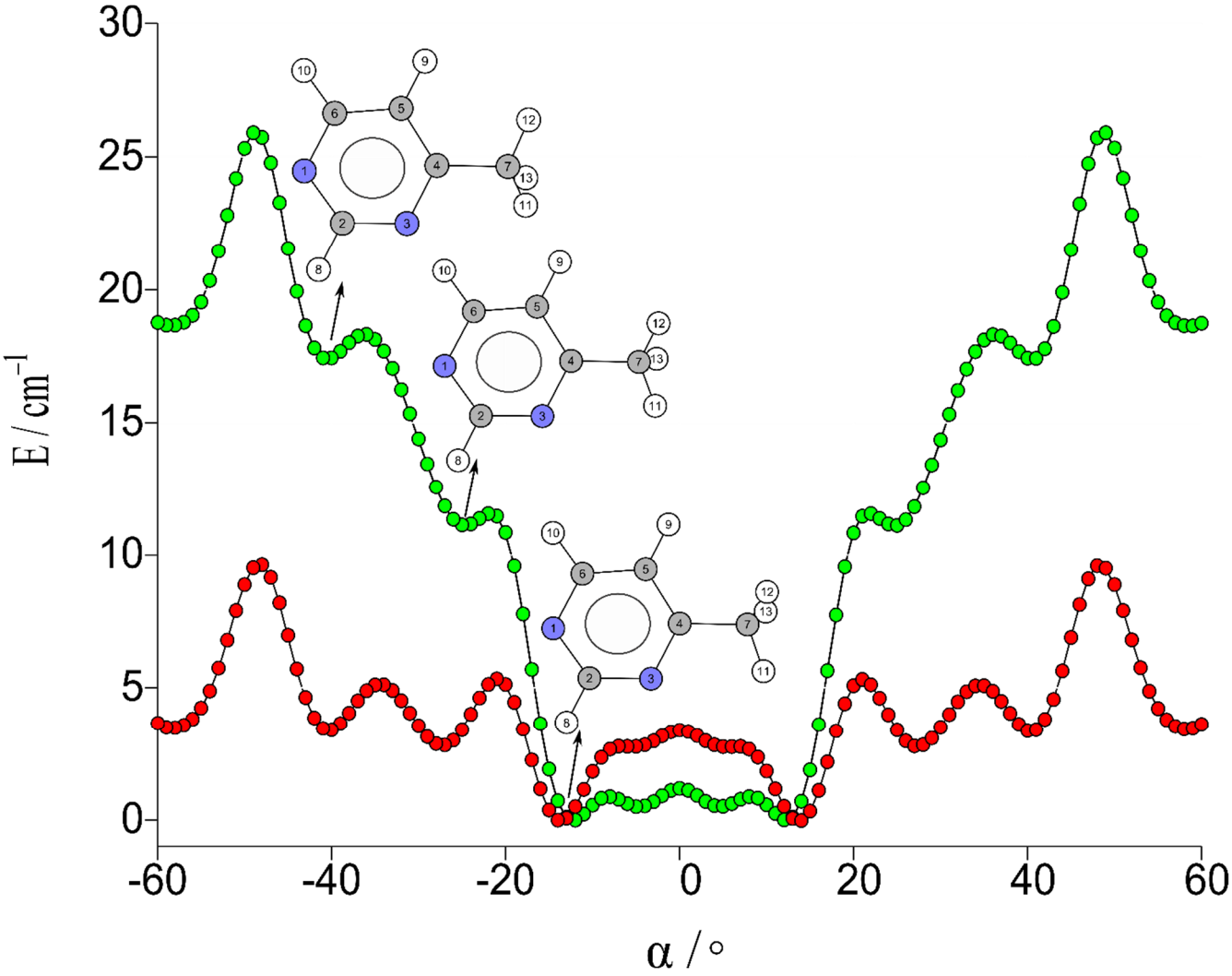

Table S-IV: Observed frequencies ($\nu_{obs.}$) of the A and E species of 4-methylpyrimidine. $\nu_{calc.}$ are the calculated frequencies; $\nu_{obs.}-\nu_{calc.}$ values as obtained after a fit with the program *TW21* and *BELGI-2N*. *J, K_a, K_c* are the asymmetric top rotational quantum numbers of the lower energy level; *J', K_a', K_c'* are those of the upper energy level. F_1 and *F* quantum numbers are defined in Eqn. (35) Chapter II.

	J'	*K_a'*	*K_c'*	*J*	*K_a*	*K_c*	Sym	F_1'	*F'*	F_1	*F*	$\nu_{obs.}$	$\nu_{obs.} - \nu_{calc.}$	$\nu_{obs.} - \nu_{calc.}$
	Upper level			Lower level								GHz	*TW21*/kHz	*BELGI*/kHz
1.	1	1	1	0	0	0	A	0	1	1	1	7.961839	−1	3
								0	1	1	2	7.961839	−1	3
								2	2	1	1	7.962196	0	0
								2	2	1	2	7.962196	0	0
								1	0	1	1	7.962538	−1	−4
								2	1	1	0	7.962926	0	14
								2	3	1	2	7.962990	3	4
								1	2	1	1	7.963332	0	−1
								1	2	1	2	7.963332	0	−1
								1	1	1	1	7.964420	−1	0
								1	1	1	2	7.964420	−1	0
2.	1	1	0	1	0	1	A	1	2	0	1	4.240563	−2	0
								2	1	2	2	4.240780	1	0
								0	1	1	2	4.240848	−3	−5
								2	3	2	3	4.241193	−11	−11
								2	1	1	0	4.242167	−1	−3
								1	1	2	1	4.242450	1	4
								2	3	1	2	4.242596	3	2
								1	2	2	3	4.242615	−1	1
								1	0	2	1	4.243058	−2	1
								2	2	1	2	4.243066	2	2
3.	2	0	2	1	0	1	A	2	2	2	1	8.892945	0	1
								2	2	2	3	8.892971	0	0
								2	2	2	2	8.893019	1	1
								2	3	2	3	8.893109	0	0
								1	1	0	1	8.893289	−3	−2
								1	2	0	1	8.893406	1	2
								1	0	0	1	8.893581	1	1
								2	2	1	1	8.894332	−1	0
								3	3	2	2	8.894473	2	2
								3	4	2	3	8.894650	0	0
4.	2	0	2	1	1	1	A	2	2	1	2	5.436827	−2	−1

								2	3	1	2	5.436964	−3	−2
								2	1	1	0	5.437820	−1	1
								2	2	2	2	5.437964	−1	−1
								2	3	2	2	5.438104	2	1
								3	3	1	2	5.438292	10	11
								2	2	0	1	5.438320	−1	−4
								1	0	1	1	5.438399	0	−1
								3	4	2	3	5.438848	−3	−5
								1	1	1	2	5.439200	−1	1
								1	2	1	2	5.439311	−3	−1
								3	3	2	2	5.439420	1	2
5.	2	1	1	1	1	0	A	3	2	1	2	9.797868	0	−1
								2	3	1	2	9.798070	2	3
								3	2	2	2	9.798807	−2	−3
								2	3	2	2	9.799007	−3	−1
								1	1	1	0	9.799065	1	−2
								2	2	1	2	9.799234	−1	−2
								3	3	1	2	9.799378	2	1
								3	2	2	1	9.799753	2	3
								3	4	2	3	9.799896	1	1
								3	3	2	2	9.800314	−4	−4
								3	3	2	3	9.800783	−6	−5
								2	1	0	1	9.800797	−1	3
								3	2	0	1	9.801026	2	5
								2	2	2	1	9.801117	−1	0
								1	1	2	1	9.801416	−2	−3
								1	2	0	1	9.801710	−2	−32
6.	2	1	2	1	0	1	A	1	1	0	1	11.682561	2	4
								2	3	2	3	11.682933	4	4
								2	3	2	2	11.682975	0	−1
								1	0	0	1	11.683344	0	3
								3	3	2	2	11.683649	2	1
								2	2	1	1	11.683819	−1	−2
								3	4	2	3	11.684276	1	3
								3	2	2	2	11.684657	1	2
								1	2	2	1	11.684828	−1	2
								3	3	1	2	11.684996	4	4
								1	2	1	2	11.686243	−3	−1
								1	0	1	1	11.686755	−1	1
								2	3	1	2	11.684315	−3	−4
								2	1	1	0	11.684476	−1	−2

								3	2	2	1	11.684582	−1	1
								3	2	2	2	11.684661	5	6
								1	2	2	1	11.684828	−1	2
								3	3	1	2	11.684988	−4	−4
								1	1	1	1	11.685971	−1	1
								1	1	1	2	11.685997	−4	−2
7.	2	1	2	1	1	1	A	2	1	1	1	8.225808	−1	−2
								2	2	1	2	8.226316	−1	−1
								2	3	1	2	8.226787	1	2
								2	3	2	3	8.227129	−1	−3
								1	1	1	1	8.227380	1	2
								2	2	2	2	8.227450	−2	−4
								2	3	2	2	8.227921	−1	−2
								1	0	1	1	8.228164	0	2
								3	2	1	2	8.228464	−4	−1
								3	4	2	3	8.228486	10	10
								3	3	2	2	8.228596	1	1
								1	2	2	1	8.229123	4	−8
								3	2	2	2	8.229603	−1	0
								1	2	2	2	8.229857	8	9
								3	2	0	1	8.229960	1	−1
8.	2	2	0	1	1	1	A	1	0	1	1	21.069526	−5	−4
								1	1	1	1	21.069817	−1	−2
								3	2	1	1	21.070421	−3	−2
								1	2	1	2	21.070795	0	2
								1	1	1	2	21.070902	−6	−4
								1	2	2	1	21.071202	0	−12
								3	4	2	3	21.071948	3	3
								2	3	1	2	21.073144	1	5
								2	3	2	3	21.073485	−1	−1
								2	2	2	1	21.073684	−1	−14
								2	1	1	0	21.073868	−3	1
								2	2	2	2	21.074414	−1	0
								2	2	0	1	21.074773	2	0
9.	2	2	1	2	1	2	A	1	1	1	0	12.722221	−1	−3
								1	2	1	2	12.722736	5	5
								1	0	1	1	12.722927	−3	−3
								1	2	3	2	12.722979	2	2
								3	4	3	4	12.724128	7	7
								2	1	1	0	12.724462	0	−1
								1	1	2	1	12.724569	−8	−6

								1	2	2	3	12.724661	2	5
								1	1	2	2	12.725156	−2	0
								2	2	1	1	12.725302	4	3
								3	4	2	3	12.725480	13	15
								3	3	2	3	12.725532	6	8
								2	3	3	4	12.725608	7	7
								2	3	3	3	12.726273	−1	0
								2	1	2	1	12.726814	−3	−1
								2	3	2	3	12.726955	9	10
								2	2	2	2	12.727450	0	2
10.	3	0	3	2	0	2	A	3	3	3	2	13.058428	0	0
								3	3	3	3	13.058740	0	−2
								3	4	3	4	13.058930	0	−1
								3	2	3	2	13.058964	−3	−3
								3	3	2	2	13.060197	3	2
								4	4	3	3	13.060327	0	1
								4	5	3	4	13.060594	1	1
								4	3	3	2	13.060647	0	0
11.	3	0	3	2	1	2	A	3	4	3	3	10.269978	−1	−2
								3	3	2	3	10.270239	2	2
								2	2	1	2	10.270520	−4	−6
								4	3	1	2	10.270535	5	4
								3	3	2	2	10.270704	−2	−2
								4	3	3	2	10.270771	−4	−6
								2	3	1	2	10.270921	0	−1
								4	5	3	4	10.270969	0	−1
								4	4	3	3	10.271149	−1	0
								2	1	1	1	10.271386	0	−1
								4	3	3	3	10.271787	4	3
								4	4	2	3	10.271823	0	1
								2	2	2	1	10.272339	−1	0
								2	2	2	3	10.272450	−2	−1
								2	3	2	3	10.272839	−9	−8
								2	2	2	2	10.272921	−1	1
								2	1	2	2	10.273535	−3	−1
12.	3	1	2	2	1	1	A	3	2	3	3	14.616421	1	3
								3	2	2	2	14.616560	−1	0
								2	1	1	1	14.617349	−5	−7
								3	4	3	4	14.617580	−1	2
								3	4	2	3	14.617995	0	0
								4	4	3	3	14.618369	2	3

								4	5	3	4	14.618413	0	0
								2	2	1	1	14.618465	−4	−4
								2	3	2	3	14.619332	−2	−5
13.	3	1	3	2	0	2	A	3	4	3	4	15.060610	−1	−2
								3	2	3	2	15.060713	−3	−3
								3	4	3	3	15.060837	2	−1
								3	3	2	2	15.061490	−1	−3
								4	4	3	3	15.061559	1	1
								3	4	2	3	15.062152	0	−1
								4	5	3	4	15.062252	0	2
								2	3	2	3	15.064270	−1	2
								2	1	2	1	15.064622	−3	−1
								2	1	2	2	15.064822	−4	−2
14.	3	2	2	3	1	3	A	2	1	2	1	13.971764	−4	−5
								2	3	2	3	13.972195	9	9
								4	3	4	3	13.972350	−16	−16
								4	4	4	4	13.973581	0	0
								3	2	3	2	13.974115	3	5
								3	4	3	4	13.974306	1	4
								3	3	3	3	13.975104	2	4
15.	4	1	4	3	0	3	A	4	4	3	3	18.249072	1	0
								3	3	2	2	18.249106	−2	−2
								5	5	4	4	18.249203	0	1
								3	4	2	3	18.249654	0	1
								5	6	4	5	18.249788	0	2
16.	4	2	2	3	2	1	A	4	3	3	2	18.991076	14	15
								4	4	3	3	18.991403	−8	−8
								5	4	4	3	18.991534	−1	−2
								5	6	4	5	18.991609	0	0
								3	4	2	3	18.991678	2	2
								5	5	4	4	18.991819	2	1
								3	3	2	2	18.991954	2	1
17.	4	2	3	3	2	2	A	4	4	3	3	17.933834	−2	−2
								4	5	3	4	17.933900	−1	−1
								4	3	3	2	17.933923	5	5
								5	5	4	4	17.934464	−1	−1
								5	6	4	5	17.934536	−1	−2
								5	4	4	3	17.934561	8	8
								3	3	2	2	17.934624	−7	−7
								3	4	2	3	17.934698	1	1
18.	4	1	3	4	0	4	A	4	5	3	4	9.056321	2	4

								4	3	5	4	9.056372	−2	0
								4	5	5	6	9.056733	0	2
								4	3	3	3	9.056837	−3	−3
								4	3	4	3	9.058164	−1	2
								4	5	4	5	9.058507	1	5
								3	3	3	3	9.059059	−1	−3
								4	5	4	4	9.059226	0	3
								5	5	5	5	9.059301	−1	−1
								5	6	4	5	9.059546	1	2
								4	4	4	4	9.059753	0	3
								3	4	4	5	9.059903	−1	−1
19.	5	1	5	4	1	4	A	5	5	4	4	20.152819	−1	−2
								4	4	3	3	20.152842	3	3
								6	6	5	5	20.152942	1	2
								5	6	4	5	20.152976	2	2
								4	5	3	4	20.153011	−2	−2
								6	7	5	6	20.153070	−1	−1
20.	5	1	4	5	0	5	A	4	3	4	3	12.218585	−7	−10
								6	5	6	5	12.218790	−3	−4
								5	6	5	6	12.219763	2	6
								4	4	4	4	12.220502	−1	−3
								6	6	6	6	12.220689	3	3
								5	5	5	5	12.221250	−1	2
21.	3	2	2	2	1	1	A	2	2	1	1	23.887414	0	2
								4	4	3	3	23.887574	1	2
								3	3	2	2	23.887715	0	1
								2	3	1	2	23.888391	−2	31
								4	5	3	4	23.888470	3	4
								3	4	2	3	23.888888	7	5
								4	3	3	2	23.889081	−1	1
								3	2	2	1	23.889307	0	0
22.	3	2	1	2	2	0	A	3	4	2	3	13.980010	0	1
								3	3	2	2	13.980336	0	1
								4	3	3	2	13.981400	3	1
								3	2	3	2	13.981459	−6	−5
								4	5	3	4	13.981463	−6	−7
								2	3	1	2	13.982254	2	1
								2	2	1	1	13.982619	0	1
								2	2	1	2	13.982731	0	0
23.	3	2	2	2	2	1	A	4	4	3	3	13.521111	0	0
								4	5	3	4	13.521168	−2	−2

								4	3	3	2	13.521197	6	5
								2	2	1	1	13.521948	0	0
								2	3	1	2	13.521976	−2	−3
								2	1	1	0	13.522025	1	0
24.	3	1	2	3	0	3	A	3	2	2	1	6.702415	−1	1
								3	4	2	3	6.702903	1	3
								4	3	2	3	6.703232	−2	6
								3	4	4	5	6.703433	−3	−1
								4	3	4	3	6.703619	−6	−40
								4	3	2	2	6.703626	−3	−33
								3	3	2	3	6.703739	1	1
								4	5	4	5	6.704269	1	0
								2	3	2	2	6.704639	2	0
								3	4	3	4	6.705100	1	4
								2	2	2	2	6.705238	−1	−3
								4	4	4	4	6.705606	−1	−1
								4	3	3	3	6.705845	0	36
								4	5	3	4	6.705934	3	3
								3	3	3	3	6.706350	0	1
								4	4	3	4	6.706778	−1	1
								2	3	3	3	6.706853	0	1
								2	2	3	2	6.706914	−2	−1
								4	4	3	3	6.707195	2	3
								2	2	3	3	6.707453	−2	−2
25.	3	1	2	3	1	3	A	4	5	4	5	4.702612	3	1
								3	4	4	4	4.702696	1	2
								3	4	3	4	4.703420	1	5
26.	4	0	4	3	0	3	A	4	5	4	5	16.968039	−1	−3
								4	4	3	4	16.968981	−2	−2
								3	3	2	3	16.968992	0	1
								3	3	2	2	16.969386	−3	−2
								4	4	3	3	16.969399	2	1
								5	5	4	4	16.969523	1	2
								3	4	2	3	16.969692	−2	−1
								4	5	3	4	16.969703	1	0
								4	3	3	2	16.969738	−2	−2
								5	6	4	5	16.969814	1	1
								5	4	4	3	16.969851	1	1
27.	4	1	4	3	0	3	A	4	4	3	3	18.249071	0	−1
								3	3	2	2	18.249107	−2	−1
								5	5	4	4	18.249203	0	1

								3	4	2	3	18.249654	0	1
								4	3	3	2	18.249734	1	0
								3	2	2	1	18.249766	−6	−4
								5	6	4	5	18.249788	0	2
								5	4	4	3	18.249904	0	1
25.	4	1	4	3	1	3	A	4	3	4	3	16.246239	0	−3
								4	5	4	5	16.246332	−1	−4
								4	4	3	4	16.246975	−1	−1
								3	3	2	3	16.247108	−1	−2
								5	5	4	4	16.247971	0	1
								3	4	2	3	16.248053	1	2
								5	4	4	3	16.248091	1	1
								5	6	4	5	16.248129	1	1
								3	2	2	2	16.249079	−2	−2
								5	4	4	4	16.249305	−1	−1
								3	3	3	3	16.250025	−1	2
								3	4	3	4	16.250171	1	4
26.	5	0	5	4	0	4	A	5	4	5	4	20.688998	1	−2
								5	5	4	5	20.689785	0	0
								4	4	3	4	20.689828	−3	−2
								5	5	4	4	20.690505	0	0
								4	4	3	3	20.690531	−1	−1
								6	6	5	5	20.690614	0	1
								5	6	4	5	20.690773	0	−1
								5	4	4	3	20.690786	−3	−4
								4	3	3	2	20.690801	−3	−2
								6	7	5	6	20.690869	0	0
								6	5	5	4	20.690886	1	1
27.	5	0	5	4	1	4	A	4	3	3	2	19.410747	−1	−2
								5	4	4	3	19.410799	4	3
								4	4	3	3	19.410820	8	8
								5	5	4	4	19.410831	0	0
								4	5	3	4	19.410842	2	2
								6	7	5	6	19.410895	1	0
								6	6	5	5	19.410931	−1	−1
								4	3	3	3	19.412027	0	−1
								6	5	5	5	19.412166	−1	−1
28.	5	1	4	4	1	3	A	4	4	3	3	23.851980	5	5
								6	6	5	5	23.851996	−1	−1
								5	5	4	4	23.852005	2	2
								5	6	4	5	23.852028	0	−1

								4	5	3	4	23.852076	−1	−2
								5	4	4	3	23.852095	1	0
								6	5	5	4	23.852149	−1	−2
								6	7	5	6	23.852163	2	2
								4	3	3	2	23.852204	−2	−2
29.	5	1	5	4	0	4	A	5	5	4	4	21.432494	0	−1
								4	4	3	3	21.432559	0	0
								6	6	5	5	21.432621	0	0
								5	6	4	5	21.432926	0	0
								5	4	4	3	21.432959	−3	−4
								4	5	3	4	21.432974	0	1
								6	7	5	6	21.433045	0	1
								6	5	5	4	21.433097	−1	0
30.	5	2	3	4	2	2	A	6	5	5	4	24.106533	14	13
								6	7	5	6	24.106565	15	15
								6	6	5	5	24.106719	0	−1
								4	4	3	3	24.106752	−2	−2
31.	5	3	2	4	3	1	A	5	6	4	5	23.068007	0	0
								5	5	4	4	23.068156	−1	−1
								6	7	5	6	23.068698	−1	−2
								6	6	5	5	23.068827	5	5
								4	5	3	4	23.068854	−2	−2
								4	4	3	3	23.069002	−1	−1
32.	5	3	3	4	3	2	A	5	6	4	5	22.838267	−2	−2
								5	5	4	4	22.838328	0	0
								6	5	5	4	22.838951	−7	−7
								6	7	5	6	22.838973	3	3
								4	5	3	4	22.839125	3	3
								4	4	3	3	22.839168	−2	−2
33.	5	2	3	5	1	4	A	5	6	6	7	9.771636	6	10
								6	7	6	6	9.771803	4	3
								6	5	4	5	9.771845	1	3
								4	5	4	4	9.771887	2	4
								6	7	6	7	9.772384	1	2
								4	5	4	5	9.772423	−2	1
								6	6	6	6	9.772656	1	1
								5	4	5	4	9.772746	−1	1
								5	6	5	6	9.772802	0	1
								5	5	5	5	9.773081	1	−28
								4	5	5	5	9.773369	−1	−2
								6	5	5	4	9.773406	1	1

								6	7	5	6	9.773558	4	2
								4	3	5	4	9.773643	−4	−6
								4	5	5	6	9.773869	−3	−4
								6	6	5	5	9.773911	3	1
								4	4	5	5	9.774052	−4	−6
34.	5	2	4	5	1	5	A	4	3	4	3	17.775570	−5	−6
								4	5	4	5	17.775823	−1	−2
								6	7	6	7	17.775975	2	1
								5	4	5	4	17.776715	−4	−1
								4	4	4	4	17.776788	0	0
								5	6	5	6	17.776888	2	4
								6	6	6	6	17.777018	−1	0
								5	5	5	5	17.777886	−1	2
35.	5	3	3	5	2	4	A	4	3	4	3	20.182166	−5	−7
								4	5	4	5	20.182230	−1	−2
								6	5	6	5	20.182339	−2	−3
								6	7	6	7	20.182420	6	5
								4	4	4	4	20.182567	−1	−3
								6	6	6	6	20.182750	3	1
								5	4	5	4	20.183209	0	0
								5	6	5	6	20.183275	3	2
36.	6	0	6	5	0	5	A	6	6	5	5	24.338135	1	0
								5	5	4	4	24.338165	1	1
								7	7	6	6	24.338222	0	0
								6	7	5	6	24.338340	0	−1
								5	6	4	5	24.338373	2	2
								7	8	6	7	24.338417	0	0
37.	6	0	6	5	1	5	A	5	5	4	4	23.596136	−2	−2
								6	6	5	5	23.596146	1	1
								6	7	5	6	23.596185	−2	−3
								5	6	4	5	23.596197	−1	−1
								7	6	6	5	23.596206	0	0
								7	7	6	6	23.596216	3	2
								7	8	6	7	23.596240	−1	−1
								7	8	6	7	23.596240	−1	−1
38.	6	1	6	5	1	5	A	6	6	5	5	23.995949	−1	−1
								5	5	4	4	23.995966	2	2
								7	7	6	6	23.996033	1	0
								6	5	5	4	23.996066	−2	−3
								6	7	5	6	23.996079	1	1
								5	6	4	5	23.996102	0	−1

								7	6	6	5	23.996124	−2	−2
								7	8	6	7	23.996146	0	0
39.	6	1	5	6	0	6	A	5	4	5	4	16.016406	−2	−5
								7	6	7	6	16.016547	2	0
								5	6	5	6	16.016718	0	−2
								7	8	7	8	16.016794	5	3
								5	5	5	5	16.018234	−1	−3
								7	7	7	7	16.018382	3	2
								6	6	6	6	16.018984	1	5
								6	5	6	5	16.017219	−1	1
								6	7	6	7	16.017460	2	5
40.	6	2	4	6	1	5	A	7	6	7	6	10.819958	−3	3
								5	4	5	4	10.820016	−2	−2
								7	8	7	8	10.820179	1	1
								5	6	5	6	10.820226	−2	0
								6	5	6	5	10.820442	−2	0
								6	7	6	7	10.820541	0	2
								5	6	6	6	10.821401	−1	−3
								5	6	6	7	10.821729	−4	−4
								7	7	6	6	10.822067	3	2
								5	5	6	6	10.822209	−5	−7
41.	6	2	5	6	1	6	A	5	4	5	4	20.292354	−2	−3
								5	6	5	6	20.292558	−2	−3
								7	8	7	8	20.292668	3	4
								6	5	6	5	20.293285	−1	2
								6	7	6	7	20.293435	2	5
								5	5	5	5	20.293557	−2	−2
								7	7	7	7	20.293721	1	2
								6	6	6	6	20.294459	0	4
42.	6	3	3	6	2	4	A	5	6	5	5	15.835685	−5	−6
								6	7	5	6	15.835889	8	8
								5	5	5	5	15.836110	0	−1
								7	7	7	7	15.836183	2	1
								5	6	5	6	15.836501	−1	−2
								7	8	7	8	15.836641	3	2
								6	7	6	7	15.837074	0	−2
								6	5	6	5	15.837151	2	0
43.	7	1	6	7	0	7	A	6	5	6	5	20.162834	−3	−5
								8	7	8	7	20.162941	3	1
								6	7	6	7	20.163075	1	−1
								8	9	8	9	20.163144	5	3

								7	6	7	6	20.163584	−2	0
								7	8	7	8	20.163776	3	5
								6	6	6	6	20.164487	0	−1
								8	8	8	8	20.164606	4	3
								8	9	7	8	20.165140	−4	−2
								7	7	7	7	20.165202	1	4
								6	6	7	7	20.166783	10	13
44.	7	2	5	7	1	6	A	6	5	6	5	12.798725	−3	−3
								8	7	8	7	12.798885	−3	−1
								8	9	8	9	12.798902	2	1
								6	7	6	7	12.798924	−3	−2
								7	8	7	8	12.799251	1	3
								6	6	6	6	12.799697	−2	−3
								8	8	8	8	12.799752	1	0
								7	7	7	7	12.799914	−2	−1
								8	7	7	7	12.800166	0	0
								6	7	7	7	12.800413	−1	−3
								6	7	7	8	12.800493	−4	−4
45.	7	2	6	7	1	7	A	6	5	6	5	23.155225	−2	−3
								8	7	8	7	23.155327	0	0
								6	7	6	7	23.155394	−1	−2
								8	9	8	9	23.155478	5	4
								7	6	7	6	23.156019	−1	1
								7	8	7	8	23.156149	2	4
								6	6	6	6	23.156392	−2	−2
								8	8	8	8	23.156516	1	2
								7	7	7	7	23.157167	0	3
50.	7	3	4	7	2	5	A	6	6	6	6	14.854401	1	0
								8	8	8	8	14.854445	0	0
								6	7	6	7	14.854651	−1	−1
								6	5	6	5	14.854706	−5	−4
								8	9	8	9	14.854716	0	0
								8	7	8	7	14.854730	2	2
								7	7	7	7	14.854804	−1	−2
								7	8	7	8	14.855030	1	−1
								7	6	7	6	14.855064	−3	−5
51.	7	3	5	7	2	6	A	6	5	6	5	22.418219	−5	−8
								6	7	6	7	22.418312	0	−2
								8	9	8	9	22.418383	3	0
								6	6	6	6	22.418827	−4	−6
								7	6	7	6	22.418855	−1	−1

								8	8	8	8	22.418913	−1	−2
								7	8	7	8	22.418933	4	3
								7	7	7	7	22.419443	0	−1
52.	8	1	7	8	0	8	A	7	6	7	6	24.381020	−14	−17
								9	8	9	8	24.381115	3	0
								7	8	7	8	24.381214	0	−3
								9	10	9	10	24.381278	6	4
								8	7	8	7	24.381720	0	1
								8	9	8	9	24.381868	4	5
								8	8	8	8	24.383141	2	5
53.	8	2	6	8	1	7	A	9	8	9	8	15.741787	−2	−2
								7	8	7	8	15.741866	3	2
								8	7	8	7	15.742085	−3	−1
								8	9	8	9	15.742218	0	3
								7	7	7	7	15.742863	−2	−3
								9	9	9	9	15.742912	0	−1
								8	8	8	8	15.743165	−1	1
54.	8	3	5	8	2	6	A	7	7	7	7	14.435692	0	−1
								9	10	9	10	14.435745	0	0
								8	8	9	8	14.435792	−2	−2
								9	8	8	8	14.435896	−1	3
								8	9	8	9	14.435996	−1	−1
55.	8	3	6	8	2	7	A	7	6	7	6	24.173724	−4	−7
								9	8	9	8	24.173791	−4	−6
								7	8	7	8	24.173816	2	0
								9	10	9	10	24.173868	2	0
								8	7	8	7	24.174263	−4	−5
								8	9	8	9	24.174342	0	0
								7	7	7	7	24.174415	−1	−3
								9	9	9	9	24.174480	0	−1
								8	8	8	8	24.174946	6	6
56.	9	2	7	9	1	8	A	8	7	8	7	19.517464	−5	−6
								10	9	10	9	19.517535	0	−1
								8	9	8	9	19.517620	0	−1
								10	11	10	11	19.517640	3	2
								9	8	9	8	19.517871	−3	0
								9	10	9	10	19.517999	1	3
								8	8	8	8	19.518739	−1	−2
								10	10	10	10	19.518784	0	0
								9	9	9	9	19.519095	−1	1
57.	1	1	0	0	0	0	E	0	1	1	2	10.049289	0	−1

								2	1	1	1	10.050270	−1	−4
								2	3	1	2	10.050402	2	3
								2	2	1	1	10.050555	0	0
								1	1	1	0	10.051143	−1	−3
								1	2	1	2	10.051216	−1	0
								1	0	1	1	10.051370	0	−2
58.	1	1	1	0	0	0	E	0	1	1	2	6.448599	0	−1
								2	2	1	1	6.449451	−1	−2
								2	3	1	2	6.449590	1	3
								2	1	1	0	6.449631	0	1
								1	0	1	1	6.450044	1	−3
								1	2	1	2	6.450182	1	1
								1	1	1	2	6.450300	0	−1
59.	2	0	2	1	0	1	E	2	2	2	1	8.882802	1	−1
								2	2	2	2	8.882872	2	−1
								2	3	2	3	8.882974	2	0
								2	1	2	1	8.883013	−1	−1
								1	1	0	1	8.883150	−3	0
								1	2	0	1	8.883269	1	1
								1	0	0	1	8.883453	1	0
								2	2	1	1	8.884191	0	1
								3	3	2	2	8.884325	2	1
								2	3	1	2	8.884363	2	−1
								3	4	2	3	8.884517	3	1
								3	2	2	1	8.884585	−11	2
								1	1	1	1	8.886566	2	2
								1	1	1	2	8.886591	−1	0
								1	1	1	0	8.886632	−1	−3
								1	2	1	1	8.886683	0	1
								1	2	1	2	8.886710	−2	1
								1	0	1	1	8.886866	−1	0
60.	2	1	1	1	1	0	E	2	1	1	0	9.327708	0	2
								2	1	1	1	9.327934	1	2
								2	3	1	2	9.328063	−1	3
								2	2	2	2	9.328770	0	−10
								3	4	2	3	9.329425	−1	1
								3	2	2	1	9.329531	0	−1
								3	3	2	2	9.329739	2	0
								2	1	0	1	9.329789	1	1
								3	3	2	3	9.329894	2	−1
								1	2	2	1	9.330017	0	−2

								1	1	2	1	9.330259	−2	−1
								3	2	0	1	9.330518	1	2
								1	0	0	1	9.330573	1	−2
								1	2	0	1	9.331002	9	−1
								1	1	0	1	9.331242	−1	−2
61.	2	1	2	1	0	1	E	3	3	2	2	10.641157	2	0
								3	4	2	3	10.641561	0	3
								2	2	1	1	10.641595	1	1
								2	2	1	2	10.641623	−4	1
								3	2	2	1	10.641742	1	0
								3	2	2	2	10.641811	0	−1
								2	3	1	2	10.641927	0	0
								3	3	1	2	10.642504	0	1
62.	2	1	2	1	1	1	E	2	2	1	1	8.697133	0	9
								2	2	1	2	8.697243	−2	−1
								2	1	1	1	8.697515	1	2
								2	3	1	2	8.697548	2	0
								2	1	1	0	8.697769	1	2
								2	2	2	1	8.697789	−2	−5
								3	3	2	2	8.698854	5	1
								1	2	1	2	8.699034	0	2
								3	4	2	3	8.699163	0	0
								3	2	2	2	8.699507	−3	0
								1	2	2	1	8.699583	−3	0
								3	2	0	1	8.700358	2	−2
								1	1	0	1	8.700435	1	1
								1	2	0	1	8.700615	0	2
								1	0	0	1	8.700964	5	0
63.	2	2	0	2	1	1	E	1	0	1	1	12.663580	2	−1
								1	2	1	1	12.663689	−4	5
								1	1	1	1	12.663751	−2	−1
								1	2	1	2	12.663925	−2	0
								1	1	1	2	12.663990	2	−3
								1	2	3	2	12.664409	−3	−3
								3	2	3	3	12.664683	−1	2
								3	3	3	3	12.664863	2	0
								1	2	2	3	12.664941	2	−1
								3	2	3	2	12.665174	−2	5
								3	4	3	4	12.665205	1	3
								2	3	3	4	12.666705	3	−4
								2	2	3	2	12.666802	1	−2

								2	3	2	3	12.667253	0	−3
								2	1	2	1	12.667417	2	2
								2	2	2	1	12.667528	−2	−5
64.	2	2	1	2	1	2	E	3	2	3	2	9.921755	−1	−1
								3	3	3	2	9.921988	0	1
								3	4	3	4	9.922031	0	1
								1	2	2	3	9.922246	−2	−1
								1	1	2	2	9.922638	0	2
								3	3	3	3	9.922643	−1	2
								3	2	2	1	9.922904	2	2
								2	3	3	4	9.923543	−1	−1
								2	3	2	3	9.924567	1	3
								2	2	2	3	9.924662	1	−2
								2	2	2	2	9.924968	2	−1
65.	3	0	3	2	0	2	E	3	3	3	3	13.023722	1	−2
								3	4	3	4	13.023924	0	−2
								3	2	3	2	13.023960	−1	−3
								2	2	1	2	13.024901	0	0
								2	2	1	1	13.025018	1	−1
								3	3	2	2	13.025176	−2	2
								4	4	3	3	13.025307	6	−1
								3	4	2	3	13.025467	0	−1
								3	2	2	1	13.025533	−2	1
								4	5	3	4	13.025592	−1	2
								4	3	3	2	13.025649	2	1
								4	3	3	3	13.025977	−1	−1
								2	2	2	2	13.027392	−2	0
								2	3	2	3	13.027665	2	1
66.	3	1	3	2	0	2	E	3	3	3	2	14.372966	3	0
								3	2	1	1	14.373219	−17	−4
								3	3	3	3	14.373300	−1	4
								3	4	3	4	14.373735	1	−2
								3	2	3	2	14.373813	−1	−3
								2	2	1	1	14.374425	0	0
								4	4	3	3	14.374714	−2	1
								3	3	2	2	14.374744	1	−3
								2	3	1	2	14.374908	−1	−1
								4	5	3	4	14.375262	1	3
								3	2	2	1	14.375387	2	2
								3	2	2	2	14.375578	−2	−18
								4	3	3	3	14.375742	0	−2

								4	4	2	3	14.376019	−2	1
								2	2	2	2	14.376798	3	0
								2	3	2	3	14.377256	6	1
67.	1	0	1	0	0	0	E	2	2	1	1	4.507146	−8	−2
								2	3	1	2	4.507193	0	1
								2	1	1	0	4.507217	0	−1
68.	1	1	0	1	0	1	E	2	1	0	1	5.541032	−2	2
								2	2	0	1	5.541313	−2	2
								1	1	0	1	5.541900	−2	−2
								1	2	0	1	5.541973	1	1
								1	0	0	1	5.542127	3	−2
								2	3	2	3	5.543210	−2	3
								2	2	2	1	5.543343	−4	6
								2	2	2	2	5.543399	1	−8
								0	1	1	1	5.543459	−1	−1
								0	1	1	2	5.543487	−2	−1
								1	1	2	1	5.543927	0	−1
								1	2	2	3	5.544023	1	−1
								1	0	2	1	5.544153	0	−1
								2	1	1	0	5.544515	1	0
								2	3	1	2	5.544599	0	3
								1	1	1	1	5.545314	−3	−2
								1	1	1	2	5.545340	0	−3
								1	2	1	1	5.545386	−1	0
								1	2	1	2	5.545413	1	0
								1	0	1	1	5.545540	1	−2
69.	2	0	2	1	1	1	E	2	2	1	1	6.939721	0	1
								2	1	1	1	6.939932	−2	1
								2	3	1	2	6.939985	0	0
								2	1	1	0	6.940186	3	1
								2	2	2	1	6.940390	−1	0
								2	2	2	2	6.940565	2	−3
								2	3	2	3	6.940579	2	0
								2	1	2	2	6.940778	−1	−1
								3	2	1	1	6.941502	0	1
								3	3	2	2	6.942020	1	1
								3	4	2	3	6.942121	0	0
								3	2	2	1	6.942168	1	−3
								1	2	1	2	6.942331	3	0
								3	2	2	2	6.942351	−1	2
								1	0	1	1	6.942395	0	−1

								1	2	0	1	6.943913	2	1
								1	0	0	1	6.944097	−2	1
70.	2	1	1	1	1	1	E	2	1	1	1	12.928778	−3	1
								2	2	1	1	12.929035	0	0
								2	3	1	2	12.929098	−3	3
								2	2	2	2	12.929883	3	0
								1	2	1	2	12.930112	−2	0
								3	2	2	1	12.930179	2	3
								3	4	2	3	12.930234	2	−2
								3	3	2	2	12.930842	1	0
								1	2	0	1	12.931693	−2	0
								1	1	0	1	12.931930	−2	−4
71.	2	2	0	1	1	0	E	1	1	1	0	21.992909	19	−4
								1	2	1	2	21.993002	1	0
								1	1	1	2	21.993065	0	−5
								1	2	1	1	21.993074	0	2
								1	1	1	1	21.993137	−2	−3
								3	3	2	2	21.994603	−4	1
								3	4	2	3	21.994628	−2	2
								3	2	2	1	21.994703	0	1
								3	3	2	3	21.994755	−4	−3
								1	1	0	1	21.994993	−7	−2
								2	1	1	0	21.995140	−1	19
								2	3	1	2	21.995317	6	1
								2	2	1	2	21.995393	0	−1
								2	2	1	1	21.995463	0	−2
								2	3	2	2	21.995975	3	−2
								2	2	2	2	21.996051	2	−4
								2	3	2	3	21.996131	1	−2
								2	1	2	1	21.996219	−1	0
72.	2	2	1	1	1	1	E	1	0	1	1	18.619542	2	−4
								1	2	1	1	18.619669	0	−7
								1	2	1	2	18.619795	0	−1
								1	1	1	2	18.619886	1	6
								1	2	2	1	18.620346	−4	0
								3	2	2	1	18.621086	−2	0
								3	4	2	3	18.621196	0	3
								3	3	2	2	18.621495	−1	1
								2	3	1	2	18.622113	1	1
73.	2	1	1	2	0	2	E	2	1	1	0	5.986382	0	0
								2	3	1	2	5.986766	2	2

								2	2	1	1	5.986942	−1	1
								1	2	1	2	5.987781	−2	0
								2	3	3	3	5.987806	3	2
								1	1	1	0	5.987833	1	−5
								2	2	3	3	5.987862	−1	−2
								1	2	1	1	5.987898	1	−1
								3	2	3	2	5.988004	−2	−1
								3	4	3	4	5.988115	−2	0
								3	3	3	3	5.988822	−2	−1
								2	3	2	3	5.989113	−1	3
								2	2	2	2	5.989314	0	−1
								1	0	2	1	5.989629	1	−4
								3	4	2	3	5.989659	−2	2
								3	2	2	2	5.989786	−3	1
								1	2	2	3	5.990125	−12	−2
								3	3	2	2	5.990275	1	2
								1	1	2	1	5.990300	0	−2
								1	1	2	2	5.990511	2	−2
74.	2	2	0	2	1	2	E	1	1	1	0	16.894718	0	−4
								1	2	1	2	16.895003	1	−2
								1	1	1	2	16.895070	2	−2
75.	3	1	2	2	0	2	E	3	2	1	1	20.252973	−1	1
								3	2	3	2	20.253564	2	−1
								2	1	1	0	20.253848	−1	−5
								3	2	3	3	20.253883	−2	−11
								2	3	1	2	20.254389	−3	0
								4	3	3	2	20.254609	0	1
								4	5	3	4	20.254757	−2	1
								3	2	2	1	20.255136	0	2
								3	4	2	3	20.255404	1	3
								4	4	3	3	20.255646	0	2
								3	3	2	2	20.255901	0	0
								4	3	2	2	20.256390	2	1
								2	3	2	3	20.256734	1	−1
								2	2	2	1	20.257169	−1	−2
								2	2	2	2	20.257379	−2	−3
76.	3	1	2	2	1	1	E	3	3	3	3	14.265629	−2	1
								3	4	3	4	14.265745	−2	0
								3	2	2	2	14.266031	−1	1
								3	4	2	3	14.266293	−1	1
								3	3	2	2	14.266587	0	1

								4	3	3	2	14.266603	−1	0
								2	3	1	2	14.266610	0	2
								4	4	3	3	14.266822	0	0
								2	2	1	1	14.266868	3	−1
								2	2	1	2	14.267108	3	−2
								4	4	3	4	14.267292	1	−1
								2	1	2	1	14.267467	−4	−5
								2	3	2	3	14.267622	−1	−4
77.	3	1	3	2	1	2	E	3	3	3	3	12.616459	0	−3
								3	2	3	2	12.616655	1	−2
								3	4	3	4	12.616693	1	−3
								3	3	2	3	12.617038	1	0
								3	3	2	2	12.617342	1	−1
78.	3	2	1	2	2	0	E	3	2	2	1	13.725319	2	3
								3	4	2	3	13.725362	1	3
								3	3	2	2	13.725499	−2	1
								3	3	2	3	13.725573	−1	−3
								4	3	3	3	13.726619	1	0
								3	4	3	3	13.726736	1	2
								4	3	3	2	13.726801	0	0
								4	5	3	4	13.726826	0	1
								4	4	3	3	13.726919	1	2
								3	3	3	2	13.727134	3	1
								2	3	1	2	13.727623	1	2
								2	2	1	1	13.727779	−1	1
								2	2	1	2	13.727844	3	−2
79.	3	2	2	2	1	2	E	2	1	1	0	23.732364	−1	−3
								4	3	1	2	23.732734	0	0
								2	3	1	2	23.732819	0	−1
								2	1	1	1	23.732894	−2	−2
								3	2	1	1	23.732944	0	0
								4	3	3	2	23.732988	2	0
								3	4	3	3	23.733779	2	3
								4	4	3	3	23.734024	1	0
								3	2	2	1	23.734164	−1	−1
								3	4	2	3	23.734356	0	4
								2	1	2	2	23.734504	1	−2
								4	4	2	3	23.734600	1	0
								3	3	2	2	23.734936	1	1
80.	3	2	2	2	2	1	E	3	2	2	2	13.809584	2	−1
								2	3	2	2	13.809639	0	−1

								3	2	2	1	13.809735	2	2
								3	4	2	3	13.809790	−2	2
								3	3	2	2	13.809968	0	2
								4	3	3	3	13.811000	0	−1
								4	3	3	2	13.811231	−2	0
								4	5	3	4	13.811265	−1	1
								4	4	3	3	13.811384	1	2
								2	3	1	2	13.812057	0	0
								2	2	1	1	13.812259	1	2
81.	3	1	2	3	0	3	E	3	2	2	1	7.227305	0	1
								3	4	2	3	7.227740	2	3
								3	2	4	3	7.227916	0	−1
								3	3	2	3	7.228092	0	0
								3	4	4	5	7.228271	0	2
								3	3	4	3	7.228472	3	0
								2	1	2	1	7.228485	1	−3
								3	3	2	2	7.228510	−2	1
								4	3	2	3	7.228579	1	−1
								4	3	4	3	7.228961	−3	1
								2	3	2	3	7.229069	3	−2
								4	5	4	5	7.229167	1	1
								3	4	3	4	7.229937	−1	3
								4	4	4	4	7.230336	0	−1
								3	3	3	3	7.230728	−1	1
								4	5	3	4	7.230833	1	3
								4	3	3	3	7.231215	2	1
								2	3	3	4	7.231266	0	−2
								4	4	3	3	7.231922	2	1
								2	2	3	3	7.232205	2	−3
82.	3	1	2	3	1	3	E	3	4	2	3	5.878149	0	3
								3	2	2	2	5.878548	1	1
								3	4	4	5	5.878600	−2	0
								3	3	4	3	5.878707	1	0
								2	1	2	1	5.878771	1	−4
								4	3	2	3	5.878988	−2	0
								3	3	2	2	5.879105	0	3
								4	3	4	3	5.879194	1	0
								3	4	4	4	5.879386	−4	3
								4	5	4	5	5.879498	−1	2
								3	2	3	2	5.879751	0	2
								4	4	4	3	5.879901	−2	0

								2	2	2	3	5.879978	0	−4
								3	4	3	4	5.880126	0	4
83.	3	2	1	3	1	2	E	4	5	4	5	12.125388	4	1
								4	4	4	5	12.125609	0	−2
								4	3	3	3	12.125853	−2	−2
								3	4	3	4	12.126324	4	0
								3	2	3	2	12.126438	0	−6
								2	2	3	2	12.126695	1	−3
								3	3	3	2	12.126741	1	−1
84.	3	2	1	3	1	3	E	2	1	2	1	18.003980	−2	−4
								2	3	2	3	18.004416	0	−2
								4	3	4	3	18.004560	0	−1
								4	5	4	5	18.004886	0	3
								2	2	2	2	18.005242	2	−2
								3	3	2	2	18.005286	0	−3
								3	4	4	4	18.005710	6	3
								4	4	4	4	18.005890	1	0
								4	5	3	4	18.006408	−2	3
								2	2	3	2	18.006449	0	2
								4	4	3	4	18.006629	1	0
								3	3	3	3	18.007342	1	1
								3	3	3	3	18.007342	3	1
85.	3	2	2	3	1	2	E	2	2	2	2	5.234916	2	0
								2	3	2	3	5.235134	1	2
								4	4	4	4	5.235213	−2	0
								4	3	4	3	5.235543	2	5
								4	5	4	5	5.235580	−1	0
86.	3	2	2	3	1	3	E	2	1	2	1	11.114152	1	−4
								3	2	2	1	11.114203	−3	−1
								2	3	2	3	11.114611	−2	−1
								4	3	4	3	11.114732	1	0
								4	5	4	5	11.115078	0	2
								3	4	4	4	11.115899	1	2
								4	4	4	4	11.116145	0	0
								3	2	3	2	11.116361	1	−1
								3	4	3	4	11.116640	0	4
								2	2	3	2	11.116701	−2	−1
								4	4	3	4	11.116886	0	2
								3	3	3	4	11.116914	−1	−1
								3	2	3	3	11.117211	2	0
								2	3	3	3	11.117268	1	2

								3	3	3	3	11.117594	−1	1
87.	4	0	4	3	1	2	E	4	4	3	3	9.675993	2	−2
								5	5	4	4	9.676511	−2	1
								3	3	2	2	9.676725	1	3
								4	5	3	4	9.677096	−1	−4
								5	6	4	5	9.677976	3	−1
								5	4	4	3	9.678220	−1	1
								3	4	4	3	9.678444	1	0
								3	2	2	1	9.678562	0	5
								5	4	3	3	9.678707	0	0
88.	4	0	4	3	0	3	E	4	5	4	5	16.905367	10	−2
								4	3	4	3	16.905384	7	0
								3	3	2	2	16.906710	−7	−2
								4	4	3	3	16.906722	1	1
								5	5	4	4	16.906846	0	0
								4	5	3	4	16.907036	2	3
								4	3	3	2	16.907068	1	−2
								5	6	4	5	16.907144	8	1
								5	4	4	3	16.907180	−7	1
89.	4	0	4	3	1	3	E	4	4	3	3	15.557150	0	1
								5	4	2	3	15.557216	−1	8
								4	3	3	2	15.557224	−1	7
								3	3	2	2	15.557299	−2	−6
								5	4	4	3	15.557414	0	0
								3	4	2	3	15.557433	0	1
								5	5	4	4	15.557444	0	3
								5	6	4	5	15.557474	−1	1
								3	2	2	2	15.558295	0	8
								5	4	4	4	15.558437	0	−8
								3	3	3	2	15.558510	0	2
90.	4	1	4	3	0	3	E	4	4	4	4	17.785105	0	−4
								4	5	4	5	17.785527	−1	−4
								4	3	4	3	17.785570	0	−3
								3	3	2	2	17.786665	−2	0
								4	4	3	3	17.786692	−1	−1
								5	5	4	4	17.786782	−1	0
								3	4	2	3	17.787139	−2	0
								4	5	3	4	17.787194	−1	−1
								4	3	3	2	17.787258	−2	−1
								5	6	4	5	17.787278	−2	0
								5	4	4	3	17.787369	0	0

								3	2	2	2	17.787872	0	−1
								5	5	3	4	17.787930	0	2
								5	4	4	4	17.788038	−1	−1
								3	3	3	3	17.788882	1	0
								3	4	3	4	17.789336	1	1
91.	4	1	3	3	1	2	E	4	4	4	4	19.111592	1	0
								4	5	4	5	19.111753	0	1
								3	2	2	2	19.111987	1	−3
								4	3	3	3	19.112137	−10	−1
								4	5	3	4	19.112649	2	0
								4	3	3	2	19.112694	0	0
								3	4	2	3	19.112730	0	0
								4	4	3	3	19.112786	0	0
								5	4	4	3	19.112800	0	0
								5	6	4	5	19.112823	0	1
92.	4	1	3	3	2	1	E	4	5	3	4	6.986327	−1	2
								4	4	3	3	6.986601	−1	1
								4	4	2	3	6.986871	1	2
								4	4	4	3	6.986924	0	−8
								5	4	3	3	6.987103	−1	1
								5	6	4	5	6.987435	1	0
								5	5	4	4	6.987866	−1	1
								3	3	2	2	6.988139	1	0
93.	4	1	4	3	1	3	E	4	3	4	3	16.435805	−1	−3
								4	5	4	5	16.435858	0	−3
								4	4	3	4	16.436442	2	−1
								3	3	2	3	16.436655	−1	−1
								4	4	3	3	16.437121	−1	0
								3	3	2	2	16.437258	−5	0
								5	5	4	4	16.437377	−2	0
								4	5	3	4	16.437384	2	1
								5	4	4	3	16.437603	−1	0
								5	6	4	5	16.437610	4	2
								3	2	2	2	16.438466	−1	−1
								5	4	4	4	16.438634	−5	0
94.	4	1	3	3	2	2	E	4	3	3	2	13.876084	2	3
								4	5	3	4	13.876135	−2	0
								4	4	3	3	13.876348	−12	0
								4	4	2	3	13.876672	−7	−3
								4	4	4	3	13.876761	11	1
								5	4	3	3	13.876851	1	1

								5	6	4	5	13.877241	5	−1
								3	4	3	3	13.877273	0	2
								3	2	2	1	13.877461	1	−2
								3	4	2	3	13.877593	2	−5
								5	5	4	4	13.877614	0	3
								3	3	2	2	13.877882	0	−2
95.	4	2	3	3	1	2	E	3	3	2	2	23.738924	1	−12
								5	5	4	4	23.739075	0	−7
								3	4	2	3	23.739192	0	12
								5	6	4	5	23.739445	7	1
								5	4	4	3	23.739462	0	4
								4	4	3	3	23.739646	1	−1
								4	5	3	4	23.739772	1	0
								4	3	3	2	23.739905	0	0
96.	4	2	2	3	2	1	E	4	5	3	4	18.478634	0	1
								4	4	3	3	18.478673	2	1
								5	6	4	5	18.479212	1	1
								5	4	4	3	18.479248	1	0
								5	5	4	4	18.479335	−1	0
								3	4	3	4	18.479354	−2	7
								3	3	2	2	18.479477	−2	0
97.	4	2	3	3	2	2	E	4	4	3	3	18.503209	1	1
								4	5	3	4	18.503259	2	1
								4	3	3	2	18.503292	2	0
								5	6	4	5	18.503864	1	0
								5	5	4	4	18.503871	1	2
								5	4	4	3	18.503920	1	1
								3	3	2	2	18.504021	0	1
								3	4	2	3	18.504047	0	−1
98.	4	3	2	3	3	1	E	3	4	3	4	18.309063	−1	−3
								3	3	3	3	18.309127	−1	−1
								4	5	3	4	18.309798	−2	1
								4	4	3	3	18.309864	−4	2
								5	6	4	5	18.311139	0	1
								5	5	4	4	18.311194	2	2
								3	4	2	3	18.311658	−1	1
								3	3	2	2	18.311720	1	1
99.	4	1	3	4	0	4	E	4	3	3	2	9.432954	−2	0
								4	5	5	6	9.433776	0	0
								4	4	3	4	9.433854	−1	0
								4	4	5	4	9.434079	0	0

								3	2	3	2	9.434282	−3	−5
								4	4	3	3	9.434580	1	−3
								3	4	3	4	9.434775	−1	−3
								5	6	5	6	9.434846	2	1
								4	3	4	3	9.435228	−1	2
								4	5	4	5	9.435553	1	4
								3	3	3	3	9.436074	−3	−4
								5	5	5	5	9.436314	4	0
								4	4	4	4	9.436793	3	2
								5	4	4	4	9.437293	−2	0
								3	3	4	3	9.437367	0	−2
								5	5	4	4	9.438026	0	3
100.	4	1	3	4	1	4	E	3	4	3	4	8.554659	2	−4
								5	6	5	6	8.554711	0	1
								4	3	4	3	8.555040	−2	3
								4	5	4	5	8.555392	3	4
101.	4	2	3	4	0	4	E	3	4	3	4	14.061223	0	−5
								5	4	5	4	14.061242	3	4
								5	6	5	6	14.061469	−1	2
								3	3	3	3	14.062211	2	−3
								4	3	4	3	14.062438	2	1
								5	5	5	5	14.062572	2	−1
								4	5	4	5	14.062676	−1	3
								4	4	4	4	14.063653	0	1
102.	4	2	2	4	1	3	E	4	4	5	5	11.490840	0	−1
								4	5	3	4	11.490898	−1	5
								3	2	3	3	11.490907	2	0
								4	3	3	2	11.491053	1	5
								3	3	3	3	11.491338	5	0
								5	5	5	5	11.491471	3	2
								3	4	3	4	11.491610	4	3
								5	6	5	6	11.491778	−2	3
								5	4	5	4	11.491814	−2	0
								4	4	4	4	11.492072	1	−1
								4	5	4	5	11.492308	1	0
								4	3	4	3	11.492380	1	−1
								5	5	4	4	11.492702	−1	1
								4	4	4	3	11.492721	1	1
								5	6	4	5	11.492848	3	3
103.	4	2	3	4	1	3	E	4	3	3	2	4.625882	−2	4
								5	6	5	5	4.625971	1	3

								4	5	5	6	4.626053	1	−1
								3	3	3	3	4.626134	4	−2
								5	5	5	5	4.626259	3	0
								4	4	4	4	4.626861	−3	0
								4	5	4	5	4.627123	3	0
								4	3	4	3	4.627209	−2	−1
104.	4	2	3	4	1	4	E	4	3	3	2	13.179984	1	−1
								4	5	3	4	13.180373	3	2
								3	2	3	2	13.180689	1	−4
								5	4	5	4	13.181048	−3	−1
								3	4	3	4	13.181111	3	−2
								5	6	5	6	13.181335	−1	3
								4	5	5	5	13.181780	0	2
								3	2	3	3	13.181897	−2	−5
								3	4	3	3	13.182005	−1	1
								4	3	4	3	13.182248	−4	0
								3	3	3	3	13.182260	−4	−1
								4	5	4	5	13.182517	−2	6
								5	5	5	5	13.182637	−1	0
105.	4	3	1	4	2	2	E	3	3	3	3	20.019838	−5	−3
								3	4	3	4	20.019996	0	4
								5	5	5	5	20.020129	−3	−2
								5	6	5	6	20.020311	−3	0
								4	4	4	4	20.021326	−5	−3
								4	5	4	5	20.021431	0	−2
								4	3	4	3	20.021475	0	−5
106.	4	3	2	4	2	3	E	3	3	3	3	16.521681	1	−1
								3	4	3	4	16.521757	0	1
								5	5	5	5	16.521984	−1	0
								5	4	5	4	16.522064	0	−2
								5	6	5	6	16.522074	−1	3
								4	4	4	4	16.523185	0	−1
								4	5	4	5	16.523228	0	−1
								4	3	4	3	16.523252	2	−3
107.	5	0	5	4	0	4	E	5	6	5	6	20.615993	−1	−2
								5	5	4	5	20.616755	−2	0
								6	6	5	6	20.616800	1	1
								5	5	4	4	20.617505	0	−1
								4	4	3	3	20.617531	−1	0
								6	6	5	5	20.617614	0	0
								5	6	4	5	20.617768	1	−1

								4	3	3	2	20.617795	1	1
								6	7	5	6	20.617863	2	0
								6	5	5	4	20.617878	0	2
								4	4	4	4	20.619741	0	2
								4	5	4	5	20.619982	−1	1
108.	5	0	5	4	1	4	E	5	5	4	4	19.737535	0	1
								4	4	3	3	19.737579	0	0
								5	4	4	3	19.737592	−1	−2
								5	6	4	5	19.737608	−1	1
								4	3	3	2	19.737616	−1	1
								6	6	5	5	19.737679	−3	1
								6	5	5	4	19.737689	−2	2
								6	7	5	6	19.737728	−1	0
109.	5	1	5	4	0	4	E	5	5	4	4	21.125528	3	−1
								4	4	3	3	21.125563	−1	−1
								6	6	5	5	21.125635	3	−1
								5	6	4	5	21.125903	−1	−1
								4	5	3	4	21.125926	1	−1
								6	7	5	6	21.126000	−1	−1
								6	5	5	4	21.126039	0	−1
								4	4	4	4	21.127771	3	−1
								4	5	4	5	21.128115	−2	1
								4	3	4	3	21.128231	0	2
110.	5	1	4	4	1	3	E	4	4	3	3	23.710655	−2	4
								6	6	5	5	23.710677	1	−1
								4	4	3	3	23.710655	−2	4
								6	6	5	5	23.710677	−1	−1
								5	6	4	5	23.710690	−1	1
								4	5	3	4	23.710735	15	−1
								5	4	4	3	23.710744	8	0
								6	7	5	6	23.710811	1	3
111.	5	1	4	4	2	2	E	5	4	4	3	12.218361	−1	−2
								5	6	4	5	12.218381	−2	0
								5	5	4	4	12.218580	−1	−2
112.	5	1	4	4	2	3	E	5	4	4	3	19.083535	−1	2
								5	6	4	5	19.083565	0	0
								5	5	4	4	19.083794	5	0
								5	5	4	5	19.084023	0	1
								6	5	5	4	19.084171	−4	15
								6	7	5	6	19.084194	−2	8
								4	3	3	2	19.084251	−1	0

								4	5	3	4	19.084284	1	−2
								6	6	5	5	19.084418	0	−1
								4	4	3	3	19.084515	−2	−1
113.	5	2	4	4	2	3	E	5	5	4	4	22.999050	2	0
								5	6	4	5	22.999130	1	−1
								6	5	5	5	22.999167	−2	5
								6	6	5	5	22.999350	1	0
								4	4	3	3	22.999391	0	−3
								6	7	5	6	22.999477	−1	−1
								6	5	5	4	22.999492	2	−1
								4	5	3	4	22.999499	0	1
								4	3	3	2	22.999560	−2	0
114.	5	3	2	4	3	1	E	5	4	4	3	22.914448	2	−1
								5	6	4	5	22.914461	0	3
								5	5	4	4	22.914552	0	2
								6	5	5	4	22.915136	2	−2
								6	7	5	6	22.915156	0	1
								6	6	5	5	22.915217	1	1
								4	5	3	4	22.915310	3	−1
								4	3	3	2	22.915326	−2	2
								4	4	3	3	22.915396	0	1
115.	5	3	3	4	3	2	E	5	4	4	3	23.034213	−1	−2
								5	6	4	5	23.034233	−2	2
								5	5	4	4	23.034354	1	0
								6	5	5	4	23.034909	−12	0
								6	7	5	6	23.034931	0	1
								6	6	5	5	23.035023	3	0
								4	5	3	4	23.035087	−2	0
								4	3	3	2	23.035098	1	2
								4	4	3	3	23.035203	−3	−2
116.	5	1	4	5	0	5	E	5	5	6	5	12.526858	0	1
								5	4	4	4	12.527147	1	−1
								4	3	4	3	12.527324	4	−5
								6	5	6	5	12.527517	−2	−1
								5	6	6	6	12.527654	2	−12
								4	5	4	5	12.527716	−2	−3
								6	7	6	7	12.527792	1	1
								5	4	5	4	12.528188	0	0
								5	6	5	6	12.528473	1	4
117.	5	2	4	5	1	5	E	4	3	4	3	15.934472	0	−5
								6	5	6	5	15.934690	−1	−2

								4	5	4	5	15.934798	1	−1
								6	7	6	7	15.934947	−1	2
								5	4	5	4	15.935674	−1	1
								5	6	5	6	15.935903	0	4
								4	4	4	4	15.936041	−2	−4
								6	6	6	6	15.936288	1	1
118.	6	0	6	5	0	5	E	6	6	5	5	24.273790	−2	−1
								5	5	4	4	24.273819	0	1
								7	7	6	6	24.273878	1	1
								6	7	5	6	24.273988	0	−1
								5	6	4	5	24.274019	−1	1
								7	8	6	7	24.274063	−1	−1
119.	6	0	6	5	1	5	E	6	6	5	5	23.765766	−2	−1
								5	5	4	4	23.765786	−1	0
								6	5	5	4	23.765838	1	−2
								7	7	6	6	23.765856	−1	1
								5	6	4	5	23.765883	0	−2
								7	6	6	5	23.765900	−2	1
								7	8	6	7	23.765927	1	1
120.	6	1	5	5	2	3	E	6	6	5	5	16.790508	−2	−1
								6	7	5	6	16.790668	−3	−2
								6	5	5	4	16.790725	0	−2
								7	7	6	6	16.790897	−1	−1
								5	5	4	4	16.790951	0	−2
121.	6	1	6	5	0	5	E	6	6	5	5	24.544172	0	0
								5	5	4	4	24.544208	−3	0
								7	7	6	6	24.544262	0	0
								6	7	5	6	24.544424	0	−3
								6	5	5	4	24.544434	−1	0
								5	6	4	5	24.544459	−3	−1
								7	8	6	7	24.544505	1	−3
								7	6	6	5	24.544518	−3	1
122.	6	1	6	5	1	5	E	6	6	5	5	24.036147	0	−1
								5	5	4	4	24.036175	−1	−1
								7	7	6	6	24.036240	3	0
								6	5	5	4	24.036281	−2	−3
								6	7	5	6	24.036291	1	0
								5	4	4	3	24.036299	−3	0
								5	6	4	5	24.036327	0	−1
								7	6	6	5	24.036351	−1	−3
								7	8	6	7	24.036371	−1	1

123.	6	1	5	6	0	6	E	5	4	5	4	16.257901	6	−6
								7	6	7	6	16.258037	0	−2
								5	6	5	6	16.258205	−1	−4
								7	8	7	8	16.258282	4	2
								6	5	6	5	16.258706	0	1
								6	7	6	7	16.258939	1	4
								5	5	5	5	16.259685	−2	−5
								7	7	7	7	16.259832	1	0
								6	6	6	6	16.260430	1	2
124.	6	2	4	6	1	5	E	6	6	7	6	11.782592	−4	1
								5	6	5	5	11.782605	−1	6
								5	4	5	4	11.782773	−1	0
								5	6	5	6	11.782889	−2	0
								7	8	7	8	11.782905	0	3
								6	5	6	5	11.783160	−3	1
								6	7	6	7	11.783233	0	3
								5	5	5	5	11.783273	0	−2
								7	7	7	7	11.783333	2	1
								6	6	6	6	11.783557	1	1
125.	6	2	5	6	1	6	E	5	4	5	4	19.048266	−1	−6
								7	6	7	6	19.048413	−1	−2
								5	6	5	6	19.048510	−1	−3
								6	5	6	5	19.049238	1	0
								6	7	6	7	19.049419	5	3
								5	5	5	5	19.049696	0	−4
								7	7	7	7	19.049868	2	0
126.	6	3	3	6	2	4	E	5	5	5	5	18.586953	3	1
								7	7	7	7	18.587029	0	3
								5	6	5	6	18.587343	1	2
								7	8	7	8	18.587454	−1	0
								6	6	6	6	18.587568	2	0
								6	7	6	7	18.587906	0	−1
								6	5	6	5	18.587979	5	1
127.	6	3	4	6	2	5	E	6	6	7	6	17.253191	1	8
								5	6	5	6	17.253298	0	1
								7	6	7	6	17.253344	1	3
								7	8	7	8	17.253381	0	5
								5	5	5	5	17.253709	1	1
								7	7	7	7	17.253822	−1	2
								6	5	6	5	17.253952	−5	2
								6	7	6	7	17.254028	−2	5

								6	6	6	6	17.254400	−5	2
128.	7	2	5	7	1	6	E	8	7	8	7	13.485243	−3	5
								6	7	6	7	13.485287	1	1
								7	6	7	6	13.485505	−1	2
								7	8	7	8	13.485618	0	4
								6	6	6	6	13.486023	1	0
								8	8	8	8	13.486073	−1	0
								7	7	7	7	13.486289	0	0
129.	7	2	6	7	1	7	E	7	6	7	6	22.312266	0	−3
								7	8	7	8	22.312410	−1	0
								6	6	6	6	22.312734	1	−6
								8	8	8	8	22.312860	0	−3
130.	7	3	4	7	2	5	E	6	6	6	6	17.428089	3	2
								8	8	8	8	17.428130	1	1
								6	7	6	7	17.428455	3	2
								7	7	7	7	17.428513	0	2
								8	9	8	9	17.428529	4	1
								6	5	6	5	17.428544	1	2
								7	8	7	8	17.428832	−1	0
								7	6	7	6	17.428887	5	−1
131.	7	3	5	7	2	6	E	6	5	6	5	18.873972	−1	1
								8	7	8	7	18.874077	2	1
								6	7	6	7	18.874099	1	3
								7	6	7	6	18.874618	1	3
								7	8	7	8	18.874720	0	6
								6	6	6	6	18.874786	0	0
								8	8	8	8	18.874875	0	5
132.	8	2	6	8	1	7	E	9	8	9	8	16.306885	0	0
								7	8	7	8	16.306961	0	−3
								9	10	9	10	16.306976	0	4
								8	7	8	7	16.307186	0	0
								8	9	8	9	16.307316	0	4
								7	7	7	7	16.307948	0	−1
								8	8	8	8	16.308261	0	2